Charles University in Prague

Faculty of Medicine in Pilsen

Doctoral thesis

Cognitive and emotional abnormalities in cerebellar mutant mice

Mgr. Jan Tůma

Supervisor: **Doc. MUDr. František Vožeh, CSc.**

Advisors: **MUDr. Jan Cendelín, Ph.D.**

Pascal Hilber, Ph.D., HDR

Study programme: **Physiology and Pathological Physiology**

Department of Pathophysiology

Pilsen 2015

DECLARATION

I hereby declare that this thesis is based on experiments performed at the Department of Pathophysiology and Laboratory of Neurodegenerative Disorders (Biomedical Centre) of the Faculty of Medicine in Pilsen, Charles University in Prague during my Ph.D. studies and was written by me. All sources of information are reported in the list of references. This thesis was not used to obtain any other or similar degree. I agree with permanent deposition of my thesis in the Centre for Scientific Information in Faculty of Medicine in Pilsen, Charles University in Prague. I also agree with permanent deposition of my thesis in the database of the inter-university project Theses.cz for the purposes of a continuous surveillance of comparability of degree dissertations.

This work was financially supported by grants GAUK 58509 and 613112, SV No. 262805 and No. 260175, PRVOUK P36, COST No. LD12057 and LD12056 and project CZ.1.05/2.1.00/03.0076 from European Regional Development Fund.

Pilsen 2015

…….....

Mgr. Jan Tůma

ACKNOWLEDGEMENT

I would like to thank my supervisor, Doc. MUDr. František Vožeh, CSc., for the opportunity to work on this project and for his help during my Ph.D. studies. Special thanks belong to my advisor MUDr. Jan Cendelín, Ph.D. for leading my work, his scientific suggestions and advice, as well as friendly discussions. I would also like to thank my French advisor Pascal Hilber, Ph.D., HDR for his help and inspiring advice.

My further thanks goes to all my past and present colleagues from the Department of Pathophysiology as well as other departments and laboratories in the Faculty of Medicine in Pilsen. Especially I would like to thank to Helena Geciová and Irena Pojarová for their enormous technical and friendly help. I would like to also thank Doc. Mgr. Vladimír Sládek, Ph.D. for his scientific enthusiasm and stimulating discussions.

I would also like to express my warmest thanks to my family for their support and help during my studies.

Last, but not least, my heartfelt thanks belong to my wife Jana for her love, endless patience and understanding, as well as help with my work.

CONTENTS

LIST OF ABBREVIATIONS

Agtpbp1 – ATP/GTP binding protein 1 gene [*Mus musculus*]

Agtpbp1 – ATP/GTP binding protein 1 [*Mus musculus*] (synonym: CCP1, Nna1)

ACTH – adrenocorticotropic hormone

ADCA – autosomal dominant cerebellar ataxia

AMPA – α-amino-3-hydroxy-5-methyl-4-isoxazolepropionic acid receptor

AMPK – 5' adenosine monophosphate-activated protein kinase

AOA – ataxia with oculomotor apraxia

ATP – adenosine triphosphate

ATXN2 – Ataxin-2 protein [*Homo sapiens*] (synonym: *SCA2*)

ATXN2 – Ataxin-2 protein [*Homo sapiens*]

BDNF – brain-derived neurotrophic factor

Cbln1 – cerebellin 1 precursor protein [*Mus musculus*]

CCP1 – cytosolic carboxypeptidase 1 (see ATP/GTP binding protein 1)

CNS – central nervous system

DRPLA – dentatorubral-pallidoluysian atrophy

EA – episodic ataxia

FMR1 – fragile X mental retardation 1 gene [*Homo sapiens*]

FXTAS – fragile X-associated tremor/ataxia syndrome

GABA – γ-aminobutyric acid

GAD – GABA-synthesizing enzyme glutamate decarboxylase

GluR*δ2* – δ2 glutamate receptor

Grid2 – δ2 glutamate receptor gene [*Mus musculus*]

GRID2 – δ2 glutamate receptor gene [*Homo sapiens*]

HPA – Hypothalamo-Pituitary-Adrenal

IGF-I – Insulin-like growth factor I

iGluR – ionotropic glutamate receptor

KA – kainic acid

Lc – Lurcher

PKC – protein kinase C

PF-PC LTD – parallel fibre-Purkinje cell long-term depression

MLCK1 – myosin light chain kinase 1

MSA – multiple system atrophy

MSA-C – multiple system atrophy (cerebellar subtype)

MSA-P – multiple system atrophy (parkinsonian subtype)

NMDA – *N*-Methyl-D-aspartic acid

NRXN – neurexin

OKR – optokinetic reflex

OPCA – olivopontocerebellar atrophy

pcd – Purkinje cell degeneration mice

Pcp2 – Purkinje cell protein 2 gene [*Mus musculus*]

Pcp2 – Purkinje cell protein 2 [*Mus musculus*] (synonym: L7)

PFS – posterior fossa syndrome

polyQ – polyglutamine tract

SAOA – sporadic adult-onset ataxia

SCA – spinocerebellar ataxia

SCA2 – spinocerebellar ataxia type 2

SCA2 –spinocerebellar ataxia type 2 gene (see: *ATXN2*)

SGP2 – sulfated glycoprotein 2

Shh – Sonic hedgehog [*Mus musculus*]

VOR – vestibulo-ocular reflex

SUMMARY

The cerebellum is traditionally considered a structure responsible for the control of motor function. Nevertheless, during the last three decades, it has been revealed that the cerebellum is also involved in attention, perception, mood, speech, nonmotor learning, and memory. Hereditary cerebellar ataxias represent a heterogeneous group of neurodegenerative disorders with a variety of neurological and systemic symptoms. Variability of human hereditary ataxias is also reflected in animal models of cerebellar disorders. The most frequently used animal models are *Lurcher* and *Purkinje cell degeneration* (*pcd*) mutant mice.

The main aim of this thesis was to analyze and compare the spatial and emotional behavior of these cerebellar mutants. Additional aims were to study the impact of abnormal behavior on breeding capacity in *Lurcher* mice and to assess the applicability of cerebellar mutants as models for experimental therapy of cerebellar degeneration.

We have confirmed several behavioral impairments in both *Lurcher* and *pcd* mutant mice. Nevertheless, we have found that the manifestation of spatial behavior deficit is different in these two cerebellar mutants. Based on our findings, we propose that the deficit of spatial performance in cerebellar mutants may potentially arise from a combination of 1) cognitive disturbances, 2) sensory deficits, 3) motor impairments, and finally, 4) affective disorder. Moreover, resulting spatial behavior could also be modified by the specific effect of mutation, genetic background, and sex. We have also shown that abnormal behavior, e.g. maternal infanticide leads to decreased breeding capability in *Lurcher* females. Although we have shown that embryonic cerebellar grafts survive well in both *Lurcher* and SCA2 mice, the morphology of the graft did not promise any strong specific behavioral effects.

SOUHRN

Mozeček je tradičně spojován s kontrolou a exekucí motorických funkcí. Nicméně, poslední tři dekády výzkumu ukazují, že mozeček hraje svou roli i v řízení pozornosti, percepce, nálady, řeči, nemotorického učení a paměti. Hereditární mozečkové ataxie představují heterogenní skupinu neurodegenerativních onemocnění s širokou škálou neurologických a systémových symptomů. Variabilita dědičných ataxií je také reflektována v širokém spektru zvířecích modelů. Nejčastěji používanými jsou mutantní myši *Lurcher* a *Purkinje cell degeneration* (*pcd*).

Hlavním cílem této práce bylo analyzovat a porovnat prostorové a emoční chování u myší typu *Lurcher* a *pcd*. Dalšími cíli bylo zkoumat vliv abnormálního chování myší typu *Lurcher* na jejich reprodukční úspěšnost a ověřit využitelnost mozečkových mutantů jako modelů pro experimentální terapii olivocerebelární degenerace.

Výsledky této práce potvrdily řadu behaviorálních poruch u myší typu *Lurcher* a *pcd*. Nicméně ukázali jsme, že poruchy prostorového chování se u těchto mutantů liší. Na základě našich výsledků se domníváme, že deficit v prostorovém chování u mozečkových mutantů může vznikat kombinací těchto faktorů: 1) kognitivního deficitu, 2) senzorických poruch, 3) motorických obtíží a 4) afektivních změn. Výsledné projevy prostorového chování mohou být navíc dále determinovány specifickým efektem mutace, genetického pozadí a/nebo pohlavím. Ukázali jsme také, že abnormální chování, např. mateřská infanticida u samic myší typu *Lurcher* vede k jejich sníženému reprodukčnímu potenciálu. Navzdory dobré schopnosti embryonálního transplantátu přežívat v mozečku myší typu *Lurcher* i SCA2, morfologie transplantátu nenaznačovala žádný silný specifický behaviorálně-funkční efekt.

1 INTRODUCTION

Cerebellum, “little brain” in Latin, has always been seen as a distinct subdivision of the brain (Glickstein et al., 2009). It is located in the posterior cranial fossa, underneath the occipital and temporal lobes of the cerebral cortex. The cerebellum is present in all vertebrates (Larsell, 1967; Nieuwenhuys, 1967). Most of them have even one or more additional structures that are histologically similar to the cerebellum and are known as cerebellum-like structures (Bell, 2002).

1.1 Gross anatomy

The gross anatomy of the cerebellum varies from a simple dome-like structure in amphibians and reptiles, to the more complicated shapes in fish, birds and mammals (Voogd and Glickstein, 1998). The internal organization of the mammal cerebellum is similar to the cerebral hemispheres. It consists of three major parts: 1) cortex, repeatedly folded around, 2) the four-pairs of cerebellar nuclei deeply buried 3) in the middle of cerebellar white matter. In the sagittal section, the white matter branches into the highly folded gray matter of the cortex and creates a typical pattern, termed *arbor vitae* (tree of life). The cerebellum is morphologically distinguished into three lobes: rostral lobe, caudal lobe and flocculonodular lobe. The flocculonodular lobe (also known as the vestibulocerebellum or archicerebellum) is the phylogenetically oldest portion and is located on the inferior surface. The vestibulocerebellum receives vestibular, visual, and motor information, and sends its output exclusively to the brainstem vestibular nuclei (Naito et al., 1995; Barmack, 2003). The vestibulocerebellum is involved in the maintenance of body balance, coordination of eye movements and transforms the head-centered vestibular afferent information into earth-referenced self-motion and spatial orientation signals (Yakusheva et al., 2007).

The remaining two lobes, rostral and caudal lobes reflect the phylogenesis as well as functions of the cerebellum only partially. For this reason, longitudinal zones also distinguish the cerebellum into the 1) vermis, the most medial portion, 2) paravermis, intermediate parts and 3) hemispheres, the largest and most lateral

parts of the cerebellum. The vermis and paravermis constitute a structure termed spinocerebellum (or paleocerebellum). The spinocerebellum receives information from a wide range of sensory systems, including vestibular, visual, somatosensory, proprioceptive, and auditory, as well as information from the motor cortex via pontocerebellar nuclei. The spinocerebellum also processes signals related to the autonomic, visceral, cardiovascular, and immune functions. Its axons target cerebellar nuclei, e.g. interpositus nuclei and fastigial nuclei, which in turn send outputs to the vestibular and reticulospinal systems, as well as to the thalamus and superior colliculus. There are also a sparser number of collaterals projecting to the spinal cord and pons (Bagnall et al., 2012). The spinocerebellum regulates muscle tone and adapts the body to changing circumstances.

The most lateral part of the cerebellar cortex is termed cerebrocerebellum (or neocerebellum). This phylogenetically youngest structure receives diverse information from various areas of the cerebral cortex. The cerebrocerebellum projects to the cerebellar nuclei, particularly the dentate nuclei, whose predominant output is to the thalamus and reticular formation (Bagnall et al., 2012). Lateral portions of the cerebellum play an important role in motor learning and cognitive processes (see review Timmann et al., 2010). Three prominent stalks, cerebellar peduncles, connect the cerebellum to the rest of the brain. Afferent fibers come by this way to the cerebellar cortex, from where the circuit continues to the cerebellar nuclei and their axons form the efferent pathways leaving the cerebellum through the cerebellar peduncles.

1.2 Cerebellar development

The cerebellar primordium arises from dorsal rhombomere 1 of the anterior hindbrain (Millen and Gleeson, 2008). Early cerebellar development requires a contribution from the posterior mesencephalon (Martinez and Alvarado-Mallart, 1989) and the alar plate of rhombomere 2 (Marin and Puelles, 1995) as well as adjacent fourth ventricle roof plate signaling (Chizhikov et al., 2006; Wilson et al., 2007). Between mouse embryonic days 9 and 12, the rostral-caudal axis of dorsal rhombomere 1 rotates 90 degrees into the medial-lateral axis of the wing-like bilateral cerebellar primordium (Sgaier et al., 2005). As cerebellar development progresses,

the two lateral primordia fuse on the dorsal midline over the fourth ventricle to establish the medial vermis and lateral cerebellar hemispheres (Louvi et al., 2003; for review see Millen and Gleeson, 2008).

Cerebellar patterning is dependent on morphogenic factors secreted by the rhombic lip and roof plate, leading to the formation of two germinal centers that will give rise to multiple cerebellar neuronal types and subtypes (for review see Consalez et al., 2007). These neurogenic centers, the upper rhombic lip and ventricular zone, contain gene expression microdomains, and regulate the genesis of neuronal precursors fated to adopt GABAergic and glutamatergic phenotypes, respectively (for review see Consalez et al., 2007). Upper rhombic lip and ventricular zone segmentation therefore reflect the origin of the two main neuronal types of the adult cerebellum, Purkinje cells and granule cells, respectively. The mutual exclusivity of Purkinje cell and granule cell precursors is defined by the expression of *Ptf1a* (Hoshino et al., 2005) and *Atoh1* (*Math1*) genes (Ben-Arie et al., 1997; Machold and Fishell, 2005), respectively (for review see Butts et al., 2007).

Purkinje cells are born at the onset of cerebellar neurogenesis (for mouse between embryonic days 10.5 (E10.5) and E12.5; Miale and Sidman, 1961; for review see Sotelo and Rossi, 2007). The adult Purkinje cell phenotype is acquired through a complex sequence of processes, including migration from the ventricular zone to the cortex, formation of the Purkinje cell plate and arrangement into the final monolayer, axonal growth, and expansion of the dendritic tree (for review see Sotelo and Rossi, 2007). The mouse granule cell precursors begin to proliferate in the upper rhombic lip in E10 and thereafter start to migrate tangentially in latero-medial and postero-anterior directions to cover the superficial zone of the cerebellum, called the external granular layer (Miale and Sidman, 1961; for review see Komuro et al., 2007). After clonal expansion in the external granular layer, the granule cell precursors begin to produce postmitotic granule cells which start to migrate toward their final destination within the internal granular layer located underneath of Purkinje cell layer (Komuro and Yacubova, 2003). During the migration, granule cells transform their shape from a vertically elongated spindle to spherical (Komuro and Rakic, 1998; for review see Komuro et al., 2007). The transit amplification of granule cell precursors within the external granular layer is driven by sonic hedgehog

(Shh) morphogenic factor secreted by Purkinje cells (Dahmane and Ruiz i Altaba, 1999; Lewis et al., 2004) that determines the size of the external granular layer and hence, the degree of cerebellar foliation (Corrales et al., 2004; Corrales et al., 2006).

1.3 Cerebellar circuits

The cerebellar cortex is functionally built from Purkinje cells that are large projection neurons, and several types of interneurons: granule cells, Golgi cells, stellate cells, basket cells, unipolar brush cells, Lugaro cells and candelabrum cells (Jaarsma et al., 1998; Laine and Axelrad, 1998; Voogd and Glickstein, 1998; Schilling et al., 2008). The three-layer cortex receives information from three extracerebellar afferent inputs: the mossy fibers, the climbing fibers, and diffusely organized monoaminergic and cholinergic afferents (Voogd and Glickstein, 1998).

Granule cells are small glutamatergic neurons, and are the most common cells in the cerebellum as well as in the entire brain (2.7×10^7 in mouse; 1.1×10^{11} in human) (Voogd and Glickstein, 1998; Huang and Ricklefs, 2007). Granule cells create the deepest layer of the cerebellar cortex. Excitatory mossy fibers ascend to the granular layer and their terminals (rosettes) contact dendrites of ~20-30 granule cells in complex synapses (glomeruli) (Voogd and Glickstein, 1998; Bagnall et al., 2012). Granule cells mostly have 3-5 short dendrites each terminating in a glomerulus; thus each granule cell receives inputs from 3 to 5 mossy fibers (Bagnall et al., 2012). Unmyelinated axons of granule cells ascend toward the superficial, cell-poor molecular layer of the cerebellar cortex, where they bifurcate into long T-shaped branches, termed parallel fibers. Each parallel fiber reaches up to 0.2 cm and 1 cm in the mouse and human, respectively, through the cortex and makes up to 400 and 2,000 synapses with Purkinje cells in the mouse and human, respectively (Voogd and Glickstein, 1998; Huang and Ricklefs, 2007; Bagnall et al., 2012).

Purkinje cells are large γ-aminobutyric acid (GABA)-ergic neurons, which serve as the sole output of the cerebellar cortex (Voogd and Glickstein, 1998). Their somas are located in a single row, between the deep granular layer and superficial molecular layer. The flattened dendritic trees of Purkinje cells are oriented to the perpendicularly running parallel fibers. The long parallel fibers may arise from the granule cells of different cerebellar zones (see above), thus each Purkinje cell might

receive information about sensory conditions (Voogd and Glickstein, 1998), and hypothetically also about internal states, and the plans of the individual (Bagnall et al., 2012). It is hypothesized that Purkinje cells respond to the stimulation from parallel fibers with the modulated discharge of short simple spikes (20-60 impulses/s) (Barmack and Yakhnitsa, 2008). The second major input to the cerebellum are climbing fibers, which originate from contralateral inferior olivary neurons. After birth, each Purkinje cell is innervated by multiple climbing fibers with similar synaptic strength, but during development, a one-to-one connection between a climbing fiber and Purkinje cell is established in an activity-dependent manner (see review Hashimoto and Kano, 2013). A single climbing fiber comprises a number of synaptic contacts onto the soma and dendrites of Purkinje cell. The simultaneous release of glutamate from each of these synapses results in a postsynaptic current that evokes a low-frequency multi-peak action potential termed “complex spike”. Each complex spike consists of a burst of five to six action potentials (Llinas and Sugimori, 1980; Barski et al., 2003; Bagnall et al., 2012).

The myelinated axons of Purkinje cells project ipsilaterally in cerebellar nuclei and certain brainstem nuclei. In cerebellar nuclei, axonal terminations of Purkinje cells diverge into three types of neurons: 1) GABAergic neurons, which project to the inferior olive subregions and closing an inhibitory feedback loop, 2) large excitatory neurons and 3) short-axon inhibitory neurons with an unknown function (Bagnall et al., 2012).

There are several types of cerebellar interneurons, which modulate the functional circuit of the cerebellum. The Golgi cell terminals contribute to the cerebellar glomeruli and provide a feed-backward inhibition to the granule cells (Voogd and Glickstein, 1998; Barmack and Yakhnitsa, 2008). They also inhibit unipolar brush cells (Dugue et al., 2005). Stellate and basket cells are localized in the molecular layer and provide a feed-forward inhibition to the Purkinje cells (Voogd and Glickstein, 1998; Barmack and Yakhnitsa, 2008). Unipolar brush cells amplify vestibular primary afferent mossy fiber projections through synaptic feed-forward excitation onto the granule cells (Barmack and Yakhnitsa, 2008). Lugaro cells are found between the Purkinje cell layer and upper part of the granule cell layer (Schilling et al., 2008). Simat et al. (2007) showed that Lugaro cells account for about

one third of all inhibitory neurons in the granular layer. It is thought that Lugaro interneurons are the primary targets of the serotonergic inputs into the cerebellar cortex (Dieudonne and Dumoulin, 2000). Candelabrum cells are the most recently delineated distinct neuronal phenotype of the cerebellar cortex (Laine and Axelrad, 1994; Schilling et al., 2008). Candelabrum cell somas are located within the Purkinje cell layer. Typically, these cells have one or two long dendrites which ascend almost vertically to the molecular layer, and several short dendrites, which project onto the granular layer (Schilling et al., 2008). The afferent inputs of the candelabrum cells or their targets have not been elucidated. Nevertheless, recent studies from a monkey (*Macaca*) cerebellum showed that candelabrum cells are immunoreactive for glycine, GABA, and GAD (the GABA-synthesizing enzyme glutamate decarboxylase), and thus indicated that candelabrum cells use GABA and glycine as transmitters (Crook et al., 2006).

Although, the structure of the cerebellar circuit is highly stereotyped, the topography of the cerebellar circuit is described at least by three distinct maps, defined by different patterns of climbing fiber input, mossy fiber input, and Purkinje cell phenotype (Cerminara et al., 2013). According to this notion, the cytoarchitecture of the cerebellar cortex is divisible into a number of 1 to 2 mm wide sagittal zones, each receiving climbing fibers from a circumscribed part of the inferior olive and projecting to a specific deep cerebellar nuclei (see reviews Voogd and Bigare, 1980; Garwicz et al., 1998). High-resolution electrophysiological mapping experiments have shown that these zones can be further divided into narrower (0.1 – 0.3 mm) longitudinal strips, termed “microzones” (Ekerot et al., 1991; for reviews see Garwicz et al., 1998; Cerminara et al., 2013). It is thought that climbing fiber microzones and their associated input and output connections represent basic operational units of the cerebellum (see review Ruigrok, 2011). In addition, the micromapping of mossy fiber projections suggests that they form a “patched” mosaic of receptive fields within the cerebellar cortex (Cerminara et al., 2013). Besides the climbing fiber microzones and mossy fiber patches, Purkinje cells are also organized into rostro-caudally extended bands defined by the expression of aldolase C (zebrin II) enzyme (Brochu et al., 1990). This Purkinje cell compartmentalization corresponds with the organization of cerebellar nuclei and it is speculated that aldolase C-positive and -negative

compartments are generally associated with somatosensory and other functions, respectively (Sugihara, 2011).

1.4 Cerebellar functions

1.4.1 Motor control and learning

From an historical point of view, the cerebellum has been primarily considered a motor structure. Patients with cerebellar lesions often display symptoms related to inappropriate force production (Holmes, 1917), difficult compensation of torque interaction during multi-joint movements (Bastian et al., 1996; Bastian et al., 2000), and/or individual muscle activity (Thach, 1968; Smith, 1981; Frysinger et al., 1984; for review see Ebner et al., 2011). The cerebellum is also important for motor learning. Cerebellar motor learning is required to obtain procedural skills (Schonewille et al., 2010).

The conceptual framework for the generation of fast, coordinated movements is based on the central nervous system (CNS) implementing internal models that can mimic the input/output information, or their inverses, of the motor apparatus (for reviews see Kawato, 1999; Ebner, 2007). There are two main classes of internal models. Forward internal models can use efferent copies of motor commands and predict the sensory consequences of actions (for reviews see Wolpert et al., 1998; Ebner, 2007). Inverse internal models calculate necessary feedforward motor commands from desired trajectory information (for review see Kawato, 1999). The internal model hypotheses propose that the brain needs to predict feedback control, since biological feedback loops are slow and have small gains (for reviews see Kawato, 1999; Ebner, 2007).

Ito (1970) proposed that the cerebro-cerebellar communication loop constitutes a unique internal feedback that simulates the kinematics of the controlled object and in this way, the primary motor cortex should be able to perform a precise movement using this internal forward model instead of external feedback from the real controlled object. Miall et al. (2007) also suggested another closely related idea, that the cerebellum calculates a “state estimate” by combining sensory information about the last known position of the arm with predictions of its responses to recent

movement commands, and thereby accurately plans and controls movements. Motor learning by repeated practice can be considered to be a process whereby the internal forward model is formed and remodeled in the cerebellum through modification of the input-output relationship of the involved microcomplex (Ito, 2012). During motor learning, the first execution of movement is very slow because it cannot be adequately preprogramed and instead it is performed largely by cerebral intervention using long-loop sensory feedback. Nevertheless, with practice a greater amount of movement can be preprogramed and thus, executed more rapidly (Kawato et al., 1987).

Based on the theoretical frameworks of Marr (1969) and Albus (1971), Ito et al. (1982) suggested long-term depression at parallel-fiber Purkinje cell synapses (PF-PC LTD) as an essential cellular mechanism of motor learning (for review see Hirano, 2014). Over the past decades, the PF-PC LTD as a primary cellular mechanism of cerebellar-dependent motor learning has been studied in different cerebellar conditioning tasks, e.g. adaptation of the vestibulo-ocular reflex (VOR) (Ito, 1982; De Zeeuw et al., 1998) or eyeblink conditioning (Delgado-Garcia and Gruart, 2002; De Zeeuw and Yeo, 2005; Thompson, 2005). Although many studies have supported the involvement of PF-PC LTD in motor learning (for details see Ito, 2012), there are also reports suggesting that motor learning can occur without PF-PC LTD (van Alphen and De Zeeuw, 2002; Welsh et al., 2005; Schonewille et al., 2011; for review see Hirano, 2014). Therefore, the contribution of other mechanisms, e.g. changes in basal electrophysiological function and/or use-dependent neuronal plasticity, to cerebellar motor learning cannot be excluded (Schonewille et al., 2011).

1.4.2 Perceptual functions

Observations from anatomical and electrophysiological studies as well as clinical reports showed that the cerebellum is also involved in perceptual processes (for review see Baumann et al., 2015). While damage to the cerebellum does not lead to complete loss of sensory function, it is apparent that it affects some sensory and perceptual processes, such as motion and time perception, or the ability to recognize perceptual sequences (for review see Baumann et al., 2015).

Yakusheva et al. (2007) found that Purkinje cell activity in vermal lobules 9 (uvula) and 10 (nodulus) reflects the critical computation of transforming head-centered vestibular signals into earth-referenced self-motion and spatial orientation information. Since our motion sensors are fixed to the head, they measure linear acceleration and angular rotation within the head- and not earth-centered reference frame (Angelaki et al., 1999; Green and Angelaki, 2004; Yakusheva et al., 2007). Cerebellar Purkinje cells seem to be crucial for this computational step that encodes inertial motion perception (Yakusheva et al., 2007). Moreover, there are several considerable lines of evidence that the cerebellum contributes to visual and auditory processing (Snider and Stowell, 1944; Thier et al., 1999; Parsons et al., 2009; Yakusheva et al., 2013; for review see Baumann et al., 2015), as well as timing perception (Perrett et al., 1993; Koekkoek et al., 2003; Bares et al., 2007; Rahmati et al., 2014; for review see Baumann et al., 2015).

Currently, there are three hypotheses that explain the role of the cerebellum in information processing. A prominent hypothesis is a form of internal model of sensory events that predict input/output information (see above; for reviews see Kawato, 1999; Ebner, 2007; Baumann et al., 2015). An alternative hypothesis proposes that the cerebellum facilitates perception by monitoring and coordinating the acquisition of sensory inputs (Bower, 1997; for review see Baumann et al., 2015). The last hypothesis suggests that the cerebellum plays a role of internal timing device that provides separate timing computations for different tasks (Keele and Ivry, 1990; for review see Baumann et al., 2015).

It was also found that the cerebellum is one of the most consistently responsive brain structures to nociceptive stimuli (Saab and Willis, 2003; Moulton et al., 2010). Moulton et al. (2010) speculated that the cerebellum is an integrator of multiple effector systems, including affective processing, pain modulation, and sensorimotor processing, and plays a cross-modal modulatory role in adaptation to pain and/or injury.

1.4.3 Cognitive and affective functions

The results from neuroanatomical, neuroimaging and experimental as well as clinical studies from the past decades have substantially extended the functional role

of the cerebellum to cognitive and affective regulation (for reviews see Baillieux et al., 2008; Leiner, 2010). The mapping of the human cerebellum with regard to cognitive and emotional processing began in the 1980s (Leiner et al., 1986; Petersen et al., 1989), however some earlier studies already reported some behavioral anomalies occurring in association with cerebellar lesions or disorders (for reviews see Baillieux et al., 2008; Buckner, 2013). Despite sporadic findings supporting a more general role of the cerebellum in non-motor functions, the first comprehensive study in patients with disease confined to the cerebellum was conducted by Schmahmann and Sherman (Schmahmann and Sherman, 1997). The Schmahmann's syndrome (or cerebellar cognitive affective syndrome) in terms of cognitive and affective operations is characterized by 1) executive dysfunction such as disturbances in planning, set-shifting, abstract reasoning and working memory, 2) visuo-spatial deficits, such as impaired visuo-spatial organization and memory, 3) mild language symptoms including agrammatism and anomia and finally 4) behavioral-affective disturbances, consisting of blunting of affect or disinhibited and inappropriate behavior (Schmahmann and Sherman, 1997; for reviews see Schmahmann, 2004; Baillieux et al., 2008; Bodranghien et al., 2015). Another well-known clinical entity with a cognitive and behavioral profile closely resembling Schmahmann's syndrome is the posterior fossa syndrome (PFS, for reviews see De Smet et al., 2007; Baillieux et al., 2008). Although PFS is an etiologically heterogeneous clinical condition that may develop following acute cerebellar damage, it mostly occurs after posterior fossa tumor surgery in children or adolescents (for review see De Smet et al., 2007). However, adult patients have also been reported (De Smet and Marien, 2012; Marien et al., 2013). PFS consists of a broad spectrum of linguistic, especially transient mutism, and cognitive as well as behavioral-affective disturbances (for reviews see Pollack, 1997; Baillieux et al., 2008).

The clinical as well as anatomical and functional imaging studies have shown that separated and topographically-organized cerebellar subsystems are involved in cognitive functions, sensorimotor and emotional processing (Kalashnikova et al., 2005; Lie et al., 2006; Stoodley and Schmahmann, 2010). Functional and anatomical tracing studies have indicated that the cerebellum is linked with autonomic (Andrezik et al., 1984; Haines and Dietrichs, 1984), limbic (Anand et al., 1959; Harper and

Heath, 1973; Heath, 1973; Annoni et al., 2003), associative as well as sensorimotor regions of the cerebral cortex (Schmahmann and Pandya, 1997b, a; for review see Glickstein and Doron, 2008). The bidirectional connections of the cerebellum with cortex regions involved in perception of socially salient emotion material, including the posterior parietal cortex and prefrontal cortex were also revealed (Schmahmann, 1991; Middleton and Strick, 2001; Dum and Strick, 2003; Kelly and Strick, 2003; for review see Turner et al., 2007). In addition, reciprocal connections link the cerebellum with brainstem areas containing neurotransmitters involved in mood regulation, including serotonin, norepinephrine, and dopamine (Dempesy et al., 1983; Marcinkiewicz et al., 1989; for review see Turner et al., 2007).

Strong fronto-cerebellar connectivity, consisting of closed cortico-cerebellar loops in which the dorsolateral part of the prefrontal cortex connects to the cerebellum via pontine nuclei while the cerebellum projects back to the prefrontal cortex via the dentate nucleus and thalamus (Schmahmann and Pandya, 1997b), elucidates cerebellar involvement in executive functions, including multitasking, problem-solving and inhibition, necessary to plan and direct goal-oriented behavior (for review see Baillieux et al., 2008). Although, the cerebellar contribution to motor learning is well known (see above), the last studies also extended the role of the cerebellum in non-motor learning tasks (Drepper et al., 1999; Neau et al., 2000) and memory (Appollonio et al., 1993; Paulesu et al., 1993; Gottwald et al., 2004; Ziemus et al., 2007). Moreover, experimental studies with various mouse models of cerebellar disorders showed the disruption of spatial behavior (for reviews see Cendelin and Vozeh, 2007; Lalonde and Strazielle, 2007; Cendelin, 2014). The subsequent studies demonstrated that cerebellar Purkinje cells play a critical role in the integration of internal (idiothetic) signals generated by vestibular cues, optic flow and proprioception (Angelaki and Hess, 2005; Yakusheva et al., 2007; Brooks and Cullen, 2009; Yakusheva et al., 2013). Rochefort et al. (2011; 2013) also found that the disruption of cerebellar self-motion signal processing affects the hippocampal place cells' spatial code and showed that the cerebellum participates in the construction of a hippocampal spatial representation map (Passot et al., 2012; Onuki et al., 2015).

In the 1920s, Sir Gordon M. Holmes reported that the patients with cerebellar lesions manifested abnormal speech (Holmes, 1922) and currently, the cerebellar contribution to motor speech regulation is widely accepted (for review see Baillieux et al., 2008). Nevertheless, the data from the last decades has indicated that the cerebellum is also involved in non-motor linguistic processes, such as language perception, speech motor planning, word production, verbal working memory, phonological and semantic verbal fluency, reading and writing (for review see Marien et al., 2014).

1.5 Cerebellar disorders

With regard to multiple functions of cerebellum, its dysfunction can manifest itself in terms of a variety of clinical signs. Usually the main motor signs are cerebellar ataxia, i.e. lack of motor coordination, kinetic tremor, passivity, dysmetria and oculomotor deficit (e.g. nystagmus, macrosaccadic oscillation). Furthermore, cerebellar affection is also manifested with cognitive inefficiency, and psychiatric disturbances (Schmahmann and Sherman, 1997; Schmahmann, 2004; Manto, 2005; Massaquoi, 2012). In most of the progressive cerebellar disorders, pathogenesis of dysfunction is due to degeneration of cerebellar cortex and its afferent or efferent fiber connections (Klockgether, 2007).

The classification of ataxias (wide spectrum of progressive cerebellar disorders with ataxia as the leading symptom) distinguishes between hereditary and non-hereditary ataxias. Hereditary ataxias are related to a genetic deficit and can be divided into four groups: autosomal dominant ataxias, autosomal recessive ataxias, mitochondrial ataxias, and X-linked ataxias (Brusse et al., 2007). The non-hereditary ataxias are separated into sporadic degenerative ataxias, such as multiple system atrophy (MSA), and acquired ataxias, such as alcoholic cerebellar degeneration (Klockgether, 2007). This classification is strictly based on etiology but does not take into consideration pathogenic aspects. According to pathogenic factors the ataxias can be classified into five categories: mitochondrial, metabolic, defective DNA repair, abnormal protein folding and degradation and channelopathies (Filla and De Michele, 2012). None of these classifications is optimal. Furthermore, some authors combine both classifications and thus could be related to more than one category and the

terminology becomes confusing, e.g. Friedreich's ataxia is autosomally recessively inherited with affection of mitochondrial functions (see below) and therefore sometimes categorized as mitochondrial ataxia together with mitochondrially inherited ataxias. For the next section of this paper, the classification with priority to the genetic point of view will be used.

1.5.1 Cerebellar ataxias

Autosomal dominant ataxias

Autosomal dominant ataxias comprise spinocerebellar ataxias (including dentatorubral-pallidoluysian atrophy, abbreviated DRPLA) and the episodic ataxias (for reviews see Di Donato, 1998; Manto, 2005; Jen, 2008; Matilla-Duenas, 2008). Spinocerebellar ataxias (SCAs, previously named autosomal dominant cerebellar ataxias, ADCAs) represent a genetically and clinically heterogeneous group of cerebellar disorders where the age of onset of clinical symptoms is usually between 30 and 50 years of age. However, early onset in childhood and onset in later decades after 60 years have been reported for specific SCA subtypes (Matilla-Duenas et al., 2006; Matilla-Duenas, 2008). SCAs were initially classified according to clinical and neuropathological descriptions (Harding, 1993), but current numbering corresponds to the order of gene description (Di Donato, 1998; Manto, 2005). This molecular classification is currently the most accepted by the scientific and medical community. The pathogenesis of SCAs is still poorly understood, the genetic analyses, epidemiologic data, neuropathological investigations as well as experiments with animal models have provided important new insights into the pathogenic mechanisms. At least 30 dominantly inherited SCA subtypes have been described up to now, and the genes and molecular defects are identified and characterized in 17 of them (Matilla-Duenas et al., 2006).

In seven SCA subtypes, the causative molecular defects result from translation of CAG trinucleotide (DNA sequence coding for glutamine) expansions encoding a polyglutamine (polyQ) repeat in encoded proteins. This group comprises SCAs 1, 2, 3 (or Machado-Joseph disease), 6, 7, 17 (or Huntington's disease-like 4), and DRPLA (Kanazawa, 1999; Matilla-Duenas, 2008). These diseases belong to a larger group of progressive neurodegenerative disorders, such as Huntington's disease, with a

synthesis of polyQ-containing protein aggregates forming characteristic nuclear or cytoplasmic inclusions (Zoghbi and Orr, 2000). In the second group of SCAs, including SCAs 8, 10, 12, and the chromosome 16q22.1-linked ADCA (16q-ADCA), the mutations are located outside of the coding region of the disease-related genes apparently leading to alternations in gene expression (SCA12 and 16q-ADCA) or to trans-dominant RNA gain-of-function effects (SCAs 8 and 10) (Matilla-Duenas, 2008). In SCA8, recent evidence suggests that an expanded polyQ within *SCA8* gene (resulting from the translation of the opposite strand) might also contribute to disease pathogenesis and therefore the hypothesis that SCA8 may be caused by both RNA and protein dominant gain-of-function mechanisms (both CUG and CAG expansion induce toxicity) has been proposed (Moseley et al., 2006). A third group of SCA subtypes including SCAs 5, 11, 13, 14, 27 and 28 are caused by mutations resulting in alterations of amino acid composition leading to dysregulation of protein function (Matilla-Duenas, 2008). In the remaining 13 types of SCAs (SCAs 4, 9, 15, 16, 18, 19, 20, 21, 22, 23, 24, 25 and 26), the genes and thus mutations still remain to be identified and characterized.

Hereditary episodic ataxias (EAs) represent a phenotypically and genetically heterogeneous group of rare monogenic disorders that manifest as attacks of imbalance and incoordination, often with associated progressive ataxia (Jen et al., 2007; Jen, 2008). The genes affected by mutation comprise neuronal voltage-gated potassium and calcium channels, which are widely distributed in the nervous system, but are particularly abundant in the cerebellum (Jen et al., 2007). Although, the molecular identification of these genes have broadened the clinical spectrum of EAs (up to now 7 EAs have been described), mechanisms for how mutations in the ion channel genes cause a wide spectrum of paroxysmal neurological symptoms (e.g. epilepsy, migraine, dystonia, myasthenia and even intermittent coma) and lead to progressive neurodegeneration is still poorly understood (Jen et al., 2007; Jen, 2008).

Autosomal recessive ataxias

Autosomal recessive cerebellar ataxias constitute a heterogeneous group of rare neurodegenerative disorders associated with various neurologic, ophthalmologic and systemic symptoms (see reviews Di Donato et al., 2001; Palau and Espinos, 2006). Most of the recessive ataxias have childhood onset, but a minority of them can also

have adult onset, often associated with milder phenotypes (Di Donato et al., 2001; Palau and Espinos, 2006). Some types of recessive ataxia show a regional distribution, e.g. ataxia oculomotor apraxia type I (AOA1) is the most frequent in Portugal and Japan (Brusse et al., 2007). The most frequent recessive ataxias are Friedreich's ataxia and ataxia telangiectasia (Brusse et al., 2007).

Besides Friedreich's ataxia and ataxia telangiectasia, there is a wide spectrum of other autosomal recessive ataxias, e.g. AOA1, AOA2, ataxia with vitamin E deficiency, Niemann-Pick C disease and Wilson's disease. Moreover, the increasing quality of diagnostic and molecular methods have still broadened the group of autosomal recessive ataxias. For example, Hills et al. (2013) reported a recessively inherited syndrome caused by mutation in the gene encoding δ2 glutamate receptor (*GRID2*) leading to cerebellar ataxia and eye movement abnormalities. Surprisingly, a similar loss-of-function mutation in *GRID2* ortholog gene has been previously described and studied as a spontaneous mutation in an animal model, *hotfoot* (*Grid2*^{ho}) mice (Lalouette et al., 1998). For a detailed description of the function of the receptor see below in chapter 1.5.1 *Lurcher* mice.

Mitochondrial ataxias

Mitochondrial ataxias constitute a group of disorders caused by mutations in mitochondrial genes with matrilineal inheritance or sporadic occurrence. Some authors also include this group of ataxias with defects in nuclear DNA encoded mitochondrial proteins (Brusse et al., 2007), but this classification could lead to inexact categorization (see above). Most of the mitochondrial genes are involved in energy production. Mutations in mitochondrial DNA cause different diseases with ataxia as a main symptom, especially in Kearns–Sayre syndrome, May–White syndrome, mitochondrial neurogastrointestinal encephalomyopathy, Leigh syndrome and retinitis pigmentosa, mitochondrial encephalomyopathy, lactic acidosis with stroke-like episodes, and myoclonus epilepsy with ragged red fibers (Manto and Marmolino, 2009; Filla and De Michele, 2012).

X-linked ataxias

X-linked ataxias are related to the X chromosome inheritance. The most common is fragile X-associated tremor/ataxia syndrome (FXTAS), caused by

premutation size expansion of CGG trinucleotide (55 to 200 CGG repeats) in *fragile X mental retardation 1* gene (*FMR1*). The FXTAS is a neurodegenerative disorder with neuropathological hallmarks, such as brain atrophy, white matter lesions in the cerebellar peduncle and/or brain stem and intranuclear inclusion bodies (Hall et al., 2014). The clinical symptoms of FXTAS are characterized by intention tremor, cerebellar gait ataxia and parkinsonism (Hall et al., 2014). More than 50% of FXTAS patients show cognitive and behavioral changes, including executive function impairments, mood dysregulation, and risk of mood and anxiety disorders (Bourgeois et al., 2007; Bourgeois et al., 2011; Juncos et al., 2011).

Non-hereditary ataxias

There is also a wide spectrum of sporadic degenerative ataxias and acquired ataxias. In many cases of sporadic adult-onset ataxias, a genetic or a specific acquired cause cannot be found (Klockgether, 2010). The multiple system atrophy (MSA) is the most common cause (30%) of isolated late-onset cerebellar ataxia (Brusse et al., 2007). MSA is a sporadic, adult disease with progressive neurodegeneration in the cerebellum, basal ganglia, brain stem and intermediolateral cell columns of the spinal cord encompassing the former disease categories striatonigral degeneration, sporadic olivopontocerebellar atrophy (OPCA) and Shy-Drager syndrome (Abele et al., 2002). MSA can be clinically classified by motor presentations into two major categories. Parkinsonian features predominate in 80% of patients (MSA-P subtype), and cerebellar ataxia is the main motor feature in 20% of patients (MSA-C subtype) (Wenning et al., 1994; Wenning et al., 2004). MSA-C is characterized by gait ataxia, limb kinetic ataxia, scanning dysarthria, and cerebellar oculomotor disturbances (Wenning et al., 2004).

Sporadic degenerative ataxias that are distinct from MSA-C have recently been designated as sporadic adult-onset ataxia of unknown etiology (SAOA) or idiopathic late-onset cerebellar ataxia (Abele et al., 2002). SAOA is defined by: progressive ataxia, disease onset after the age of 20 years, no acute or subacute disease onset, no evidence of a causative gene mutation, no established symptomatic cause and no possible or probable MSA according to established clinical criteria (Klockgether, 2012). These criteria enable distinguishing SAOA from the hereditary ataxias, the acquired ataxias and MSA. SAOA also cannot be considered as a distinct disease

entity, but rather as a heterogeneous group of disorders with unknown etiology defined by a characteristic clinical syndrome and exclusion of known diseases.

Acquired ataxias represent a heterogeneous group of diseases with known causes including autoimmune, toxic, infectious factors and vitamin deficiency and manifesting with ataxia as a predominant clinical symptom.

1.5.2 Therapeutic strategies

Although there is increasing insight into the genetic and pathophysiological mechanisms underlying hereditary ataxias, therapeutic options modifying neurodegenerative process are still very limited (Brusse et al., 2007). Vitamin deficiency, intoxication, autoimmune processes, some endocrine disorders or some of the autosomal recessive ataxias (e.g. ataxia with vitamin E deficiency) are often treatable causes of ataxia. Treatment of underlying malignancy may also improve or cure paraneoplastic syndromes. While for most of the patients with cerebellar ataxia, symptomatic therapy (e.g. dopaminergic, anticholinergic or beta-blockers therapy) may relieve symptoms (Brusse et al., 2007), an effective causal therapy for most of the hereditary ataxias is still lacking.

One of the potential approaches to therapy of cerebellar degenerative disorders is neurotransplantation. Although this therapy still represents more likely experimental possibilities, there are first attempts to introduce this approach into human medicine (e.g. Wu et al., 1991; Lee et al., 2008; Tian et al., 2009).

1.6 Mouse models of cerebellar degeneration

The broad spectrum of human cerebellar degenerative disorders is also reflected in animal models of cerebellar ataxias (see reviews Lalonde and Strazielle, 2007; Manto and Marmolino, 2009; Cendelin, 2014). Mouse models are widely used to study symptoms, pathogenesis, and cell death mechanisms, as well as to develop and test therapeutic approaches for these diseases (Cendelin, 2014). Depending on the origin of pathological mutation, there are either spontaneous or transgenic/induced mouse mutants. Spontaneous mutations constitute models of cerebellar disorders, but mostly they do not represent identical mutations to those known in human medicine.

Contrary to the naturally occurring ataxic mice, there are a substantial number of transgenic mice with induced mutations (Manto and Marmolino, 2009).

For the purpose of this thesis, three mouse models of hereditary cerebellar ataxia will be reviewed. *Lurcher* mice represent a spontaneous semi-dominant mutation, *Purkinje cell degeneration* (*pcd*) mice represent a spontaneous recessive mutation and the mouse model of SCA2 represents transgenic dominant mutation.

1.6.1 *Lurcher* mice

Description of the mutant

Lurcher (*Lc*) mice were discovered and described as a spontaneous mutation in a Mi^{wh} homozygous male in Medical Research Council's Radiological Research Unit at Harwell, England in 1954 (Phillips, 1960). *Lurcher* mutation (gene symbol: $Grid2^{Lc}$) is a base-pair substitution (G-to-A) that changes a nonpolar alanine into a polar threonine in the transmembrane domain III of the mouse ionotropic δ2 glutamate receptor (GluRδ2; gene symbol *Grid2*) (Zuo et al., 1997). Locus of the $Grid2^{Lc}$ mutation was found on chromosome 6 (Zuo et al., 1995; De Jager et al., 1997). The allele was described as autosomal semi-dominant (Phillips, 1960). Homozygous mutants are not viable and die shortly after birth due to the massive loss of mid- and hindbrain neurons (Cheng and Heintz, 1997; Resibois et al., 1997). Later a second *Lc* allele (Lc^{J}; gene symbol: $Grid2^{Lc\text{-}J}$), which is phenotypically indistinguishable from the original $Grid2^{Lc}$, was found as a spontaneous mutation in the inbred strain BALB/cByJ at The Jackson Laboratory in 1993 (De Jager et al., 1997). There are several strains of *Lurcher* mice, e.g. B6 x B6CBCa Aw-J/A-Grid2^{Lc} T(2;6)7Ca MitfMi-wh/J, B6CBACa Aw-J/A-Grid2^{Lc}/J, B6 x BALB/cByJ-Grid2^{Lc}-J/J, and C3H (Cendelin and Vozeh, 2007). *Lurcher* mice are fertile and mating capable cerebellar mutants, but their breeding capacity is limited due to litter size reduction (Phillips, 1960).

Morphological and cellular changes

The cerebellar cytoarchitecture in *Lurcher* mutants is severely disrupted by progressive postnatal loss of virtually all Purkinje cells and the vast majority of granule cells and inferior olivary neurons (Caddy and Biscoe, 1975; Caddy and

Biscow, 1976; Wilson, 1976). Neurodegeneration in *Lurcher* mice is initially seen in all four transverse zones: the anterior (lobules I–V), central (lobules VI, VII), posterior (lobules VIII, dorsal IX), and nodular (ventral lobule IX and lobule X) zone (Duffin et al., 2010). Due to this massive degeneration, the cerebellum of adult *Lurcher* heterozygotes is considerably macroscopically reduced (Wilson, 1976; Cendelin and Vozeh, 2007; Vogel et al., 2007). For a comparison of *Lurcher* mutant and wild type cerebellum see Figure 1A,B.

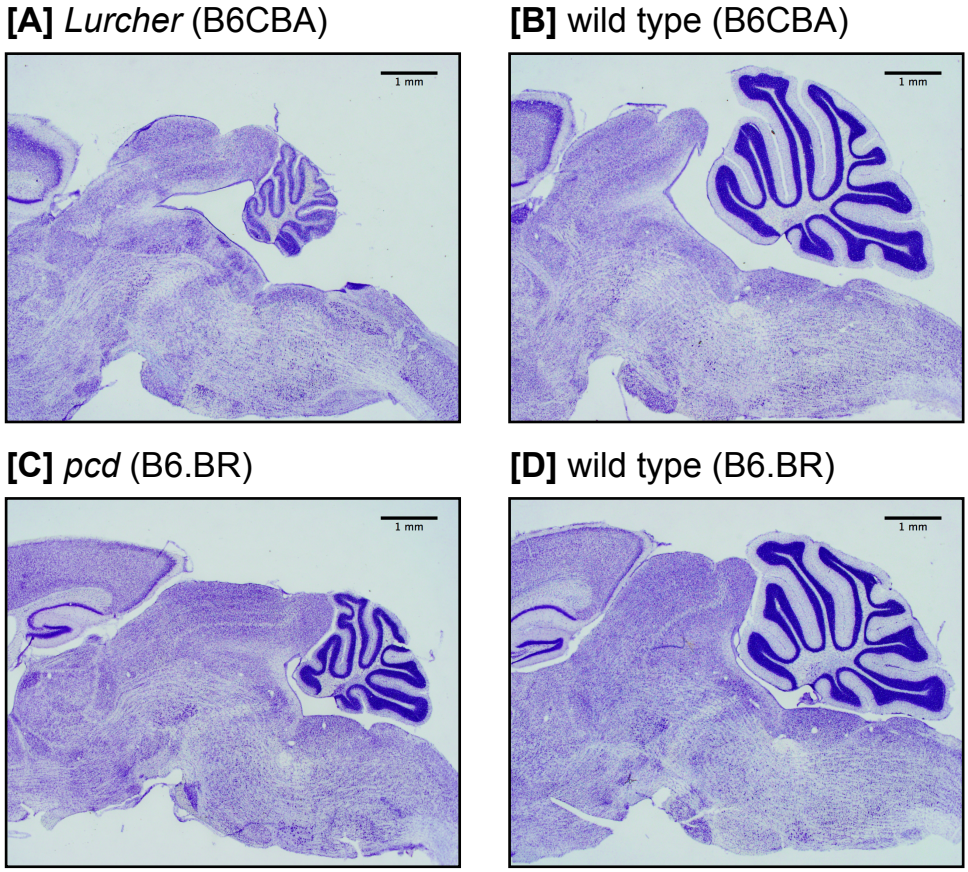

Figure 1: Sagittal sections of the cerebellum of [A] *Lurcher* (B6CBA), [B] wild type (B6CBA), [C] *pcd* (B6.BR) and [D] wild type (B6.BR) males.

Lurcher mutants show severe defects in Purkinje cells and granule cells soon after birth. Purkinje cell abnormalities appear at postnatal day 3 or 4 (P3-P4) in the form of crowding failure of nuclear growth, and condensed or lessened cytoplasm; Purkinje cell death is apparent at P4-P6 depending on the cerebellar lobule (Swisher

and Wilson, 1977). Caddy and Biscoe (1979) described that intensive reduction of Purkinje cells proceeds between P8 and P25 and practically all of the Purkinje cells degenerate by 3 months after birth. Surviving Purkinje cells are restricted to the paraflocculus/flocculus and the nodular zone and could be detected as late as at P146 (~5 months) (Duffin et al., 2010).

Perishing Purkinje cells show various structural and ultrastructural changes characteristic of various cell death mechanisms (see above): necrosis (dilatation of cytoplasmic organelles, fragmentation of the nuclear membrane without chromatin condensation and characteristic destruction of the cytoplasm by non-lysosomal degradation), apoptosis (nuclear pyknosis, DNA fragmentation, cytoplasmic membrane blebbing, late rupture of the nuclear membrane, cell shrinkage, and removal by phagocytes) and autophagy (sequestration of cytoplasmic organelles by autophagosomes and their further degradation by delivery to the lysosomes) (Dumesnil-Bousez and Sotelo, 1992; Norman et al., 1995; Dusart et al., 2006; Wang et al., 2006; Purkartova and Vozeh, 2013). Despite the abnormalities in early developing Purkinje cells, the onset of the synaptogenesis between Purkinje cells and their specific inputs (parallel fibers, climbing fibers and basket cell axons) takes place on schedule, and at P8 no defect has been detected. Nevertheless, on and after P10, the rate of parallel fiber synaptogenesis declines, only a few climbing fibers translocate from their initial soma contacts to their peridendritic locations, and basket cell axons fail to completely surround the Purkinje cell somas (Heckroth et al., 1990; Dumesnil-Bousez and Sotelo, 1992). Based on these findings, Dumesnil-Bousez and Sotelo (1992) suggested that the *Grid2*^{Lc} mutation delays the neuron maturation.

Extensive degeneration of Purkinje cells, the key neurons in the olivocerebellar circuitry, also induces retrograde degeneration of their primary afferents, granule cells and inferior olivary neurons. Granule cell death is common before and during granule cell migration, from P2 to P18. A decrease of these cells in the generative layers of the external granular layer is seen as early as P2 in the lobulus simplex and by P6 in the uvula (Swisher and Wilson, 1977). Loss of granule cells is greater than the proliferation and migration from the external granular layer since there is never an increase in cell number seen in the internal granule layer of the wild type mice (Caddy and Biscoe, 1979). The cell extinction, reflected in reduced

growth of the molecular and granular layers (Swisher and Wilson, 1977), affects almost 90% of the granule cells in *Lurcher* mice (Caddy and Biscoe, 1979). Loss of inferior olivary neurons is apparent at P11 and in adult *Lurcher* mutants represents 70-75% of complete neuronal population (Caddy and Biscoe, 1979). In contrast to reduced synaptogenesis between climbing fibers and Purkinje cells, the synapses between climbing fibers and Golgi, granule, basket and stellate cells seem to be unaffected (Caddy and Biscoe, 1979).

A quantitative analysis of the deep cerebellar nuclei in *Lurcher* mutant mice revealed an overall 60% decrease in volume (Heckroth, 1994a). The principal neurons are slightly reduced in number (20% decrease) in the nuclear complex, while the population of small neurons is reduced by 37% in the interposed nucleus and dentate nuclei, but is unchanged in the fastigial nucleus (Heckroth, 1994a). In a later study, Sultan et al. (2002) confirmed the mild degeneration (a reduction by 20%) of glutamatergic principal neurons and more pronounced GABAergic (by 42%) and glycinergic neurons (by 45%). From the point of view of cytological components, the loss of myelinated axons and boutons accounts for 59% of the cerebellar nuclei atrophy, an additional 2% represents loss of nuclear neurons and another 8.3% represents reduction in dendritic arbors. The remaining 30.7% of the lost nuclear volume results from reduced volume of glial processes, vascular elements, and intercellular space (Heckroth, 1994b). These findings suggest that the massive deafferentation of cerebellar nuclei occurring between P10-P30 in *Lurcher* mutant mice has a relatively mild effect on the principal neurons of cerebellar nuclei (Heckroth, 1994a).

Role of GluRδ2 and cell death mechanism

The *Grid2*^{Lc} is a gain-of-function mutation that changes GluRδ2 into a leaky membrane channel leading to chronic cell depolarization (Zuo et al., 1997). The δ-subfamily of ionotropic glutamate receptors (iGluRs) consists of the GluRδ1 and GluRδ2. Although the δ receptors have been considered as "orphan receptors" because they do not form functional glutamate-gated ion channels, later studies have demonstrated that the GluRδ2 plays a crucial role in cerebellar function (Kashiwabuchi et al., 1995). *In situ* hybridization and immunogold electron microscopy revealed that GluRδ2 are selectively expressed in parallel fiber-Purkinje

cell synapses (Araki et al., 1993) and show close spatial association with AMPA GluR2/3 receptors (Landsend et al., 1997). Although, the GluRδ2 can form heteromeric receptors with AMPA and kainate receptors *in vitro* (Kohda et al., 2003) the vast majority of the GluRδ2 were not coassembled with AMPA or kainate receptors *in vivo* (Mayat et al., 1995; Kohda et al., 2003). Nevertheless, it has been found that GluRδ2 regulates AMPA receptor endocytosis during cerebellar PF-PC LTD induction (Kohda et al., 2013), which is an important cellular mechanism for memory formation (Ito, 2002). Uemura (2010) also showed that the N-terminal domain of GluRδ2 interacts with presynaptic neurexins (NRXNs) cerebellin 1 precursor protein (Cbln1) and suggested that the GluRδ2 mediates cerebellar parallel fiber-Purkinje cell synapse formation (Kashiwabuchi et al., 1995; Kurihara et al., 1997; Takeuchi et al., 2008). These results indicated that GluRδ2 plays a direct role in synapse formation and synaptic plasticity (Yuzaki, 2004), which underlie development, learning and memory (Ito, 1989; Bliss and Collingridge, 1993).

Although the GluRδ2 is probably not a functionally active ion channel (see above), the *Grid2*^{Lc} mutation indicates that the receptor can act as an ion channel. The ability of *Grid2*^{Lc} mutation to form GluRδ2 into a channel pore may just be a function that was lost during evolution (Yuzaki, 2004). Although the *Grid2*^{Lc} mutation and its effect on GluRδ2 is well characterized, the mechanism of cell death is still being discussed (Armstrong et al., 2011). The cell-autonomous Purkinje cell death has been alternately described as necrotic (Dumesnil-Bousez and Sotelo, 1992), apoptotic (Norman et al., 1995; Wullner et al., 1995; Selimi et al., 2000b) and autophagic (Yue et al., 2002; Wang et al., 2006; Yue, 2010) depending on morphological and molecular criteria (Vogel et al., 2007; Armstrong et al., 2011). Necrotic cell death hypothesis based on some ultrastructural evidence was suggested before the *Grid2*^{Lc} mutation had been identified. Dumesnil-Bousez and Sotelo (1992) described necrotic process based on the morphological abnormalities of Purkinje cells seen after P12, such as axonal swelling, perinuclear clumps of chromatin and altered mitochondria (enlarged, with dilated cristae) as well as a generally delayed process of maturation evidenced in dendritic trees (hyperspinous dendrites, delayed formation of proximal and distal compartments) and in cell bodies (incomplete development of basal polysomal mass).

Since the *Grid2*^{Lc} mutation changing the GluRδ2 into a constitutively opened membrane channel was identified, the mode of cell death was characterized as excitotoxic with apoptosis as an endpoint (Norman et al., 1995; Zuo et al., 1997; Armstrong et al., 2011). Moreover, Norman et al. (1995) demonstrated that dying *Lurcher* Purkinje cells exhibit characteristic morphologic features of apoptosis, including nuclear condensation, axon beading, membrane blebbing and the presence of mRNA for sulfated glycoprotein 2 (SGP2), a marker for apoptotic death in T-cells and prostate epithelial cells. Using the TUNEL labelling method, additional studies identified DNA fragmentation resulting from apoptotic signaling cascades (Norman et al., 1995; Wullner et al., 1995; Selimi et al., 2000a). Furthermore, increased expression of the pro-apoptotic Bax protein along with c-Jun phosphorylation and caspase-8 and -9 expression from P9 to P30 in *Lurcher* Purkinje cells was found (Wullner et al., 1998; Lu and Tsirka, 2002). However, it is not known if all of these proteins are overexpressed in the same Purkinje cells (Armstrong et al., 2011). Contrary to these findings, Selimi et al. (2000a) found that activated caspase-3, a key mediator of apoptotic cell death, is expressed only in few scattered *Lurcher* Purkinje cells. Zanjani et al. (1998a; 1998b) also showed that blockade of apoptosis by manipulating the expression of pro- and anti-apoptotic proteins has had limited success in *Lurcher* Purkinje cell survival. All of these reports demonstrated that apoptosis could play only a limited role in *Lurcher* Purkinje cell death (Armstrong et al., 2011).

Autophagy hypothesis, as the second form of programmed cell death asserted in *Lurcher* neurodegeneration, arose from the study by Yue et al. (2002). Autophagy-related programmed cell death is a dynamic process involving rearrangement of subcellular membranes into autophagosomes and autophagic vacuoles, which engulf the cytoplasmic matrix and organelles and deliver them to lysosomes for degradation (Klionsky and Emr, 2000; Yue et al., 2002). Although, the autophagic pathways might be a phylogenetically older programmed cell death mechanism than apoptosis (Schwartz et al., 1993), both apoptosis and autophagy share several common regulatory elements (Xue et al., 1999; Tukaj, 2013). Once these signals are activated, autophagy may be able to cause cell death even in the presence of apoptosis inhibitors (Klionsky and Emr, 2000). These findings are in

accordance with a report of limited success to maintain *Lurcher* Purkinje cell survival after blocking apoptosis using increased expression of anti-apoptotic proteins (Klionsky and Emr, 2000). Autophagic pathways for bulk degradation of subcellular constituents are hyperactivated in many neurodegenerative disorders such as Huntington's disease (Sapp et al., 1997; Kegel et al., 2000; Petersen et al., 2001), Alzheimer's disease (Cataldo et al., 1996; Nixon et al., 2000) and Parkinson's disease (Anglade et al., 1997).

Autophagic cell death hypothesis postulated for *Lurcher* mutants supposes that GluRδ2 induces autophagy by the interaction via its C-terminus with the PSD-95/Dlg/ ZO-1 (PDZ)-domain-containing protein n-PIST (neuronal isoform of protein-interacting specifically with TC10) that forms a complex with the autophagy-related protein Beclin1, thereby regulating the formation of autophagosomes (Yue et al., 2002; Yue, 2010). The expression of GluRδ2^{Lc}, but not GluRδ2^{wt}, has been shown to lead to the formation of Beclin1-positive autophagosome-like vesicles and to an increase of cell death (Yue et al., 2002). Nevertheless, Zanjani et al. (2009) pointed out that the accumulation of autophagosomes in *Lurcher* Purkinje cell axon terminals (Wang et al., 2006) is due to the chronic depolarization of the cell body or is directly linked to the release of Beclin1 from the mutant receptor. The reevaluation of the "autophagic cell death" hypothesis in *Lurcher* mutants showed that the expression of GluRδ2^{Lc} decreased intracellular ATP (adenosine triphosphate) levels in a manner that was dependent on the extracellular Na^+ concentrations and activated AMPK (5' adenosine monophosphate-activated protein kinase) before autophagy was activated (Nishiyama et al., 2010). Based on these findings, Nishiyama et al. (2010) proposed that decreased ATP levels, which were probably caused by the overactivation of Na^+/K^+ ATPase in response to constitutive Na^+ currents associated with GluRδ2^{Lc} channels, activate AMPK and autophagy pathways. Therefore, activation of autophagy might have a homeostatic protective role in maintaining intracellular ATP and the *Lurcher* Purkinje cell death is rather necrotic with autophagic features (Nishiyama and Yuzaki, 2010).

Neurochemical abnormalities

Besides the abnormality of GluRδ2, *Lurcher* mutant mice also show changes in concentrations of several neurotransmitters, their metabolites and densities of receptors. A selective reduction of glutamate concentration was found in the cerebellum, hippocampus and entorhinal-piriform area (Reader et al., 1998). Strazielle et al. (2000) also reported lower density of AMPA, *N*-methyl-D-aspartic acid (NMDA) and kainate glutamate receptors, in the cerebellar cortex of *Lurcher* mutants compared to the wild type mice, while in the cerebellar nuclei only KA receptors were diminished. In other brain regions (limbic system, motor cerebral cortical regions, neostriatum and thalamus), the alterations always followed the same pattern characterized by a decrease of NMDA and kainate receptors but with an increase of AMPA sites (Strazielle et al., 2000). While the concentrations of GABA, Glycine, Aspartate, Dopamine and Taurine remain unchanged in *Lurcher's* cerebellum, their levels were significantly lower in the entorhinal-piriform area compared with wild type mice (Reader et al., 1998). On the other hand, higher concentrations of noradrenaline and serotonin in the mutant cerebellum were described (Strazielle et al., 1996; Le Marec et al., 1999; Reader et al., 2000). Apart from neurotransmitter systems, *Lurcher* mutants also showed changes in concentration of some metabolites, enzyme activity and expression of certain genes in the cerebellum or even in some other brain regions (for details see reviews Cendelin and Vozeh, 2007; Lalonde and Strazielle, 2007; Vogel et al., 2007).

Behavioral characteristics

The progressive cerebellar degeneration in *Lurcher* mutant mice affects a broad spectrum of behavioral functions and provides insights into the role of the cerebellum in circuitries related to motor, cognitive and emotional processing. Heterozygous mutants develop more slowly than control mice of the same strain (Vogel et al., 2007). They show lower body weight from the end of the first postnatal months compared to the healthy littermates and this reduced body weight remains during adulthood (Thullier et al., 1997)

Lurcher mice are characterized with marked cerebellar ataxia. The gait is wobbly, lurching and with tendency to fall to either side (Phillips, 1960). The ataxic

gait is not accompanied by trembling to the extent shown by other cerebellar mutants, but rather by jerky up and down movements (Phillips, 1960). The step ratio and interlimb coupling are more variable in *Lurchers* animals than in healthy animals (Fortier et al., 1987). The disorganization of the cyclic limb movements as well as irregular EMG pattern seen in the *Lurcher* mutants during walking were not observed during swimming (Fortier et al., 1987). Gait analysis showed differences in some gait components (e.g. stand, stride length, swing speed); however these differences could be partially explained by different speeds of movement (Cendelin et al., 2010).

Skeletal muscles of *Lurcher* mice are more fragile due to reduced muscle protein content (Hartmann et al., 2001). Motor disabilities of *Lurcher* mice result in poor performance in several motor skill tests. Affected dynamic equilibrium and motor coordination were observed in the treadmill (Le Marec and Lalonde, 2000) and rotarod test (Thullier et al., 1997; Hilber and Caston, 2001). The wooden beam (Le Marec et al., 1997), slanted ladder (Krizkova and Vozeh, 2004; Cendelin et al., 2008) and unstable platform (Hilber et al., 1999) tests showed impaired static equilibrium. Furthermore, *Lurcher* mice exhibited a decrease of muscular strength observed in the horizontal wire (bar) or coat-hanger tests (Lalonde et al., 1992; Hilber and Caston, 2001). In spite of their motor deficits, *Lurcher* mutants have an ability for motor learning and their performance improves when the task is repeated (Lalonde, 1994; Lalonde and Thifault, 1994; Lalonde et al., 1996; Hilber and Caston, 2001; Cendelin et al., 2008). However their ability to learn decreases with age (Hilber and Caston, 2001). *Lurcher* mice also showed changes in the oculomotor system. Although they possess both optokinetic (OKR) and VOR compensatory reflexes, they are unable to modify either of these reflexes in the course of training (van Alphen et al., 2002).

Massive loss of Purkinje cells induces various cognitive and behavioral disturbances in *Lurcher* mice. They show poor performance in spatial tasks, mainly in the Morris water maze (Lalonde et al., 1988; Hilber et al., 1998; Porras-Garcia et al., 2005; Cendelin et al., 2008). While in the task with a hidden escape platform, healthy controls decrease their escape latencies (or trajectory lengths) with training, *Lurcher* mice showed only mild or no improvement (Lalonde et al., 1988; Porras-Garcia et al., 2005; Cendelin et al., 2008). They also have difficulties in the visible platform task (Lalonde et al., 1988). Therefore, the deficit in visuomotor coordination has been

suggested as a key factor in the acquisition of spatial tasks (Lalonde et al., 1988; Lalonde and Thifault, 1994). *Lurcher* mutants show impaired simultaneous spatial discrimination learning (Lalonde et al., 1993a), spatial working as well as reference memory (Belzung et al., 2001) and long-term spatial memory (Hilber et al., 1998). All of these findings suggest that *Lurcher* mice are unable to construct a cognitive map and they use an associative route strategy rather than true spatial strategy based on cognitive mapping (Hilber et al., 1998).

The poor performance of *Lurcher* mutants in spatial tests could also be partially explained by their decreased motivation to explore the novel environment (Lalonde et al., 1993b; Monnier and Lalonde, 1995; Caston et al., 1998). Not only spatial learning disturbances, but also changes in classical conditioning of eyelid response were reported in *Lurcher* mice (Porras-Garcia et al., 2005; Porras-Garcia et al., 2010). Despite the learning curves of *Lurcher* mice during classical conditioning of eyelid responses being similar to normal mice, the amplitudes of the learned response are significantly lower (Porras-Garcia et al., 2005). Moreover, electrophysiological recordings of the interpositus and red nuclei in *Lurcher* mutants during eyeblink conditioning suggested compensatory mechanisms in the absence of the cerebellar cortex during performance of learned movements (Porras-Garcia et al., 2010; Porras-Garcia et al., 2013).

Lurcher mice exhibited not only motor and cognitive deficits (see above), but also alteration in emotional processing (Monnier and Lalonde, 1995; Hilber et al., 2004). Frederic et al. (1997) showed that exposure of *Lurcher* mutants to a novel environment increased adrenocorticotropic hormone (ACTH) and corticosterone plasma levels (hormonal stress indicators) 3.5-fold and 1.8-fold, respectively, in *Lurcher* compared to normal mice, while the basal levels of circulating ACTH and corticosterone were similar to wild type mice. The exposure to anxiogenic situations induced less anxious behavior with higher blood corticosterone level than in the wild type mice (Hilber et al., 2004; Lorivel et al., 2010). The contrast between less anxiety-like behavior and elevated levels of corticosterone during stressful situations suggest that *Lurcher* mice have reduced capacity to inhibit selective components of natural behaviors (Frederic et al., 1997; Hilber et al., 2004). An inhibition deficit was demonstrated by their decreased ability to produce prepulse inhibition of the acoustic

startle response (Porras-Garcia et al., 2005) or the immobility response (Lalonde, 1998). The discrepancy between the HPA axis reaction and the disproportional neural control of behavior could be due to an affection of the sensorimotor gating mechanism (Porras-Garcia et al., 2005).

Lurcher mice in experimental therapy

Lurcher mice do not constitute an identical model of a known human disease, but their neurological similarities with the human spinocerebellar atrophy allow for considering heterozygous *Lurchers* animals as a partial model of this pathology (Hilber et al., 2004). Moreover, Coutelier et al. (2015) recently reported similar putative gain-of-function mutation of *GRID2* gene in human patients with congenital and mild adult-onset cerebellar ataxia. *Lurcher* mutants are also used as an animal model for the study of autistic spectrum disorders due to their developmental loss of Purkinje cells and some behavioral abnormalities (Dickson et al., 2010; Rogers et al., 2013).

While Heckroth et al. (1998) described some advantages of this mouse model for the cerebellar neurotransplantation therapy, Triarhou (1996) remarked that the restoration of developmental perturbed cerebellar circuit of the *Lurcher* mice by means of neural transplantation poses some serious limitations. The *Lurcher* host cerebellum was used for the graft of embryonic cell suspension (Tomey and Heckroth, 1993), solid pieces of embryonic cerebellum (Dumesnil-Bousez and Sotelo, 1993; Cendelin et al., 2009b, a; Cendelin et al., 2012) and various types of stem cells (Jones et al., 2010; Houdek et al., 2012). The graft survival rate depends on the grafted cells as well as on the properties of the host tissue (Rossi and Cattaneo, 2002). Despite grafted embryonic cerebellar cells being able to survive and differentiate into Purkinje neurons, their dendrites fail to adopt a characteristic planar disposition inside the host cerebellum (Triarhou, 1996). Moreover, there is very little evidence for functional recovery (Jones et al., 2010).

1.6.2 *Purkinje cell degeneration* mice

Description of the mutant

Purkinje cell degeneration (*pcd*) mice occur as spontaneous autosomal recessive mutants in the C57BR/cdJ strain at The Jackson Laboratory (Mullen et al., 1976). *Pcd* mice carry a mutation that affects the *Agtpbp1* gene located on chromosome 13 (Fernandez-Gonzalez et al., 2002). *Agtpbp1* gene encodes the cytosolic carboxypeptidase 1 (CCP1) that belongs to the metallocarboxypeptidase gene family. Several spontaneous (*Agtpbp1*$^{pcd\text{-}1J}$, *Agtpbp1*$^{pcd\text{-}2J}$, *Agtpbp1*$^{pcd\text{-}3J}$, *Agtpbp1*$^{pcd\text{-}5J}$, *Agtpbp1*$^{pcd\text{-}7J}$), induced (*Agtpbp1*$^{pcd\text{-}4J}$, *Agtpbp1*$^{pcd\text{-}6J}$) and transgenic (*Agtpbp1*$^{pcd\text{-}Tg(Dhfr)1Jwg}$) mutants with similar phenotypes have been discovered or generated, respectively (for reviews see Wang and Morgan, 2007; Cendelin, 2014).

Morphological and cellular changes

The deficiency of CCP1 in *pcd* mice leads to a number of cellular defects, including abnormal accumulation of polysomes in Purkinje cells (Landis and Mullen, 1978), affected transcription, and DNA repair in Purkinje cells and mitral cells of the olfactory bulb (Valero et al., 2006; Baltanas et al., 2011), endoplasmic reticulum stress in Purkinje cells (Kyuhou et al., 2006), formation of axonal spheroids (Baurle and Grusser-Cornehls, 1994), mitochondrial dysfunction (Chakrabarti et al., 2010), elevated autophagy (Berezniuk et al., 2010), and abnormal dendritic development (Li et al., 2010). Although CCP1 was originally described as an ATP/GTP-binding protein related to zinc carboxypeptidase (Harris et al., 2000), there is no experimental evidence for this, and the purported ATP/GTP-binding pocket is only distantly related to that of well-studied ATP/GTP-binding proteins (Berezniuk et al., 2012). Berezniuk et al. (2012) demonstrated that CCP1 processes glutamate residues from C-terminus of α- as well as β-tubulin. Rogorowski et al. (2010) also showed that the removal of gene-encoded glutamic acids from the C-termini of proteins is not specific to tubulin but affects a range of substrates including myosin light chain kinase 1 (MLCK1). Consistent with the enzymatic activity of CCP1, it has been shown that tubulin polyglutamination is highly increased specifically in brain areas, such as the cerebellum and olfactory bulb which degenerate in the *pcd* mice (Rogowski et al., 2010). Cartelli et al. (2010) described that disruption in tubulin dynamics could

consequently induce mitochondrial dysfunction and cause neurodegeneration. Abnormalities in mitochondria in *pcd* mice were also reported by Chakrabarti et al. (2010). Downregulation of tubulin polyglutamination subsequently leads to partial prevention of neurodegeneration in these mutants (Rogowski et al., 2010).

The predominant pathology in *pcd* mutants is the loss of Purkinje cells (Figure 1C,D). The pathogenic process may be summarized as abnormal inclusions and organelles within the soma of Purkinje cells (for review see Wang and Morgan, 2007). These changes are well marked before the onset of ataxia and extinction of the first Purkinje cells, the number of which is within normal range before P21 (Landis and Mullen, 1978). In addition, affected Purkinje cells also possess unusual configurations of endoplasmic reticulum with associated electron-dense particles similar to but larger than ribosomes, mature and forming intracisternal A particles and nematosomes (Landis and Mullen, 1978).

The death of Purkinje cells in *pcd* mice has been suggested as apoptotic via the activation of caspase-3 and subsequent fragmentation of DNA (Kyuhou et al., 2006). In addition to the activation of apoptosis in Purkinje cells, many activated microglia were found in the molecular layer of the cerebellar cortex (Kyuhou et al., 2006). Chakrabarti et al. (2009) later reported that *pcd* mice on the Bax null background obtained by the intercrossing of pcd^{5J} with Bax knock-out mice did not show any differences in the onset of ataxia. In neurons, both the intrinsic as well as extrinsic pathways of apoptosis require Bax activation for execution of cell death. Based on these findings, the *pcd* phenotype is not modified by Bax gene dosage and the classic apoptosis is not responsible for Purkinje cell death. The subsequent ultrastructural studies indicated increased autophagy pathway in Purkinje cells, and yielded evidence for mitophagy (Chakrabarti et al., 2009).

The loss of Purkinje cells occurs over a relatively brief period of time. However, the progress of cell extinction shows a different tempo in individual regions of the cerebellum (for review see Wang and Morgan, 2007). In 22- and 24-day old mutants, 25-50% of the Purkinje cells in the vermis had degenerated (Mullen et al., 1976). In 29-day old *pcd* mice, the only surviving Purkinje cells were found in the nodulus, flocculus, paraflocculus and ventral side of the uvula of the vermis, where many Purkinje cells were still present at this time. At 5 weeks of age, some

Purkinje cells still survived in these regions, but by 7 weeks only a few of them remained, mainly in the lobule X (Mullen et al., 1976; Landis and Mullen, 1978). Before the *pcd* Purkinje cells became extinct, they appeared to receive all their appropriate synaptic contacts (Landis and Mullen, 1978). However, some disruption of synaptogenesis between parallel fibers and Purkinje cell spines occurred at late stages of development. Some Purkinje cell spines lacked presynaptic elements (naked spines) and postsynaptic thickenings were present along the Purkinje cell dendritic shafts with parallel fibers appearing to make synaptic contacts directly onto the shafts (Landis and Mullen, 1978). Heterozygous *pcd* mutants also showed progressive and age-related loss of Purkinje cells. 17-month old both male and female heterozygous mice lost ~18% of their Purkinje cells. Contrary to the homozygous mice, the loss of Purkinje cells in heterozygous *pcd* mutants apparently occurred evenly throughout the cerebellum. Nevertheless, this degree of Purkinje cell degeneration did not lead to any detectable locomotor deficit (Doulazmi et al., 2002).

The degeneration of Purkinje cells triggers a secondary loss of cerebellar granule cells. Reduction of cerebellar granule cells is exponentially progressive (Triarhou, 1998). In 3-month old *pcd* mice the granule cell layer appeared relatively normal in thickness; however, pyknotic nuclei were evident and there was a mild to moderate reduction in granule cell number (Triarhou, 1998). Subsequently, the loss of granule cells progressed through the mutant lifespan so that by 20 months of age ~95% had degenerated (Triarhou, 1998; for review see Wang and Morgan, 2007). There was no obvious reduction of Golgi II cells in the granular layer or of neurons in the deep cerebellar nuclei (Mullen et al., 1976). The loss of Purkinje cells in *pcd* mice also deprived inferior olivary neurons, which are their major presynaptic inputs (Ghetti et al., 1987). Ghetti et al. (1987) reported that the decline of inferior olivary neuron number in *pcd* mutants was 49% between P17 and P300 and depending on the state of their postsynaptic Purkinje cells. Moreover, Purkinje cell disappearance stimulated the development of a severe gliosis characterized by enhanced glial proliferation, as well as the release of pro-inflammatory mediators (Baltanas et al., 2013). For a comparison of *pcd* mutant and wild type cerebellum see Figure 1C,D.

Pcd mutants also showed a rapid degeneration of discrete populations of thalamic neurons between P50 and P60 (O'Gorman and Sidman, 1985). Severely

affected nuclei, in which a majority of neurons degenerated, include the central division of the mediodorsal nucleus, the ventral medial geniculate, posterior, posterior ventrolateral and posteromedial nuclei, and those portions of the ventrolateral and posteromedial nuclei which immediately surround the medial division of the ventrobasal complex (O'Gorman and Sidman, 1985). Electron and light microscopy revealed the same cytology of thalamic neuron degeneration as in Purkinje cells. At P30, the general cytological organization of thalamic neurons in medial geniculate nucleus closely resembled that of neurons in littermate controls, but neurons in *pcd* mutants were distinguished by the presence of small aggregates of fine granules, approximately 9 nm in diameter (O'Gorman, 1985; O'Gorman and Sidman, 1985). By P50 the neurons were more affected and large areas of cytoplasm were occupied exclusively by polysomes, while profiles of endoplasmatic reticulum and the Golgi apparatus appeared to be reduced (O'Gorman, 1985). *Pcd* mice also suffered from degeneration of olfactory bulb mitral cells, detectable after the second postnatal month (Greer and Shepherd, 1982). The application of the 2-deoxyglucose technique indicated that the *Agtpbp1*^{pcd} mutation causing the loss of mitral cells did not affect the ability of olfactory receptor cells to respond in a normal manner to the odor (Greer and Shepherd, 1982). However, a later study using the precise olfactometry revealed that the mutant mice exhibited a deficit in odorant detection and discrimination (Diaz et al., 2012).

Pcd mutants lose about 50% of their retinal photoreceptor cells between 3 and 5 weeks of age, and thereafter slowly lose the remaining photoreceptor cells during the first year of life (Blanks and Spee, 1992). The first sign of the retinal degeneration appearing between P13-P18 is characterized by a large number of vesicles, ranging in diameter from 150 to 350 nm, which are located in the extracellular space adjacent to the photoreceptor inner segment (Blanks et al., 1982b). By P25 there was an abundance of pyknotic photoreceptor nuclei and many outer segments were clearly disorganized. Thereafter, as the photoreceptor cells are lost, their outer segments slowly become shorter and more variable in length (LaVail et al., 1982). The electroretinographic records revealed that the retina's rod and cone systems showed a reduction in the amplitude of the electrical signal (Marchena et al., 2011). Although, the most obvious abnormality in the retina of *pcd* mice was degeneration of

photoreceptor cells, Müller cells also appeared to be affected, having swollen apical processes often seen coursing through the outer nuclear layer (Blanks et al., 1982b).

Behavioral characteristics

As found in *Lurcher* mice (see above), cerebellar degeneration in *pcd* mutants affects a wide spectrum of behavioral functions. The major neurological symptom is cerebellar ataxia that can be behaviorally detected at P22 (Mullen et al., 1976). The ataxic phenotype becomes more obvious after P28 (Mullen et al., 1976; for review see Wang and Morgan, 2007). Le Marec and Lalonde (1997) showed that *pcd* mice have shorter falling latencies and spend more time in passive rotation on the accelerating rotarod compared to the healthy control littermates. Contrary to the control mice, *pcd* mutants were not able to improve their performance on the accelerating rotarod with repeated trials (Le Marec and Lalonde, 1997). The disruption of sensorimotor skills in *pcd* mice was demonstrated during the acquisition of the slow treadmill task at low slopes. In this test, longer time spent walking, an indication of a decreased ability of coordinating whole body movements, was observed in *pcd* mice (Le Marec and Lalonde, 1998). Goodlett et al. (1992) found that despite gait abnormalities in *pcd* mice, their swimming ability was surprisingly competent. Mutants could at times adopt a normal swimming posture comparable to healthy mice, with their head above the water, forepaws inhibited, propelling with alternating hind limb kicks and using the tail in the water. Nevertheless, they did not maintain this swimming pattern for long distances, and frequently broke into a "dog-paddle" in which they used both forelimbs and hind limbs for swimming (Goodlett et al., 1992).

Besides motor disabilities, *pcd* mice have been reported to have additional behavioral deficits. 30-, 60- and 110-day old *pcd* mutants were impaired in distal-cue (spatial) navigation, but not proximal-cue (visual guidance) task in the Morris water maze (Goodlett et al., 1992). The ability to perform the proximal-cue but not distal-cue task in all three tested age groups indicates that the deficit in spatial navigation is not simply due to motor dysfunction and/or visual sensory deficits (Goodlett et al., 1992). Apart from spatial learning disturbances, *pcd* mice also have impaired eyeblink conditioning (Chen et al., 1996) that appears to be result of a deficiency in cerebellum-mediated learning (Chen et al., 1999).

Agtpb1^{pcd} mutations were reported for several mouse strains, e.g. C57BL/6J (Marchena et al., 2011), C57BR/cdJ (Mullen et al., 1976), B6C3Fe-a/a (Le Marec and Lalonde, 1997), BALB/cByJ (Rogowski et al., 2010), DBA/2J (Chakrabarti et al., 2009), SM/J (Fernandez-Gonzalez et al., 2002). Although the mice with *Agtpb1*^{pcd} mutation can survive to at least 17 months, generally older mutants are in poorer health, being lighter in weight and less active than littermates (Mullen et al., 1976). The adult *pcd* females are fertile, but have difficulties in rearing the few litters they produce (Mullen et al., 1976). Male *pcd* mice are sterile, because they have reduced numbers of sperm that are abnormally shaped and non-motile (Mullen et al., 1976; Handel et al., 1988). Nevertheless, they are capable of mating, as evidenced by vaginal plugs in estrus females (Mullen et al., 1976).

Pcd mice in experimental therapy

Like *Lurcher* mice, *pcd* mutants do not constitute an identical model of a known human disease. Nevertheless, due to their multiple system disorders, *pcd* mutants are often used as an animal model for studying the developmental loss of Purkinje cells (for review see Wang and Morgan, 2007), olfactory bulb degeneration (Diaz et al., 2012) and retinal degeneration (Chang et al., 2002).

A number of studies have shown that transplantation of wild type cerebellar primordia into the *pcd* mice either as cell suspensions (Sotelo and Alvarado-Mallart, 1986; Chang and Ghetti, 1993; Triarhou et al., 1995; Zhang et al., 1996) or as solid graft (Sotelo and Alvarado-Mallart, 1987a, b) can mitigate some aspects of the *pcd* phenotype. Although the normal mouse cerebellum contains about 200,000 Purkinje cells, in engrafted experiments as few as 3,000 Purkinje cells per cerebellum were sufficient to improve motor function (for review see Wang and Morgan, 2007). Diaz et al. (2012) also showed that the transplantation of adult wild type bone marrow-derived cells into the *pcd* mouse tail vein generated a large population of microglial cells in the olfactory bulb and reduced the degenerative process of this structure. The alleviation of mitral cell degeneration was accompanied by functional recovery witnessed by significantly improved olfactory detection and enhanced odor discrimination (Diaz et al., 2012). Moreover, several transplantation therapy approaches have been taken to actually prevent Purkinje cell degeneration in *pcd* mutants (for details see review Wang and Morgan, 2007). It has been reported that

the subcutaneous implantation of neuroprotectant insulin-like growth factor I (IGF-I) microspheres improved motor coordination of *pcd* mice (Carrascosa et al., 2004).

1.6.3 Mouse model of spinocerebellar ataxia type 2 (SCA2 mice)

Description of the mutant

Transgenic SCA2 mice carrying human ataxin-2 gene (*ATXN2*), with an enlarged CAG repeat sequence was first developed by the team of prof. Stefan Pulst in Cedar-Sinai Medical Centre in Los Angeles, USA (Huynh et al., 2000). The first mouse transgenic model of SCA2 was generated by microinjection of transgenic construct containing a full length human *ATXN2* (formerly *SCA2*) cDNA (with a 58 CAG repeat) as well as the mouse Purkinje cell protein 2 (*Pcp2*) promoter into pronuclei of the B6D2F1 mouse strain, a C57BL/6J x DBA/1J hybrid (for details see Huynh et al., 2000). Using this method, 4 human mutant founder lines carrying 58 CAG repeats (*Pcp2-ATXN2*^{Q58}), Q58-5, Q58-5B, Q58-11 and Q58-19, were generated, but only Q58-5B, Q58-11 and Q58-19 were able to produce offspring (Huynh et al., 2000). Later, several other SCA2 models have been generated. Besides *Pcp2-ATXN2*^{Q58} mice, expression of full-length *ATXN2* is targeted to Purkinje cells using *Pcp2* promoter also in the *Pcp2-ATXN2*^{Q127} mouse model with 127 CAG triplets (Hansen et al., 2013). Aguiar et al. (2006) developed a SCA2 mouse model with 75 CAG repeats under the *ATXN2* self-promoter control (*ATXN2*^{Q75}). Damrath et al. (2012) generated another SCA2 mouse model carrying 42 CAG triplets under the control of the endogenous murine *ATXN2* promoter (*ATXN2*^{Q42}). The last developed mouse transgenic model of SCA2 at this time was created by transgenesis using human bacterial artificial chromosomes (BACs) (Dansithong et al., 2015). BAC approach enables introducing an entire human gene including introns and regulatory regions into the mouse genome. Models generated by BAC approach often have lower genomic copy numbers than conventional cDNA models resulting in more physiological expression levels and potentially more faithful late onset of disease (Dansithong et al., 2015). Mice with the *ATXN2* BAC transgene have 72 CAG repeats in the *ATXN2* gene (BAC- *ATXN2*^{Q72}) (Dansithong et al., 2015).

Cellular and morphological changes

ATXN2 protein is widely expressed in the mammalian nervous system (Pulst et al., 1996; Kiehl et al., 2000). It is involved in the regulation of epidermal growth factor receptor (Nonis et al., 2008) and inositol 1,4,5-triphosphate receptor whereby increased cytosolic calcium occurs with CAG triplet expansion (Liu et al., 2009). The functions of ATXN2 protein are also associated with the endoplasmic reticulum (van de Loo et al., 2009), Golgi complex (Huynh et al., 2003) and translational regulation (Ciosk et al., 2004). Furthermore, ATXN2 is important in energy metabolism, weight regulation (Kiehl et al., 2006; Lastres-Becker et al., 2008) and also demonstrates its role in RNA metabolism due to the interaction with multiple RNA binding proteins (Shibata et al., 2000; Ciosk et al., 2004; Nonhoff et al., 2007; Elden et al., 2010).

In SCA2, expansion of CAG triplets in exon 1 of the *ATXN2* gene causes expansion of polyQ domain in ATXN2 protein (Dansithong et al., 2015). It is thought that the toxic gain-of-function protein aggregation affects RNA processing, resulting in degenerative processes affecting preferentially cerebellar neurons (Damrath et al., 2012). Larger polyQ expansions have been associated with greater pathology (van de Warrenburg et al., 2005; Matilla-Duenas et al., 2014). The expression of human cytosolic protein ATXN2 with polyQ tract in transgenic SCA2 mouse lines leads to formation of cytoplasmic, but not nuclear, microaggregates (Huynh et al., 2000; Damrath et al., 2012). Microaggregate accumulation resulting in impaired RNA processing as well as protein synthesis (Thangima Zannat et al., 2011) is possibly critical for Purkinje cells with their large ribosomal machinery (Damrath et al., 2012). The accumulation of microaggregates is accompanied with progressive loss of Calbindin-28K in Purkinje cells (Huynh et al., 2000; Aguiar et al., 2006; Hansen et al., 2013). Huynh et al. (2000) showed that whereas at four weeks Calbindin-28K labeling was strong in healthy *Pcp2-ATXN2*^{Q22} and wild type mice, in the *Pcp2-ATXN2*^{Q58} homozygotes it had already been reduced. The progressive reduction of Calbindin-28K protein was also confirmed by decreased *Calb1* gene transcription until 8 weeks in *Pcp2-ATXN2*^{Q127} and 9 weeks in BAC-*ATXN2*^{Q72} mouse lines, respectively (Hansen et al., 2013; Dansithong et al., 2015). Transcriptional changes were also observed in other Purkinje cell specific genes, such as *Pcp2* and *Grid2* (Hansen et al., 2013; Dansithong et al., 2015). Although Calbindin reduction has also

been reported in SCA1 mutant mice (Vig et al., 1998) and abnormalities in handling of calcium fluxes have been implicated in neurodegenerative process in general (for reviews see Felix, 2000; Bidaud et al., 2006), there is a debate as to whether elevated calcium is a primary contributor to subsequent loss of Purkinje cells (Schwaller et al., 2002). Cellular changes in SCA2 transgenic mice are followed by decrease of firing frequency of Purkinje cells, first shown at 6 weeks, loss of dendritic arbor, soma shrinkage and finally by extinction of Purkinje cells (Aguiar et al., 2006; Hansen et al., 2013). At 24-27 weeks, Purkinje cell number is reduced by 50-53% in *Pcp2-ATXN2*^{Q58} lines (Huynh et al., 2000). In *Pcp2-ATXN2*^{Q127} mice the reduction in Purkinje cell number as well as reduction of thickness of molecular layer was not seen until after 12 weeks (Hansen et al., 2013).

Functional changes

The loss of the Purkinje cells in SCA2 mouse model is accompanied by a progressive functional deficit. The SCA2 mice with *Pcp2-ATXN2*^{Q58} have a 19% reduction of stride length at 8 weeks (Q58-19 line) and at 16 weeks (all three Q58 lines) respectively (Huynh et al., 2000). Huynh et al. (2000) also found that *Pcp2-ATXN2*^{Q58} mice with neurodegenerative phenotypes had a tendency to fold their hind legs when held by the tail for at least one minute. Clasping was observed at 16-20 weeks in the Q58-19 line and at 8-12 months in the Q58-11 line. In Q58-5B line, no clasping was observed up to 26 weeks of age (Huynh et al., 2000). The mice with human *Pcp2-ATXN2*^{Q22} did not show clasping up to 12 months of age (Huynh et al., 2000). In the rotarod test, Q58-11 and Q58-5B lines confirmed progressive functional deficits observed in transgenic *Pcp2-ATXN2*^{Q58} mice (see above). At 6 weeks, motor performance of transgenic animals was not different from that of wild type mice, at 16 weeks homozygous *Pcp2-ATXN2*^{Q58} mice already performed poorly on rotarod testing, whereas heterozygous *Pcp2-ATXN2*^{Q58} animals performed like wild type mice did (Huynh et al., 2000). At 26 weeks, both heterozygous and homozygous *Pcp2-ATXN2*^{Q58} mice showed severely impaired motor performance compared to the wild type mice and animals expressing *Pcp2-ATXN2*^{Q22} (Huynh et al., 2000). In *ATXN2*^{Q75} mice, the rotarod test revealed significant differences in motor performance compared to the healthy littermates at 20 weeks of age (Aguiar et al., 2006). In BAC-*ATXN2*^{Q72} the motor deficit began at 16 weeks of age (Dansithong et

al., 2015). The earliest onset of SCA2 motor symptoms was found in the transgenic mouse line with the longest polyQ repeats. The deterioration of motor performance in mice with *Pcp2-ATXN2*^{Q127} began at 8 weeks with progressive worsening of symptoms with age (Hansen et al., 2013). It seems that the morphological changes as well as motor decline in SCA2 transgenic mice was more severe in lines with longer CAG repeats (for review see Cendelin, 2014). This phenomenon is in agreement with inverse association observed between the size of polyQ repeat and the age of onset in SCA2 human patients (Pulst et al., 1996; Pulst et al., 2005).

SCA2 mice in experimental therapy

SCA2 transgenic mice constitute an animal model of human pathology. Therefore they serve as an ideal model for experimental therapy. Nevertheless, there are only a few studies with a therapeutic approach. Liu et al. (2009) demonstrated that glutamate exposure induced more pronounced Purkinje cell death in *Pcp2-ATXN2*^{Q58} cell cultures compared to the wild type cells and that the application of dantrolene, a calcium stabilizer, attenuated the glutamate-induced cell death. Furthermore, in animal experiments it has been shown that long-term feeding of *Pcp2-ATXN2*^{Q58} mice with dantrolene alleviated age-dependent motor deficits and reduced loss of Purkinje cells observed in untreated *Pcp2-ATXN2*^{Q58} animals by 12 months of age (Liu et al., 2009). Chang et al. (2011) also reported that intravenous transplantation of human mesenchymal stem cells effectively improved rotarod performance of SCA2 transgenic mice and delayed the onset of motor function deterioration. On the other hand, intracranial transplantation failed to achieve such a therapeutic effect (Chang et al., 2011).

2 AIMS

The general aim of this thesis was to contribute to the understanding of the cerebellar involvement in behavioral processes, particularly spatial behavior and the impact of cerebellar degeneration. For this purpose, mouse models of olivocerebellar degeneration were used. Most of this work was focused on the analysis of spatial and emotional behavior in *Lurcher* and *pcd* mutant mice. The second part of this thesis was to elaborate on the breeding capacity of *Lurcher* mice and the therapeutic potential of cerebellar mutants as models for experimental therapy of cerebellar degeneration.

The specific aims of this thesis were the following:

1) Cognitive and emotional processing in *Lurcher* mice

To assess exploratory behavior of *Lurcher* mice

To assess visual guidance and spatial learning of *Lurcher* mice

To assess anxiety and depressive-like behavior of *Lurcher* mice

2) Comparison of cognitive and emotional processing in *Lurcher* and *pcd* mice

To compare exploratory behavior of the mutants

To compare visual guidance and spatial learning of the mutants

To compare anxiety and depressive-like behavior of the mutants

3) Fertility and maternal behavior in *Lurcher* mice

To test fertility of *Lurcher* females

To test maternal behavior of *Lurcher* females

4) Experimental therapy in mouse models of cerebellar degeneration

To test applicability of mouse models of cerebellar degeneration in experimental therapy

3 RESULTS

3.1 List of original articles

1. Maternal infanticide and low maternal ability in cerebellar mutants *Lurcher*
Jan Tuma, Jan Cendelin and Frantisek Vozeh
Neuroendocrinology Letters 2013; 34(7): 618-623

2. Mutation-related differences in exploratory, spatial, and depressive-like behavior in *pcd* and *Lurcher* cerebellar mutant mice
Jan Tuma, Yaroslav Kolinko, Frantisek Vozeh and Jan Cendelin
Frontiers in Behavioral Neuroscience 2015; 9: 116

3. Morphological analysis of embryonic cerebellar grafts in SCA2 mice
Zdenka Purkartova, Jan Tuma, Martin Pesta, Vlastimil Kulda, Lucie Hajkova, Ondrej Sebesta, Frantisek Vozeh and Jan Cendelin
Neuroscience Letters 2014; 558: 154-158

4. The effect of genetic background on behavioral manifestation of *Grid2^{Lc}* mutation
Jan Cendelin, Jan Tuma, Ivana Korelusova and Frantisek Vozeh
Behavioural Brain Research 2014; 271: 218-227

5. Transplantation of embryonic cerebellar grafts improves gait parameters in ataxic *Lurcher* mice
Vaclav Babuska, Zbynek Houdek, Jan Tuma, Zdenka Purkartova, Jana Tumova, Milena Kralickova, Frantisek Vozeh and Jan Cendelin
Cerebellum 2015; 14(6): 632-641

ORIGINAL ARTICLES

Article 1

Jan Tuma, Jan Cendelin and Frantisek Vozeh

Maternal infanticide and low maternal ability in cerebellar mutants *Lurcher*

Neuroendocrinology Letters 2013; 34(7): 618-623

ORIGINAL ARTICLE

Maternal infanticide and low maternal ability in cerebellar mutants *Lurcher*

Jan Tuma [1,2], Jan Cendelin [1,2], Frantisek Vozeh [1,2]

1 Department of Pathophysiology, Faculty of Medicine in Pilsen, Charles University, Czech Republic
2 Biomedical Centre, Faculty of Medicine in Pilsen, Charles University, Czech Republic

Correspondence to: Jan Tuma, MSc.
Department of Pathophysiology, Faculty of Medicine in Pilsen, Charles University
Lidicka 1, 301 66 Pilsen, Czech Republic.
tel: +420 377593365; fax: +420 377593369; e-mail: jena.tuma@gmail.com

Submitted: 2013-08-19 Accepted: 2013-09-11 Published online: 2013-12-03

Key words: ***Lurcher* mice; *Grid2*^{Lc}, breeding capacity; fertility; maternal infanticide; behavioral disinhibition**

Neuroendocrinol Lett 2013; **34**(7):618–623 **PMID:** 24464008 NEL340713A15

Abstract

OBJECTIVE: One of the common, but less studied deficiencies in mouse models of cerebellar disorders is impaired breeding capacity. Nevertheless, there is no extensive study in *Lurcher* (Grid2^{Lc}) mice, a model of olivocerebellar degeneration. The aim of this work was to analyze a breeding capacity of these mutants.
METHODS: *Lurcher* females mated with healthy wild type males were compared with two control groups: wild type females mated with wild type males and wild type females mated with *Lurcher* males. The breeding capacity of *Lurcher* mice was analyzed using a fertility rate, mating capability and pups survival rate through three consecutive litters.
RESULTS: *Lurcher* dams did not show significantly reduced fertility and mating capability. Nevertheless, their breeding capacity was affected by reduced litter size, maternal infanticide and higher pup mortality during the maternal care period.
CONCLUSION: *Lurcher* mice are fertile and mating capable cerebellar mutants, but their breeding capacity is reduced due to the postpartum behavioral abnormalities. With regard to hyper-reactivity of the hypothalamo-pituitary-adrenal axis followed by behavioral disinhibition during stressful events in *Lurcher* mutants, we hypothesize that the lower breeding capacity is associated with these endocrine and behavioral abnormalities.

Abbreviations:

Agtpbp1^{pcd}	- purkinje cell degeneration mutation
BC_a	- bias corrected and accelerated method
CMH	- Cochran-Mantel-Haenszel test
GluRδ2	- δ2 glutamate receptor
Grid2^{Lc}	- *Lurcher* mutation
HPA	- hypothalamic-pituitary-adrenal axis
Lc$^{(wt)}$	- *Lurcher* females mated with wild type males
nr	- *nervous* mutation
PP1	- postpartum day 1
PP2	- postpartum day 2
PP30	- postpartum day 30
Reln^{rl}	- *reeler* mutation
Rora^{sg}	- *staggerer* mutation
SEM	- standard error of the mean
wt$^{(Lc)}$	- wild type females mated with *Lurcher* males
wt$^{(wt)}$	- wild type females mated with wild type males

INTRODUCTION

Cerebellar disorders are associated with ataxia, dysarthria and difficulty with eye movements. Structural and/or functional cerebellar abnormalities also affect cognition, regulation of emotion and social interaction processing (Schmahmann 2004). A less expected, but common deficiency in mouse models of cerebellar disorders is impaired reproductive performance and offspring productivity. Aberrations in the vaginal estrous cycle and ovarian abnormalities have been found in *staggerer* (*Rora*^{sg}) mice (Guastavino *et al.* 2005; Guastavino & Larsson 1992). Reduced reproductive performance has also been found in *reeler* (*Reln*^{rl}) and *nervous* (*nr*) mutants (Guastavino *et al.* 1993; Sidman & Green 1970). Smaller litter size and difficulties with pup care have been described in Purkinje cell degeneration (*pcd*; *Agtpbp1*^{pcd}) mice (Mullen *et al.* 1976). It has been assumed that affected motor coordination in cerebellar mutants influences sexual activity, nest-building behavior and pup rearing (Chen *et al.* 2007; Guastavino *et al.* 1993), but other authors have suggested that this behavioral deficiency could be caused by a global effect of the mutation on other systems (e.g. endocrine system) (Bulloch *et al.* 1982).

Although mating success, reproductive performance and maternal ability in cerebellar mutant mice have occasionally been studied for a long time, none of these studies focused on *Lurcher* mice. *Lurcher* (*Grid2*$^{Lc/+}$) mutants constitute a natural model of hereditary olivocerebellar degeneration (Phillips 1960). The degenerative process is caused by a mutation of the δ2 glutamate receptor (*GluRδ2*) gene (Zuo *et al.* 1997). GluRδ2 is predominantly expressed by cerebellar Purkinje cells and, at lower levels, in some hindbrain neurons (Araki *et al.* 1993). Constitutive activation of *GluRδ2*^{Lc} causes an inward current and consequent excitotoxic death of Purkinje cells (Norman *et al.* 1995); this is followed by the death of granule, basket and stellate cells and inferior olive neurons due to the disappearance of connective pathways (Caddy & Biscoe 1979; Heckroth & Eisenman 1991; Zanjani *et al.* 2006). The mutant mice are semi-dominant heterozygous. Homozygous individuals (*Grid2*$^{Lc/Lc}$) die shortly after birth due to massive loss of mid- and hindbrain neurons (Cheng & Heintz 1997). *Lurcher* mice are characterized by the cerebellar ataxia (Hilber & Caston 2001), cognitive deficits (Hilber *et al.* 1998), behavioral disinhibition (Hilber *et al.* 2004) and hyper-reactivity of the hypothalamic-pituitary-adrenal (HPA) axis (Frederic *et al.* 1997).

Lurcher mutants are fertile, although the litter size of *Lurcher* females is reduced (Phillips 1960); however, the breeding capacity of *Lurcher* females has not been extensively studied yet. In view of this fact, our objective was to test the reproductive performance and maternal ability of *Lurcher* dams over the course of three consecutive litters and to compare them with their healthy littermate controls.

MATERIALS AND METHODS

Animals

Lurcher (Lc) mutants and their healthy wild type (wt) littermates (B6CBA strain) were used. Females were housed separately in plastic cages (20 x 25 cm) with wooden shavings in a temperature and humidity controlled room with a standard 12/12 hours light/dark cycle. Standard commercial pellet diet and water were available *ad libitum*. The experiment was performed in compliance with EU Guidelines for scientific experimentation on animals and with permission of the Ethics Committee of the Faculty of Medicine in Pilsen, CZ.

Reproductive performance, maternal ability and breeding capacity assessment

Three experimental groups of female mice were used. *Lurcher* females were mated with wild type males (Lc$^{(wt)}$, *n=13*). Two control groups consisted of wild type females mated with wild type males (wt$^{(wt)}$, *n=13*) and wild type females mated with *Lurcher* males (wt$^{(Lc)}$, *n=13*). Dams from Lc$^{(wt)}$ and wt$^{(Lc)}$ groups should have theoretically breed in Mendelian ratios, i.e. 50% *Lurcher* and 50% of wild type pups. Therefore, the wt$^{(Lc)}$ group served as an ideal control for both litter size and pup viability assessment. *Lurcher* and control females were followed through three reproduction cycles. Females were mated for the first time at the age of 2 months. Each reproduction cycle consisted of a maximum of 3 weeks of mating (the male was removed when the female became obviously pregnant, or at the end of the 3 week mating period), the residual period of gravidity (i.e. delivery would theoretically occur 0–3 weeks after the male was removed), 4 weeks of pup-rearing and 2 weeks of rest time after the pups were weaned.

The reproductive performance was evaluated using the fertility rate, mean delivery day and litter size on the second postpartum day (PP2). The fertility rate was the percentage of mated females giving birth to pups (born dead or alive). The delivery day was calculated as the sum of the mating time and the residual period of gravidity and served as an indicator of the mating time necessary for conception (assuming that the pregnancy duration was constant). Mean litter size on PP2 was calculated only for dams with at least 1 live pup at that time point. To avoid stressing the mothers, especially *Lurcher* dams, pups were not counted immediately after parturition; instead they were counted on PP2.

Maternal ability was evaluated as maternal infanticide rate and pup survival rate. The maternal infanticide rate was calculated as the percentage of dams giving birth to pups which cannibalized their complete litter on PP1. Since the pups were counted on PP2, cannibalizing only individual pups on PP1 was undetectable. Pups survival rate was calculated as the percentage of pups surviving from PP2 until weaning on PP30. To lessen the emotional hyper-reactivity of *Lurcher* mutants during stressful situations, dams were

Tab. 1. Fertility rate and mean delivery day (± SEM) of *Lurcher* and wild type control dams in individual litters.

	Fertility rate [%]				Delivery day			
	$Lc^{(wt)}$	$wt^{(Lc)}$	$wt^{(wt)}$	*p-value* [a]	$Lc^{(wt)}$	$wt^{(Lc)}$	$wt^{(wt)}$	*p-value* [b]
1st litter	83.33	83.33	92.31	0.717	28.82 (±2.78)	24.42 (±1.70)	24.08 (±0.87)	0.349
2nd litter	72.73	80.00	100.00	0.129	26.29 (±2.77)	23.22 (±1.33)	24.08 (±1.73)	0.445
3rd litter	70.00	70.00	83.33	0.679	21.71 (±0.42)	26.86 (±3.09)	27.90 (±2.54)	0.315

Note: Fertility rate = total number of females giving birth to pups (born dead or alive)/total number of mated females ×100; Delivery day = number of days after start of mating to delivery; $Lc^{(wt)}$ = *Lurcher* female mated with wild type male; $wt^{(Lc)}$ = wild type female mated with *Lurcher* male; $wt^{(wt)}$ = wild type female mated with wild type male
[a] Freeman-Halton extension of Fisher's exact test; [b] Kruskal-Wallis ANOVA.

not separated (e.g. pup weighing, nest-building behavior scoring) from their pups to avoid modifying natural maternal behavior.

Breeding capacity was the number of live pups at weaning time (PP30). All mated females were involved in the assessment of this parameter. The number represents the number of pups produced in one litter per one female of the group and it is the final measure of both reproductive performance and maternal care ability.

Statistical analysis

The comparison of *Lurchers* ($Lc^{(wt)}$) fertility rate and maternal infanticide rate for three consecutive litters with each control group of wild type dams ($wt^{(wt)}$, $wt^{(Lc)}$) was performed using the Cochran-Mantel-Haenszel (CMH) test for $2 \times 2 \times K$ contingency tables. CMH statistics allows for the analysis of three nominal variables ($2 \times 2 \times K$), where two variables are independent (groups) and the third variable identifies the repeats (litters). The homogeneity of odds ratios, assumptions for the CMH test, was verified using the Breslow-Day test. The analysis of each litter was done separately using the Freeman-Halton extension of Fisher's exact test for 2×3 tables and Fisher's exact test for post-hoc analyses to find any differences between two groups. The mean delivery day, pup survival rate and mean litter size were evaluated using the Kruskal-Wallis ANOVA. Multiple comparisons were performed using the bootstrapping 95% confidence intervals (95% CI) for the difference in the means and two-sample permutation test. The 95% CI for the difference in means was estimated using the bias corrected and accelerated (BC_a) method. The BC_a method can be applied to the construction of nonparametric confidence intervals. The two-sample permutation test requires few assumptions (e.g. normal distribution) and thus can be used for post hoc analysis with Kruskal-Wallis ANOVA. Both resampling procedures were based on 10,000 replicates. Violation of Gaussian distribution assumption was verified using the Shapiro-Wilk test. Differences were considered statistically significant if $p<0.05$. Statistical analyses were performed using R 2.14.0 (GNU) for Mac OS X. Quantitative data are presented as mean ± standard error of the mean (SEM).

RESULTS

Results of the reproductive performance assessment are presented in Table 1. *Lurcher* dams did not show any significant changes in fertility rate (CMH test: $Lc^{(wt)}$ vs. $wt^{(wt)}$: $\chi^2=2.46$, $p=0.117$; $Lc^{(wt)}$ vs. $wt^{(Lc)}$: $\chi^2=0.05$, $p=0.825$). Mutant fertility rates were not been significantly changed over three consecutive litters compared to both control groups (see Table 1). *Lurcher* dams also did not show significantly increased delivery day compared to control dams (see Table 1).

Although, mutant dams had no problems with mating and pregnancy, the CMH test showed a higher maternal infanticide incidence in *Lurchers,* within all three litters ($Lc^{(wt)}$ vs. $wt^{(wt)}$: $\chi^2=7.62$, $p=0.006$; $Lc^{(wt)}$ vs. $wt^{(Lc)}$: $\chi^2=12.10$, $p=0.001$), with the most prominent incidence in the 1st litter (see Table 2). Maternal infanticide was observed on PP1, and probably occurred immediately after parturition. Although the cause of pup death on PP1 could not be specified, pieces of carcass were not found; therefore the missing pups were assumed to be cannibalized. Since almost all litters of *Lurcher* females, during the first reproduction cycle, were cannibalized, pup survival rate as well as mean litter size on PP2 and PP30 could not be evaluated for the first litter. Consequently both of these parameters

Tab. 2. Maternal infanticide rate of *Lurcher* and wild type control dams in individual litters. Data are presented as a mean (± SEM).

	Maternal infanticide rate [%]			
	$Lc^{(wt)}$	$wt^{(Lc)}$	$wt^{(wt)}$	*p-value* [a]
1st litter	80.00	0.00	8.33	**<0.001** *
2nd litter	25.00	0.00	7.69	0.431
3rd litter	42.86	14.29	30.00	0.393

Note: Maternal cannibalism rate = total number of maternal cannibalism incidence/total number of parturitions × 100; $Lc^{(wt)}$ = *Lurcher* female mated with wild type male; $wt^{(Lc)}$ = wild type female mated with *Lurcher* male; $wt^{(wt)}$ = wild type female mated with wild type male
[a] Freeman-Halton extension of Fisher's exact test
* $Lc^{(wt)}$ vs. $wt^{(Lc)}$: $p<0.001$; $Lc^{(wt)}$ vs. $wt^{(wt)}$: $p=0.002$; $wt^{(wt)}$ vs. $wt^{(Lc)}$: $p=1.000$ (Fisher's exact post-hoc test).

were analyzed for all three litters together. The results from the mean litter size and pup survival rate are presented in Table 3. *Lurcher* dams showed significantly lower litter size on PP2 and PP30 as well as a lower pup survival rate compared to both groups of wild type controls. Breeding capacity of $wt^{(Lc)}$ and $wt^{(wt)}$ control groups was similar since no significant differences in: (1) fertility rate (CMH test: $wt^{(wt)}$ vs. $wt^{(Lc)}$: $\chi^2=1.70$, $p=0.192$; see Table 1), (2) delivery day (see Table 1), (3) maternal infanticide (CMH test: $wt^{(wt)}$ vs. $wt^{(Lc)}$: $\chi^2=0.76$, $p=0.384$; see Table 2) or (4) pups survival rate and litter size on PP2 and PP30 (see Table 3) were found.

DISCUSSION

Reproductive performance, maternal ability and overall breeding capacity of *Lurcher* females were studied. Although, *Lurcher* dams did not show any changes in reproductive performance compared to both control groups, maternal ability to progress pups from delivery to weaning was significantly affected. This behavioral disruption led to an overall decrease in breeding capacity of mutants.

Lurcher females did not show significantly altered fertility rate or delivery day. The reproductive system, namely conception capability and course of pregnancy in *Lurcher* females, does not seem to be markedly affected by the mutation. Mutation related motor disturbances present in *Lurchers* probably do not interfere with mating and sexual activity. Furthermore, the absence of differences between wild type females mated with wild type males and those mated with *Lurchers* suggest normal fertility and sexual activity in *Lurcher* males. These results are in contrast with previous findings for other cerebellar mutants, where mating impairment was likely, at least in part, a consequence of gait abnormalities, problems with body balance and reduced male fertility (Guastavino 1982; Guastavino *et al.* 1993). The only impairment of reproductive performance in *Lurcher* females was smaller litter size on PP2. The present study was not focused on prenatal examination of the number of fertilized oocytes or number of embryos. Therefore it is difficult to associate the reduced litter size, shortly after birth, as being prenatal related or perinatal related, i.e. natural pup death or maternal cannibalism.

Increased maternal infanticide, especially in primiparous dams and lower pup survival rate indicated poor maternal ability in *Lurcher* mutants. With regard to previously published results for other cerebellar mutants (Boufares *et al.* 1993; Bulloch *et al.* 1982) and unpublished observations, it was not assumed that maternal ability impairment was due to motor disorder in *Lurcher* dams. More likely it is indicative of a deficit in sensorimotor integration and affected emotionality of *Lurcher* mutants (Hilber *et al.* 2004; Porras-Garcia *et al.* 2005).

The cerebellar cortex can exert tonic inhibition on the amygdala, hippocampus and septum relative to the Papez circuit (Snider & Maiti 1976). Disruption of this suppression, by the mutant-related disappearance of Purkinje cells in *Lurcher* mutants, can induce changes in emotional behavior followed by an inability to select information during stressful events and the consequent loss of dependence on the environmental context.

Although, *Lurcher* mice have normal basal levels of adrenocorticotropic hormone (ACTH) and corticosterone (CORT), both hormones are dramatically elevated during mild stressful situations including common daily low stress events (Frederic *et al.* 1997), e.g. home-cage cleaning, handling or transfer to laboratory. Increased levels of corticotropin-releasing hormone (CRH), followed by increased CORT secretion, in cerebellar mutants (Frederic *et al.* 1997; Frederic *et al.* 2006), can influence the function of the amygdala and hippocampus, which are sensitive to both of these hormones (Giesbrecht *et al.* 2010; Maras & Baram 2012; Kavushansky & Richter-Levin 2006). The amygdala as well as hippocampus are also involved in the sensorimotor gating system (Miller *et al.* 2010), and play a role in stress and anxiety-related behavior. Therefore, affection of the central inhibitory system, together with the HPA axis hyper-reactivity, in *Lurcher* mutants can trigger a disproportionate behavioral reaction (Lorivel *et al.* 2010) and abnormal maternal behavior, e.g., neglecting, eating or killing their own pups. This hypothesis is supported by Poley (1974) who described higher stress reactivity to environmental stimuli as a factor causing maternal infanticide or cannibalism in rodents. The effect of CORT could be potentiated by the physiological increase in CORT level after the parturition (Zarrow *et al.* 1972) which has been suggested to modulate ongoing maternal behavior (Rees *et al.* 2004).

Tab. 3. Litter size and pup survival rate of *Lurcher* and wild type control dams. Data are presented as mean (± SEM).

	Litter size PP2	Litter size PP30	Pup survival rate
$Lc^{(wt)}$	3.92 (±0.47)	1.78 (±0.72)	49.21 (±17.84)
$wt^{(Lc)}$	6.65 (±0.31)	6.15 (±0.35)	91.86 (±3.59)
$wt^{(wt)}$	5.81 (±0.61)	5.61 (±0.60)	95.37 (±2.89)
p-value [a]	**0.008** [*]	**0.002** [†]	**0.015** [‡]

Note: Pup survival rate = number of weaned pups/number of live pups at PP2 × 100; PP2 = post-partum day 2; PP30 = post-partum day 30 (the weaning time); $Lc^{(wt)}$ = *Lurcher* female mated with wild type male; $wt^{(Lc)}$ = wild type female mated with *Lurcher* male; $wt^{(wt)}$ = wild type female mated with wild type male

[a] Kruskal-Wallis ANOVA with difference of means (95% CI for difference) and two-sample permutation test as a post-hoc analysis

[*] $Lc^{(wt)}$ vs. $wt^{(Lc)}$: –2.74 (–3.96, –1.72), $p<0.001$; $Lc^{(wt)}$ vs. $wt^{(wt)}$: –1.89 (–0.49, –2.15), $p=0.028$; $wt^{(wt)}$ vs. $wt^{(Lc)}$: 0.85 (–0.44, 2.22), $p=0.229$

[†] $Lc^{(wt)}$ vs. $wt^{(Lc)}$: –4.38 (–5.84, –2.65), $p<0.001$; $Lc^{(wt)}$ vs. $wt^{(wt)}$: –3.83 (–5.66, –1.89), $p<0.001$; $wt^{(wt)}$ vs. $wt^{(Lc)}$: 0.54 (–0.82, 1.84), $p=0.433$

[‡] $Lc^{(wt)}$ vs. $wt^{(Lc)}$: –42.65 (–79.17, –5.56), $p=0.001$; $Lc^{(wt)}$ vs. $wt^{(wt)}$: –46.16 (–82.32, –10.33), $p<0.001$; $wt^{(wt)}$ vs. $wt^{(Lc)}$: –3.52 (–12.02, 5.61), $p=0.806$.

Finally, the altered litter size on PP2 could be also related to the HPA axis being much more sensitive to environmental stimuli in *Lurcher* mutants compared to wild type mice (Frederic *et al.* 1997; Hilber *et al.* 2004). Chronically increased levels of ACTH and CORT inhibit follicle development, luteinizing hormone secretion and ovulation (Brann & Mahesh 1991). Therefore HPA axis hyper-reactivity may negatively influence oocyte development in *Lurcher* females.

In conclusion, *Lurcher* females showed reduced breeding capacity compared with healthy littermates. We hypothesize that, unlike other cerebellar mutants, anatomical disturbances of the reproductive system and motor impairment probably play a minor role in *Lurcher* mutant mice. Reduced numbers of offspring from *Lurcher* females is likely due to fewer pups being born and poor pup survival. Both these factors can be explained by HPA axis hyper-reactivity affecting oocyte development and triggering behavioral disinhibition caused by disruption of the central inhibitory system. The high incidence of maternal infanticide in *Lurchers* was probably a consequence of their behavioral disinhibition and abnormal stress reactivity, the pathogenesis of which involves the disappearance of cerebellar Purkinje cells. The hypothesis that HPA axis abnormalities and their secondary endocrine and behavioral consequences are probably responsible for the majority of reproduction disturbances in *Lurchers* is worth further examination using prenatal and behavioral studies.

ACKNOWLEDGEMENTS

We would like to thank to Helena Geciova, Irena Pojarova, Patrik Galeta, Ladislav Pecen. The study was supported by the Grant Agency of Charles University, Grant No. 613112 and SVV No. 266 803, Charles University Research Fund P36, COST No. LD12057 and LD12056 of the Ministry of Education, Youth and Sport of the Czech Republic and project CZ.1.05/2.1.00/03.0076 from European Regional Development Fund.

REFERENCES

1 Araki K, Meguro H, Kushiya E, Takayama C, Inoue Y, Mishina M (1993). Selective expression of the glutamate receptor channel delta 2 subunit in cerebellar Purkinje cells. Biochem Biophys Res Commun. **197**: 1267–1276.
2 Boufares S, Guastavino JM, Larsson K (1993). Restoration of staggerer mouse maternal behavior following long-term breeding selection. Physiol Behav. **53**: 1151–1155.
3 Brann DW, Mahesh VB (1991). Role of corticosteroids in female reproduction. FASEB J. **5**: 2691–2698.
4 Bulloch K, Hamburger RN, Loy R (1982). Nest-building behavior in two cerebellar mutant mice: staggerer and weaver. Behav Neural Biol. **36**: 94–97.
5 Caddy KW, Biscoe TJ (1979). Structural and quantitative studies on the normal C3H and Lurcher mutant mouse. Philos Trans R Soc Lond B Biol Sci. **287**: 167–201.
6 Frederic F, Chautard T, Brochard R, Chianale C, Wollman E, Oliver C, Delhaye-Bouchaud N, Mariani J (1997). Enhanced endocrine response to novel environment stress and endotoxin in Lurcher mutant mice. Neuroendocrinology. **66**: 341–347.
7 Frederic F, Chianale C, Oliver C, Mariani J (2006). Enhanced endocrine response to novel environment stress and lack of corticosterone circadian rhythm in staggerer (Rora sg/sg) mutant mice. J Neurosci Res. **83**: 1525–1532.
8 Giesbrecht CJ, Mackay JP, Silveira HB, Urban JH, Colmers WF (2010). Countervailing modulation of Ih by neuropeptide Y and corticotrophin-releasing factor in basolateral amygdala as a possible mechanism for their effects on stress-related behaviors. J Neurosci. **30**: 16970–16982.
9 Guastavino JM (1982). Sexual experience and successful mating in staggerer mutant mice. Behav Process. **7**: 183–188.
10 Guastavino JM, Boufares S, Crusio WE (2005). Ovarian abnormalities in the staggerer mutant mouse. Scientific World Journal. **5**: 661–664.
11 Guastavino JM, Larsson K (1992). The staggerer gene curtails the reproductive life span of females. Behav Genet. **22**: 101–112.
12 Guastavino JM, Larsson K, Allain C, Jaisson P (1993). Neonatal vestibular stimulation and mating in cerebellar mutants. Behav Genet. **23**: 265–269.
13 Heckroth JA, Eisenman LM (1991). Olivary morphology and olivocerebellar topography in adult lurcher mutant mice. J Comp Neurol. **312**: 641–651.
14 Hilber P, Caston J (2001). Motor skills and motor learning in Lurcher mutant mice during aging. Neuroscience. **102**: 615–623.
15 Hilber P, Jouen F, Delhaye-Bouchaud N, Mariani J, Caston J (1998). Differential roles of cerebellar cortex and deep cerebellar nuclei in learning and retention of a spatial task: studies in intact and cerebellectomized lurcher mutant mice. Behav Genet. **28**: 299–308.
16 Hilber P, Lorivel T, Delarue C, Caston J (2004). Stress and anxious-related behaviors in Lurcher mutant mice. Brain Res. **1003**: 108–112.
17 Chen YT, Collins LL, Uno H, Chou SM, Meshul CK, Chang SS, Chang C (2007). Abnormal cerebellar cytoarchitecture and impaired inhibitory signaling in adult mice lacking TR4 orphan nuclear receptor. Brain Res. **1168**: 72–82.
18 Cheng SS, Heintz N (1997). Massive loss of mid- and hindbrain neurons during embryonic development of homozygous lurcher mice. J Neurosci. **17**: 2400–2407.
19 Kavushansky A, Richter-Levin G (2006). Effects of stress and corticosterone on activity and plasticity in the amygdala. J Neurosci Res. **84**: 1580–1587.
20 Lorivel T, Gras M, Hilber P (2010). Effects of corticosterone synthesis inhibitor metyrapone on anxiety-related behaviors in lurcher mutant mice. Physiol Behav. **101**: 309–314.
21 Maras PM, Baram TZ (2012). Sculpting the hippocampus from within: stress, spines, and CRH. Trends Neurosci. **35**: 315–324.
22 Miller EJ, Saint Marie LR, Breier MR, Swerdlow NR (2010). Pathways from the ventral hippocampus and caudal amygdala to forebrain regions that regulate sensorimotor gating in the rat. Neuroscience. **165**: 601–611.
23 Mullen RJ, Eicher EM, Sidman RL (1976). Purkinje cell degeneration, a new neurological mutation in the mouse. PNAS. **73**: 208–212.
24 Norman DJ, Feng L, Cheng SS, Gubbay J, Chan E, Heintz N (1995). The lurcher gene induces apoptotic death in cerebellar Purkinje cells. Development. **121**: 1183–1193.
25 Phillips R (1960). "Lurcher", a new gene in linkage group XI of the house mouse. J Genet. **57**: 35–42.
26 Poley W (1974). Emotionality related to maternal cannibalism in BALB and C57BL mice. Anim Learn Behav. **2**: 241–244.
27 Porras-Garcia E, Cendelin J, Dominguez-Del-Toro E, Vozeh F, Delgado-Garcia JM (2005). Purkinje cell loss affects differentially the execution, acquisition and prepulse inhibition of skeletal and facial motor responses in Lurcher mice. Eur J Neurosci. **21**: 979–988.

28 Rees SL, Panesar S, Steiner M, Fleming AS (2004). The effects of adrenalectomy and corticosterone replacement on maternal behavior in the postpartum rat. Horm Behav. **46**: 411–419.
29 Schmahmann JD (2004). Disorders of the cerebellum: ataxia, dysmetria of thought, and the cerebellar cognitive affective syndrome. J Neuropsychiatry Clin Neurosci. **16**: 367–378.
30 Sidman RL, Green MC (1970). "Nervous," a new mutant mouse with cerebellar disease. Les Mutants Pathologiques ches l'Animal, Centre National De la Recherche. Saboury M. Paris**:** 69–79.
31 Snider RS, Maiti A (1976). Cerebellar contributions to the Papez circuit. J Neurosci Res. **2**: 133–146.
32 Zanjani SH, Selimi F, Vogel MW, Haeberle AM, Boeuf J, Mariani J, Bailly YJ (2006). Survival of interneurons and parallel fiber synapses in a cerebellar cortex deprived of Purkinje cells: studies in the double mutant mouse Grid2Lc/+;Bax(–/–). J Comp Neurol. **497**: 622–635.
33 Zarrow MX, Schlein PA, Denenberg VH, Cohen HA (1972). Sustained corticosterone release in lactating rats following olfactory stimulation from the pups. Endocrinology. **91**: 191–196.
34 Zuo J, De Jager PL, Takahashi KA, Jiang W, Linden DJ, Heintz N (1997). Neurodegeneration in Lurcher mice caused by mutation in delta2 glutamate receptor gene. Nature. **388**: 769–773.

Article 2

Jan Tuma, Yaroslav Kolinko, Frantisek Vozeh and Jan Cendelin

Mutation-related differences in exploratory, spatial, and depressive-like behavior in *pcd* and *Lurcher* cerebellar mutant mice

Frontiers in Behavioral Neuroscience 2015; 9: 116

frontiers in Behavioral Neuroscience

ORIGINAL RESEARCH
published: 12 May 2015
doi: 10.3389/fnbeh.2015.00116

Mutation-related differences in exploratory, spatial, and depressive-like behavior in *pcd* and *Lurcher* cerebellar mutant mice

Jan Tuma[1,2], *Yaroslav Kolinko*[1,3], *Frantisek Vozeh*[1,2] and *Jan Cendelin*[1,2]*

[1] Laboratory of Neurodegenerative Disorders, Faculty of Medicine in Pilsen, Biomedical Centre, Charles University in Prague, Pilsen, Czech Republic, [2] Department of Pathophysiology, Faculty of Medicine in Pilsen, Charles University in Prague, Pilsen, Czech Republic, [3] Department of Histology and Embryology, Faculty of Medicine in Pilsen, Charles University in Prague, Pilsen, Czech Republic

The cerebellum is not only essential for motor coordination but is also involved in cognitive and affective processes. These functions of the cerebellum and mechanisms of their disorders in cerebellar injury are not completely understood. There is a wide spectrum of cerebellar mutant mice which are used as models of hereditary cerebellar degenerations. Nevertheless, they differ in pathogenesis of manifestation of the particular mutation and also in the strain background. The aim of this work was to compare spatial navigation, learning, and memory in *pcd* and *Lurcher* mice, two of the most frequently used cerebellar mutants. The mice were tested in the open field for exploration behavior, in the Morris water maze with visible as well as reversal hidden platform tasks and in the forced swimming test for motivation assessment. *Lurcher* mice showed different space exploration activity in the open field and a lower tendency to depressive-like behavior in the forced swimming test compared with *pcd* mice. Severe deficit of spatial navigation was shown in both cerebellar mutants. However, the overall performance of *Lurcher* mice was better than that of *pcd* mutants. *Lurcher* mice showed the ability of visual guidance despite difficulties with the direct swim toward a goal. In the probe trial test, *Lurcher* mice preferred the visible platform rather than the more recent localization of the hidden goal.

Keywords: *Lurcher*, olivocerebellar degeneration, *pcd*, spatial learning, water maze

OPEN ACCESS

Edited by:
Denise Manahan-Vaughan, Ruhr University Bochum, Germany

Reviewed by:
Carsten T. Wotjak, Max-Planck-Institute of Psychiatry, Germany
Olivia Andrea Masseck, Ruhr University Bochum, Germany

***Correspondence:**
Jan Cendelin, Laboratory of Neurodegenerative Disorders, Faculty of Medicine in Pilsen, Biomedical Centre, Charles University in Prague, Alej Svobody 1655/76, Pilsen 323 00, Czech Republic
jan.cendelin@lfp.cuni.cz

Received: *15 January 2015*
Accepted: *21 April 2015*
Published: *12 May 2015*

Citation:
Tuma J, Kolinko Y, Vozeh F and Cendelin J (2015) Mutation-related differences in exploratory, spatial, and depressive-like behavior in pcd and Lurcher cerebellar mutant mice. Front. Behav. Neurosci. 9:116. doi: 10.3389/fnbeh.2015.00116

Introduction

Neurodegenerative disorders affecting the olivo-cerebellar system are manifested by well-characterized motor disorders. Nevertheless, the cerebellum is also involved in cognitive and behavioral processes, abnormalities of which have been described in humans (Schmahmann and Sherman, 1997; Cooper et al., 2010; Fancellu et al., 2013; Marien and Beaton, 2014), as well as in a wide spectrum of cerebellar mutant mice (for review see Manto and Marmolino, 2009; Cendelin, 2014). Cerebellar mutants are variable relative to the feature and extent of the cerebellar and extra-cerebellar neuronal degeneration. Moreover, the mutations appear in different mouse strains and these mutants retain specific phenotypic traits of the original strains. The importance of the genetic background for behavioral manifestation has been shown in gain-of-function (Cendelin et al., 2014) as well as loss-of-function mutations (Lalouette et al., 2001). Furthermore,

the review by D'hooge and de Deyn (2001) showed that sex differences, age, nutrition, stress, infections as well as experimental protocol, apparatus, and data analysis could markedly influence results in the Morris water maze task (Morris, 1984). With respect to these facts, it is therefore difficult to compare the behavioral phenotype of various mutations in mice of different background strains from different studies. On the other hand, the identification and understanding of specific impairments related to a particular mutation should be of interest regarding the variability of human hereditary cerebellar degenerations (Manto, 2005) and the use of mouse models for the development of disease-targeted therapeutic approaches.

In the present study, the behavioral phenotype of two of the most frequently used mouse models of olivocerebellar degeneration, *Lurcher* and *Purkinje cell degeneration* (*pcd*), were studied. *Lurcher* mice (Phillips, 1960) constitute the semi-dominant gain-of-function mutation in the δ2 glutamate receptor (GluRδ2) gene that changes the receptor into a leaky membrane channel, which chronically depolarizes the cell membrane (Zuo et al., 1997). GluRδ2 is expressed predominantly by Purkinje cells (Araki et al., 1993) and therefore, cell-autonomous degeneration of Purkinje cells is a primary effect of the mutation (Wetts and Herrup, 1982a,b). Virtually all Purkinje cells disappear by 3 months of age (Caddy and Biscoe, 1979). Fast reductions of cerebellar interneurons and inferior olive neuron numbers are due to secondary target-related cell death (Caddy and Biscoe, 1979; Wetts and Herrup, 1982a,b; Zanjani et al., 2006). *Lurchers* are characterized by ataxia (Fortier et al., 1987), spatial orientation impairments (Lalonde et al., 1988; Cendelin et al., 2008), and alterations of anxiety-related behaviors (Hilber et al., 2004). *Lurcher* mutation exists in two phenotypically undistinguishable alleles, the original one, $Grid2^{Lc}$ (Zuo et al., 1997), and $Grid2^{Lc-J}$ (de Jager et al., 1997). For experiments, $Grid2^{Lc}$ mutants have been used, e.g., in B6CBA and C3H (Caddy and Biscoe, 1979; Cendelin et al., 2014) strain backgrounds.

Pcd mice (Mullen et al., 1976) carry a recessive loss-of-function mutation in the gene encoding the cytosolic ATP/GTP binding protein 1 (*Agtpb1*), a.k.a. *Nna1* (Fernandez-Gonzalez et al., 2002). *Nna1* is expressed throughout the brain and retina with prominence in cerebellar Purkinje cells (Mullen et al., 1976; Baltanas et al., 2011), mitral cells of the olfactory bulb (Greer and Shepherd, 1982), thalamic neurons (O'Gorman, 1985; O'Gorman and Sidman, 1985), and retinal photoreceptors (Blanks et al., 1982; Lavail et al., 1982). Histopathological analysis of *pcd* mice revealed rapid Purkinje cell loss between the third and fourth postnatal week (Baltanas et al., 2013), slowly progressive cerebellar granule cell degeneration, moderate reduction of the deep cerebellar nuclei, and slow degeneration of inferior olivary neurons that are supposed to be secondary to the loss of Purkinje cells (Ghetti et al., 1987; Triarhou et al., 1987). The photoreceptor decrease progresses slowly and even after 9 months of life, some photoreceptors are retained (Marchena et al., 2011). *Pcd* mice suffer from ataxia (Mullen et al., 1976; Goodlett et al., 1992) and a deterioration of spatial navigation learning (Goodlett et al., 1992). The *pcd* mutation exists in several different alleles (Wang and Morgan, 2007). *Pcd* mice carrying the original allele $Agtpbp1^{pcd}$ have been used for experiments, e.g., in B6.BR (Vinueza Veloz et al., 2014), C57BL/6J (Zhang et al., 1996), or B6C3Fe (Rotter et al., 2000) strains.

Both mutants constitute a distinct type of mutation affecting the olivo-cerebellar system either exclusively (*Lurcher*) or inclusively (*pcd*) and determining a strong pathological phenotype. Distinct histopathological similarities predestine them to frequent mutual comparisons, mostly often indirect (Furuya et al., 1994; Lalonde and Thifault, 1994; Le Marec and Lalonde, 1997, 2000), but none of these studies have involved systematic experiments. Therefore, the aim of this study was to test the behavioral phenotype of *pcd* and *Lurcher* mice with particular attention paid to cognitive and emotional disturbances under the same environmental conditions. We also aimed to assess the comparability of the mutants, which are not commercially available in identical strains. Thus, healthy littermates were also tested to assess the role of the genetic backgrounds.

Materials and Methods

Animals

Two cohorts of adult (3 months) B6.BR pcd^{1J} and B6CBA *Lurcher* mutants and their healthy wild type littermates of both sexes were used (for *n*, see **Table 1**). Both B6.BR *pcd* and wild type mice were obtained by crossing heterozygous males and females. Both B6CBA *Lurcher* and wild type mice were obtained by crossing wild type females with heterozygous *Lurcher* males. All animals were housed in the same breeding facility under standard laboratory conditions in a temperature and humidity controlled room with a 12/12 h light/dark cycle (6 a.m. to 6 p.m.). The tests were performed during the light phase of the cycle. Animals were kept in plastic cages with wooden shavings and maintained with a standard commercial pellet diet and water *ad libitum*. All experimental procedures were performed in compliance with the EU Guidelines for Scientific Experimentation on Animals and with the permission of the Ethical Commission of the Faculty of Medicine in Pilsen.

Experimental Design

To eliminate the influence of the tests on behavior, two cohorts of mice were used. Cohort A was used for analysis of the explorative behavior in the open field and spatial learning, orientation and navigation in the Morris water maze. Cohort B was used for assessment of motivation and depressive-like behavior in the water environment. The body weight of mice from both cohorts was measured on the first day of the experiment before the tests. For behavioral tests and body weight evaluation, male and female mice were considered separate experimental groups. Since *pcd* mice are known to suffer from retinal degeneration (Blanks et al., 1982; Lavail et al., 1982), the retinas of samples of *pcd* mutants were examined stereologically and compared with those from their B6.BR wild type littermates as well as with retinas of B6CBA *Lurcher* and wild type mice to assess the presence and extent of photoreceptor degeneration at the time of finishing the behavioral testing.

TABLE 1 | Mean ± SEM (*n*) body weight of 3-month-old *pcd* and *Lurcher* mice and their healthy littermate controls (separately for both cohorts).

	B6.BR		B6CBA	
	pcd	**wild type**	***Lurcher***	**wild type**
COHORT 1				
Females (g)	15.96 ± 1.262 (16)	21.57 ± 0.986 (22)	20.49 ± 1.847 (17)	22.00 ± 1.887 (21)
Males (g)	19.56 ± 2.350 (16)	26.51 ± 2.509 (17)	24.79 ± 1.847 (19)	27.89 ± 1.885 (18)
COHORT 2				
Females (g)	15.53 ± 2.911 (14)	22.32 ± 1.052 (13)	20.01 ± 1.507 (14)	22.92 ± 1.168 (12)
Males (g)	19.03 ± 3.199 (11)	27.81 ± 1.519 (16)	24.56 ± 1.272 (12)	28.47 ± 1.574 (15)

Behavioral Testing

Open Field

Explorative behavior and spontaneous motor activity were analyzed using the open field test. The apparatus consisted of a white open top plastic box (50 × 50× 50 cm) with an illumination intensity of 20 lux at the box floor level. The subject was placed in the center of the open field and left undisturbed for 5 min. The apparatus was cleaned with 70% ethanol between subjects. The activity was recorded using EthoVision® XT 7.1 (Noldus Information Technology b.v., Netherlands). The locomotion activity (% of the test duration), distance moved (cm), thigmotaxis (% moved distance in the 3 cm border zone), and mean walking speed (cm/s) were evaluated.

Morris Water Maze Task

The goal-directed navigation and spatial learning were evaluated using a Morris water maze task (Morris, 1984). The apparatus consisted of a circular white plastic pool (100 cm in diameter × 55 cm in height), with the water level set at a height of 35 cm above the base. The pool was filled with water (26 ± 2°C) and illuminated with 70 lux at the water surface. Escape from the water was provided by a transparent circular PlexiGlass platform (7.5 cm in diameter; 0.5 cm below the water level). Four starting points around the circumference of the pool were arbitrarily designated: North (N), South (S), West (W), and East (E). Each animal performed four trials per day-session with 16 min inter-trial intervals. The subject was introduced into the pool facing the wall in one of four starting positions. The maximal time for the platform location was 60 s. If the mouse did not locate the platform within the allotted time, it was manually placed on the platform. After each trial, the mouse was left on the platform for 30 s.

The water maze test consisted of 12 consecutive day-sessions arranged into three phases: visible platform test (day-sessions 1–5), reversal hidden platform test (day-sessions 6–11), and probe trial (day-session 12). For the visible platform test, the hidden escape platform position was highlighted by a cylindrical label (3 cm in diameter; 5 cm in height) with vertical black and white stripes mounted 12 cm above the submerged platform. The label served as a cue for visual goal-directed navigation. Platform position and starting point order is schematically depicted in **Figure 1**. For the probe trial, the escape platform was removed, and each mouse was allowed to swim freely for 60 s per trial.

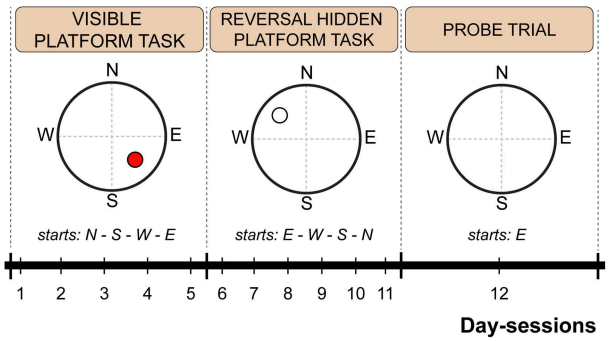

FIGURE 1 | Scheme of the Morris water maze protocol indicating time schedule, platform position and starting point sequence. The red circle indicates a visible platform position. An empty circle indicates a hidden platform position. Dashed lines represent imaginary quadrant borders.

The movement of the mice in the maze was recorded using EthoVision® XT 7.1. Escape latencies (s) and distance moved (cm) were measured as the basic parameters of the performance in the Morris water maze task. Swimming speed during periods of activity (i.e., excluding floating periods) was calculated to assess the swimming ability of the mice and to evaluate the relationship between latency and distance moved. Mouse navigation and orientation relative to the escape platform position was determined as the heading angle error and direct swim percentage. The heading angle error was measured as a deviation from a direct line from the starting point to the center of the platform. As direct swim, those trials with a shorter distance moved than the length of a direct line connecting the starting point and the platform multiplied by 1.3 were considered (Cendelin et al., 2014). The exploration strategy was evaluated using thigmotaxis (% moved distance in the 10 cm margin zone of the maze). Floating (% of time spent inactive) was assessed as a specific behavioral event. Spatial learning and memory were assessed using the preference for the NW or SW quadrant, respectively (% of distance moved), for the first 30 s of the first start of the probe trial only to avoid the effect of adaptation on the missing platform.

Forced Swimming Test

The motivation to swim and depressive-like behavior were analyzed using the Porsolt's forced swimming test (Porsolt et al., 1979). Mice were immersed in a glass water tank (diameter:

18 cm; height: 26 cm; water depth: 19 cm). The water was maintained at 26 ± 2°C and illuminated with 70 lux at the water surface. The mouse was left to swim without any possibility of escape for 15 min per day-session for three consecutive days. Immobility periods were recorded using EthoVision® XT 7.1, and relative immobility (% of total time) was calculated. To assess the development of depressive-like behavior within a day-session, immobility periods were evaluated separately in three 5-min time-bouts for each day-session.

Quantitative Histology of the Retina

The presence and extent of retinal degeneration in *pcd* mutants ($n = 8$) compared with their healthy littermates ($n = 8$) and B6CBA mice (*Lurcher*: $n = 8$; WT: $n = 8$) was assessed using stereological analysis. Paraformaldehyde-fixed right eyes of four females and four males per group were processed into 10 µm thick serial sections with random orientation. Every fifteenth section was stained with Gill's hematoxylin and scanned as a stack of four 2.5 µm optical sections using an Olympus C-5060 digital camera coupled to an Olympus CX31 microscope (Olympus, Tokyo, Japan) using an 60× objective with a numerical aperture of 1.35. To count the retinal photoreceptor cell nuclei, nine dissector-counting frames were randomly imposed on each stack (Glaser et al., 2007), taking into account only those optical dissectors located in the outer nuclear layer (ONL) of the retina (352 ± 15 dissectors for each animal). The volume of the retina and total number of photoreceptor nuclei were estimated using the fractionator method. Finally, the number of photoreceptor nuclei was related to the retina volume and numerical density was determined (Gundersen, 1986; Boyce et al., 2010). The mean coefficient of sampling error (CE) was 4.7% for the ONL volume and 4.4% for the retina volume (Gundersen and Jensen, 1987).

Statistical Analysis

Data were analyzed using traditional statistical tests extended with a non-parametric permutational approach (Pesarin and Salmaso, 2010). Three-Way ANOVA or Three-Way ANOVA with repeated measurements were evaluated, and the following factors were analyzed: type—cerebellar mutant (CM)/wild type (WT), strain—B6CBA/B6.BR, sex—female/male, and within-group factors day-session and/or time-bout (session, bout; if applicable). Interactions of these factors were also assessed. All ANOVA-tests were followed by planned comparisons performed using *t*-tests with a Bonferroni correction for repeated measurements (day-session and/or time-bout). The data ordered in a paired design were analyzed using the paired *t*-test. The preference for the selected quadrants was verified using the one-sample *t*-test against a value of 25%, which represents a random occurrence. The data are presented as mean ± SEM. $p < 0.05$ was considered statistically significant. Reported *F* and *t*-values are considered as F_0 and t_0, respectively, before the start of permutational tests. ANOVAs and *t*-tests were performed with maximal 5000 and 10,000 permutations, respectively. Statistical analyses were conducted using the R version 3.1.2 for Mac OS.

Results

Body Weight

The mean body weight of mice is presented in **Table 1**. Both *pcd* and *Lurcher* mutants showed significantly reduced body weights compared to their healthy counterparts. Moreover, *pcd* mice showed significantly lower body weights compared to *Lurchers,* even though the wild type mice for both groups were not different (for statistics see Supplementary Table 1).

Open Field

Spatial distribution of the exploratory activity in the open field is presented in **Figure 2A**. Despite an evident preference for corners of the square arena in all experimental groups, B6CBA mice, and especially B6CBA *Lurchers,* showed a higher tendency to explore the entire arena. The significance of individual parameters measured in the open field on individual factors (type, strain, sex) and their interactions are shown in **Table 2**.

Distance moved is shown in **Figure 2B**. While *pcd* females moved a shorter distance in the open field than B6.BR wild type females, *Lurcher* females walked longer distances than B6CBA wild type females. In males, no significant differences were found between mutant and wild type mice. Wild type females and *pcd* and wild type males of the B6.BR strain had longer distances moved than did their B6CBA counterparts. *Pcd* males moved longer distances than *pcd* females ($t = -3.68$, $p < 0.001$) and B6CBA wild type males moved longer distances than females ($t = -2.40$, $p < 0.020$).

Locomotion activity is shown in **Figure 2C**. The activity was higher in *Lurcher* females than in B6CBA wild type females and in *pcd* males than in B6.BR wild type males. Strain comparison showed higher activity in B6.BR wild type females, mutant and wild type males than in their B6CBA counterparts. *Pcd* males had higher locomotion activity than *pcd* females ($t = -3.76$, $p < 0.001$), and B6CBA wild type males were more active than females ($t = -2.52$, $p < 0.013$).

Thigmotaxis is displayed in **Figure 2D**. Thigmotaxis was significantly lower in *Lurcher* males than in B6CBA wild type males. B6.BR males showed higher thigmotaxis than B6CBA males. There was no effect of sex on thigmotaxis in the open field.

The parameter walking speed is shown in **Figure 2E**. Walking speed in the open field arena was lower in *pcd* females than in B6.BR wild type females, in *pcd* males than in B6.BR wild type males, and in *Lurcher* males than in B6CBA wild type males. Strain comparison showed that *pcd* females walked slower than *Lurcher* females, but *pcd* males were faster than *Lurcher* males. Both B6.BR wild type females and males achieved a higher walking speed than B6CBA wild type mice. *Pcd* males showed higher walking speed than *pcd* females ($t = -3.59$, $p < 0.001$), and B6CBA wild type males walked faster than females ($t = -2.02$, $p < 0.048$).

Morris Water Maze

Parameters measured in the Morris water maze are displayed in **Figures 3–5**. For the significance of the effect of individual factors (type, strain, sex, day-session) and their interactions on parameters measured in the Morris water maze, see **Tables 3**, **4**.

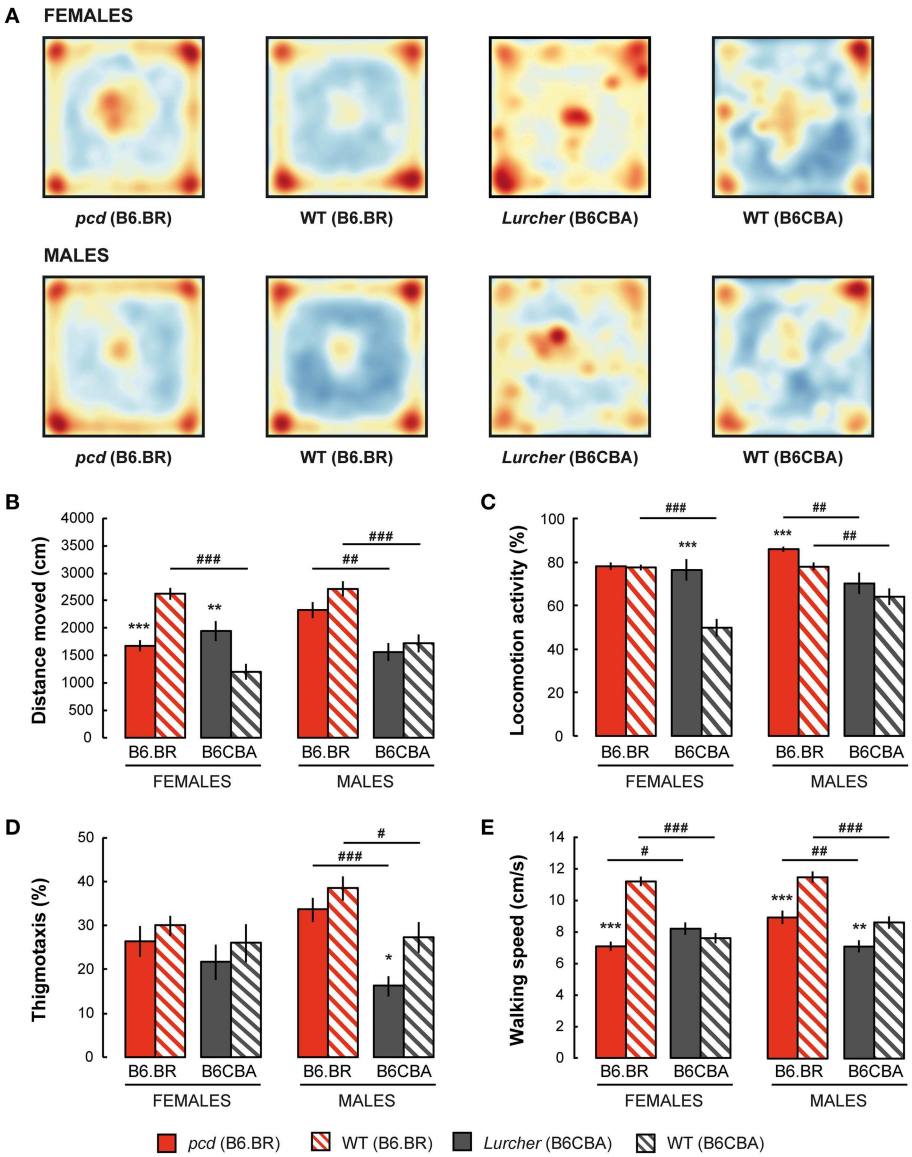

FIGURE 2 | Open field test: (A) Superposition of trajectories (frequency of animal presence) for females and males in the arena; (B) Total distance moved (cm); (C) Percentage of time spent with locomotion activity (%); (D) Percentage of thigmotaxis (% moved distance in the 3 cm border zone) and (E) Mean walking speed (cm/s) during locomotion activity periods. Statistical significance was evaluated using a permutational *t*-test. Within-strain comparison: $^{*}p < 0.05$, $^{**}p < 0.01$, and $^{***}p < 0.001$. Between-strain comparison: $^{\#}p < 0.05$, $^{\#\#}p < 0.01$, and $^{\#\#\#}p < 0.001$. Data are presented as mean ± SEM.

Typical examples of trajectory shapes observed during the experiment are shown in **Figures 6A–F**.

Escape Latencies

Escape latencies in the Morris water maze (**Figure 3A**) were significantly longer in both types of cerebellar mutants than in their wild type littermates during the test with the visible as well as the hidden platform. The only day on which the difference was low (for the B6.BR mice, it was insignificant) was the first day with the hidden platform moved into the opposite quadrant (D6). Strain comparison showed smaller differences in both mutant as well as wild type mice. Compared with *Lurchers*, *pcd* mice (both males and females) had longer latencies in the visible platform task, while no differences between the mutants were found during the hidden platform task. In addition, B6.BR wild type mice achieved worse results than their B6CBA counterparts did (for females, only at the beginning of the visible platform task, but for males also at the end of the hidden platform task). The direct comparison of females and males showed differences in B6.BR wild type mice only on the day-session 3 ($t = -5.28$, $p < 0.001$) and day-session 5 ($t = -2.72$, $p = 0.023$).

Distance Moved

Distance moved (**Figure 3B**) was significantly longer in *Lurcher* mice compared with wild type B6CBA mice on all days of the test. On the other hand, *pcd* mice showed a markedly longer

TABLE 2 | Open field test: statistical significances of the between-group factors (type, strain, and sex) and their interactions.

Between-group factors	Distance		Locomotion		Thigmotaxis		Walking speed	
	$F_{(1, 138)}$	p	$F_{(1, 138)}$	p	$F_{(1, 138)}$	p	$F_{(1, 138)}$	P
Type	3.24	0.045	18.12	<0.001	6.32	0.007	55.21	<0.001
Strain	48.45	<0.001	37.04	<0.001	15.63	<0.001	49.22	<0.001
Sex	4.14	n.s.	2.80	n.s.	1.48	n.s.	4.28	0.020
Type:Strain	21.06	<0.001	6.12	0.005	0.54	n.s.	31.48	<0.001
Type:Sex	0.66	n.s.	1.76	n.s.	0.70	n.s.	0.30	n.s.
Strain:Sex	2.08	n.s.	0.00	n.s.	4.41	0.032	4.77	0.023
Type:Strain:Sex	12.46	<0.001	8.38	0.004	0.33	n.s.	13.01	<0.001

Permutational Three-Way ANOVA.

trajectory than wild type B6.BR mice only in the visible platform task, except for on the first day, while the difference appeared only occasionally in the next phase. In wild type mice, mild strain differences appeared only in the visible platform task. Nevertheless, in the mutants, a significant difference appeared in the hidden platform task when the distance moved was markedly longer in *Lurchers* than in *pcd* mice. Sex differences were found only on the day-session 3 in B6.BR wild type mice ($t = -2.72$, $p = 0.037$).

Swimming Speed

Swimming speed (**Figure 3C**) was significantly lower in *pcd* mice than in other mice.

On the other hand, *Lurchers* did not swim slower than their wild type littermates. *Lurcher* males were even significantly faster than wild type ones on day-session 1. Strain comparison showed a slower swimming speed in B6.BR wild type mice than in B6CBA ones, namely in the visible platform phase. There were no significant sex differences in swimming speed.

Heading Deviation

Heading deviation error (**Figure 4A**) was significantly higher in mutant mice than in their wild type littermates. In the B6.BR strain, the differences were mainly seen in the visible platform task, while, in the B6CBA strain, they were significant for almost the entire course of the experiment. In females, no strain differences were seen. B6.BR wild type males were occasionally worse than B6CBA males. The only sex difference in heading deviation error was found on the day-session 10 in B6.BR wild type mice ($t = -3.42$, $p = 0.011$).

Direct Swim

The percentage of direct swim trials (**Figure 4B**) was high in wild type mice of both strains in the visible platform task except for the first day session. Also, on some days of the hidden platform task, wild type mice showed a significantly higher percentage of direct swim trials than their mutant littermates. In mutant mice, direct swim trials were rare in both phases of the test. Strain differences showing better performance in B6CBA mice were only seen for a few day-sessions and mainly for wild type mice. Males and females did not differ in direct swim percentage.

Thigmotaxis

Thigmotaxis (**Figure 5A**) was significantly higher in both cerebellar mutants than in wild type animals on most days of the water maze test. Strain differences, on the other hand, were poor. The only difference between males and females was found on the day-session 5 in B6.BR wild type mice ($t = -3.19$, $p = 0.010$).

Floating Analysis

Floating analysis (**Figure 5B**) revealed almost no differences in the percentage of time spent without activity between mutant and wild type mice. Nevertheless, in cerebellar mutants, a strain difference was observed, since floating behavior was very rare in *Lurcher* mutants. B6.BR wild type males spent significantly more time floating than females on the day-session 3 ($t = -3.47$, $p = 0.003$), day-session 4 ($t = -2.86$, $p = 0.015$), day-session 5 ($t = -2.87$, $p = 0.013$), and day-session 7 ($t = -2.87$, $p = 0.035$).

Morris Water Maze Task Acquisition

Significance of the within factor (day-session) indicated the importance of development of the parameters during the course of the Morris water maze test (**Tables 3, 4**). Learning process, which was manifested as a shortening of escape latencies (**Figure 3A**, **Table 5**) and distance moved (**Figure 3B**, **Table 5**), was detectable for the visible platform task in all groups of mice and for the hidden platform task for both B6CBA and B6.BR wild type mice and B6CBA *Lurcher* males. *Lurcher* females and both *pcd* males and females did not learn the hidden platform task (**Table 5**). Wild type mice of both strains also showed a significant decrease of heading deviation error (**Figure 4A**, **Table 5**) and an increase of the direct swim percentage (**Figure 4B**, **Table 5**) during both visible and hidden platform tasks. *Lurcher* mice improved heading deviation and direct swim percentage (males only) during the visible platform task, but not during the hidden platform task. *Pcd* mice did not improve their heading deviation or direct swim percentage in either of the tasks.

Change of the platform position and its concealment (compare day-sessions 5 and 6) led to significant prolongation of both latencies and distance moved in all groups of mice (**Figures 3A,B**, **Table 5**), an increase in heading deviation error in all groups except *pcd* females (**Figure 4A**, **Table 5**) and a decrease in the direct swim percentage in wild type mice and *Lurcher*

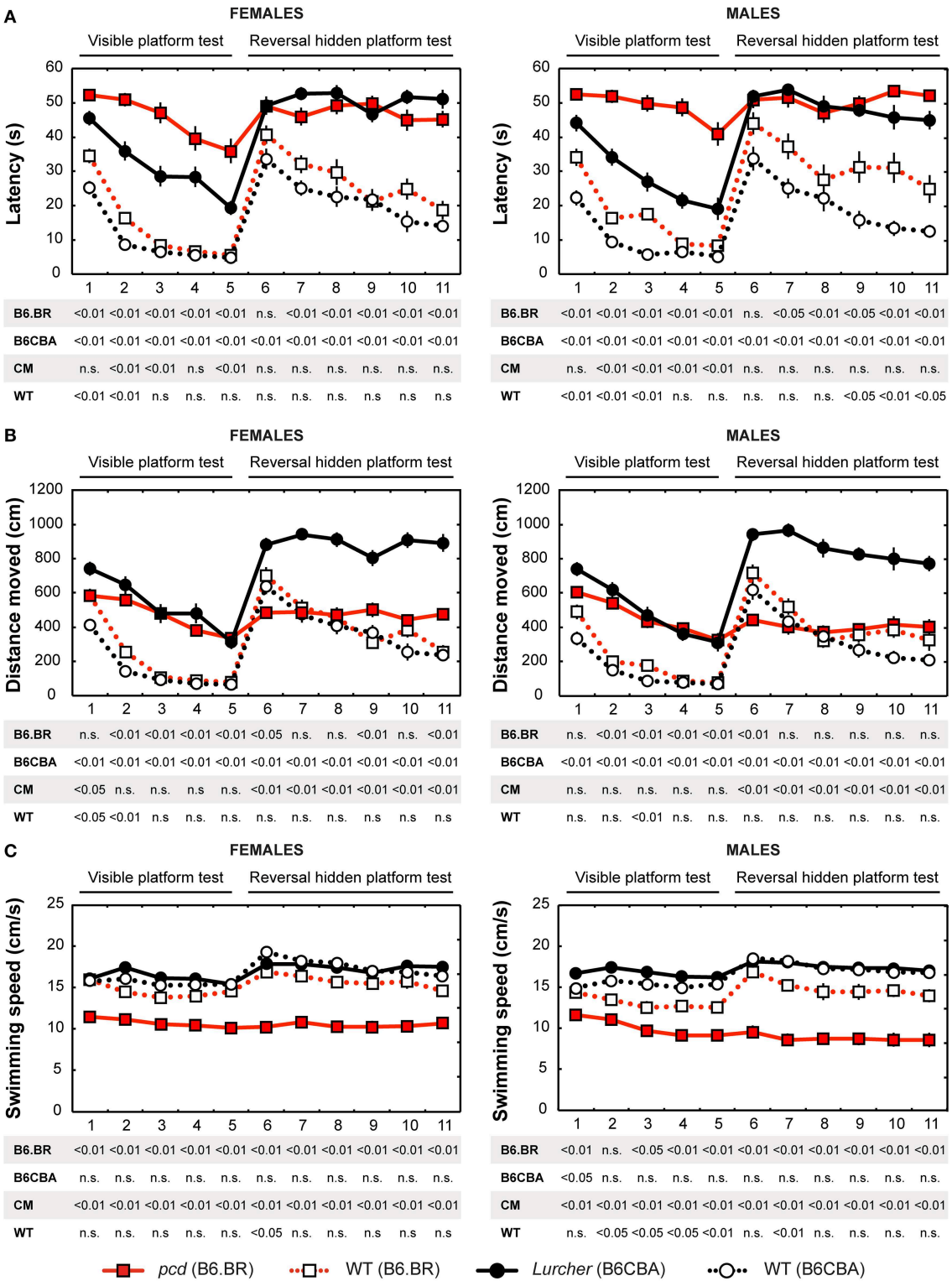

FIGURE 3 | Morris water maze: (A) Mean escape latency (s); (B) Total distance moved (cm) and (C) Mean swimming speed during periods of active swimming (cm/s). Statistical significance was evaluated using permutational *t*-test with Bonferroni correction for the repeated measurement for within-strain comparisons (*pcd* vs. B6.BR wild type, *Lurcher* vs. B6CBA wild type) as well as for between-strain comparisons of cerebellar mutants (CM; *pcd* vs. *Lurcher*) and wild types (WT; B6.BR WT vs. B6CBA WT). Data are presented as mean ± SEM.

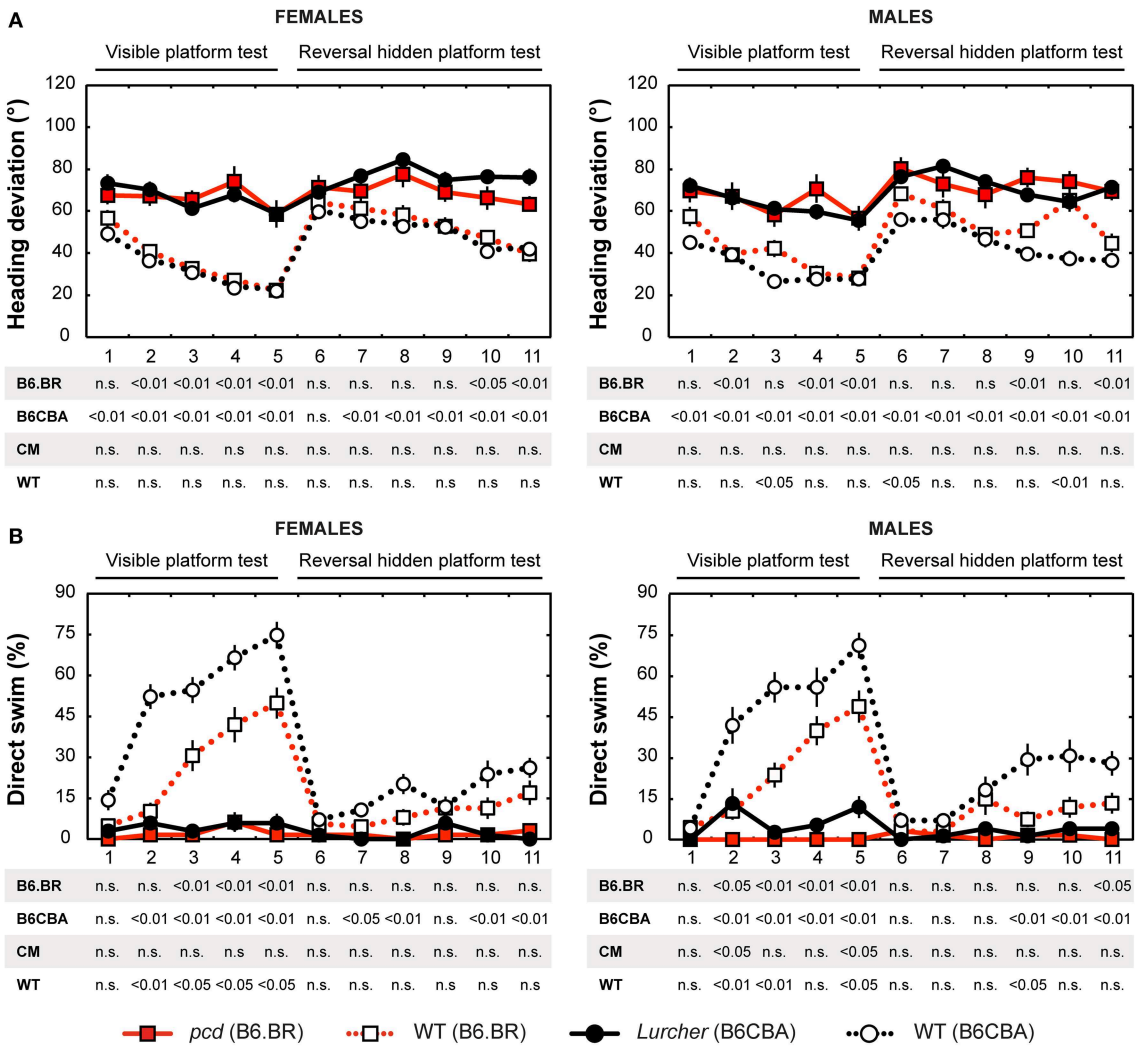

FIGURE 4 | Morris water maze: (A) Heading deviation (°) from the direct swim to the platform and (B) Percentage of direct swim trials (%). Statistical significance was evaluated using permutational *t*-test with Bonferroni correction for the repeated measurement for within-strain comparisons (*pcd* vs. B6.BR wild type, *Lurcher* vs. B6CBA wild type) as well as for between-strain comparisons of cerebellar mutants (CM; *pcd* vs. *Lurcher*) and wild types (WT; B6.BR WT vs. B6CBA WT). Data are presented as mean ± SEM.

males (**Figure 4B**, **Table 5**). The effect of change of the platform position and its concealment is also shown in Supplementary Figure 1.

Probe Trial

Probe trial on the last day of the Morris water maze test showed a mild preference for the NW quadrant in which the hidden platform was localized for the previous 6 day-sessions in B6CBA and B6.BR wild type mice. Surprisingly, both types of cerebellar mutants showed a significant preference for the SE quadrant, where the visible platform was localized during the first phase of the water maze test (**Figure 6G**). These findings were confirmed by the measurement of latency of the first occurrence in the former position of the visible and hidden platform (Supplementary Figure 2).

Forced Swimming Test

Depressive-like behavior, which manifested as a state of immobility in the Porsolt's forced swimming test, is presented in **Figure 7**. The analysis showed a significant between-group effect of the type and strain, but not their interaction (**Table 6**). Nevertheless, a Three-Way ANOVA showed a significant effect of type:sex as well as type:strain:sex factor interactions (**Table 6**). A repeated measurement ANOVA also showed a significant within-group factor effect of the time-bout and day-session (**Table 6**).

Total length of immobility in *pcd* females did not significantly differ from that in B6.BR wild type females (except the first 5 min time-bout in day-session 3). On the contrary, *pcd* males showed less immobility than B6.BR wild type males (**Figure 7**). In B6CBA mice, both *Lurcher* females and males had a shorter duration of immobility than did wild type mice in most time-bouts of day-session 2 and 3 (**Figure 7**). The occurrence of immobility

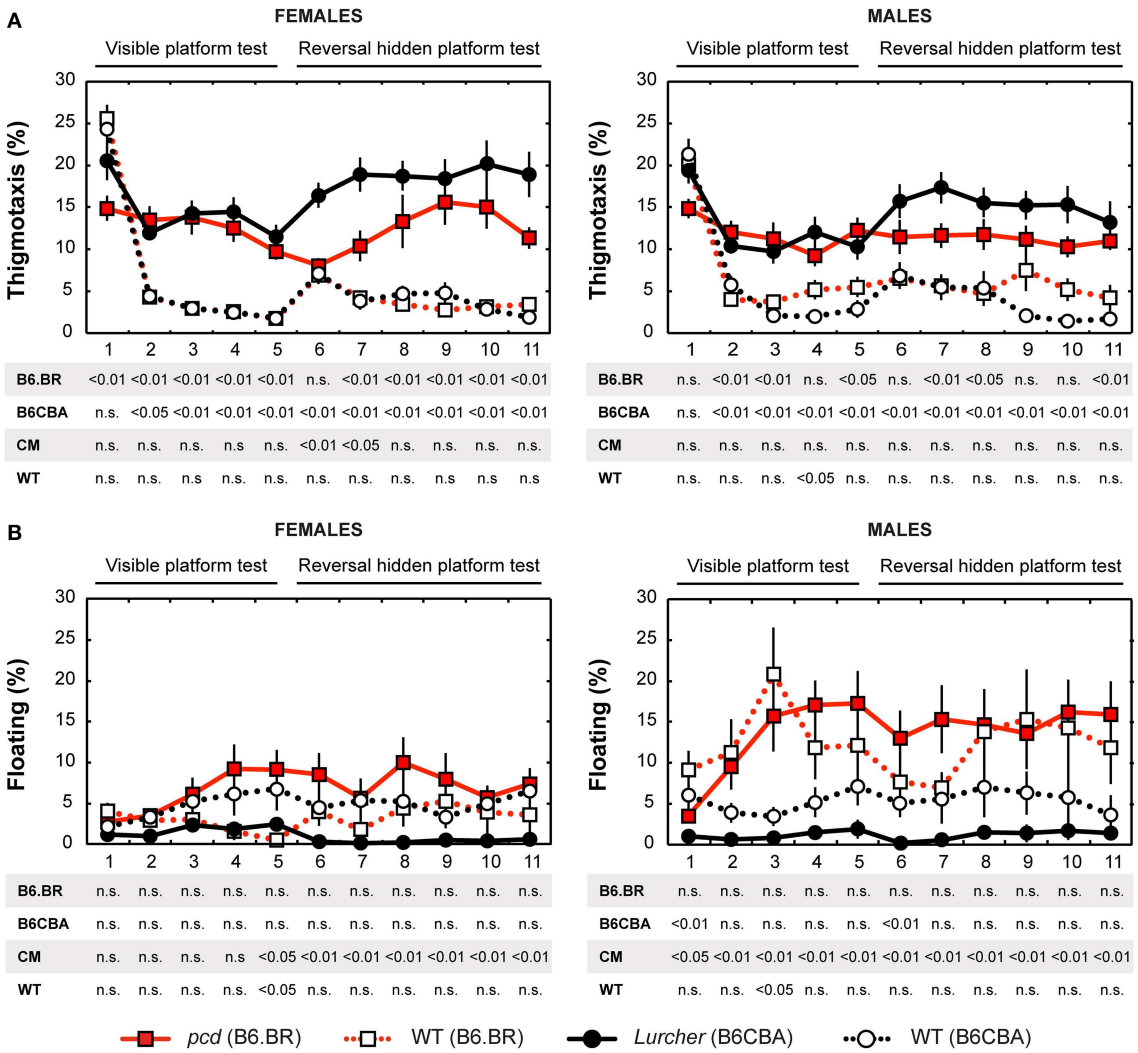

FIGURE 5 | Morris water maze: (A) Percentage of thigmotaxis (% of distance moved in 10 cm border zone) and (B) Percentage of floating (% of time spent without swimming). Statistical significance was evaluated using permutational *t*-test with Bonferroni correction for the repeated measurement for within-strain comparisons (*pcd* vs. B6.BR wild type, *Lurcher* vs. B6CBA wild type) as well as for between-strain comparisons of cerebellar mutants (CM; *pcd* vs. *Lurcher*) and wild types (WT, B6.BR WT vs. B6CBA WT). Data are presented as mean ± SEM.

periods was very low in *Lurcher* mice; thus, their immobility state duration was significantly shorter than in *pcd* mice in each day-session for females and the last 2 day-sessions for males. B6CBA wild type females showed less immobility than B6.BR wild type females in the first time-bout for day-session 1 and 2 as well as the first two time-bouts on day-session 3. The sex differences were found in *pcd* mice; males showed less immobility than females (**Figure 7**).

Furthermore, while the immobility was permanently rare in *Lurchers*, its duration increased from the day-session 1 to 3 in other mice (**Table 7**). For pair comparison of time-bout 1 vs. time-bout 3 for each day-session, see Supplementary Table 2.

Quantitative Histology

Stereological analysis showed only an insignificant reduction in the density of retinal photoreceptors nor ONL volume relative to whole retina volume in *pcd* mutants compared with their healthy littermates, or with B6CBA *Lurcher* and wild type mice (**Figure 8**).

Discussion

In this study, we have shown specific features of spatial performance and behavioral differences in response to the Morris water maze task in *pcd* and *Lurcher* mice, the most frequently used mouse models of olivocerebellar degeneration (for review, see Lalonde and Strazielle, 2007; Cendelin, 2014). Although it has been described that the neurodegenerative process disrupts spatial learning in both mutants, specific features of their spatial performance, which are presented here, have not been reported and sufficiently explained before, and even

TABLE 3 | Morris water maze—escape latency, distance moved, and swimming speed: statistical significances of the between-group factors (type, strain, and sex) and within-group factors (session) as well as their interactions.

VISIBLE PLATFORM TASK						
Between-group factors	**Latency**		**Distance moved**		**Swimming speed**	
	$F_{(1, 138)}$	p	$F_{(1, 138)}$	p	$F_{(1, 138)}$	p
Type	665.03	<0.001	424.95	<0.001	15.29	<0.001
Strain	100.00	<0.001	0.01	n.s.	148.94	<0.001
Sex	0.70	n.s.	1.18	n.s.	2.41	n.s.
Type:Strain	31.43	<0.001	15.00	<0.001	58.87	<0.001
Type:Sex	0.11	n.s.	0.03	n.s.	1.62	n.s.
Strain:Sex	4.91	n.s.	0.07	n.s.	3.88	0.043
Type:Strain:Sex	0.57	n.s.	0.17	n.s.	0.01	n.s.
Within-group factors	$F_{(4, 552)}$	p	$F_{(4, 552)}$	p	$F_{(4, 552)}$	p
Session	221.38	<0.001	251.08	<0.001	13.52	<0.001
Type:Session	15.50	<0.001	17.14	<0.001	2.22	n.s.
Strain:Session	1.66	n.s.	0.47	n.s.	7.08	<0.001
Sex:Session	1.62	n.s.	0.95	n.s.	0.90	n.s.
Type:Strain:Session	14.23	<0.001	11.25	<0.001	0.95	n.s.
Type:Sex:Session	0.68	n.s.	2.79	<0.001	0.09	n.s.
Strain:Sex:Session	2.01	n.s.	0.80	n.s.	0.21	n.s.
Type:Strain:Sex:Session	2.62	0.037	1.50	n.s.	0.85	n.s.
REVERSAL HIDDEN PLATFORM TASK						
Between-group factors	**Latency**		**Distance moved**		**Swimming speed**	
	$F_{(1, 138)}$	p	$F_{(1, 138)}$	p	$F_{(1, 138)}$	p
Type	291.22	<0.001	192.35	<0.001	57.66	<0.001
Strain	6.71	0.005	89.06	<0.001	163.72	<0.001
Sex	0.66	n.s.	3.50	n.s.	2.72	n.s.
Type:Strain	11.03	0.008	176.79	<0.001	60.70	<0.001
Type:Sex	0.07	n.s.	0.48	n.s.	0.14	n.s.
Strain:Sex	4.45	0.025	0.01	n.s.	2.48	0.048
Type:Strain:Sex	0.05	n.s.	1.50	n.s.	0.43	n.s.
Within-group factors	$F_{(5, 690)}$	p	$F_{(5, 690)}$	p	$F_{(5, 690)}$	p
Session	28.67	<0.001	43.91	<0.001	16.82	<0.001
Type:Session	15.68	<0.001	20.09	<0.001	5.42	<0.001
Strain:Session	1.13	n.s.	1.33	n.s.	0.47	n.s.
Sex:Session	1.09	n.s.	1.11	n.s.	0.62	n.s.
Type:Strain:Session	1.21	n.s.	1.75	0.025	0.45	n.s.
Type:Sex:Session	0.13	n.s.	0.82	n.s.	0.92	n.s.
Strain:Sex:Session	2.07	n.s.	0.90	n.s.	1.05	n.s.
Type:Strain:Sex:Session	1.79	n.s.	1.26	n.s.	0.18	n.s.

Permutational Three-Way ANOVA with repeated measurements.

contradict some earlier opinions (Goodlett et al., 1992; Lalonde and Thifault, 1994). With regard to many factors that could influence the performance of the mice in behavioral tests, e.g., specific mutations, genetic background, sex, and the environment (for review, see Wolfer and Lipp, 2000; D'hooge and de Deyn, 2001), we performed a detailed comparative behavioral analysis of spatial navigation, learning and memory in *pcd* and *Lurcher* mutants. In order to assess specific behavioral abnormalities that could influence performance in the spatial navigation task, open field and forced swimming tests were done.

Behavior of *Pcd* and *Lurcher* Mutants in the Open Field and Forced Swimming Test

The type of the mutation, background strain and sex influenced behavior in both open field and forced swimming tests. The effect of sex of experimental animals was relatively stronger in

TABLE 4 | Morris water maze—heading deviation, direct swim percentage, thigmotaxis, and floating: statistical significances of the between-group factors (type, strain, and sex) and within-group factors (session) as well as their interactions.

VISIBLE PLATFORM TASK								
Between-group factors	**Heading**		**Direct swim**		**Thigmotaxis**		**Floating**	
	$F_{(1, 138)}$	*p*	$F_{(1, 138)}$	*p*	$F_{(1, 138)}$	*p*	$F_{(1, 138)}$	*p*
Type	314.21	<0.001	553.17	<0.001	101.37	<0.001	0.29	n.s.
Strain	1.45	n.s.	80.97	<0.001	0.39	n.s.	16.35	<0.001
Sex	0.02	n.s.	2.87	n.s.	1.89	n.s.	12.13	<0.001
Type:Strain	1.17	n.s.	37.56	<0.001	1.80	n.s.	5.82	0.037
Type:Sex	2.08	n.s.	2.46	n.s.	1.78	n.s.	1.11	n.s.
Strain:Sex	0.52	n.s.	0.03	n.s.	0.73	n.s.	13.43	<0.001
Type:Strain:Sex	0.10	n.s.	2.21	n.s.	0.05	n.s.	0.42	n.s.
Within-group factors	$F_{(4, 552)}$	*p*	$F_{(1, 138)}$	*p*	$F_{(4, 552)}$	*p*	$F_{(4, 552)}$	*p*
Session	43.71	<0.001	75.07	<0.001	214.95	<0.001	7.79	<0.001
Type:Session	11.01	<0.001	52.12	<0.001	60.72	<0.001	3.11	0.003
Strain:Session	0.96	n.s.	7.20	<0.001	1.65	n.s.	3.61	<0.001
Sex:Session	0.23	n.s.	0.46	n.s.	3.58	n.s.	1.44	n.s.
Type:Strain:Session	2.57	0.034	3.13	<0.001	3.61	<0.001	6.90	<0.001
Type:Sex:Session	0.91	n.s.	0.19	n.s.	3.39	<0.001	0.45	n.s.
Strain:Sex:Session	0.14	n.s.	0.61	n.s.	1.20	n.s.	6.03	<0.001
Type:Strain:Sex:Session	1.44	n.s.	0.81	n.s.	0.73	n.s.	0.55	n.s.
REVERSAL HIDDEN PLATFORM TASK								
Between-group factors	**Heading**		**Direct swim**		**Thigmotaxis**		**Floating**	
	$F_{(1, 138)}$	*p*	$F_{(1, 138)}$	*p*	$F_{(1, 138)}$	*p*	$F_{(1, 138)}$	*p*
Type	174.80	<0.001	113.05	<0.001	124.96	<0.001	0.07	n.s.
Strain	0.90	n.s.	16.52	<0.001	6.76	0.008	13.07	<0.001
Sex	0.36	n.s.	0.51	n.s.	0.62	n.s.	5.87	0.018
Type:Strain	8.64	<0.001	13.26	<0.001	10.45	<0.001	6.64	<0.001
Type:Sex	0.30	n.s.	0.16	n.s.	2.31	n.s.	0.00	n.s.
Strain:Sex	6.36	0.014	1.40	n.s.	1.39	n.s.	4.40	n.s.
Type:Strain:Sex	0.02	n.s.	0.39	n.s.	0.00	n.s.	0.01	n.s.
Within-group factors	$F_{(5,690)}$	*p*	$F_{(5,690)}$	*p*	$F_{(5,690)}$	*p*	$F_{(5,690)}$	*p*
Session	16.00	<0.001	12.51	<0.001	3.28	n.s.	2.14	0.022
Type:Session	5.30	<0.001	9.32	<0.001	7.53	<0.001	0.51	n.s.
Strain:Session	2.77	<0.001	1.96	<0.001	1.77	n.s.	1.28	n.s.
Sex:Session	3.62	0.005	0.72	n.s.	2.07	<0.001	1.36	n.s.
Type:Strain:Session	0.82	n.s.	0.83	n.s.	0.94	n.s.	1.27	n.s.
Type:Sex:Session	1.65	n.s.	1.26	n.s.	2.65	0.024	1.23	n.s.
Strain:Sex:Session	2.78	0.013	1.26	n.s.	0.43	n.s.	1.17	n.s.
Type:Strain:Sex:Session	0.15	n.s.	2.55	0.005	3.01	0.004	0.62	n.s.

Permutational Three-Way ANOVA with repeated measurements.

these tests than in the Morris water maze and was, in this case, sufficient to completely invert the differences. In the open field, B6.BR mice showed typical preference to the corners of the arena, while, in B6CBA mice, the activity was more dispersed through the arena. Such higher dispersion of the activity was more marked in *Lurchers* than in their wild type littermates. Abnormal exploration has been reported also by Caston et al. (1998) who found significantly reduced exploratory behavior in *Lurchers* despite an increase in spontaneous activity. The most obvious phenomenon observed in the forced swimming test was the absence of floating even during later phases of each day-session of the forced swimming test and the absence of an increase of floating duration across the day-sessions in *Lurcher* mice. While tendency toward inactivity and depressive-like behavior were

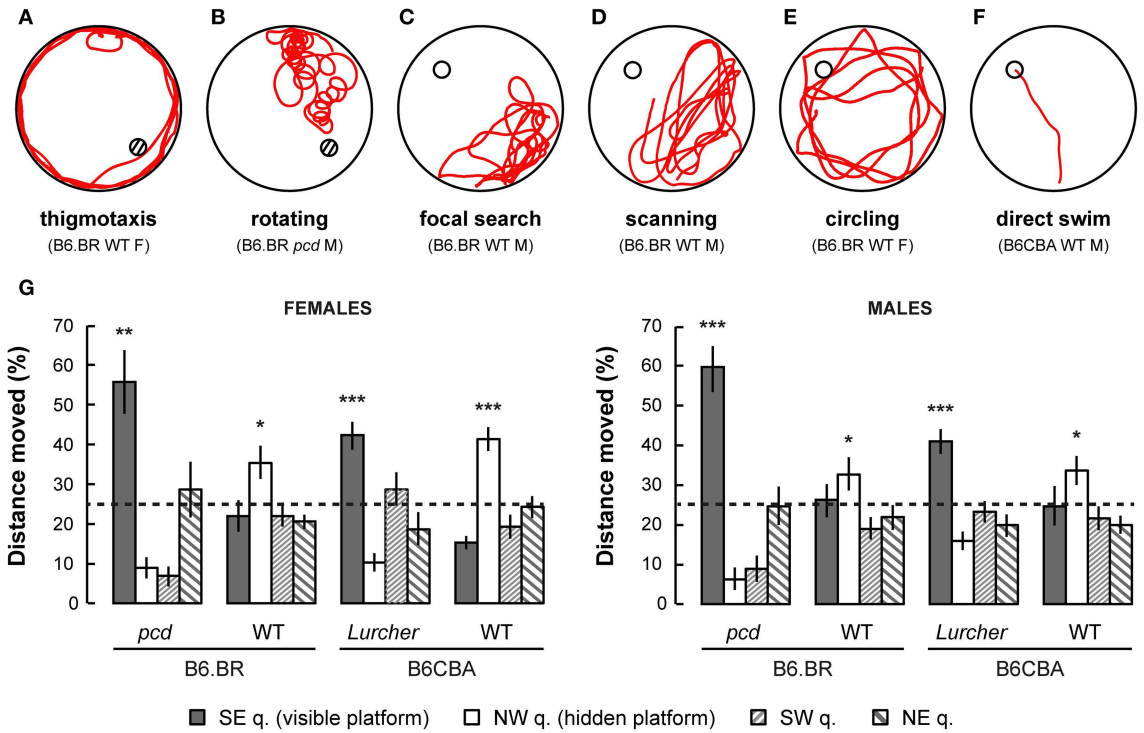

FIGURE 6 | Examples of typical trajectories (A–F) of cerebellar mutants and wild type mice. (A) Thigmotaxis (e.g., B6.BR WT female, day-session 1, trial 1) was typical for *Lurcher* (Lc) and both B6.BR and B6CBA wild type (WT) mice on the first day-session. **(B)** Rotation (e.g., *pcd* male, day-session 1, trial 1) was an abnormal trajectory pattern that occurred in both cerebellar mutants in all day-sessions. **(C)** Focal search (e.g., B6.BR WT male, day-session 6, trial 1) in area of previous platform position appeared in WT and *Lc* mice immediately after change of the platform position (day-session 6). **(D)** Scanning (e.g., B6.BR WT male, day-session 6, trial 3) or **(E)** circling (e.g., B6.BR WT female, day-session 7, trial 1) strategy was used by WT mice before they learned the new platform position. **(F)** Direct swim (e.g., B6CBA WT male, day-session 11, trial 3) typical for WT mice in day-sessions 2–5 (visible platform) and appearing also in WT mice at the end of hidden platform task, but not in cerebellar mutants. Hatched circles indicate position of visible platform empty circles indicate position of hidden platform. **(G)** Morris water maze (probe trial): Percentage of distance moved through individual quadrants during the first 30 s of the first trial (E-starting position) of day-session 12. Statistical significance was evaluated using one-sample permutational *t*-test against 25% value, which represents a random occurrence: $^{*}p < 0.05$ and $^{**}p < 0.01$, $^{***}p < 0.001$. Data are presented as mean ± SEM.

observed in *pcd* mice, *Lurchers* showed rather inadequate high activity.

Features of behavior seen in both open field and forced swimming tests comply with behavioral disinhibition affecting *Lurcher* mice (Frederic et al., 1997; Lalonde, 1998; Hilber et al., 2004; Porras-Garcia et al., 2005). The discrepancy between less fear-related behavior and elevated levels of corticosterone during stressful situations (Frederic et al., 1997; Hilber et al., 2004; Lorivel et al., 2014), a lack of prepulse inhibition and an inability to produce the immobility response suggest that *Lurcher* mice have a reduced capacity to inhibit selective components of natural behaviors due to an affection of the sensorimotor gating mechanism (Lalonde, 1998; Porras-Garcia et al., 2005). In *pcd* mice, only indirect evidence suggesting the possibility of some level of behavioral disinhibition and perseveration were reported in studies of spontaneous alternation, exploration and habituation (Lalonde et al., 1987, 1989). Since more dispersed activity in the open field and less frequent immobility in the forced swimming test were also in B6CBA wild type mice as compared with B6.BR wild type mice, these phenomena are not only due to the *Lurcher* phenotype, but might be at least a partially strain-related phenomenon.

Performance of *Pcd* and *Lurcher* Mutants in the Morris Water Maze Tests

Both *pcd* and *Lurcher* cerebellar mutants showed poor performance in the Morris water maze. Despite finding a marked improvement in *Lurcher* mice during the visible platform task, the results were worse than in wild type controls, and there were only a few trials with a direct swim toward the goal. The results for learning the hidden platform position were much worse, and among cerebellar mutants, it was detectable only in *Lurcher* males. This complies with earlier findings (Lalonde and Thifault, 1994; Cendelin et al., 2014), and may support the hypothesis that *Lurcher* mice have impaired visuomotor integration suggested by Lalonde and Thifault (1994). Nevertheless, visuomotor integration ability seems to be partially preserved in *Lurchers*, since they are able to learn the visual platform task. Preference for the zone of the previous platform position during the first trial after changing the platform position (analogy of probe trial)

TABLE 5 | Morris water maze: statistical significances of change between or during individual phases.

VISIBLE PLATFORM TASK (DAY-SESSION 1 VS. DAY-SESSION 5)								
	Latency		Distance moved		Heading		Direct swim	
Females	***t***	***p***	***t***	***p***	***t***	***p***	***t***	***p***
pcd B6.BR	4.90	<0.001	7.43	<0.001	1.39	n.s.	−1	n.s.
Wild type B6.BR	14.25	<0.001	13.28	<0.001	9.46	<0.001	−7.51	<0.001
Lurcher B6CBA	8.82	<0.001	7.83	<0.001	3.06	0.007	−0.81	n.s.
Wild type B6CBA	11.44	<0.001	9.52	<0.001	4.93	<0.001	−9.55	<0.001
Males	***t***	***p***	***T***	***p***	***t***	***p***	***t***	***p***
pcd B6.BR	3.80	0.002	7.99	<0.001	2.06	n.s.	0	n.s.
Wild type B6.BR	9.54	<0.001	9.26	<0.001	5.50	<0.001	−6.67	<0.001
Lurcher B6CBA	9.23	<0.001	8.74	<0.001	3.68	0.001	−2.96	0.016
Wild type B6CBA	7.27	<0.001	6.68	<0.001	5.11	<0.001	−14.75	<0.001
REVERSAL HIDDEN PLATFORM TASK (DAY-SESSION 6 VS. DAY-SESSION 11)								
	Latency		Distance moved		Heading		Direct swim	
Females	***t***	***p***	***T***	***p***	***t***	***p***	***t***	***p***
pcd B6.BR	1.14	n.s.	0.22	n.s.	1.17	n.s.	−0.56	n.s.
Wild type B6.BR	6.00	<0.001	7.52	<0.001	4.09	<0.001	4.55	<0.001
Lurcher B6CBA	−0.58	n.s.	−0.15	n.s.	−1.47	n.s.	1.73	n.s.
Wild type B6CBA	6.23	<0.001	7.27	<0.001	4.35	<0.001	11.12	<0.001
Males	***t***	***p***	***t***	***p***	***t***	***p***	***t***	***p***
pcd B6.BR	−0.43	n.s.	1.12	n.s.	1.96	n.s.	0	n.s.
Wild type B6.BR	3.63	0.004	4.38	<0.001	3.66	0.002	7.32	<0.001
Lurcher B6CBA	3.16	0.004	3.65	0.002	1.41	n.s.	1.68	n.s.
Wild type B6CBA	5.62	<0.001	6.22	<0.001	4.50	<0.001	7.62	<0.001
PLATFORM TRANSITION (DAY-SESSION 5 VS. DAY-SESSION 6)								
	Latency		Distance moved		Heading		Direct swim	
Females	***t***	***p***	***t***	***p***	***t***	***p***	***t***	***p***
pcd B6.BR	−3.23	0.006	−2.93	0.011	−1.78	n.s.	0	n.s.
Wild type B6.BR	−13.71	<0.001	−13.16	<0.001	−15.43	<0.001	7.8	<0.001
Lurcher B6CBA	−8.76	<0.001	−9.28	<0.001	−2.51	0.025	1.14	n.s.
Wild type B6CBA	−10.42	<0.001	−12.56	<0.001	−8.48	<0.001	11.78	<0.001
Males	***t***	***p***	***t***	***p***	***t***	***p***	***t***	***p***
pcd B6.BR	−2.64	0.020	−2.19	0.042	−2.80	0.016	−1.46	n.s.
Wild type B6.BR	−11.81	<0.001	−12.63	<0.001	−10.13	<0.001	7.91	<0.001
Lurcher B6CBA	−8.55	<0.001	−8.35	<0.001	−4.55	<0.001	2.96	0.016
Wild type B6CBA	−8.36	<0.001	−9.60	<0.001	−6.91	<0.001	13.83	<0.001

Permutational paired t-test.

also supports the idea that *Lurcher* mutants have some level of spatial learning ability that seems to be strongly dependent on the possibility of visual guidance training, which was constituted in our study by the 5 day-sessions of the visual platform task. Poor performance in the hidden platform task, on the other hand, may suggest a severe spatial learning deficit.

Although it has been reported in *pcd* mice that their performance in the visual platform task is not impaired compared to wild type controls (Goodlett et al., 1992), we observed poor performance of *pcd* mice in both visual and hidden platform tasks. The first study of spatial navigation in *pcd* mice used quite small experimental groups of male mice (Goodlett et al., 1992). In the present study, the results are based on larger samples, and males and females were analyzed separately.

An interesting phenomenon seen in the probe trial was the marked preference for the quadrant in which the visible

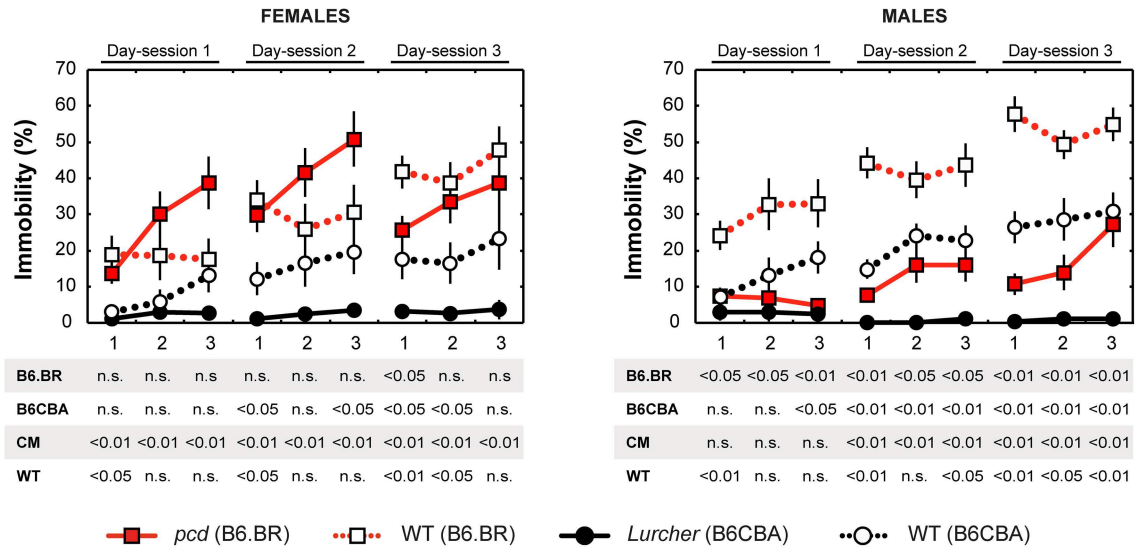

FIGURE 7 | Forced swimming test: percentage of immobility state (% of time spent without moving). Statistical significance was evaluated using a permutational *t*-test with a Bonferroni correction for the repeated measurement for within-strain comparisons (*pcd* vs.B6.BR wild type, *Lurcher* vs. B6CBA wild type) and for between-strain comparisons of cerebellar mutants (CM; *pcd* vs. *Lurcher*) and wild types (WT; B6.BR WT vs. B6CBA WT). Sex differences were significant in *pcd* mutants only from day-session 1, time-bout 2 until day-session 3, time-bout 1 ($t = 3.13$, $p = 0.011$; $t = 4.05$, $p = 0.003$; $t = 3.89$, $p = 0.004$; $t = 2.90$, $p = 0.030$; $t = 3.67$; $p = 0.005$; $t = 2.93$, $p = 0.019$, respectively). Data are presented as mean ± SEM.

platform was localized, and the omitting of the quadrant of the more recent localization of the hidden platform in both types of cerebellar mutants. In *pcd* mice, this is an artifact of spending a long time in the proximity of the starting point due to low activity. Furthermore, the reversal hidden platform task seemed to be extremely difficult for *Lurchers*. The preference of the original target quadrant could be explained by the behavioral inflexibility of *Lurcher* mice (Dickson et al., 2010). Behavioral flexibility, inhibitory response, and working memory are high-level cognitive skills, which enable the effective execution of goal-directed behaviors (Dalley et al., 2004). These skills have consistently been shown to be dependent on the prefrontal cortex (Dalley et al., 2004; Robbins and Arnsten, 2009). It has been demonstrated that the cerebellum modulates the prefrontal cortex activity (Strick et al., 2009; Rogers et al., 2013). Behavioral inflexibility, as well as behavioral disinhibition, which are closely related to inhibitory response (Young et al., 2009), suggested the affection of higher cognitive skills in *Lurcher* mutants. Thus, the poor performance of cerebellar mutants in the water maze task could be caused by at least four types of factors or their combinations: (1) Cognitive disorders, (2) Sensory disorders, (3) Motivation and behavioral abnormalities, and (4) Motor deficits. The performance is further modified by differences in manifestation of the mutations, strain, and sex.

Role of Cognition

The Morris water maze task requires at least two types of non-motor learning. First, association between the platform and escape from the maze must be created. Second, the animal must start to learn the position of the platform. Associative learning processes are supposed to be strongly related to the cerebellum (Gruart et al., 1997; Jimenez-Diaz et al., 2004; for review, see Thompson and Steinmetz, 2009; Perciavalle et al., 2013) and its abnormalities have been described in both *Lurcher* and *pcd* mutants (Chen et al., 1996; Porras-Garcia et al., 2005, 2010; Brown et al., 2010). Thus, delayed association between the platform and water escape could affect the motivation to learn its position in cerebellar mutants.

Traditionally, spatial cognition is related to the hippocampus (O'Keefe and Nadel, 1978). Nevertheless, the cerebellum participates in the construction of hippocampal spatial representation and, thus, plays an important role in goal-directed navigation (Rochefort et al., 2011, 2013; Onuki et al., 2013). Therefore, it could be assumed that the absence of Purkinje cells in both *pcd* and *Lurcher* mice might have a strong impact on the hippocampal processes involved in solving spatial tasks.

Role of Sensory Impairments

Since good vision is crucial for spatial navigation, retinal degeneration could be an important factor that strongly influences behavior, namely spatial performance in *pcd* mice. Nevertheless, the retinal degeneration in *pcd* mice is only slowly progressive (Blanks et al., 1982; Lavail et al., 1982; Blanks and Spee, 1992; Marchena et al., 2011), and we have found only an insignificant reduction of photoreceptor density in the retinas of *pcd* mice at the age at which they were tested for spatial orientation. Despite this, some impact of vision problems on behavior during spatial tasks could not be excluded due to the possible functional imperfection of a degenerating retina even

TABLE 6 | Forced swimming test: statistical significances of the between-group factors (type, strain, and sex) and within-group factors (bout, session) as well as their interactions.

	Immobility	
Between-group factors	$F_{(1, 99)}$	*p*
Type	39.45	<0.001
Strain	76.79	<0.001
Sex	0.03	n.s.
Type:Strain	0.43	n.s.
Type:Sex	18.15	<0.001
Strain:Sex	2.10	n.s.
Type:Strain:Sex	7.17	0.013
Within-group factors	$F_{(2, 198)}$	*p*
Bout	23.02	0.011
Type:Bout	2.65	0.025
Strain:Bout	1.69	n.s.
Sex:Bout	1.37	n.s.
Type:Strain:Bout	17.60	<0.001
Type:Sex:Bout	2.87	0.023
Strain:Sex:Bout	1.13	n.s.
Type:Strain:Sex:Bout	1.67	n.s.
Within-group factors	$F_{(1, 99)}$	*p*
Session	29.48	<0.001
Type:Session	12.91	<0.001
Strain:Session	5.00	0.005
Sex:Session	0.72	n.s.
Type:Strain:Session	0.24	n.s.
Type:Sex:Session	0.27	n.s.
Strain:Sex:Session	0.10	n.s.
Type:Strain:Sex:Session	0.03	n.s.
Within-group factors	$F_{(2, 198)}$	*p*
Bout:Session	1.83	n.s.
Type:Bout:Session	1.08	n.s.
Strain:Bout:Sesion	1.22	n.s.
Type:Strain:Bout:Session	1.15	n.s.
Sex:Bout:Session	0.30	n.s.
Type:Sex:Bout:Sesion	3.56	n.s.
Strain:Sex:Bout:Sesion	0.41	n.s.
Type:Strain:Sex:Bout:Session	2.63	n.s.

Permutational Three-Way ANOVA with repeated measurements.

TABLE 7 | Forced swimming test: paired comparison of day-session 1 and 3 for each time-bout.

Groups	Time-bout (min)	Females		Males	
		t	*p*	*t*	*p*
pcd B6.BR	00 – 05	−4.60	<0.001	−0.86	n.s.
	05 – 10	−0.53	n.s.	−1.44	n.s.
	10 – 15	0.01	n.s.	−3.22	0.006
Wild type B6.BR	00 – 05	−4.07	0.003	−7.48	<0.001
	05 – 10	−3.30	0.012	−2.46	0.028
	10 – 15	−5.17	0.001	−2.93	0.011
Lurcher B6CBA	00 – 05	−1.22	n.s.	1.04	n.s.
	05 – 10	0.14	n.s.	0.66	n.s.
	10 – 15	−0.51	n.s.	0.60	n.s.
Wild type B6CBA	00 – 05	−2.93	0.011	−4.24	<0.001
	05 – 10	0.14	n.s.	0.66	n.s.
	10 – 15	−1.36	n.s.	−2.41	0.033

Permutational paired t-test.

before a reduction of photoreceptor number becomes evident (Marchena et al., 2011).

However, in addition, the cerebellar disorder itself may lead to severe sensory dysfunctions by at least two mechanisms—affection of perceptual processes and oculomotor abnormalities. The cerebellum is associated with perceptual systems including vision, proprioception and self-motion perception, and cerebellar lesions lead to a wide range of sensory impairments (for review, see Baumann et al., 2015). Therefore, cerebellar disorders may severely affect spatial orientation ability due to the inappropriate acquisition and processing of information necessary for space navigation.

Control of oculomotor function is important for sighting fixation and for the visual following of an object by a moving individual. In *Lurchers,* abnormalities of the optokinetic and vestibuloocular reflexes were described by van Alphen et al. (2002). Since cerebellar Purkinje cells control oculomotor coordination, including optokinetic and vestibuloocular reflexes (for review, see Angelaki and Hess, 2005; Yakusheva et al., 2007), oculomotor problems could be expected also in *pcd* mice, in which, however, the vestibuloocular reflex has been found to be almost normal (Killian and Baker, 2002).

For all of these reasons, sensory problems can be expected to play a significant role in navigation difficulties in cerebellar mutants. In the visible goal task, these problems may be less important than in the case of the hidden goal task, since the goal represents a single and marked intramaze object of interest instead of multiple extramaze landmarks necessary for hidden goal location.

Role of Motivation and Behavioral Abnormalities

Paradoxically, *pcd* mice showed short distances moved. This fact can be explained by low swimming activity and longer periods of floating compared with *Lurchers*. Therefore, their trajectory was relatively short, even in the case where they did not reach the platform and spent the entire trial slowly swimming with floating periods, while *Lurcher* mice spent this time intensively swimming. Higher tendency of inactivity in *pcd* mice and higher swimming activity in *Lurcher* mice were also seen in the forced swimming test. Floating is a behavioral phenomenon that may substantially influence the results of the water maze tasks (Llano Lopez et al., 2010) or may be a

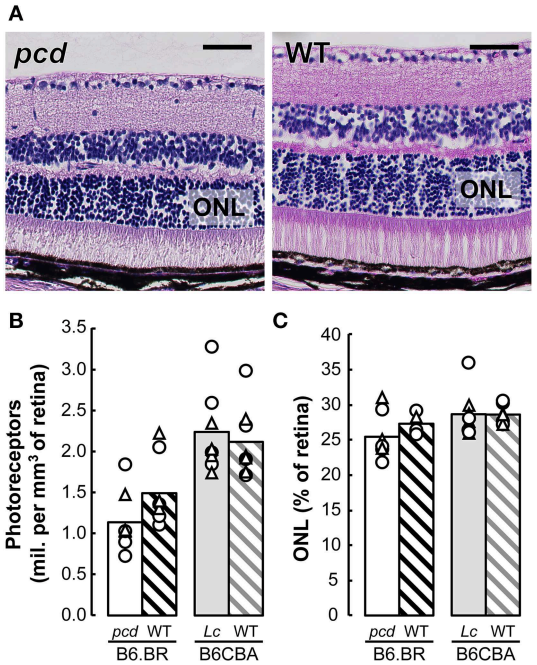

FIGURE 8 | (A) Histology of the retina in *pcd* and B6.BR wild type (WT) mice stained with Gill's hematoxylin. The bars indicate 50 μm. **(B)** Mean number of photoreceptors in outer nuclear layer (ONL) per mm^3 of the retina and **(C)** mean volume of ONL expressed as percentage of whole retina volume in *pcd*, B6.BR WT, *Lurcher* (Lc) and B6CBA WT mice. Values of individual animals are indicated by △ for females and ○ for males.

response to a difficult task as a manifestation of depressive-like behavior and learned helplessness (Porsolt et al., 1979). Potential sight impairment due to retinal degeneration and poor fitness related to low body weight may make the spatial task too difficult for *pcd* mice, which might induce learned helplessness.

Role of Motor Impairment

For performance in the water maze task, swimming and direction maintenance abilities are required. Motor impairment has been shown many times in cerebellar mutants (Fortier et al., 1987; Lalonde et al., 1996; Le Marec and Lalonde, 1997, 1998; Cendelin et al., 2008, 2014). On the other hand, Fortier et al. (1987) showed a normal EMG pattern in swimming *Lurcher* mice, but not in walking ones, suggesting that swimming is not as affected by the ataxia as gait. Furthermore, *Lurcher* mice achieved the same swimming speed as wild type mice. In *pcd* mice, low swimming speed could account for their abnormal swimming pattern (Goodlett et al., 1992), but also for lower activity or worse fitness. Nevertheless, in both *Lurcher* and *pcd* mice, we have observed a high incidence of rotating, but almost no direct swim trials. A low frequency of direct swim was even seen in *Lurcher* mice at the end of the visible platform task when they showed an improving ability to reach the visible goal. Therefore, motor deficiency does not seem to affect swimming ability, but rather, could influence trajectory shape and disable the maintenance of a straight course toward the goal in cerebellar mutants.

Role of the Mutation, Strain Background and Sex

Poor spatial performance is a strong phenotypic manifestation of particular mutations in *pcd* and *Lurcher* mice. These symptoms are easily detectable by the tests, and other factors, such as strain and sex, seem to only slightly modulate performance. Sex dimorphism as a function of brain structures related to both behavioral processes and motor control has been described (Arvidsson et al., 2014), and significant sex differences were even reported in neurological manifestations of mutations in mice (Walton et al., 2012; Truong et al., 2013).

More problematic is the comparison of the manifestation of mutations. Despite the main features and extent of cerebellar degeneration being similar, *pcd* and *Lurcher* mice differ in a number of aspects. The overall performance of *pcd* mice in the Morris water maze was worse than in *Lurchers*. $Grid2^{Lc}$ and $Agtpb1^{pcd}$ mutations not only differ in the mechanism of cell death activation, but the spectrum of extracerebellar brain damage and the affection of other tissues was wider with the $Agtpb1^{pcd}$ mutation. Therefore, in this case, modifying factors have a broader range of targets. Particularly, retinal degeneration (Blanks et al., 1982; Lavail et al., 1982; Blanks and Spee, 1992; Marchena et al., 2011) and expression of *Nna1* in the skeletal muscles (Harris et al., 2000) are important. Since strain differences between B6CBA and B6.BR wild type mice were also observed in the present study, genetic background plays a role. *Pcd* and *Lurcher* mice are not commercially available on the same strain background. Therefore, it is difficult to unambiguously distinguish a specific mutation effect from the modifying effect of strain-specific phenotypic traits, the importance of which was particularly shown for floating behavior.

Recently, we have shown that, despite the *Lurcher* mutation having a strong manifestation, the phenotype could be modulated by genetic background (Cendelin et al., 2014). Considering the magnitude of differences between the same mutants in different strains and between different mutants, we could conclude that strain differences could be sufficient to cover or mitigate some of the mutation-related differences.

Conclusion

We have confirmed the severe impairments in cognitive and behavioral tests in both *pcd* and *Lurcher* mutant mice. Contrary to previous studies (Goodlett et al., 1992; Lalonde and Thifault, 1994), we found that visuomotor integration is only partially disabled in *Lurchers,* and that *pcd* mice failed in both visual and hidden goal tests, using large samples of mice. Overall performance in the Morris water maze test was better in *Lurcher* mutants than in *pcd* mice. The effect of the mutation as well as of the genetic background was seen. The deficit of spatial performance in cerebellar mutants may potentially arise from a combination of cognitive, sensory, emotional, and motor disturbances, all of which are expected to be of different importance in various mutants. Mutation-related differences

could be potentiated by specific phenotypic traits of different strains of origin than these mutants.

Acknowledgments

The authors would like to thank Helena Geciova. Irena Pojarova, and Dr. Pavel Ostasov for their technical assistance and Dr. Milena Kralickova for institutional support. COST Grant No. LD12057 of the Ministry of Education, Youth and Sport of the Czech Republic.

Supplementary Material

The Supplementary Material for this article can be found online at: http://journal.frontiersin.org/article/10.3389/fnbeh.2015.00116/abstract

References

Angelaki, D. E., and Hess, B. J. (2005). Self-motion-induced eye movements: effects on visual acuity and navigation. *Nat. Rev. Neurosci.* 6, 966–976. doi: 10.1038/nrn1804

Araki, K., Meguro, H., Kushiya, E., Takayama, C., Inoue, Y., and Mishina, M. (1993). Selective expression of the glutamate receptor channel delta 2 subunit in cerebellar Purkinje cells. *Biochem. Biophys. Res. Commun.* 197, 1267–1276. doi: 10.1006/bbrc.1993.2614

Arvidsson, E., Viereckel, T., Mikulovic, S., and Wallen-Mackenzie, A. (2014). Age- and sex-dependence of dopamine release and capacity for recovery identified in the dorsal striatum of C57/Bl6J mice. *PLoS ONE* 9:e99592. doi: 10.1371/journal.pone.0099592

Baltanas, F. C., Berciano, M. T., Valero, J., Gomez, C., Diaz, D., Alonso, J. R., et al. (2013). Differential glial activation during the degeneration of Purkinje cells and mitral cells in the PCD mutant mice. *Glia* 61, 254–272. doi: 10.1002/glia.22431

Baltanas, F. C., Casafont, I., Lafarga, V., Weruaga, E., Alonso, J. R., Berciano, M. T., et al. (2011). Purkinje cell degeneration in pcd mice reveals large scale chromatin reorganization and gene silencing linked to defective DNA repair. *J. Biol. Chem.* 286, 28287–28302. doi: 10.1074/jbc.M111.246041

Baumann, O., Borra, R. J., Bower, J. M., Cullen, K. E., Habas, C., Ivry, R. B., et al. (2015). Consensus paper: the role of the cerebellum in perceptual processes. *Cerebellum* 14, 197–220. doi: 10.1007/s12311-014-0627-7

Blanks, J. C., Mullen, R. J., and Lavail, M. M. (1982). Retinal degeneration in the pcd cerebellar mutant mouse. II. Electron microscopic analysis. *J. Comp. Neurol.* 212, 231–246. doi: 10.1002/cne.902120303

Blanks, J. C., and Spee, C. (1992). Retinal degeneration in the pcd/pcd mutant mouse: accumulation of spherules in the interphotoreceptor space. *Exp. Eye Res.* 54, 637–644. doi: 10.1016/0014-4835(92)90019-O

Boyce, R. W., Dorph-Petersen, K. A., Lyck, L., and Gundersen, H. J. (2010). Design-based stereology: introduction to basic concepts and practical approaches for estimation of cell number. *Toxicol. Pathol.* 38, 1011–1025. doi: 10.1177/0192623310385140

Brown, K. L., Agelan, A., and Woodruff-Pak, D. S. (2010). Unimpaired trace classical eyeblink conditioning in Purkinje cell degeneration (pcd) mutant mice. *Neurobiol. Learn. Mem.* 93, 303–311. doi: 10.1016/j.nlm.2009.11.004

Caddy, K. W., and Biscoe, T. J. (1979). Structural and quantitative studies on the normal C3H and Lurcher mutant mouse. *Philos. Trans. R. Soc. Lond. B Biol. Sci.* 287, 167–201. doi: 10.1098/rstb.1979.0055

Caston, J., Chianale, C., Delhaye-Bouchaud, N., and Mariani, J. (1998). Role of the cerebellum in exploration behavior. *Brain Res.* 808, 232–237. doi: 10.1016/S0006-8993(98)00847-6

Cendelin, J. (2014). From mice to men: lessons from mutant ataxic mice. *Cerebellum Ataxias* 1:4. doi: 10.1186/2053-8871-1-4

Cendelin, J., Korelusova, I., and Vozeh, F. (2008). The effect of repeated rotarod training on motor skills and spatial learning ability in Lurcher mutant mice. *Behav. Brain. Res.* 189, 65–74. doi: 10.1016/j.bbr.2007.12.013

Cendelin, J., Tuma, J., Korelusova, I., and Vozeh, F. (2014). The effect of genetic background on behavioral manifestation of Grid2 mutation. *Behav. Brain. Res.* 271C, 218–227. doi: 10.1016/j.bbr.2014.06.023

Chen, L., Bao, S., Lockard, J. M., Kim, J. K., and Thompson, R. F. (1996). Impaired classical eyeblink conditioning in cerebellar-lesioned and Purkinje cell degeneration (pcd) mutant mice. *J. Neurosci.* 16, 2829–2838.

Cooper, F. E., Grube, M., Elsegood, K. J., Welch, J. L., Kelly, T. P., Chinnery, P. F., et al. (2010). The contribution of the cerebellum to cognition in spinocerebellar ataxia type 6. *Behav. Neurol.* 23, 3–15. doi: 10.1155/2010/724861

Dalley, J. W., Cardinal, R. N., and Robbins, T. W. (2004). Prefrontal executive and cognitive functions in rodents: neural and neurochemical substrates. *Neurosci. Biobehav. Rev.* 28, 771–784. doi: 10.1016/j.neubiorev.2004.09.006

de Jager, P. L., Zuo, J., Cook, S. A., and Heintz, N. (1997). A new allele of the lurcher gene, lurcherJ. *Mamm. Genome* 8, 647–650. doi: 10.1007/s003359900530

D'hooge, R., and de Deyn, P. P. (2001). Applications of the Morris water maze in the study of learning and memory. *Brain Res. Brain Res. Rev.* 36, 60–90. doi: 10.1016/S0165-0173(01)00067-4

Dickson, P. E., Rogers, T. D., Del Mar, N., Martin, L. A., Heck, D., Blaha, C. D., et al. (2010). Behavioral flexibility in a mouse model of developmental cerebellar Purkinje cell loss. *Neurobiol. Learn. Mem.* 94, 220–228. doi: 10.1016/j.nlm.2010.05.010

Fancellu, R., Paridi, D., Tomasello, C., Panzeri, M., Castaldo, A., Genitrini, S., et al. (2013). Longitudinal study of cognitive and psychiatric functions in spinocerebellar ataxia types 1 and 2. *J. Neurol.* 260, 3134–3143. doi: 10.1007/s00415-013-7138-1

Fernandez-Gonzalez, A., La Spada, A. R., Treadaway, J., Higdon, J. C., Harris, B. S., Sidman, R. L., et al. (2002). Purkinje cell degeneration (pcd) phenotypes caused by mutations in the axotomy-induced gene, Nna1. *Science* 295, 1904–1906. doi: 10.1126/science.1068912

Fortier, P. A., Smith, A. M., and Rossignol, S. (1987). Locomotor deficits in the mutant mouse, Lurcher. *Exp. Brain Res.* 66, 271–286. doi: 10.1007/BF00243304

Frederic, F., Chautard, T., Brochard, R., Chianale, C., Wollman, E., Oliver, C., et al. (1997). Enhanced endocrine response to novel environment stress and endotoxin in Lurcher mutant mice. *Neuroendocrinology* 66, 341–347. doi: 10.1159/000127257

Furuya, S., Irie, F., Hashikawa, T., Nakazawa, K., Kozakai, A., Hasegawa, A., et al. (1994). Ganglioside GD1 alpha in cerebellar Purkinje cells. Its specific absence in mouse mutants with Purkinje cell abnormality and altered immunoreactivity in response to conjunctive stimuli causing long-term desensitization. *J. Biol. Chem.* 269, 32418–32425.

Ghetti, B., Norton, J., and Triarhou, L. C. (1987). Nerve cell atrophy and loss in the inferior olivary complex of "Purkinje cell degeneration" mutant mice. *J. Comp. Neurol.* 260, 409–422. doi: 10.1002/cne.902600307

Glaser, J., Greene, G., and Hendricks, S. (2007). *Stereology for Biological Research with a Focus on Neuroscience.* Williston, VT: MBF Press.

Goodlett, C. R., Hamre, K. M., and West, J. R. (1992). Dissociation of spatial navigation and visual guidance performance in Purkinje cell degeneration (pcd) mutant mice. *Behav. Brain. Res.* 47, 129–141. doi: 10.1016/S0166-4328(05)80119-6

Greer, C. A., and Shepherd, G. M. (1982). Mitral cell degeneration and sensory function in the neurological mutant mouse Purkinje cell degeneration (PCD). *Brain Res.* 235, 156–161. doi: 10.1016/0006-8993(82)90206-2

Gruart, A., Pastor, A. M., Armengol, J. A., and Delgado-Garcia, J. M. (1997). Involvement of cerebellar cortex and nuclei in the genesis and control of unconditioned and conditioned eyelid motor responses. *Prog. Brain Res.* 114, 511–528. doi: 10.1016/S0079-6123(08)63383-X

Gundersen, H. J. (1986). Stereology of arbitrary particles. A review of unbiased number and size estimators and the presentation of some new ones, in memory of William R. Thompson. *J. Microsc.* 143, 3–45. doi: 10.1111/j.1365-2818.1986.tb02764.x

Gundersen, H. J., and Jensen, E. B. (1987). The efficiency of systematic sampling in stereology and its prediction. *J. Microsc.* 147, 229–263. doi: 10.1111/j.1365-2818.1987.tb02837.x

Harris, A., Morgan, J. I., Pecot, M., Soumare, A., Osborne, A., and Soares, H. D. (2000). Regenerating motor neurons express Nna1, a novel ATP/GTP-binding protein related to zinc carboxypeptidases. *Mol. Cell Neurosci.* 16, 578–596. doi: 10.1006/mcne.2000.0900

Hilber, P., Lorivel, T., Delarue, C., and Caston, J. (2004). Stress and anxious-related behaviors in Lurcher mutant mice. *Brain Res.* 1003, 108–112. doi: 10.1016/j.brainres.2004.01.008

Jimenez-Diaz, L., Navarro-Lopez Jde, D., Gruart, A., and Delgado-Garcia, J. M. (2004). Role of cerebellar interpositus nucleus in the genesis and control of reflex and conditioned eyelid responses. *J. Neurosci.* 24, 9138–9145. doi: 10.1523/JNEUROSCI.2025-04.2004

Killian, J. E., and Baker, J. F. (2002). Horizontal vestibuloocular reflex (VOR) head velocity estimation in Purkinje cell degeneration (pcd/pcd) mutant mice. *J. Neurophysiol.* 87, 1159–1164. doi: 10.1152/jn.00219.2001

Lalonde, R. (1998). Immobility responses in Lurcher mutant mice. *Behav. Genet.* 28, 309–314. doi: 10.1023/A:1021627631721

Lalonde, R., Filali, M., Bensoula, A. N., and Lestienne, F. (1996). Sensorimotor learning in three cerebellar mutant mice. *Neurobiol. Learn. Mem.* 65, 113–120. doi: 10.1006/nlme.1996.0013

Lalonde, R., Lamarre, Y., and Smith, A. M. (1988). Does the mutant mouse lurcher have deficits in spatially oriented behaviours? *Brain Res.* 455, 24–30. doi: 10.1016/0006-8993(88)90109-6

Lalonde, R., Manseau, M., and Botez, M. I. (1987). Spontaneous alternation and habituation in Purkinje cell degeneration mutant mice. *Brain Res.* 411, 187–189. doi: 10.1016/0006-8993(87)90699-8

Lalonde, R., Manseau, M., and Botez, M. I. (1989). Exploration and habituation in Purkinje cell degeneration mutant mice. *Brain Res.* 479, 201–203. doi: 10.1016/0006-8993(89)91354-1

Lalonde, R., and Strazielle, C. (2007). Spontaneous and induced mouse mutations with cerebellar dysfunctions: behavior and neurochemistry. *Brain Res.* 1140, 51–74. doi: 10.1016/j.brainres.2006.01.031

Lalonde, R., and Thifault, S. (1994). Absence of an association between motor coordination and spatial orientation in lurcher mutant mice. *Behav. Genet.* 24, 497–501. doi: 10.1007/BF01071563

Lalouette, A., Lohof, A., Sotelo, C., Guenet, J., and Mariani, J. (2001). Neurobiological effects of a null mutation depend on genetic context: comparison between two hotfoot alleles of the delta-2 ionotropic glutamate receptor. *Neuroscience* 105, 443–455. doi: 10.1016/S0306-4522(01)00193-2

Lavail, M. M., Blanks, J. C., and Mullen, R. J. (1982). Retinal degeneration in the pcd cerebellar mutant mouse. I. Light microscopic and autoradiographic analysis. *J. Comp. Neurol.* 212, 217–230. doi: 10.1002/cne.902120302

Le Marec, N., and Lalonde, R. (1997). Sensorimotor learning and retention during equilibrium tests in Purkinje cell degeneration mutant mice. *Brain Res.* 768, 310–316. doi: 10.1016/S0006-8993(97)00666-5

Le Marec, N., and Lalonde, R. (1998). Treadmill performance of mice with cerebellar lesions: 1. Purkinje cell degeneration mutant mice. *Behav. Neurosci.* 112, 225–232. doi: 10.1037/0735-7044.112.1.225

Le Marec, N., and Lalonde, R. (2000). Treadmill performance of mice with cerebellar lesions: 2. Lurcher mutant mice. *Neurobiol. Learn. Mem.* 73, 195–206. doi: 10.1006/nlme.1999.3926

Llano Lopez, L., Hauser, J., Feldon, J., Gargiulo, P. A., and Yee, B. K. (2010). Evaluating spatial memory function in mice: a within-subjects comparison between the water maze test and its adaptation to dry land. *Behav. Brain. Res.* 209, 85–92. doi: 10.1016/j.bbr.2010.01.020

Lorivel, T., Roy, V., and Hilber, P. (2014). Fear-related behaviors in Lurcher mutant mice exposed to a predator. *Genes Brain Behav.* 13, 794–801. doi: 10.1111/gbb.12173

Manto, M., and Marmolino, D. (2009). Animal models of human cerebellar ataxias: a cornerstone for the therapies of the twenty-first century. *Cerebellum* 8, 137–154. doi: 10.1007/s12311-009-0127-3

Manto, M. U. (2005). The wide spectrum of spinocerebellar ataxias (SCAs). *Cerebellum* 4, 2–6. doi: 10.1080/14734220510007914

Marchena, M., Lara, J., Aijon, J., Germain, F., de La Villa, P., and Velasco, A. (2011). The retina of the PCD/PCD mouse as a model of photoreceptor degeneration. A structural and functional study. *Exp. Eye Res.* 93, 607–617. doi: 10.1016/j.exer.2011.07.010

Marien, P., and Beaton, A. (2014). The enigmatic linguistic cerebellum: clinical relevance and unanswered questions on nonmotor speech and language deficits in cerebellar disorders. *Cerebellum Ataxias* 1, 1–12. doi: 10.1186/2053-8871-1-12

Morris, R. (1984). Developments of a water-maze procedure for studying spatial learning in the rat. *J. Neurosci. Methods* 11, 47–60. doi: 10.1016/0165-0270(84)90007-4

Mullen, R. J., Eicher, E. M., and Sidman, R. L. (1976). Purkinje cell degeneration, a new neurological mutation in the mouse. *Proc. Natl. Acad. Sci. U.S.A.* 73, 208–212. doi: 10.1073/pnas.73.1.208

O'Keefe, J., and Nadel, L. (1978). *The Hippocampus as a Cognitive Map*. Oxford: Oxford University Press.

O'Gorman, S. (1985). Degeneration of thalamic neurons in "Purkinje cell degeneration" mutant mice. II. Cytology of neuron loss. *J. Comp. Neurol.* 234, 298–316. doi: 10.1002/cne.902340303

O'Gorman, S., and Sidman, R. L. (1985). Degeneration of thalamic neurons in "Purkinje cell degeneration" mutant mice. I. Distribution of neuron loss. *J. Comp. Neurol.* 234, 277–297. doi: 10.1002/cne.902340302

Onuki, Y., van Someren, E. J., de Zeeuw, C. I., and van der Werf, Y. D. (2013). Hippocampal-cerebellar interaction during spatio-temporal prediction. *Cereb. Cortex* 25, 313–321. doi: 10.1093/cercor/bht221

Perciavalle, V., Apps, R., Bracha, V., Delgado-Garcia, J. M., Gibson, A. R., Leggio, M., et al. (2013). Consensus paper: current views on the role of cerebellar interpositus nucleus in movement control and emotion. *Cerebellum* 12, 738–757. doi: 10.1007/s12311-013-0464-0

Pesarin, F., and Salmaso, L. (2010). *Permutation Tests for Complex Data: Theory, Applications and Software*. Chippenham: A John Wiley and Sons, Ltd.

Phillips, R. J. S. (1960). 'Lurcher', a new gene in linkage group XI of the house mouse. *J. Genet.* 57, 35–42. doi: 10.1007/BF02985337

Porras-Garcia, E., Cendelin, J., Dominguez-Del-Toro, E., Vozeh, F., and Delgado-Garcia, J. M. (2005). Purkinje cell loss affects differentially the execution, acquisition and prepulse inhibition of skeletal and facial motor responses in Lurcher mice. *Eur. J. Neurosci.* 21, 979–988. doi: 10.1111/j.1460-9568.2005.03940.x

Porras-Garcia, E., Sanchez-Campusano, R., Martinez-Vargas, D., Dominguez-Del-Toro, E., Cendelin, J., Vozeh, F., et al. (2010). Behavioral characteristics, associative learning capabilities, and dynamic association mapping in an animal model of cerebellar degeneration. *J. Neurophysiol.* 104, 346–365. doi: 10.1152/jn.00180.2010

Porsolt, R. D., Bertin, A., Blavet, N., Deniel, M., and Jalfre, M. (1979). Immobility induced by forced swimming in rats: effects of agents which modify central catecholamine and serotonin activity. *Eur. J. Pharmacol.* 57, 201–210. doi: 10.1016/0014-2999(79)90366-2

Robbins, T. W., and Arnsten, A. F. (2009). The neuropsychopharmacology of fronto-executive function: monoaminergic modulation. *Annu. Rev. Neurosci.* 32, 267–287. doi: 10.1146/annurev.neuro.051508.135535

Rochefort, C., Arabo, A., Andre, M., Poucet, B., Save, E., and Rondi-Reig, L. (2011). Cerebellum shapes hippocampal spatial code. *Science* 334, 385–389. doi: 10.1126/science.1207403

Rochefort, C., Lefort, J. M., and Rondi-Reig, L. (2013). The cerebellum: a new key structure in the navigation system. *Front. Neural Circuits* 7:35. doi: 10.3389/fncir.2013.00035

Rogers, T. D., Dickson, P. E., McKimm, E., Heck, D. H., Goldowitz, D., Blaha, C. D., et al. (2013). Reorganization of circuits underlying cerebellar modulation of prefrontal cortical dopamine in mouse models of autism spectrum disorder. *Cerebellum* 12, 547–556. doi: 10.1007/s12311-013-0462-2

Rotter, A., Rath, S., Evans, J. E., and Frostholm, A. (2000). Modulation of GABA(A) receptor subunit mRNA levels in olivocerebellar neurons of purkinje cell degeneration and weaver mutant mice. *J. Neurochem.* 74, 2190–2200. doi: 10.1046/j.1471-4159.2000.0742190.x

Schmahmann, J. D., and Sherman, J. C. (1997). Cerebellar cognitive affective syndrome. *Int. Rev. Neurobiol.* 41, 433–440. doi: 10.1016/S0074-7742(08)60363-3

Strick, P. L., Dum, R. P., and Fiez, J. A. (2009). Cerebellum and nonmotor function. *Annu. Rev. Neurosci.* 32, 413–434. doi: 10.1146/annurev.neuro.31.060407.125606

Thompson, R. F., and Steinmetz, J. E. (2009). The role of the cerebellum in classical conditioning of discrete behavioral responses. *Neuroscience* 162, 732–755. doi: 10.1016/j.neuroscience.2009.01.041

Triarhou, L. C., Norton, J., and Ghetti, B. (1987). Anterograde transsynaptic degeneration in the deep cerebellar nuclei of Purkinje cell degeneration (pcd) mutant mice. *Exp. Brain Res.* 66, 577–588. doi: 10.1007/BF00270691

Truong, D. T., Bonet, A., Rendall, A. R., Rosen, G. D., and Fitch, R. H. (2013). A behavioral evaluation of sex differences in a mouse model of severe neuronal migration disorder. *PLoS ONE* 8:e73144. doi: 10.1371/journal.pone.0073144

van Alphen, A. M., Schepers, T., Luo, C., and de Zeeuw, C. I. (2002). Motor performance and motor learning in Lurcher mice. *Ann. N.Y. Acad. Sci.* 978, 413–424. doi: 10.1111/j.1749-6632.2002.tb07584.x

Vinueza Veloz, M. F., Zhou, K., Bosman, L. W., Potters, J. W., Negrello, M., Seepers, R. M., et al. (2014). Cerebellar control of gait and interlimb coordination. *Brain Struct. Funct.* doi: 10.1007/s00429-014-0870-1. [Epub ahead of print].

Walton, J. C., Schilling, K., Nelson, R. J., and Oberdick, J. (2012). Sex-dependent behavioral functions of the Purkinje cell-specific Galphai/o binding protein, Pcp2(L7). *Cerebellum* 11, 982–1001. doi: 10.1007/s12311-012-0368-4

Wang, T., and Morgan, J. I. (2007). The Purkinje cell degeneration (pcd) mouse: an unexpected molecular link between neuronal degeneration and regeneration. *Brain Res.* 1140, 26–40. doi: 10.1016/j.brainres.2006.07.065

Wetts, R., and Herrup, K. (1982a). Cerebellar Purkinje cells are descended from a small number of progenitors committed during early development: quantitative analysis of lurcher chimeric mice. *J. Neurosci.* 2, 1494–1498.

Wetts, R., and Herrup, K. (1982b). Interaction of granule, Purkinje and inferior olivary neurons in lurcher chimeric mice. II. Granule cell death. *Brain Res.* 250, 358–362. doi: 10.1016/0006-8993(82)90431-0

Wolfer, D. P., and Lipp, H. P. (2000). Dissecting the behaviour of transgenic mice: is it the mutation, the genetic background, or the environment? *Exp. Physiol.* 85, 627–634. doi: 10.1111/j.1469-445X.2000.02095.x

Yakusheva, T. A., Shaikh, A. G., Green, A. M., Blazquez, P. M., Dickman, J. D., and Angelaki, D. E. (2007). Purkinje cells in posterior cerebellar vermis encode motion in an inertial reference frame. *Neuron* 54, 973–985. doi: 10.1016/j.neuron.2007.06.003

Young, S. E., Friedman, N. P., Miyake, A., Willcutt, E. G., Corley, R. P., Haberstick, B. C., et al. (2009). Behavioral disinhibition: liability for externalizing spectrum disorders and its genetic and environmental relation to response inhibition across adolescence. *J. Abnorm. Psychol.* 118, 117–130. doi: 10.1037/a0014657

Zanjani, S. H., Selimi, F., Vogel, M. W., Haeberle, A. M., Boeuf, J., Mariani, J., et al. (2006). Survival of interneurons and parallel fiber synapses in a cerebellar cortex deprived of Purkinje cells: studies in the double mutant mouse Grid2Lc/+;Bax(−/−). *J. Comp. Neurol.* 497, 622–635. doi: 10.1002/cne.21017

Zhang, W., Lee, W. H., and Triarhou, L. C. (1996). Grafted cerebellar cells in a mouse model of hereditary ataxia express IGF-I system genes and partially restore behavioral function. *Nat. Med.* 2, 65–71. doi: 10.1038/nm0196-65

Zuo, J., de Jager, P. L., Takahashi, K. A., Jiang, W., Linden, D. J., and Heintz, N. (1997). Neurodegeneration in Lurcher mice caused by mutation in delta2 glutamate receptor gene. *Nature* 388, 769–773. doi: 10.1038/42009

Conflict of Interest Statement: The authors declare that the research was conducted in the absence of any commercial or financial relationships that could be construed as a potential conflict of interest.

Supplementary Data

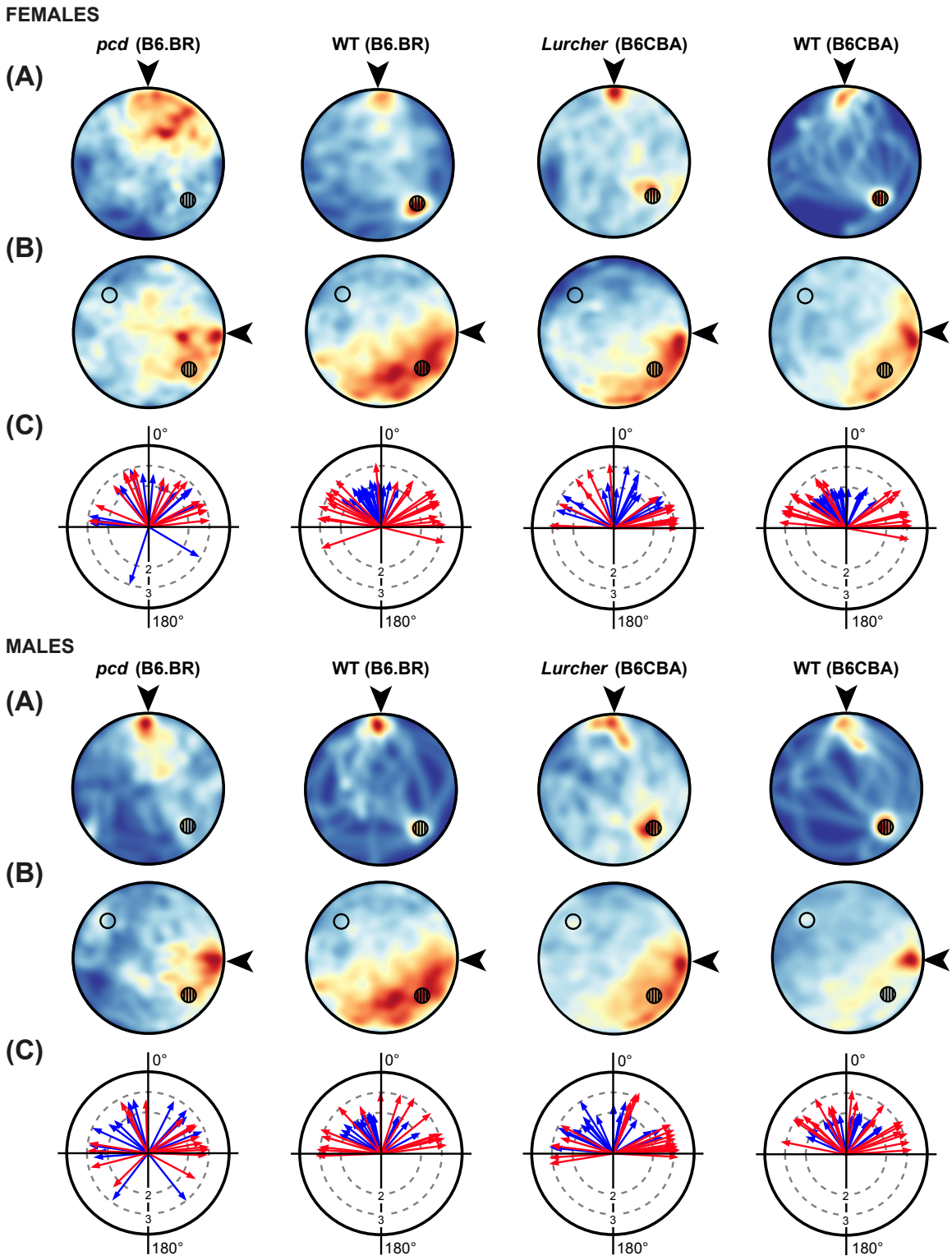
FEMALES
pcd (B6.BR)
WT (B6.BR)
Lurcher (B6CBA)
WT (B6CBA)
(A)
(B)
(C)
0°
2
3
180°
MALES
pcd (B6.BR)
WT (B6.BR)
Lurcher (B6CBA)
WT (B6CBA)
(A)
(B)
(C)
0°
2
3
180°

Supplementary Figure 1 - Effect of transition between visible platform and reversal hidden platform task in the Morris water maze. (A) Superposition of trajectories in the first trial (N-starting position depicted with arrows) of the day-session 5 (visible platform task). Hatched circles indicate the position of the visible platform. B6.BR wild type mice and both B6CBA *Lurcher* and wild type mice showed either direct or indirect swim toward the visible platform swim to the visible platform, while *pcd* mice spent most of the time floating in the start area. (B) Superposition of trajectories in the first trial (E-starting position depicted with arrows) of day-session 6 (reversal hidden platform task). Empty circles indicate current position of the hidden platform and hatched circles indicate the previous position of visible platform (visible platform task). Mice of each experimental group showed a preference for the SE quadrant with previous localization of the visible platform. Nevertheless, in *pcd* mice the area of maximum activity was focused rather in the proximity of the starting point, while in wild type mice and in *Lurchers* the center of their activity corresponded more with the previous platform position. (C) Rose graphs show trajectory vector dispersion. Blue vectors demonstrate trajectories in the first trial of day-session 5 and red vectors demonstrate trajectories in the first trial of day-session 6. Lengths of the vectors indicate distance moved in logarithmic scale (dashed circles). Directions of the vectors indicate mean deviation from direct course toward the platform (0° represents direct swim). Higher dispersion of the heading direction vectors and longer trajectories in *pcd* mice at the end of the visible platform task (day-session 5), as well as immediately after changing the platform position and its concealment (day-session 6) suggest that *pcd* mice did not search the platform in the appropriate area despite spending a lot of time there (A, B). In *Lurcher* mice, both vector direction dispersion and length in the visible platform task (day-session 5) were lower than in *pcd* mice but higher than in B6CBA and B6.BR wild type mice. The difference in vector direction dispersion and length between day-sessions 5 and 6 was also much more marked in *Lurcher* and both wild type mice than in *pcd* mice.

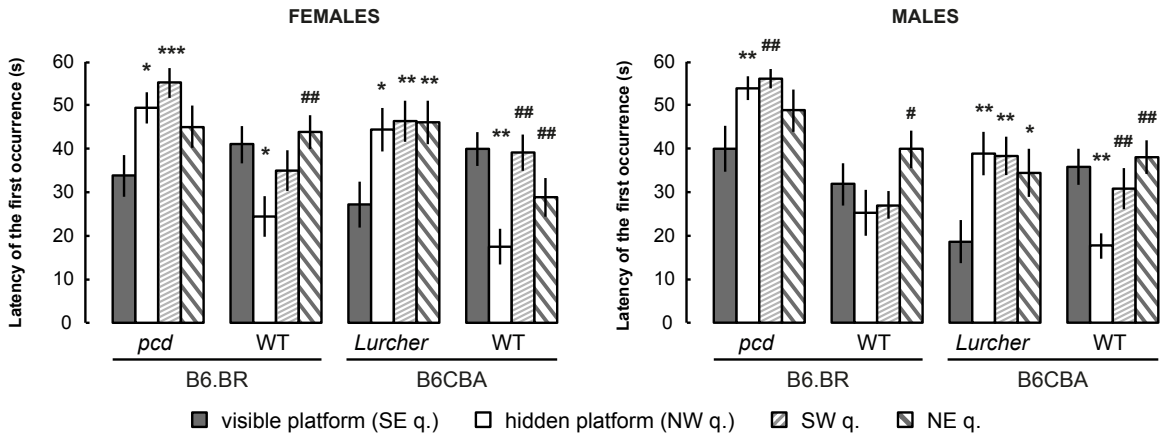

Supplementary Figure 2 - Morris water maze (probe trial): Latency of the first occurrence in the zone of former localization of the visible (center of the SE quadrant) and hidden (center of the NW quadrant) platform in the first trial (E-starting position) of day-session 12. Latencies of the first occurrence in hypothetical platforms localized in the middle of SW and NE quadrants, where the platform has never been placed are also shown. Both B6.BR and B6CBA wild type mice appeared earlier in the zone of previous localization of the hidden platform. On the other hand, cerebellar mutants showed shorter latency of first occurrence for the zone of former localization of the visible platform than for the hidden platform zone. For comparison of individual zones with visible platform zone: * $p < 0.05$, ** $p < 0.01$ and *** $p < 0.001$. For comparison of individual zones with hidden platform zone: # $p < 0.05$ and ## $p < 0.01$. Data are presented as mean ± SEM.

Supplementary Table 1 – Statistical significances of the between-group factors (type, strain and sex) and their interactions for body weight (pooled cohorts 1 and 2) as well as following planned comparisons. Permutational three-way ANOVA with repeated measurements and permutational two sample t-test.

Three-way ANOVA		
Between-group factors	$F_{(1,245)}$	*p*
Type	463.97	< 0.001
Strain	159.43	< 0.001
Sex	450.75	< 0.001
Type:Strain	86.47	< 0.001
Type:Sex	11.88	< 0.001
Strain:Sex	2.33	n.s.
Type:Strain:Sex	0.13	n.s.
Two sample t-test		
Planned comparisons	*t*	*p*
Females		
pcd vs. wild type B6.BR	-20.56	< 0.001
Lurcher vs. wild type B6CBA	-4.85	< 0.001
pcd vs. *Lurcher*	-11.58	< 0.001
WT B6.BR vs. wild type B6CBA	-1.42	n.s.
Males		
pcd vs. wild type B6.BR	-12.48	< 0.001
Lurcher vs. wild type B6CBA	-8.16	< 0.001
pcd vs. *Lurcher*	-9.33	< 0.001
WT B6.BR vs. wild type B6CBA	-2.10	0.037

Supplementary Table 2 – Forced swimming test: paired comparison of the first (time-bout 1) and the last (time-bout 3) 5 min intervals for each day-session. Permutational paired t-test.

Groups	Day-session	Females		Males	
		t	*p*	*t*	*p*
pcd B6.BR	1	-3.69	0.005	1.14	n.s.
	2	-3.86	0.004	-1.95	n.s.
	3	-2.22	0.05	-3.26	0.004
wild type B6.BR	1	0.36	n.s.	-2.16	0.045
	2	0.48	n.s.	0.13	n.s.
	3	-1.22	n.s.	0.46	n.s.
Lurcher B6CBA	1	-1.48	0.029	0.82	n.s.
	2	-1.17	n.s.	-1.05	n.s.
	3	-0.37	n.s.	-1.78	n.s.
wild type B6CBA	1	-2.70	0.009	-2.54	0.021
	2	-2.40	0.034	-2.26	0.044
	3	-0.92	n.s.	-1.05	n.s.

Article 3

Zdenka Purkartova, Jan Tuma, Martin Pesta, Vlastimil Kulda, Lucie Hajkova, Ondrej Sebesta, Frantisek Vozeh and Jan Cendelin

Morphological analysis of embryonic cerebellar grafts in SCA2 mice

Neuroscience Letters 2014; 558: 154-158

Neuroscience Letters 558 (2014) 154–158

Contents lists available at ScienceDirect

Neuroscience Letters

journal homepage: www.elsevier.com/locate/neulet

Morphological analysis of embryonic cerebellar grafts in SCA2 mice

Zdenka Purkartova[a], Jan Tuma[a,b], Martin Pesta[c], Vlastimil Kulda[d], Lucie Hajkova[c], Ondrej Sebesta[e], Frantisek Vozeh[a,b], Jan Cendelin[a,b,*]

[a] Department of Pathophysiology, Faculty of Medicine in Pilsen, Charles University, Lidicka 1, Pilsen 301 66, Czech Republic
[b] Biomedical Centre, Faculty of Medicine in Pilsen, Charles University, Husova 3, Pilsen 306 05, Czech Republic
[c] Department of Biology, Faculty of Medicine in Pilsen, Charles University in Prague, Karlovarska 48, Pilsen 301 66, Czech Republic
[d] Department of Medical Chemistry and Biochemistry, Faculty of Medicine in Pilsen, Charles University in Prague, Karlovarska 48, Pilsen 301 66, Czech Republic
[e] Laboratory of Confocal Microscopy, Faculty of Science, Charles University in Prague, Vinicna 7, Prague 2 12844, Czech Republic

HIGHLIGHTS

- Embryonic cerebellar graft survives for 12 weeks in both SCA2 and control mice.
- The grafts contained numerous Purkinje cells.
- Long distance graft-to-host axonal connections were rarely seen.
- Size of the cerebella and density of PCs did not seem to be reduced in SCA2 mice.

ARTICLE INFO

Article history:
Received 22 October 2013
Received in revised form 9 November 2013
Accepted 14 November 2013

Keywords:
Cerebellar degeneration
Neurotransplantation
Purkinje cells

ABSTRACT

SCA2 transgenic mice are thought to be a useful model of human spinocerebellar ataxia type 2. There is no effective therapy for cerebellar degenerative disorders, therefore neurotransplantation could offer hope. The aim of this work was to assess the survival and morphology of embryonic cerebellar grafts transplanted into the cerebellum of adult SCA2 mice. Four month-old homozygous SCA2 and negative control mice were treated with bilateral intracerebellar injections of an enhanced green fluorescent protein-positive embryonic cerebellar cell suspension. Graft survival and morphology were examined three months later. Graft-derived Purkinje cells and the presence of astrocytes in the graft were detected immunohistochemically. Nissl and hematoxylin–eosin techniques were used to visualize the histological structure of the graft and surrounding host tissue. Grafts survived in all experimental mice; no differences in graft structure, between SCA2 homozygous and negative mice, were found. The grafts contained numerous Purkinje cells but long distance graft-to-host axonal connections to the deep cerebellar nuclei were rarely seen. Relatively few astrocytes were found in the center of the graft. No signs of inflammation or tissue destruction were seen in the area around the grafts. Despite good graft survival and the presence of graft-derived Purkinje cells, the structure of the graft did not seem to promise any significant specific functional effects. We have shown that the graft is available for long-term experiments. Nevertheless, it would be beneficial to search for ways of enhancement of connections between the graft and host.

1. Introduction

The wide spectrum of human hereditary cerebellar degenerative diseases [1] is also reflected by the large number of mouse models of these diseases used for investigation of cerebellar functions and pathology [2]. Human autosomal dominant spinocerebellar ataxias (SCA) SCA1, SCA2, SCA3, SCA6, SCA7, and SCA17 are caused by an enlarged region of CAG trinucleotide repeats in the gene, resulting in an expansion of the polyglutamine tract (poly-Q) in the corresponding protein [1].

Transgenic mice carrying the human ataxin 2 gene, with enlarged CAG repeat sequence, are used as a model of human spinocerebellar ataxia 2 (SCA2) [3–6]. SCA2 mice suffer from a

Abbreviations: ATXN2^{Q127}, ataxin 2 with 127 glutamine repeats; DNA, Deoxyribonucleic acid; EGFP, enhanced green fluorescent protein; GAFP, glial fibrillary acidic protein; PC, Purkinje cell; pcd, Purkinje cell degeneration; PCR, polymerase chain reaction; SCA, spinocerebellar ataxia.

* Corresponding author. Tel.: +420 377 593 366; fax: +420 377 593 369.
E-mail addresses: zdenka.purkartova@lfp.cuni.cz (Z. Purkartova), jena.tuma@gmail.com (J. Tuma), martin.pesta@lfp.cuni.cz (M. Pesta), vlastimil.kulda@lfp.cuni.cz (V. Kulda), lucie.hajkova@lfp.cuni.cz (L. Hajkova), sebesta@natur.cuni.cz (O. Sebesta), frantisek.vozeh@lfp.cuni.cz (F. Vozeh), jan.cendelin@lfp.cuni.cz (J. Cendelin).

0304-3940/$ – see front matter © 2013 Elsevier Ireland Ltd. All rights reserved.
http://dx.doi.org/10.1016/j.neulet.2013.11.020

reduction in Purkinje cell (PC) number and show progressive motor deficits [3–5]. In the most frequently used natural mutant mouse models of hereditary cerebellar degeneration, such as pcd and Lurcher mice, functional deficits appear early on [7–9], while in SCA2 mice, it develops later and the onset varies based on: (1) the number of glutamine repeats, (2) line of mice and also differs between (3) homozygotes and heterozygotes [4,5]. In the SCA2 mouse line, expressing Q58 ataxin 2 (Q58-11 line), motor deficits on the rotarod test become evident at the age of 26 weeks in heterozygotes and at 16 weeks in homozygotes and the number of PCs have declined by 50% by the age of 6 months [5]. SCA2 mice, in the line expressing ataxin 2 with 127 glutamine repeats ($ATXN2^{Q127}$), have a more obvious pathological phenotype with an earlier onset [4].

Currently, therapy for hereditary cerebellar degenerations is ineffective; however, cerebellar transplantation could be promising. Several studies have shown long-term graft survival [10] and improvement of motor performance due to treatment with various neurotransplantation methods [11–14] in mouse models of cerebellar degeneration. Particularly, in C57BL/6J SCA2 transgenic mice Chang et al. [15] found that intravenous injection of human mesenchymal stem cells increased the survival of host PCs, delayed onset of disease and improved motor function. Despite the abundant research, there are no studies regarding the fate of embryonic cerebellar grafts in SCA2 mice.

The aim of this work was to assess the survival and morphology of embryonic cerebellar cell suspension grafts transplanted into the cerebellum of adult SCA2 mice.

2. Materials and methods

2.1. Animals

Cerebellar transplantation was studied in SCA2 transgenic mice of the B6D2-Tg(Pcp2SCA2)11Plt/J strain [5]. The C57BL/6-Tg(ACTB-EGFP)1Osb/J male mice were used to get graft donor embryos expressing enhanced green fluorescent protein (EGFP). Mice of both strains were purchased from The Jackson Laboratory (Bar Harbor, USA) and the colonies were then maintained in the animal facility at the Faculty of Medicine, Pilsen, CZ. The mice were kept under standard conditions with a 12:12 h light:dark cycle and water and food available *ad libitum*.

All experiments described in this article were conducted in full compliance with EU Guidelines for scientific experimentation on animals and with the permission of the Ethics Commission of the Faculty of Medicine, Pilsen, CZ. All efforts were made to minimize the number of animals used and their suffering.

2.2. Genotyping

The genotyping of SCA2 transgenic mice was performed on the basis of The Jackson Laboratory Genotyping protocols database (web page: http://www.jax.org). The Jackson Laboratory Genotyping protocol (Tg(Pcp2SCA2)11Plt-alternate1) has been designed as end point polymerase chain reaction (PCR) with the result transgene is present or not. This protocol was modified for quantitative assessment and the mice were classified into three subgroups "negative", "heterozygote", and "homozygote" according to amplification Ct. We are aware of the limitations of this approach relative to the unknown number of transgene copies inserted.

Deoxyribonucleic acid (DNA) was isolated from a piece of the mouse tail using DNeasy Blood & Tissue Kit (QIAGEN). DNA concentration was determined, and all DNA samples were diluted to a concentration of 60 ng/μl. The sequence of primers used for quantification of the transgene was as follows: transgene forward primer 13867 5′- AAT ACC TAT GAC GCC CAT GC -3′; transgene reverse primer 13868 5′- ATG AGC CCC GTA CTG AGT TG -3′. For the reference gene (internal positive control Reverse) forward primer oIMR7338 5′- CTA GGC CAC AGA ATT GAA AGA TCT-3′ and reverse primer oIMR7339 5′- GTA GGT GGA AAT TCT AGC ATC ATC C -3′ synthesized by GeneriBiotech (Hradec Kralove, Czech Republic) were used. DNA amplification was monitored with 0.5x Sybr-Green I (Molecular Probes, USA). The results of genotyping ("negative", "heterozygote", and "homozygote") were obtained according to ΔCt values (Ct for transgene minus Ct for reference gene).

For the experiment, only mice showing the maximal number of copies of the transgene, which were considered to be "homozygous" for SCA2 ($n = 15$), and negative ($n = 23$) individuals (both males and females) were used. The study was performed as a blinded-study since at the time of transplantation and histological examination the genotype of the mice was not known.

2.3. Transplantation

Embryonic cerebellar tissue was obtained from day 12 (E12, embryonic day 12) EGFP-expressing mouse embryos, which were obtained from the cross-breeding of females from the host strain with EGFP-expressing males. Donor females, with conception-timed pregnancies, were deeply anesthetized with Thiopental. Embryos were removed from the uterus, the embryonic cerebella were dissected, treated with trypsin for 10 min and mechanically suspended in the vehicle (0.9% NaCl and 0.6% glucose). The suspension concentration was adjusted to 50,000 cells/μl.

Four-months-old host mice were anaesthetized with Ketamine (100 mg/kg of the body weight) and Xylazine (16 mg/kg of the body

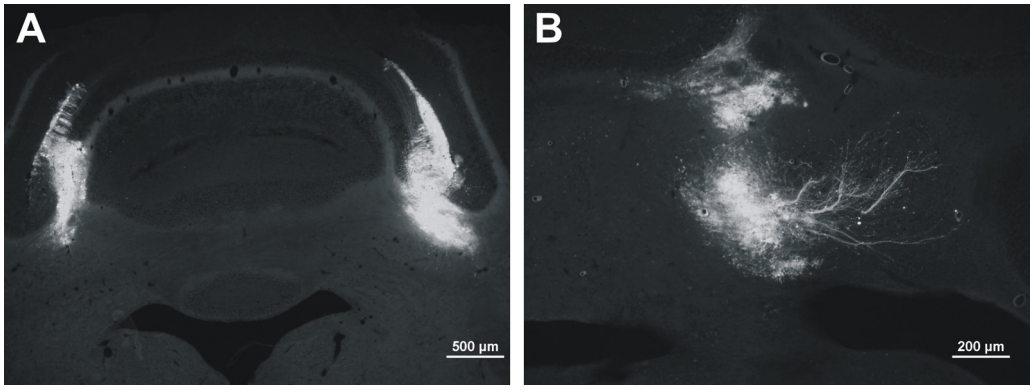

Fig. 1. A host cerebellum with the bilateral graft; the graft is located in the white matter close to the deep cerebellar nuclei and in the host cerebellar cortex; EGFP-positive fibers sprout from the right graft through the molecular layer of the cerebellar cortex and EGFP-positive Purkinje-like cells are distributed along the fissure (A; objective 4×). A subcortical graft with EGFP-positive fibers growing toward the deep cerebellar nuclei area (B; objective 10×). Native specimens, EGFP-fluorescence.

weight). The cell suspension was injected bilaterally (2 μl per site) into the host cerebellum (injection coordinates were 6.3 mm posterior to bregma, 1.5 mm lateral, 3.3 mm below the bregma) using a glass microcapillary. Injection speed was 0.5 μl/min.

2.4. Histological examination

The mice were sacrificed 12 weeks after transplantation by overdosing with thiopental and transcardially perfused with Ringer solution and 4% phosphate-buffered paraformaldehyde (pH 7.4). The brains were stored for 2 h in 4% phosphate-buffered paraformaldehyde for post-fixation and then incubated in sucrose for cryoprotection. Frontal 40 μm frozen sections were prepared. Graft identification and assessment of graft localization and presence of interactions between graft and host tissue (graft sprouting) were done in native specimens based on the natural green fluorescence of EGFP. Immunohistochemistry was used to identify PCs with anti-calbindin staining and to identify astrocytes with anti-glial fibrillary acidic protein (GFAP) staining in selected free-floating sections. In preparation for anti-calbindin staining, sections were incubated with anti-calbindin primary antibody (ab 11426, Abcam, Cambridge, United Kingdom, dilution 1:1000), overnight at room temperature and then with AlexaFluor® 594 secondary antibody (ab150076, Abcam, Cambridge, United Kingdom, dilution 1:400), for 2 h at room temperature. In preparation for anti-GFAP staining, sections were incubated with anti-GFAP primary antibody (clone G-A-5 Cy3 conjugate, Sigma–Aldrich, Saint Louis, USA, dilution 1:800), overnight at 4 °C. Remaining sections were stained using the Nissl or hematoxylin–eosin techniques, to visualize structures of the graft and surrounding host tissue.

For the basic specimen examination, an Olympus BX41 microscope (Olympus Corporation, Japan), with an epifluorescent accessory was used. Details of EGFP-positive (graft-derived) cells were imaged using a Leica TCS SP2 confocal microscope (Leica Microsystems GmbH, Germany). Co-localization of EGFP fluorescence and calbindin or GFAP positivity, indicating graft-derived PCs or astrocytes, respectively, was detected using an Olympus IX81 confocal microscope (Olympus Corporation, Japan).

2.5. Statistics

The presence of graft-derived PCs and the presence of EGFP-positive nerve fibers sprouting from the graft in homozygous SCA2 mice and negative animals were compared using Fisher's exact test. In all cases, $P < 0.05$ was considered to be statistically significant.

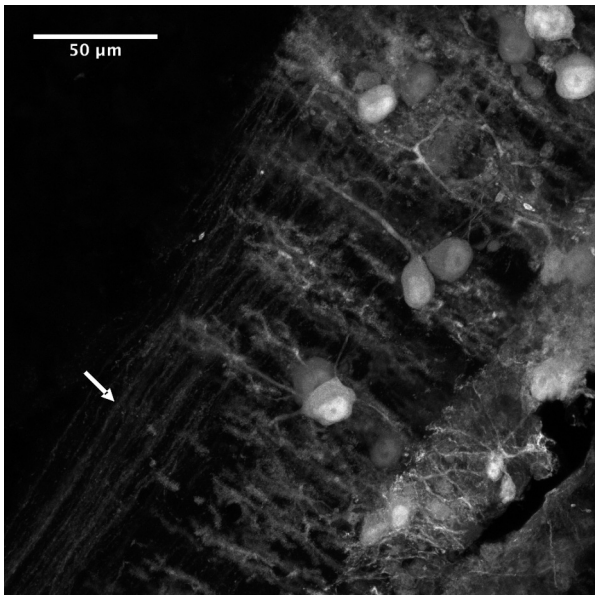

Fig. 2. Details of EGFP-positive Purkinje-like cells and EGFP-positive fibers (indicated by the arrow) perpendicular to the dendrites of the cells. Native specimen, EGFP-fluorescence, Leica TCS SP2 laser confocal microscope (objective 63×, superposition of 21 scans).

3. Results

Grafts survived in all experimental mice and there were no obvious and significant differences in graft structure between SCA2 homozygous and negative mice. In one SCA2 homozygous and one negative mouse the graft survived only unilaterally. Grafts usually consisted of a compact mass localized in the white matter close to the deep cerebellar nuclei or partially inside the nuclei. The grafts often propagated vertically into the cerebellar cortex and, in some cases, a large part of the graft was also in the cortical area (Fig. 1). In all mice the graft contained large EGFP-positive cells with cell bodies having a shape and dendritic tree arrangement typical of PCs (Fig. 2). The PC phenotype of these graft-derived cells was demonstrated by calbindin positivity (Fig. 3A and B). Graft-derived PCs

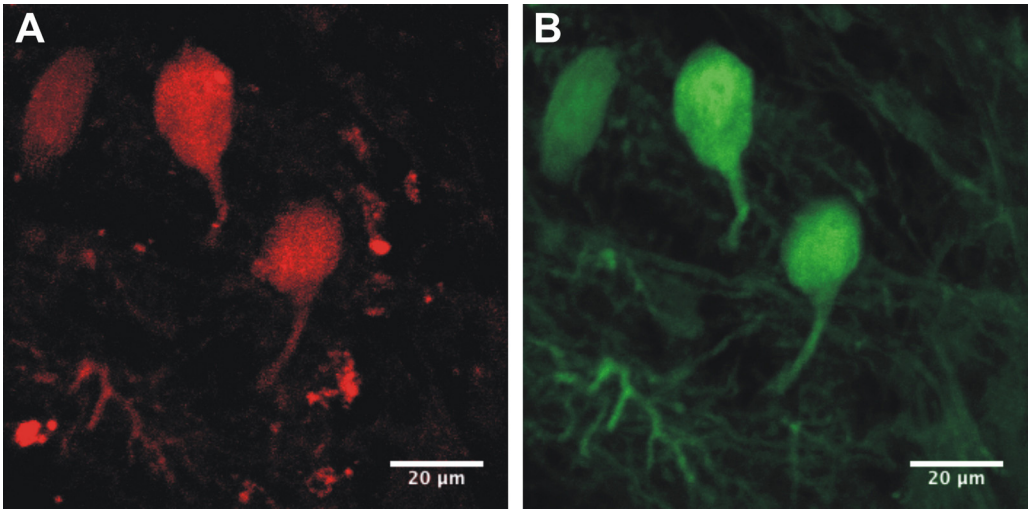

Fig. 3. Details of Purkinje-like cells showing both calbindin and EGFP-positivity. Anti-calbindin staining (A), EGFP-fluorescence (B), Olympus IX81 laser confocal microscope (objective 40×, superposition of 16 scans).

were also found outside the main graft mass, mostly along the fissures in extraparenchymal localization or in the molecular layer.

There was no significant difference in the presence of EGFP-positive fibers sprouting from the mass of the graft into the host tissue between SCA2 homozygous and negative mice (Fig. 1 A,B). Such fibers were found in 8 (53%) homozygous SCA2 mice. In 2 of them, cell fibers sprouted into the host cerebellar cortex, in 5 mice, fibers grew toward the deep cerebellar nuclei and in one mouse the fibers grew in both directions. In negative mice, cell fibers were found in 8 cases (35%). In 5 cases the fibers were in the host's cortex, in 2 mice, fibers grew toward the nuclei and in 1 mouse the fibers grew in both directions. The fibers growing into the host's cerebellar cortex were arranged in the molecular layer parallel to the cortex layer surface (Fig. 1A, Fig. 2). However, the grafts did not show the typical three-layer organization that is characteristic of the cerebellar cortex.

No signs of inflammation or destruction of host tissues were observed at the graft sites (figure not shown). In the central part of the graft, a slight increase in the density of astrocytes was observed compared with surrounding tissue of the deep cerebellar nuclei or cortex (Fig. 4A and B). The astrocytes in the graft were not EGFP-positive (Fig. 4C).

No sex differences in graft morphology were observed.

Surprisingly, the cerebella of host homozygous SCA2 mice were not markedly reduced in size and also the density of PCs did not seem to be decreased in comparison with negative animals.

4. Discussion

The embryonic cerebellar graft survived for 12 weeks in control negative as well as in SCA2 homozygous mice. There were no marked differences in graft structure between SCA2 and negative mice. The main mass of the graft was usually located in the white matter between the cortex and the deep cerebellar nuclei or in the upper part of the nuclei. Localization of embryonic cerebellar grafts under the granular layer of the cerebellar cortex, has been shown to be essential for connecting grafted PCs to the host's deep cerebellar nuclei, which is necessary for restoration of neural circuitries and cerebellar function in Purkinje cell degeneration (pcd) mice [16,17]. The granular layer acts as a barrier preventing nerve fiber sprouting toward the deep cerebellar nuclei when grafts are placed in the molecular layer [18,19]. In SCA2 mice, grafts developed into a compact mass with few nerve fibers sprouting into the host tissue; making our results similar to those described in B6CBA mice treated with the same type of graft [20]. In some cases the fibers were found in the part of the graft extending into the host's cerebellar cortex and the fibers were arranged in the molecular layer parallel to its surface like in Lurcher mice treated with solid embryonic cerebellar grafts [19,21]. Also, graft-derived PCs, which were not inside the main graft mass, were found mainly in the host cerebellar cortex. The propagation of graft-derived PCs into the host molecular layer agrees with the findings of Dumesnil-Bousez and Sotelo [19] and supports their idea that the host molecular layer exerts a positive neurotropism specific for grafted PCs. Contrary to *SCA1* mice treated with similar graft [13], organization of grafted PCs into typical layer was not so obvious and targeting the deep cerebellar nuclei by graft-derived axons was not frequent in SCA2 mice. In SCA1 mice, it has been shown that grafted neural precursor cells migrated into the cerebellar cortex only in mice with significant cell loss [11]. Lack of significant PCs reduction in homozygous SCA2 mice could explain poor and rather disorganized colonization of the host cerebellar cortex by grafted PCs.

In Lurcher mutant mice, as well as wild type mice of the B6CBA strain, treated with an embryonic cerebellar cell suspension or with a neuroprogenitor graft, experienced a massive increase in the

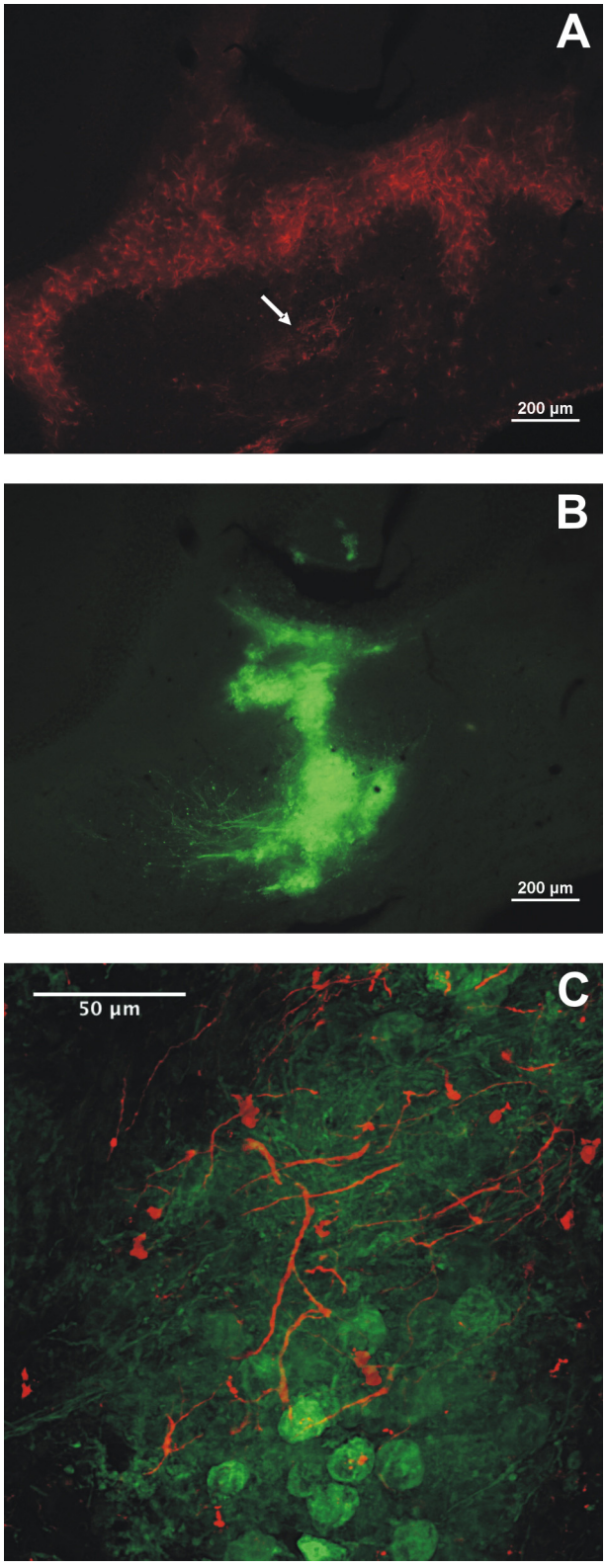

Fig. 4. Astrocytes in the graft area. Anti-GFAP staining showing astrocytes (A; objective 10×) and EGFP-fluorescence showing the graft position (B; objective 10×). The arrow indicates cluster of astrocytes inside the graft. GFAP-positive cells do not show EGFP positivity (C, Olympus IX81 laser confocal microscope, objective 20×, 2× zoom, superposition of 16 scans).

density of astrocytes inside the entire graft mass [20,22]. However, in SCA2 mice, we found relatively few astrocytes, and these tended to be in the central part of the graft, not in its periphery. These astrocytes were host-derived as they were not EGFP-positive.

Compared with most other graft types, embryonic neural cells are relatively well differentiated. When an E12 embryonic cerebellum is used as a donor, PCs are established before grafting [23] as, in the mouse cerebellum, this type of cell begins to appear between E11-13 (for review see [24]). The present study confirmed that grafted embryonic (E12) cerebellar tissue is a potent source of PCs. Donor tissue of higher embryonic age would be suitable for example for substitution of granular cells. Also the age of the graft recipient could influence the development of the graft, because progressive neurodegeneration could change the neurogenicity [25] of the recipient tissue in unknown manner.

Nevertheless, the embryonic cerebellar graft in SCA2 mice did not develop rich long-distance connections with the host's deep cerebellar nuclei, which is necessary for specific behavioral effects based on replacing lost PCs and rewiring cerebellar pathways.

On the other hand, the graft could also produce trophic effects, mediated by trophic factors (for example brain-derived neurotrophic factor, nerve growth factor, insulin-like growth factors 1 and 2, glial-derived neurotrophic factor). This mechanism could explain the development of functional restoration, despite a lack of reconnection of neural circuitries [13]. Trophic activity may be one of the main mechanisms that accounts for the prevention PCs extinction seen in association with grafted mesenchymal stem cells in mouse models of cerebellar degeneration [12,26] including SCA2 mice [15].

5. Conclusion

We have shown that the embryonic cerebellar grafts survive well in SCA2 mice and provide numerous PCs but the morphology of the graft does not promise any strong specific behavioral effects. The graft is available for long-term experiments. Nevertheless, it would be beneficial to search for ways of enhancement of connections between the graft and host.

Conflict of interest

There are no conflicts of interest to report.

Acknowledgment

The work was supported by the COST Action BM0901 grant No. LD12056 of the Ministry of Education, Youth and Sport of the Czech Republic. The authors thank Helena Geciova, Irena Pojarova, and Jan Javurek for technical assistance.

References

[1] M.U. Manto, The wide spectrum of spinocerebellar ataxias (SCAs), Cerebellum 4 (2005) 2–6.
[2] M. Manto, D. Marmolino, Animal models of human cerebellar ataxias: a cornerstone for the therapies of the twenty-first century, Cerebellum 8 (2009) 137–154.
[3] J. Aguiar, J. Fernandez, A. Aguilar, Y. Mendoza, M. Vazquez, J. Suarez, J. Berlanga, S. Cruz, G. Guillen, L. Herrera, L. Velazquez, N. Santos, N. Merino, Ubiquitous expression of human SCA2 gene under the regulation of the SCA2 self promoter cause specific Purkinje cell degeneration in transgenic mice, Neurosci. Lett. 392 (2010) 202–206.
[4] S.T. Hansen, P. Meera, T.S. Otis, S.M. Pulst, Changes in Purkinje cell firing and gene expression precede behavioral pathology in a mouse model of SCA2, Hum. Mol. Genet. 22 (2013) 271–283.
[5] D.P. Huynh, K. Figueroa, N. Hoang, S.M. Pulst, Nuclear localization or inclusion body formation of ataxin-2 are not necessary for SCA2 pathogenesis in mouse or human, Nat. Genet. 26 (2000) 44–50.
[6] J. Liu, T.S. Tang, H. Tu, O. Nelson, E. Herndon, D.P. Huynh, S.M. Pulst, I. Bezprozvanny, Deranged calcium signaling and neurodegeneration in spinocerebellar ataxia type 2, J. Neurosci. 29 (2009) 9148–9162.
[7] P. Fortier, A.M. Smith, S. Rossignol, Locomotor deficits in the cerebellar mutant mouse, Lurcher, Exp. Brain Res. 66 (1987) 271–286.
[8] V. Markvartova, J. Cendelin, F. Vozeh, Effect of dimethyl sulfoxide in cerebellar mutant Lurcher mice, Neurosci. Lett. 543 (2013) 142–145.
[9] R.J. Mullen, E.M. Eicher, R.L. Sidman, Purkinje cell degeneration, a new neurological mutation in the mouse, Proc. Nat. Acad. Sci. USA 73 (1976) 208–212.
[10] J. Cendelin, V. Babuska, I. Korelusova, Z. Houdek, F. Vozeh, Long-term survival of solid embryonic cerebellar grafts in Lurcher mice, Neurosci. Lett. 515 (2012) 23–27.
[11] S. Chintawar, R. Hourez, A. Ravella, D. Gall, D. Orduz, M. Rai, D.P. Bishop, S. Genua, S.N. Schiffmann, M. Pandolfo, Grafting neural precursor cells promotes functional recovery in an SCA1 mouse model, J. Neurosci. 21 (29) (2009) 13126–13135.
[12] J. Jones, J. Jaramillo-Merchán, C. Bueno, D. Pastor, M.C. Viso-León, S. Martínez, Mesenchymal stem cells rescue Purkinje cells and improve motor functions in a mouse model of cerebellar ataxia, Neurobiol. Dis. 40 (2010) 415–423.
[13] W.F. Kaemmerer, W.C. Low, Cerebellar allografts survive and transiently alleviate ataxia in a transgenic model of spinocerebellar ataxia Type-1, Exp. Neurol. 158 (1999) 301–311.
[14] L.C. Triarhou, W. Zhang, W.H. Lee, Amelioration of the behavioral phenotype in genetically ataxic mice through bilateral intracerebellar grafting of fetal Purkinje cells, Cell Transplant. 5 (1996) 269–277.
[15] Y.K. Chang, M.H. Chen, Y.H. Chiang, Y.F. Chen, W.H. Ma, Ch.Y. Tseng, B.W. Soong, J.H. Ho, O.K. Lee, Mesenchymal stem cell transplantation ameliorates motor function deterioration of spinocerebellar ataxia by rescuing cerebellar Purkinje cell, J. Biomed. Sci. 18 (2011) 54.
[16] C. Sotelo, R.M. Alvarado-Mallart, Reconstruction of the defective cerebellar circuitry in adult Purkinje cell degeneration mutant mice by Purkinje cell replacement through transplantation of solid embryonic implants, Neuroscience 20 (1987) 1–22.
[17] L.C. Triarhou, W.C. Low, B. Ghetti, Intraparenchymal grafting of cerebellar cell suspensions to the deep cerebellar nuclei of pcd mutant mice, with particular emphasis on re-establishment of a Purkinje cell cortico-nuclear projection, Anat. Embryol. (Berl.) 185 (1992) 409–420.
[18] B. Carletti, I.M. Williams, K. Leto, K. Nakajima, L. Magrassi, F. Rossi, Time constraints and positional cues in the developing cerebellum regulate Purkinje cell placement in the cortical architecture, Dev. Biol. 317 (2008) 147–160.
[19] N. Dumesnil-Bousez, C. Sotelo, Partial reconstruction of the adult Lurcher cerebellar circuitry by neural grafting, Neuroscience 55 (1993) 1–21.
[20] M. Cedikova, Z.Houdek, V., Babuska, V., Kulda, F., Vozeh, N., Zech, L., Cerna, K., Krakorova, M., Kralickova, J. Cendelin, Fate of two types of cerebellar graft in wild type and cerebellar mutant mice, J. Appl. Biomed.: in press.
[21] J. Cendelin, I. Korelusova, F. Vozeh, A preliminary study of solid embryonic cerebellar graft survival in adult B6CBA Lurcher mutant and wild type mice, Anat. Rec. 292 (2009) 1986–1992.
[22] Z. Houdek, J. Cendelin, V. Kulda, V. Babuska, M. Cedikova, M. Kralickova, J. Pachernik, G.B. Stefano, F. Vozeh, Intracerebellar application of P19-derived neuroprogenitor and naive stem cells to Lurcher mutant and wild type B6CBA mice, Med. Sci. Monit. 18 (2012) 174–180.
[23] B. Carletti, F. Rossi, Selective rather than inductive mechanisms favour specific replacement of Purkinje cells by embryonic cerebellar cells transplanted to the cerebellum of adult Purkinje cell degeneration (pcd) mutant mice, Eur. J. Neurosci. 22 (2005) 1001–1012.
[24] B. Carletti, F. Rossi, Neurogenesis in the cerebellum, Neuroscientist 14 (2008) 91–100.
[25] F. Rossi, E. Cattaneo, Neural stem cell therapy for neurological diseases: dreams and reality, Nat. Rev. Neurosci. 3 (2002) 401–409.
[26] M.J. Zhang, J.J. Sun, L. Qiana, Z. Liu, Z. Zhang, W. Cao, W. Li, Y. Xu, Human umbilical mesenchymal stem cells enhance the expression of neurotrophic factors and protect ataxic mice, Brain Res. 1402 (2011) 122–131.

Article 4

Jan Cendelin, Jan Tuma, Ivana Korelusova and Frantisek Vozeh

The effect of genetic background on behavioral manifestation of *Grid2*^{Lc} mutation

Behavioural Brain Research 2014; 271: 218-227

Behavioural Brain Research 271 (2014) 218–227

Contents lists available at ScienceDirect

Behavioural Brain Research

journal homepage: www.elsevier.com/locate/bbr

Research report

The effect of genetic background on behavioral manifestation of *Grid2*^{Lc} mutation

Jan Cendelin[a,b,*], Jan Tuma[a,b], Ivana Korelusova[a], Frantisek Vozeh[a,b]

[a] Department of Pathophysiology, Faculty of Medicine in Pilsen, Charles University in Prague, Lidicka 1, 301 66 Plzen, Czech Republic
[b] Biomedical Centre, Faculty of Medicine in Pilsen, Charles University in Prague, Plzen, Czech Republic

HIGHLIGHTS

- C3H mice had worse performances in the water maze than their B6CBA counterparts.
- *Lurcher* mice showed impairment of motor skills and water maze performance.
- *Lurcher* mutation induces strong pathological phenotype.
- The phenotype results from superposition of the strain and *Lurcher* mutation factors.

ARTICLE INFO

Article history:
Received 12 February 2014
Received in revised form 6 June 2014
Accepted 10 June 2014
Available online 14 June 2014

Keywords:
Ataxia
Cerebellar degeneration
Genetic background
Lurcher mice
Spatial orientation

ABSTRACT

Mutant mice are commonly used models of hereditary diseases. Nevertheless, these mice have phenotypic traits of the original strain, which could interfere with the manifestation of the mutation of interest. *Lurcher* mice represent a model of olivocerebellar degeneration, which is caused by the *Grid2*^{Lc} mutation. *Lurchers* show ataxia and various cognitive and behavioral abnormalities. The most commonly used strains of *Lurcher* mice are B6CBA and C3H, but there is no information about the role of genetic background on the *Grid2*^{Lc} manifestation. The aim of this work was to compare spatial navigation in the Morris water maze, spontaneous activity in the open field and motor skills on the horizontal wire, slanted ladder and rotarod in B6CBA and C3H *Lurcher* mutant and wild type mice. The study showed impaired motor skills and water maze performance in both strains of *Lurcher* mice. Both C3H *Lurcher* and C3H wild type mice had poorer performances in the water maze task than their B6CBA counterparts. In the open field test, C3H mice showed higher activity and lower thigmotaxis. The study showed that genetic backgrounds can modify manifestations of the *Lurcher* mutation. In this case, B6CBA *Lurcher* mice models probably have more validity when studying the behavioral aspects of cerebellar degeneration than C3H *Lurcher* mice, since they do not combine abnormalities related to the *Grid2*^{Lc} mutation with strain-specific problems.

1. Introduction

Mutant, transgenic and knock-out mice have become commonly used models of human diseases (for review see [36]). Nevertheless, these mice have the phenotypic traits of the original strain, which could interfere with the manifestation of the mutation of interest. In many mouse strains specific genetically determined abnormalities, such as sensory deficits, are standard components of the phenotype. Strain differences relative to brain morphology and physiology [20,57,58], level of anxiety and stress response [2,25,54], exploratory behavior, locomotor activity [56] and motor abilities [1,42,53] have been described. It is not surprising that strain differences in cognitive tests have also been reported [3,24,44] since these tests could easily be influenced by the variations mentioned above.

Some mutations causing specific disorders are found in several strains. The *Lurcher* mutant mouse [46], a commonly used model for olivocerebellar degeneration, is a good example.

Abbreviations: B6CBA$^{+/Lc}$, B6CBA *Lurcher* mice; B6CBA$^{+/+}$, B6CBA wild type mice; C3H$^{+/Lc}$, C3H *Lurcher* mice; C3H$^{+/+}$, C3H wild type mice; df, degree of freedom; E, East; MWM, Morris water maze; N, North; NE, North-East; NS, non-significant; OF, open field test; S, South; SEM, standard error of the mean; SW, South-West; vs., versus; W, West.

* Corresponding author at: Department of Pathophysiology, Faculty of Medicine in Pilsen, Charles University in Prague Lidicka 1, 301 66 Plzen, Czech Republic. Tel.: +420 377 593 366; fax: +420 377 593 369.
E-mail address: jan.cendelin@lfp.cuni.cz (J. Cendelin).

http://dx.doi.org/10.1016/j.bbr.2014.06.023
0166-4328/

Neurodegeneration in *Lurcher* mice is caused by a mutation (*Grid2*^{Lc}) in the δ2 glutamate receptor (GluRδ2) gene, which changes the receptor into a leaky membrane channel that chronically depolarizes the cells [60].

Homozygous mutants (*Grid2*$^{Lc/Lc}$) are not viable [11]. In heterozygous *Lurcher* mice (*Grid2*$^{+/Lc}$) the total loss of Purkinje cells and a reduction in cerebellar cortex interneurons and inferior olive neurons occurs by three months of age [4,59]. *Lurcher* mice suffer from ataxia [16,30], fail in spatial learning and orientation tasks [6,21,29,31] and exhibit changes in conditioned eyelid responses [47,48]. Additionally, hypothalamo-pituitary-adrenal axis hyper-responsiveness [17], increased plasma levels of adrenocorticotropin and corticosterone together with abnormal emotional behavior and behavioral disinhibition [23,34] and a high incidence of maternal infanticide [55] have been described in *Lurcher* mice, particularly of the B6CBA background strain. For review see [9].

The most frequently used *Lurcher* mouse strains are the C3H and B6CBA. C3H is a widely used strain. Some C3H individuals suffer from retinal degeneration determined by a homozygous combination of the *Pde6b*^{rd1} allele, which leads to a loss of the photoreceptors [10]. C3H *Lurcher* mice were used in the first detailed description of morphological changes in the cerebellum [4], although, rarely for behavioral studies [29]. The B6CBA strain is less common. Nevertheless, this strain is often used for spontaneous or transgenic neurological mutants, e.g. the *weaver* cerebellar mutant and the Huntington disease mouse model [18,19]. *Lurchers* of the B6CBA (B6CBACa/a, C57BlxCBA) strain have been used in most behavioral and neurochemical studies [6,7,22,49]. Additionally, they have been used in recent morphological studies [11,51] as well as in some studies in *Lurcher*-wild type chimeras [14,39]. Other strains of *Lurcher* mice are seldom used. The B6AKR strain was used e.g. by Zanjani et al. [59] to study survival of interneurons and parallel fiber synapses. In the inbred strain BALB/cByJ a second Lurcher allele (*Lc*^{J}), which was phenotypically indistinguishable from *Grid2*^{Lc}, was found [12].

The retinal degeneration, which impairs visual orientation, is a crucial difference between the C3H and B6CBA strains of *Lurcher* mice. The question is whether there are additional differences between C3H and B6CBA *Lurcher* mice that are not related to retinal degeneration. The role of genetic background has yet to be studied in *Lurcher* mutant mice. There are no studies directly comparing the two strains of *Lurchers* using identical experimental protocols. Moreover, there are no comparable studies describing similar parameters in different strains of *Lurchers* using similar methods. Therefore, we can only conclude that the main features of the morphological manifestation of the degeneration and motor deficit are present in both C3H and B6CBA strains of *Lurcher* mice.

Nevertheless, for an appropriate interpretation of findings of studies using mutant mouse models of human diseases it is necessary to understand all factors involved in their phenotype. The aim of this work was to assess the influence of genetic background on the manifestation of the *Grid2*^{Lc} mutation on cognitive function. Spatial performance in the Morris water task was studied and was of particular interest. Exploratory behavior and motor skills were also examined since they are essential substrates for spatial behavior.

2. Material and methods

2.1. Animals

Adult *Lurcher* mutants (*Grid2*$^{+/Lc}$) and healthy wild type (*Grid2*$^{+/+}$) littermates (both males and females equally) of the B6CBA and C3H strains were used. C3H mice were kindly provided by Dr. K. W. T. Caddy from the University College London [4,5]. B6CBA mice were kindly provided by Prof. A. Resibois from the Universiteí Libre de Bruxelles in 1998; these mice were derived from those used by Sotelo and collaborators [15,50].

Mice of both strains were housed in the same room of the breeding facility under identical conditions. Mice were kept in a room with controlled temperature (22–23 °C) and humidity (50–60%), 12/12 h light/dark cycle (6 am–6 pm) and housed 2–4 mice per cage (22 × 25 × 14 cm). The experiments were performed during the light period (8 am–2 pm). Food (standard commercial pellet diet) and water were available *ad libitum*.

Mice used in this study were obtained by crossing wild type females with *Lurcher* males. In C3H mice, the presence of retinal degeneration was determined histologically by the absence of the outer nuclear layer of the retina in hematoxylin-eosin stained sections prepared on completion of the experiments (*post mortem*). Animals affected with retinal degeneration were excluded from the study since they were not comparable with B6CBA animals.

Based on type and strain, the mice were distributed into four experimental groups: B6CBA *Lurcher* (B6CBA$^{+/Lc}$, $n = 16$, mean body weight = 24.6 g), B6CBA wild type mice (B6CBA$^{+/+}$, $n = 26$, mean body weight = 27.6 g), C3H *Lurcher* (C3H$^{+/Lc}$, $n = 16$, mean body = weight 26.7 g) and C3H wild type mice (C3H$^{+/+}$, $n = 18$, mean body weight = 29.5 g). Mean mouse age at the time of the study was 180 days.

All experiments reported here were conducted in full compliance with the EU Guidelines for scientific experimentation on animals and with the permission of the Ethics Commission of the Faculty of Medicine in Pilsen. All efforts were made to minimize discomfort.

2.2. Design of the experiment

Spatial orientation and learning were tested using a modified protocol of the Morris water maze [41], spontaneous explorative activity was examined in the open field test and motor skills were examined with a battery of standard tests. The main aim of the work was to assess spatial orientation and learning; therefore, the above mentioned tests were performed in the order mentioned to avoid any influence that 'experience with the motor tests' might have on performance in the water maze. The scheme of the experiment is shown in Fig. 1.

2.3. Experimental procedures

2.3.1. Morris water maze task

For the Morris water maze a round pool with a diameter of 95 cm, with a rim 10 cm above the water level, was used. A circular escape platform, with a diameter of 7.5 cm, was hidden 0.5 cm under the water level. Labels on the room walls served as distant visual cues. Four starting points around the circumference of the pool were arbitrary designated: North (N), South (S), West (W) and East (E). Four trials a day were performed with inter-trial intervals of 8 min. If the mouse did not reach the platform within 60 s it was manually placed upon it. After each trial the mouse was left on the platform for 30 s.

The procedure consisted of 5 phases (I–V). For the first nine days (D1–9, phase I) the starting positions were in the order N–S–W–E and the hidden platform was located in the middle of the SW quadrant of the maze. This is a common Morris water maze protocol to evaluate basal performance of mice on this task. On day 10 (D10, phase II) the platform was still in the middle of the SW quadrant, but the sequence of starting positions was E–W–S–N to change the order of the four spatial relationships between the starting point and the goal.

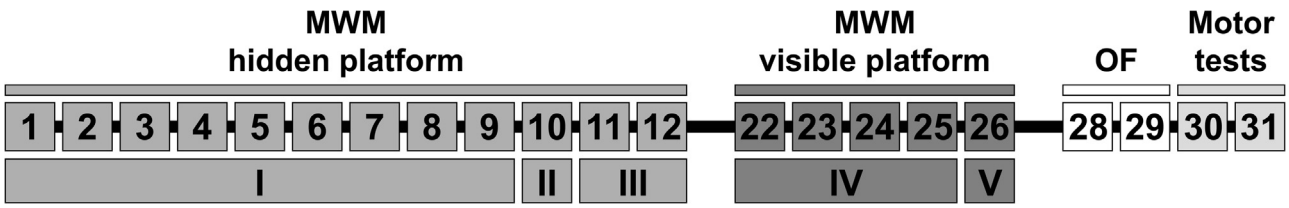

Fig. 1. Experimental protocol: The experiment lasted for 31 days (D1-D31) and consisted of 5 phases (I: hidden platform test, II: changed starting point sequence, III: changed position of the hidden platform, IV: visible platform test, V: changed position of the visible platform) involving the Morris water maze test (MWM), open field tests (OF) and motor tests.

On day 11 and 12 (D11–12, phase III) the platform was moved to the opposite quadrant (NE) and the order of the starting positions was N–S–W–E to test the ability to relearn the new goal position.

Because changes in experiment arrangement during D10–12 could confuse the mice, for the next 10 days the mice were not exposed to the maze to reduce the influence of these changes in performance of the mice in the following phase of the experiment.

On days 22–25 (D22–25, phase IV) the platform, which was in the SW quadrant, was made visible with a cylindrical label (3 cm in diameter, height of 5 cm) with vertical black and white stripes mounted 12 cm over the platform. The order of the starting positions was N–S–W–E. The purpose of this phase was to examine the ability to navigate to a visible goal.

On day 26 (D26, phase V), the visible platform was placed in the NE quadrant. The order of the starting positions was N–S–W–E. This change of visible platform position was to assess whether the mice prefer the navigation toward memorized platform position or visible goal navigation. Since the mice had experience with changes in platform position, and to avoid experience with a missing platform, no probe trials were used before the visible platform phase of the experimental procedure.

The movement of the mice in the maze was recorded using an automatic tracking system EthoVision 3.1 (Noldus Information Technology bv, Netherlands). Escape latencies (s), trajectory length (cm) and swimming velocity (cm/s) were measured as basic parameters. To assess the exploration strategy, thigmotaxis [52] was examined (i.e. the percentage trajectory length moved in the 5 cm margin zone of the maze) and percentage of direct finding type of trajectory. Trials with trajectory lengths shorter than 1.3 times the length of the shortest distance between the starting point and the platform were considered as direct finding of the platform. Mean values of four trials, done in 1 day, were calculated for each animal and each parameter.

To quantify the change in performance during or between individual phases of the experiment, ratios of trajectory lengths as the main parameter were calculated: D9/D1 – the learning effect during the initial hidden platform task, D10/D9 – the effect of changing the order of the starting positions, D11/D9 – the effect of changing the platform position, D12/D11 – the ability to learn a new platform position, D25/D22 – the learning effect during a visible platform task, D26/D25 – the effect of changing the position of the visible platform.

For the first trial (N-starting point) on D11, trajectories that moved through individual quadrants of the maze were compared in order to assess the preference for the SE quadrant, in which the platform has been originally located.

2.3.2. Open field test

Space exploration activity, which can also be influence by anxiety level, was examined in the open-field test. It was performed on day 28 (D28) and repeated in the same way on day 29 (D29). The apparatus consisted of a plastic box (40 cm × 40 cm × 40 cm) with white walls and floor. The animal was placed in the middle of the square arena and allowed to freely explore for 5 min. The apparatus was cleaned with 70% ethanol and dried between subjects. The movement of the mice was recorded using an automatic tracking system EthoVision 3.1. (Noldus Information Technology bv, Netherlands). Trajectory length (cm), locomotion activity (percentage of time spent moving) and the thigmotaxis (percentage of time spent in the 3 cm margin zone of the arena) [52] were measured.

2.3.3. Motor tests

Motor skill tests on the horizontal wire, slanted ladder and rotarod were performed on day 30 (D30) and repeated on day 31 (D31). For each mouse, each day's session consisted of four trials on the horizontal wire, slanted ladder and rotarod tasks (done in this order). Between trials mice were placed back in their home-cage for 5 min.

For the horizontal wire test the animal grasps, using its forepaws, the middle of a wire (43 cm length, 1 mm diameter) suspended 39 cm above a table between two wooden columns. The area beneath the wire was cushioned with a soft pillow. For the slanted ladder test the mouse was placed, facing up the incline, in the middle of a slanted ladder (30 cm long, 4 cm wide, inclination of 53°, with the upper end 24 cm above the table). For the rotarod test the mouse was placed on a cylinder with its head in the direction of rotation, as such, its first task was to orient itself in the opposite direction. The cylinder length was 20 cm and the diameter was 17 cm. The rotation speed was one turn per minute.

In all tests, fall latencies were measured. If the mouse did not fall or actively leave the apparatus within 60 s the trial was stopped. Mean fall latencies of the four trials were calculated for each animal, test and day. When there was active departure from the apparatus, a maximal latency of 60 s was assigned. For the wire test, active departure was by means of climbing down using one of the two wooden columns between which the wire was suspended. In the ladder test, climbing down onto the table was considered active departure. In the rotarod test, jumping from the rod was considered active departure.

2.4. Statistical analysis

A violation of the Gaussian distribution assumption was verified using the Kolmogorov–Smirnov test of normality. Because most of the analyzed parameters did not have a normal distribution, non-parametric permutation tests were used [45]. The repeated measurements in the Morris water maze, open field as well as motor function assessment were evaluated using a permutational unbalanced ANOVA with repeated measurement with two between-group factors (strain and mutation) and one within-group factor (day). Each day was then analyzed separately using a permutational two-way ANOVA. If any significance was found, post hoc tests using permutational *t*-test with Bonferroni correction for repeated measurement were calculated. To assess the difference between performances on two individual days of the tests within one group, the permutational paired *t*-test was used. To assess the significance of the change of parameters within a phase of the water

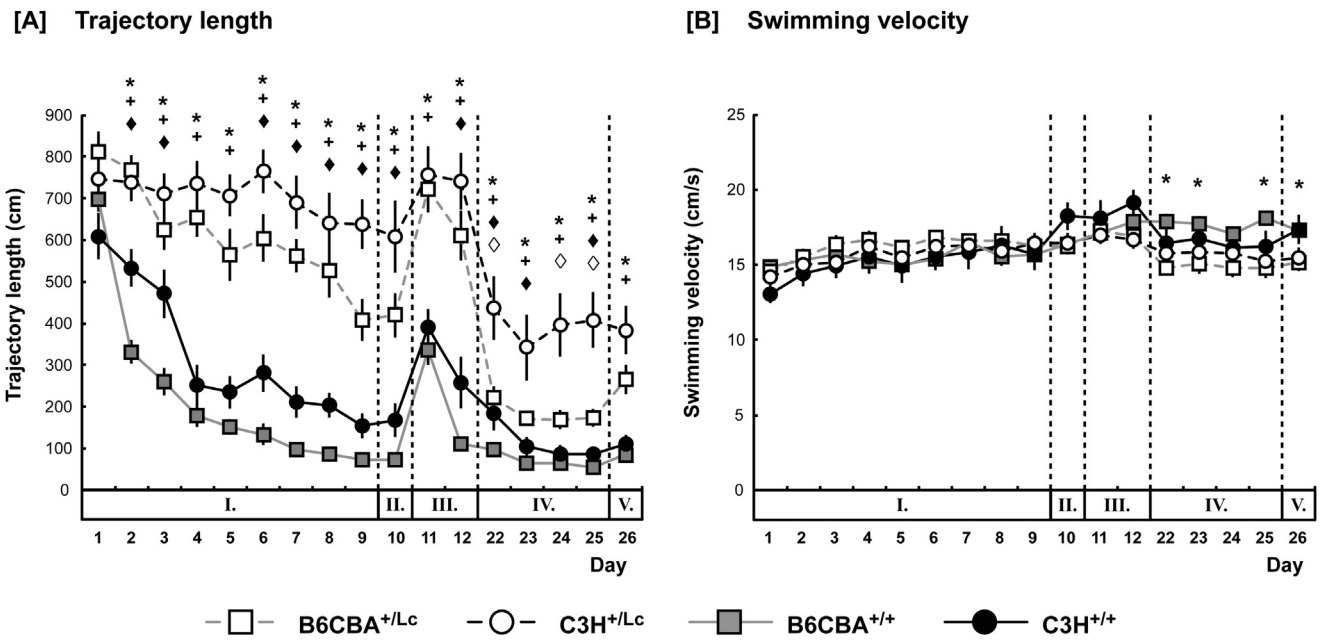

Fig. 2. Morris water maze: Mean trajectory length in cm (A) and swimming velocity in cm/s (B) in the Morris water maze (MWM) in B6CBA$^{+/Lc}$, B6CBA$^{+/+}$, C3H$^{+/Lc}$ and C3H$^{+/+}$ mice. Error bars represent SEM. I.-V. indicate individual parts of the MWM test. $P < 0.05$ is indicated by * for B6CBA$^{+/+}$ vs. B6CBA$^{+/Lc}$, by + for C3H$^{+/+}$ vs. C3H$^{+/Lc}$, by ♦ for B6CBA$^{+/+}$ vs. C3H$^{+/+}$ and by ◊ for B6CBA$^{+/Lc}$ vs. C3H$^{+/Lc}$.

maze test, a permutational ANOVA with repeated measurement was used. The preference for the SW quadrant was verified using a permutational one-sample *t*-test against 25%, which represents a random occurrence.

All permutational *t*-tests were done with 10,000 permutations. The ANOVA tests were performed with maximum of 5,000 permutations. Differences were considered statistically significant if $P < 0.05$. Statistical analyses were performed using R 2.14.0 (GNU) for Mac OS X. The data are presented as mean ± standard error of the mean (SEM).

3. Results

3.1. Morris water maze

Trajectory length, swimming velocity and statistical significance of differences in these parameters between individual experimental groups are shown in Fig. 2. Thigmotaxis and percentage of direct finding trials and statistical significance of differences in these parameters between individual experimental groups are shown in Fig. 3. Significance of the between-group effect of strain and mutation factors and their interaction on trajectory length, swimming velocity, tigmotaxis and percentage of direct finding trials is shown in Table 1. Ratios of trajectory lengths on crucial days of the experiment and significance of the between-group effect of strain and mutation factors and their interaction on the ratios is shown in Table 2. Statistical significance of changes of trajectory length between these days is shown in Table 3. Escape latencies were determined by the trajectory length and swimming velocity. The data shows that escape latencies significantly correlated with the trajectory length (for B6CBA$^{+/+}$ $R = 0.946$, $P < 0.0001$, for B6CBA$^{+/Lc}$ $R = 0.967$, $P < 0.0001$, for C3H$^{+/+}$ $R = 0.941$, $P < 0.0001$, for C3H$^{+/Lc}$ $R = 0.860$, $P < 0.0001$). Therefore the data for escape latencies are not shown.

Lurcher mice of both strains (B6CBA$^{+/Lc}$, C3H$^{+/Lc}$) achieved longer trajectories during all parts of the experiment (Fig. 2A) compared to their wild type counterparts (B6CBA$^{+/+}$, C3H$^{+/+}$). B6CBA$^{+/+}$ showed shorter trajectories than C3H$^{+/+}$ during both hidden and visible platform task. B6CBA$^{+/Lc}$, however, only had shorter trajectories than C3H$^{+/Lc}$ during the visible platform phase (Fig. 2A). Significant shortening of the trajectory length during the initial phase with the hidden platform (D1–D9) in the Morris water maze test was observed in B6CBA$^{+/+}$, B6CBA$^{+/Lc}$ and C3H$^{+/+}$ mice (Table 3). B6CBA$^{+/+}$ and C3H$^{+/+}$ mice also showed shortening of the trajectory during the visible platform task (D22–D25). In C3H$^{+/Lc}$ mice, a significant shortening of the trajectory was not observed. *Lurcher* mice of both strains (B6CBA$^{+/Lc}$, C3H$^{+/Lc}$) achieved a higher D9/D1 ratio of trajectories ($t = 7.586$, $P < 0.0001$; $t = 6.242$, $P < 0.0001$ respectively, Table 2) compared to their wild type counterparts (B6CBA$^{+/+}$, C3H$^{+/+}$). B6CBA mice had a lower D9/D1 ratio for trajectories than C3H mice (for wild type mice $t = 4.526$, $P < 0.0001$; for *Lurchers* $t = 2.918$, $P = 0.005$; Table 2).

Change of starting point sequence (D9 vs. D10) did not influence the performance of the mice in the water maze. Changing the hidden platform position (D9 vs. D11) led to a prolonged trajectory length in all experimental groups (Table 3). The D11/D9 ratio (Table 2) showed that the prolongation was higher in the wild types than in *Lurcher* mice (for B6CBA: $t = -3.06$, $P = 0.003$, for C3H: $t = -3.211$, $P < 0.0001$) and in B6CBA$^{+/Lc}$ than in C3H$^{+/Lc}$ mice ($t = -2.558$, $P < 0.011$). In the first trial (N-starting position) on D11, both B6CBA$^{+/+}$ and C3H$^{+/+}$ mice swam a significantly higher percentage of the total trajectory length ($P = 0.0007$, $P = 0.0141$ respectively) inside the SW quadrant, where the platform had been located on all previous days, compared to 25% of the trajectory length, as would be expected in a random search (Fig. 4). In *Lurcher* mice, preference for the SW quadrant was statistically insignificant. Fig. 5 also shows a preference for the SW quadrant by both B6CBA$^{+/+}$ and C3H$^{+/+}$ mice on the first trial of D11.

Learning the new position of the platform resulted in significantly shortened trajectory lengths (D11 vs. D12) in B6CBA$^{+/+}$ and B6CBA$^{+/Lc}$ mice (Table 3), but not in C3H mice. The D12/D11 ratio (Table 2) was significantly smaller in B6CBA$^{+/+}$ mice compared to B6CBA$^{+/Lc}$ ($t = 3.902$, $P < 0.0001$). Changing the position of the visible platform (D25 vs. D26) led to a longer trajectory length in B6CBA$^{+/+}$

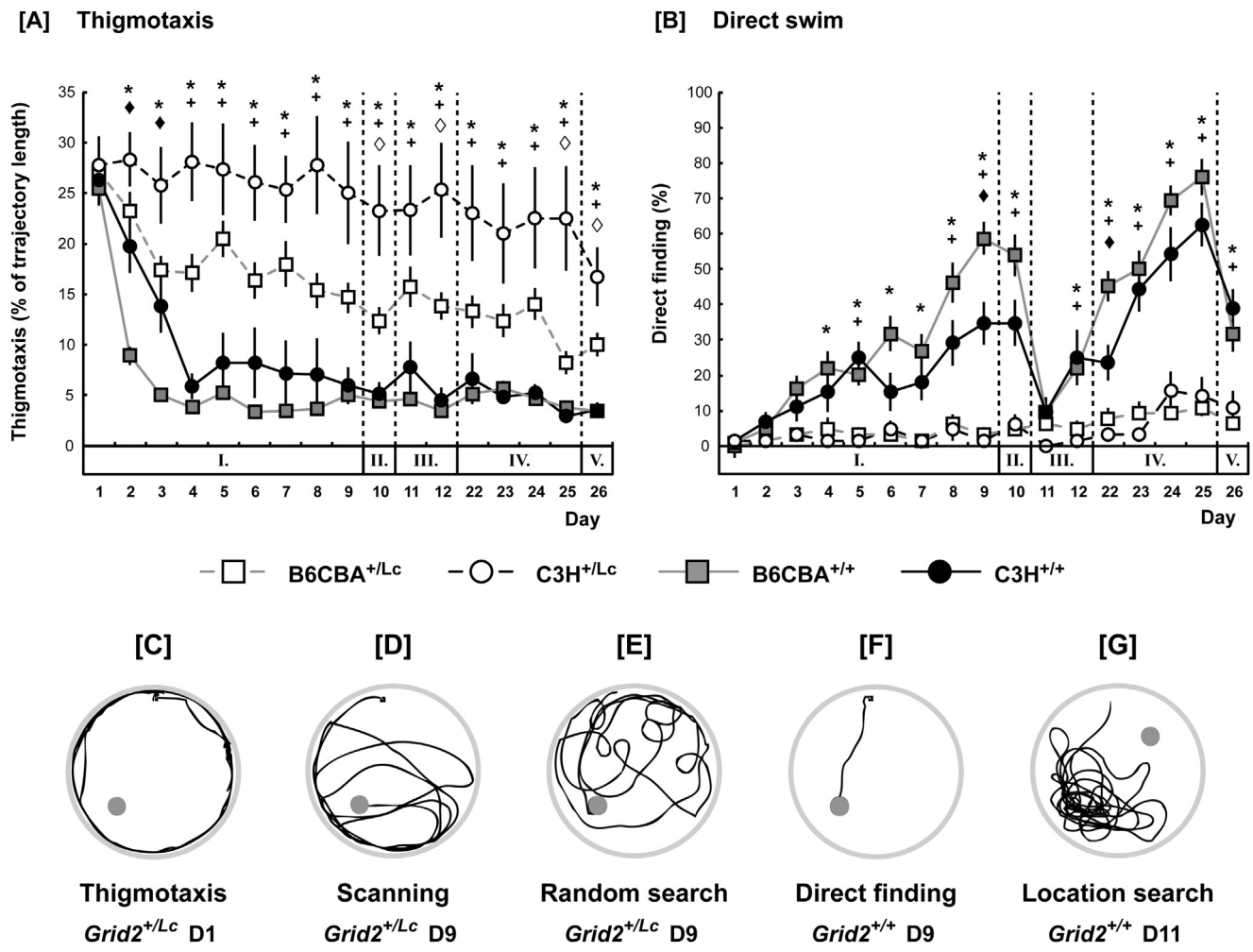

Fig. 3. Morris water maze: Mean thigmotaxis in % (A) and percentage of direct finding trials in % (B), in the Morris water maze (MWM) in B6CBA$^{+/Lc}$, B6CBA$^{+/+}$, C3H$^{+/Lc}$ and C3H$^{+/+}$ mice. Error bars represent SEM. I–V indicate individual parts of the MWM test. $P < 0.05$ is indicated by * for B6CBA$^{+/+}$ vs. B6CBA$^{+/Lc}$, by + for C3H$^{+/+}$ vs. C3H$^{+/Lc}$, by ♦ for B6CBA$^{+/+}$ vs. C3H$^{+/+}$ and by ◊ for B6CBA$^{+/Lc}$ vs. C3H$^{+/Lc}$. Examples of thigmotaxis in a *Lurcher* mouse in the first trial on D1 (C), random search (D) and scanning (E) strategy typical for *Lurcher* mice on D9, direct finding typical for wild type mice on D9 (F), and searching in zone of original platform location in a wild type mouse on D11 (G).

and B6CBA$^{+/Lc}$ mice (Table 3), but not in C3H mice. While the trajectory length on the first day of the phase with a visible platform (D22) was significantly shorter than the trajectory on the last day of the phase with a hidden platform (D9) in both B6CBA *Lurcher* ($t = 5.126$, $P = 0.0001$) and C3H *Lurcher* mice ($t = 3.464$, $P = 0.0049$), wild type mice did not perform any better when the platform was visible.

Lurcher mice showed more thigmotaxis in the water maze than their wild type counterparts during both the hidden and visible platform task (Fig. 3A). Thigmotaxis was occasionally, but not consistently higher in C3H than in B6CBA mice (Fig. 3A).

Lurcher mice of both strains had a very low percentage of direct finding trials compared with their wild type counterparts. B6CBA$^{+/+}$ mice had a significantly higher percentage of direct finding trials than C3H$^{+/+}$ mice, but only on D9 and D22 (Fig. 3B). In wild type mice of both strains the percentage increased during phase I (B6CBA$^{+/+}$: $F_{(8,200)} = 26.043$, $P < 0.0001$; C3H$^{+/+}$: $F_{(8,\ 136)} = 6.234$, $P < 0.0001$) as well as phase IV (B6CBA$^{+/+}$: $F_{(3,\ 75)} = 10.454$, $P = 0.0228$; C3H$^{+/+}$: $F_{(3,\ 57)} = 10.064$, $P = 0.0016$) of the water maze task. In C3H$^{+/+}$ mice the percentage increased during phase IV ($F_{(3,\ 45)} = 3.284$, $P = 0.0273$). Changes in both hidden (D9 vs. D11) and visible (D25 vs. D26) platform position led to a marked drop in the percentage of direct finding in wild type mice (D9 vs. D11 - B6CBA$^{+/+}$: $t = 10.923$, $P = 0.0001$, C3H$^{+/+}$: $t = 3.306$, $P = 0.0087$; D25 vs. D26 - B6CBA$^{+/+}$: $t = 5.024$, $P = 0.0002$, C3H$^{+/+}$: $t = 3.123$, $P = 0.0109$). Changes in the trajectory shape between D9 and D11 is also shown in Fig. 5).

The only difference in swimming velocity was found in the visible platform phase; B6CBA$^{+/Lc}$ mice were observed to have slower swimming velocities compared to B6CBA$^{+/+}$ mice (Fig. 2B). Swimming velocity did not differ significantly between strains (Fig. 2B).

3.2. Open field

Trajectory length, locomotion activity and thigmotaxis and statistical significance of between-group differences are shown in Fig. 6. Dependence of the parameters on mutation and strain factors and their interactions are shown in Table 4. Locomotion and thigmotaxis were significantly dependent on strain and mutation factors, but not on their interaction. Trajectory length was dependent only on mouse strain. B6CBA$^{+/Lc}$ showed higher locomotion than B6CBA$^{+/+}$ on D29 ($t = 2.8725$, $P = 0.015$). In the C3H strain, no differences between *Lurcher* mutants and wild type mice were found. Strain comparisons showed higher locomotion in C3H$^{+/+}$ compared to B6CBA$^{+/+}$ (day 28: $t = -3.8445$, $P = 0.0014$, day 29: $t = -4.0464$, $P = 0.0008$). In *Lurcher* mice, no significant difference in locomotion activity between the strains was found;

additionally, no significant differences in trajectory length and thigmotaxis between individual groups were found.

In B6CBA$^{+/+}$ mice, locomotion activity was higher in the first (D28) compared to the second open field trial (D29) ($t = 2.3667$, $P = 0.028$). B6CBA$^{+/Lc}$ mice showed significantly higher thigmotaxis on D29 than on D28 ($t = -4.4184$, $P = 0.0002$). Trajectory length did not change significantly between the first and the second trial of the open field test in any of the experimental groups.

3.3. Motor tests

Fall latencies for the horizontal wire, slanted ladder and rotarod test are shown in Fig. 7. Dependence of fall latencies on strain and the presence of mutation and interaction of these two factors is shown in Table 4. Fall latencies in all three tests were significantly dependent on mutation, but not on strain. Only the horizontal wire test showed a significant dependence on strain × mutation interaction. In all three tests of motor skills, *Lurcher* mice had shorter fall latencies than their wild type counterparts, except for C3H$^{+/Lc}$ on the wire test (Fig. 7). B6CBA$^{+/+}$ mice had longer fall latencies than C3H$^{+/+}$ on the wire test (Fig. 7). Significant motor learning effects manifested as extended latencies between the first and second testing day (D30 vs. D31) was seen only in C3H$^{+/Lc}$ mice on the rotarod test ($t = -3.2674$, $P = 0.003$).

4. Discussion

4.1. The effect of the Grid2^{Lc} mutation

We found severe impairment of performance in the spatial navigation task and motor tests in *Lurcher* mice of both strains (B6CBA and C3H). These abnormalities were in agreement with findings described in other studies of B6CBA [8,22,29,33,37,38,47] or C3H [28,29] *Lurcher* mice.

Both strains of *Lurcher* mice performed much worse on the Morris water maze with both hidden and visible platform compared to their wild type littermates, although slower swimming velocity was only seen in B6CBA *Lurcher* mice and only during the visible platform task. The higher D9/D1 ratio for trajectories in *Lurcher* mice indicated reduced learning during the hidden platform task. When the platform location was changed, wild type mice of both strains searched the area of its previous position, while *Lurchers* did

Table 1
Statistical significance (*P*-value) of the between-group effect of strain and mutation factors and their interaction (strain × mutation) across the level of repeated measurement (if any) on trajectory length, swimming velocity, thigmotaxis and percentage of direct finding trial parameters on individual phases of the Morris ware maze test. Permutational unbalanced ANOVA with repeated measurement for phase I, III and IV, two-way permutational ANOVA for phases II and V.

	Strain		Mutation		Strain × mutation	
	$F(1,72)$	P	$F(1,72)$	P	$F(1,72)$	P
Trajectory length						
I (D1–9)	23.66	<0.0001	190.29	<0.0001	0.04	NS
II (D10)	8.62	0.0146	66.54	<0.0001	0.93	NS
III (D11–12)	10.02	NS	106.84	<0.0001	0.05	NS
IV (D22–25)	17.56	<0.0001	34.58	<0.0001	6.58	0.0132
V (D26)	5.35	0.0237	53.25	<0.0001	2.22	NS
Swimming velocity						
I (D1–9)	0.37	NS	1.16	NS	0.03	NS
II (D10)	2.06	NS	1.71	NS	1.18	NS
III (D11–12)	0.45	NS	2.70	NS	1.12	NS
IV (D22–25)	0.81	NS	8.29	0.0078	2.59	NS
V (D26)	0.06	NS	6.98	0.0040	0.03	NS
Thigmotaxis						
I (D1–9)	14.92	0.0156	52.83	<0.0001	1.01	NS
II (D10)	7.23	0.0026	36.97	<0.0001	5.64	0.0174
III (D11–12)	8.78	0.0048	40.20	<0.0001	2.76	NS
IV (D22–25)	6.96	0.0128	31.45	<0.0001	5.81	0.0086
V (D26)	5.35	0.0182	45.23	<0.0001	5.04	0.04
Percentage of direct finding trials						
I (D1–9)	9.79	0.0470	83.55	<0.0001	3.12	NS
II (D10)	2.57	NS	50.24	<0.0001	3.57	NS
III (D11–12)	0.61	NS	18.98	<0.0001	1.03	NS
IV (D22–25)	15.16	0.0223	200.46	<0.0001	4.60	0.0232
V (D26)	1.41	NS	28.61	<0.0001	0.06	NS

Morris water maze – effect of strain and mutation factors.

Table 2
Mean ratios of trajectory length on individual days ± SEM showing the quantity of the change of the parameter between or during individual phases of the Morris water maze test and statistical significance (*P*-value) of the between-group effect of strain and mutation factors and their interaction (strain × mutation) on ratio of trajectory length in the Morris water maze on individual days. Permutational two-way ANOVA.

		B6CBA$^{+/Lc}$ ($n = 16$)	B6CBA$^{+/+}$ ($n = 26$)	C3H$^{+/Lc}$ ($n = 16$)	C3H$^{+/+}$ ($n = 18$)	Strain		Mutation		Strain × mutation	
						$F(1,72)$	P	$F(1,72)$	P	$F(1,72)$	P
Hidden platform learning	D9/D1	0.54 ± 0.07	0.11 ± 0.01	0.87 ± 0.09	0.27 ± 0.04	21.73	<0.0001	92.19	<0.0001	2.65	NS
Changed starting position	D10/D9	1.17 ± 0.14	1.04 ± 0.05	0.93 ± 0.10	1.25 ± 0.31	0.01	NS	0.32	NS	1.73	NS
Changed platform position	D11/D9	2.40 ± 0.42	5.49 ± 0.74	1.28 ± 0.12	3.81 ± 0.74	4.50	0.0262	18.16	<0.0001	0.18	NS
New platform position learning	D12/D11	0.90 ± 0.09	0.45 ± 0.07	1.03 ± 0.10	0.73 ± 0.21	2.58	NS	8.86	<0.0001	0.34	NS
Visible platform learning	D25/D22	0.96 ± 0.18	0.64 ± 0.06	0.99 ± 0.13	0.65 ± 0.11	0.04	NS	8.21	0.0102	0.02	NS
Changed visible platform position	D26/D25	1.78 ± 0.26	1.67 ± 0.12	1.28 ± 0.24	1.50 ± 0.18	3.07	NS	0.07	NS	0.76	NS

Morris water maze – trajectory length ratios.

Table 3
Statistical significance (*P*-value) of the change of trajectory length between or during individual phases of the Morris water maze test. Permutational ANOVA with repeated measurement for D1 D9 and D22–D25, permutation paired t-test for D9 vs. D10, D9 vs. D11, D11 vs. D12 and D25 vs. D26.

		B6CBA$^{+/Lc}$ ($n = 16$)		B6CBA$^{+/+}$ ($n = 26$)		C3H$^{+/Lc}$ ($n = 16$)		C3H$^{+/+}$ ($n = 18$)	
Hidden platform learning	D1–D9	$F(8,120) = 7.17$	$P = 0.0014$	$F(8,200) = 87.20$	$P < 0.0001$	$F(8,120) = 1.36$	NS	$F(8,136) = 28.34$	$P < 0.0001$
Changed starting position	D9 vs. D10	$t = -0.24$	NS	$t = 0.06$	NS	$t = 0.51$	NS	$t = -0.40$	NS
Changed platform position	D9 vs. D11	$t = -3.75$	$P = 0.0033$	$t = -7.12$	$P = 0.0001$	$t = -2.27$	$P = 0.0379$	$t = -4.75$	$P = 0.0004$
New platform position learning	D11 vs. D12	$t = 2.47$	$P = 0.0259$	$t = 5.88$	$P = 0.0001$	$t = 0.26$	NS	$t = 2.02$	NS
Visible platform learning	D22–D25	$F(3,45) = 2.07$	NS	$F(3,75) = 18.71$	$P < 0.0001$	$F(3,45) = 1.63$	NS	$F(3,51) = 6.45$	$P = 0.003$
Changed visible platform position	D25 vs. D26	$t = -2.23$	$P = 0.0422$	$t = -5.66$	$P = 0.0001$	$t = 0.47$	NS	$t = -1.86$	NS

Morris water maze – change of trajectory length.

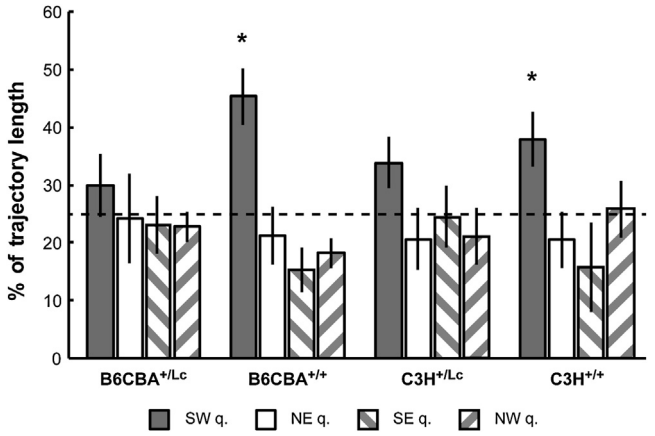

Fig. 4. Percentage of trajectory length moved through individual quadrants in the first trial (N-starting position) of the D11 (the first day with a new NE platform position) in B6CBA$^{+/Lc}$, B6CBA$^{+/+}$, C3H$^{+/Lc}$ and C3H$^{+/+}$ mice. Error bars represent SEM. The horizontal line indicates 25% level expected in random occurence. Asterisk (*) indicates $P < 0.05$ for difference of the percentage of trajectory length moved within the SW quadrant, where the platform was located previously, and expected 25% level.

not. This suggests that contrary to Lurchers, wild type mice effectively memorized the platform position. The fact that the change of the starting point sequence in the maze did not influence the performance of the mice, suggests that both wild type and *Lurcher* mice used rather allothetic navigation.

The performance of wild type mice of both strains on the last day of the initial hidden platform task was excellent (i.e. characterized by mostly direct swims toward the goal) and was similar to the performance on the visible platform task. This shows that after adequate training, wild type mice of both strains were able to locate a hidden goal with similar efficiency as a visible goal. *Lurcher* mice, on the other hand, achieved much better results when the platform was visible compared to the hidden platform task. These findings suggest that *Lurcher* mice had difficulty locating the position of the hidden goal. On the other hand, they were able to use direct visual navigation to a visible goal and were able and motivated to achieve it, though with lower efficiency than wild type mice. The difficulty in guiding themselves toward a visible goal could have been due to a deficit in visuomotor coordination [32]. The performance of *Lurcher* mice in the water maze could also be negatively influenced by their abnormal stress reactivity and behavioral disinhibition [23,35]. In this regard, failures with the hidden platform test could be attributed not only to spatial learning impairment in *Lurcher* mice, but performance could have also been influenced by higher levels of stress and anxiety during this difficult task.

Higher locomotion activity in B6CBA *Lurcher* mice, in the open field test, is in agreement with behavioral disinhibition. Despite the higher activity, *Lurcher* mice did not walk significantly longer distances compared to wild type mice, probably due to slower locomotion velocity, which could have been linked to ataxia and impairment of motor skills, which were obvious on the rotarod, ladder and horizontal wire tests.

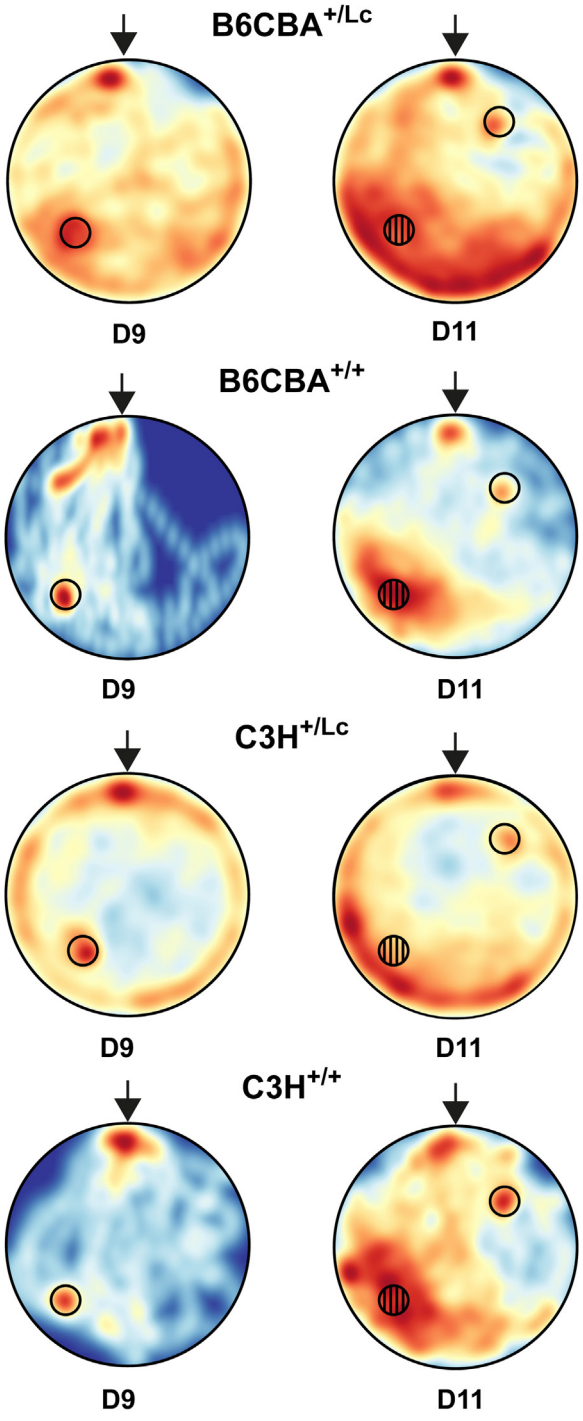

Fig. 5. Superposition of trajectories (frequency of mouse presence) in the first trial (N-starting position) on D9 and D11 respectively in B6CBA$^{+/Lc}$, B6CBA$^{+/+}$, C3H$^{+/Lc}$ and C3H$^{+/+}$ mice. The arrows indicate starting position. The empty circle indicates present platform position. For D11, the hatched circle indicates previous platform position.

4.2. The effect of the strain background

We found strain differences in performance on the Morris water maze test, independent of obvious retinal degeneration. C3H mice had poorer results than their B6CBA counterparts. The B6CBA strain was derived from the C57BL/6 and CBA strains. Mice of the C57BL/6 strain are known to perform well in the Morris water maze [26,58] and therefore they are recommended for such experiments [13]. They are also considered to be suitable for studying memory deficits in mutant mice [24]. We have shown that the B6CBA strain retained this quality from one of its parental strains. The C3H strain, on the other hand, is one of those in which retinal degeneration leading to functional blindness is known to occur. Several studies have demonstrated that this strongly modifies the behavior of mice and leads to poor performances, by C3H mice, in tasks requiring visual

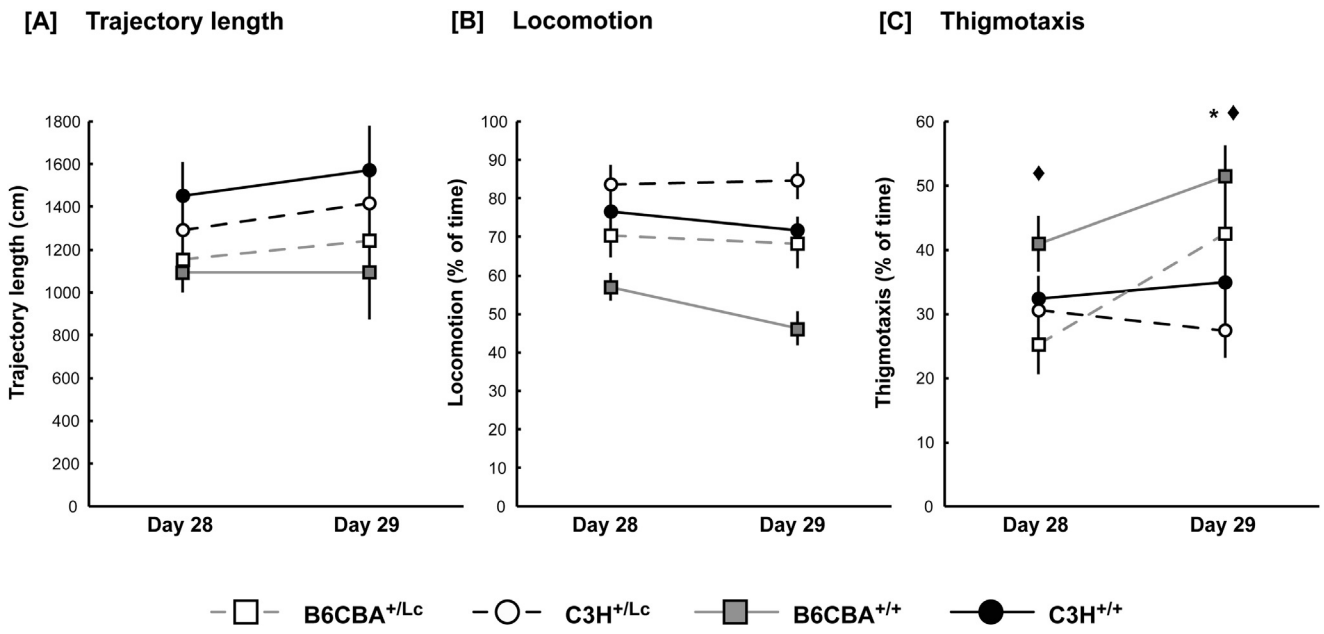

Fig. 6. Open field test: Mean trajectory length in cm (A), locomotion activity in % (B) and thigmotaxis in % (C) in B6CBA$^{+/Lc}$, B6CBA$^{+/+}$, C3H$^{+/Lc}$ and C3H$^{+/+}$ mice. Error bars represent SEM. $P < 0.05$ is indicated by * for B6CBA$^{+/+}$ vs. B6CBA$^{+/Lc}$, by + for C3H$^{+/+}$ vs. C3H$^{+/Lc}$, by ♦ for B6CBA$^{+/+}$ vs. C3H$^{+/+}$ and by ◊ for B6CBA$^{+/Lc}$ vs. C3H$^{+/Lc}$.

orientation [2,3]. Vision problems worsen performance of C3H mice in the spatial orientation and learning tests [27]. Therefore vision impairment could interfere with assessment of the *Grid2*^{Lc} mutation and prevents reliable interpretations of these cognitive tests when comparing C3H mice with other mouse strains. In our study, we used only C3H mice with intact retinas (mutation non-carriers or heterozygotes). This allowed a direct comparison between the C3H and B6CBA strains.

Using this approach, we have shown that strain specific properties were also reflected in the performance of *Lurcher* mutant mice. While *Lurcher* B6CBA mice showed a marked learning effect during the hidden platform task, C3H *Lurcher* mice showed little or no learning. Despite eliminating the influence of retinal degeneration, C3H *Lurcher* mice had more difficulties navigating to a visible platform compared with B6CBA *Lurchers*. Therefore, poor performance of C3H mice cannot be simply attributed to lack of spatial learning ability; other factors probably play a role. Because swimming velocity did not differ between the strains it cannot be explained by different swimming ability; the absence of influence of motor problems was also supported by the motor tests results. Changes in visuomotor integration, level of anxiety or behavioral abnormalities influencing the motivation to learn the position of the platform, which have been suggested as mechanisms to explain the impairment in *Lurcher* mice, could be involved in the strain differences, too. The presence of behavioral differences between strains is supported by higher locomotion activity on the open field test in C3H wild type mice. C3H/He mice have been shown to exhibit relatively low anxiogenic behavioral profiles in the elevated plus maze compared to 5 other strains, including C57BL/6J and CBA/Ca [2]. However, the meaning of this is difficult to interpret without eliminating the effects of visual impairment in C3H/He mice, since homozygosity for the *Pde6b*^{rd1} allele has been shown to result in increased activity in the open field test [40]. Functional blindness could prevent detection of anxiogenic factors in the maze. On the other hand, Ohkura et al. [43] found higher plasma levels of stress hormone corticosterone in C3H/HeN mice compared with three other mouse strains. Since *Lurcher* mice also show corticosterone elevation [23] both these factors could be mutually potentiated in C3H *Lurcher* mice.

We cannot exclude the possibility that photoreceptors in C3H mice that are heterozygous for the *Pde6b*^{rd1} allele, with morphologically intact retina, are functionally abnormal in such a way that it could impair their visual navigation using extra-maze cues, as well as direct navigation to the visible goal. Nevertheless, Owen et al. [44] found poor performance on both the hidden and visible platform Morris water maze tasks in the C3H/Ibg inbred strain carrying the retinal degeneration gene, while C3B6 F1 hybrids performed well on both tasks. This suggests that visual orientation is probably not markedly impaired in mice that are heterozygous for the *Pde6b*^{rd1} allele. To verify this hypothesis, a thorough functional examination of the visual system in C3H mice heterozygous for *Pde6b*^{rd1} allele would be necessary. The importance of visual abilities for water maze performance has been shown by Brown and Wong [3] who found a correlation between performance on visual detection tasks and the Morris water maze task with a hidden, as well as a visible platform.

The present study did not show marked strain differences in motor skills, except for the wire test, in which better performances by B6CBA wild type mice could be accounted for by their lower body weight. The ladder and rotarod tests were quite easy for wild

Table 4
Statistical significance (*P*-value) of the between-group effect of strain and mutation factors and their interaction (strain × mutation) across the level of repeated measurement on parameters measured in the open field test and fall latencies in the motor tests. Permutational unbalanced ANOVA with repeated measurements.

	Strain		Mutation		Strain × mutation	
	$F(1,72)$	P	$F(1,72)$	P	$F(1,72)$	P
Open field test						
Trajectory length	4.09	0.0398	0.01	NS	0.72	NS
Locomotion activity	24.59	<0.0001	11.58	0.0038	0.84	NS
Thigmotaxis	6.44	0.0307	4.81	0.0345	0.90	NS
Motor tests						
Horizontal wire	7.01	NS	57.68	<0.0001	10.54	0.0016
Slanted ladder	5.47	NS	298.95	<0.0001	0.16	NS
Rotarod	0.50	NS	78.85	<0.0001	0.07	NS

Open field test and motor tests – effect of strain and mutation factors.

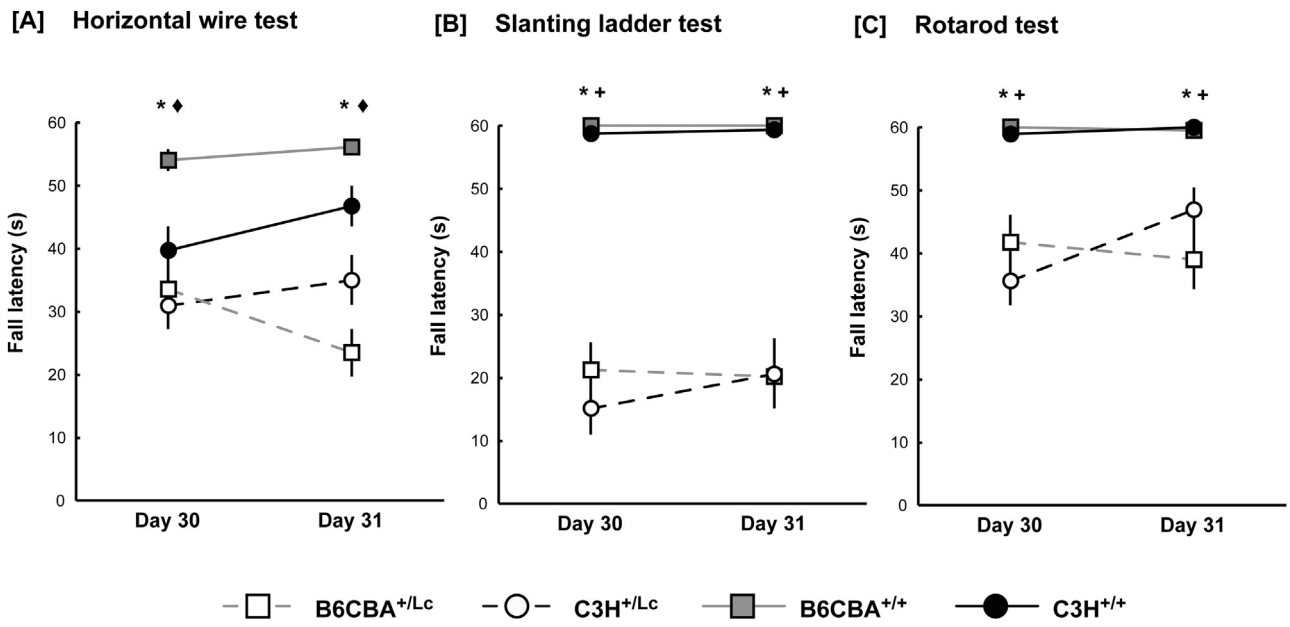

Fig. 7. Motor test: Mean fall latencies in s on the horizontal wire (A), slanting ladder (B) and rotarod (C) tests in B6CBA$^{+/Lc}$, B6CBA$^{+/+}$, C3H$^{+/Lc}$ and C3H$^{+/+}$ mice. Error bars represent SEM. $P < 0.05$ is indicated by * for B6CBA$^{+/+}$ vs. B6CBA$^{+/Lc}$, by + for C3H$^{+/+}$ vs. C3H$^{+/Lc}$, by ♦ for B6CBA$^{+/+}$ vs. C3H$^{+/+}$ and by ◊ for B6CBA$^{+/Lc}$ vs. C3H$^{+/Lc}$.

type mice, which achieved the maximum fall latency in most trials. Therefore improvement in these tests could not be seen and subtle strain differences in wild type mice could be masked.

5. Conclusion

We found performance differences in the Morris water maze task between the B6CBA and C3H strain, which were not dependent on retinal degeneration affecting some C3H mice. Strain-dependent impairment of C3H mice was analogous in both *Lurcher* mutants and wild type mice. This way, genetic background modified manifestation of the *Grid2^{Lc}* mutation. However, the final phenotype seems to be a product of the superposition of the strain and *Grid2^{Lc}* mutation effects, without any specific interference between the strain-related genetic background and the mechanism of the *Grid2^{Lc}* mutation expression. These findings indicate that the *Grid2^{Lc}* mutation induces a strong and quite stable pathological phenotype. Nevertheless, a combination of the *Lurcher* phenotype and C3H strain prevented learning in the hidden platform task. Strain-specific characteristics of the mice should be taken into account when used as a model of cerebellar degeneration. In this regard, B6CBA *Lurcher* mice seem to be a more suitable tool for investigation of behavioral aspects of cerebellar degeneration, since they do not combine abnormalities related to the *Grid2^{Lc}* mutation with strain-specific problems.

Conflict of interest

There are no conflicts of interest.

Acknowledgment

This research was supported by COST grant No. LD12056 and LD12057 of the Ministry of Education, Youth and Sport of the Czech Republic, Specific Student Research Project No. 260 053 of the Charles University, Grant Agency of the Charles University No. 613112, the Charles University Research Fund (project number P36), Faculty of Medicine in Pilsen and by project CZ.1.05/2.1.00/03.0076 from the European Regional Development Fund. We would like to thank Thomas Secrest for language editing.

References

[1] Bothe GWM, Bolivar VJ, Vedder MJ, Geistfeld JG. Behavioral differences among fourteen inbred mouse strains commonly used as disease models. Comp Med 2005;55:326–34.
[2] Brooks SP, Pask T, Jones L, Dunnett SB. Behavioural profiles of inbred mouse strains used as transgenic backgrounds. II: cognitive tests. Genes Brain Behav 2005;4:307–17.
[3] Brown RE, Wong AA. The influence of visual ability on learning and memory performance in 13 strains of mice. Learn Mem 2007;14:134–44.
[4] Caddy KWT, Biscoe TJ. Structural and quantitative studies on the normal C3H and Lurcher mutant mouse. Philos Trans R Soc London Ser B Biol Sci 1979;287:167–201.
[5] Caddy KW, Vozeh F. The effect of 3-acetylpyridine on inferior olivary neuron degeneration in Lurcher mutant and wild-type mice. Eur J Pharmacol 1997;330:139–42.
[6] Caston J, Chianale C, Delhaye-Bouchaud N, Mariani J. Role of the cerebellum in exploration behavior. Brain Res 1998;808:232–7.
[7] Caston J, Devulder B, Jouen F, Lalonde R, Delhaye-Bouchaud N, Mariani J. Role of an enriched environment on the restoration of behavioral deficits in Lurcher mutant mice. Develop Psychobiol 1999;35:291–303.
[8] Cendelin J, Korelusova I, Vozeh F. The effect of repeated rotarod training on motor skills and spatial learning ability in Lurcher mutant mice. Behav Brain Res 2008;189:65–74.
[9] Cendelin J, Vozeh F. Lurcher mouse. In: Manto M, Gruol DL, Schmahmann JD, Koibuchi N, Rossi F, editors. Handbook of the Cerebellum and Cerebellar Disorders. New York: Springer Science + Business Media; 2013. p. 1499–520.
[10] Chang B, Hawes NL, Hurd RE, Davisson T, Nusinowitz S, Heckenlively JR. Retinal degeneration mutants in the mouse. Vision Res 2002;42:517–25.
[11] Cheng SS, Heintz N. Massive loss of mid- and hindbrain neurons during embryonic development of homozygous Lurcher mice. J Neurosci 1997;17:2400–7.
[12] De Jager PL, Zuo J, Cook SA, Heintz N. A new allele of the lurcher gene, lurcher. J Mamm Genome 1997;8:647–50.
[13] D'Hooge R, De Deyn PP. Applications of the Morris water maze in the study of learning and memory. Brain Res Rev 2001;36:60–90.
[14] Dickson PE, Rogers TD, Del Mar N, Martin LA, Heck D, Blaha CD, et al. Behavioral flexibility in a mouse model of developmental cerebellar Purkinje cell loss. Neurobiol Learn Mem 2010;94:220–8.
[15] Dumesnil-Bousez N, Sotelo C. Partial reconstruction of the adult Lurcher cerebellar circuitry by neural grafting. Neuroscience 1993;55:1–21.
[16] Fortier P, Smith AM, Rossignol S. Locomotor deficits in the cerebellar mutant mouse, Lurcher. Exp Brain Res 1987;66:271–86.
[17] Frederic F, Chautard T, Brochard R, Chianale C, Wollman E, Oliver C, et al. Enhanced endocrine response to novel environment stress and endotoxin in Lurcher mutant mice. Neuroendocrinology 1997;66:341–7.
[18] Grusser C, Grusser-Cornehls U. Improvement in motor performance of Weaver mutant mice following lesions of the cerebellum. Behav Brain Res 1998;97:189–94.

[19] Guidetti P, Bates GP, Graham RK, Hayden MR, Leavitt BR, MacDonald ME, et al. Elevated brain 3-hydroxykynurenine and quinolinate levels in Huntington disease mice. Neurobiol Dis 2006;23:190–7.
[20] Guillot PV, Roubertoux PL, Crusio WE. Hippocampal mossy fiber distributions and intermale aggression in seven inbred mouse strains. Brain Res 1994;660:167–9.
[21] Hilber P, Jouen F, Delhaye-Bouchaud N, Mariani J, Caston J. Differential roles of cerebellar cortex and deep cerebellar nuclei in learning and retention of a spatial task: studies in intact and cerebellectomized lurcher mutant mice. Behav Genet 1998;28:299–308.
[22] Hilber P, Caston J. Motor skills and motor learning in Lurcher mutant mice during aging. Neuroscience 2001;102:615–23.
[23] Hilber P, Lorivel T, Delarue C, Caston J. Stress and anxious-related behaviors in Lurcher mutant mice. Brain Res 2004;1003:108–12.
[24] Holmes A, Wrenn CC, Harris AP, Thayer KE, Crawley JN. Behavioral profiles of inbred strains on novel olfactory, spatial and emotional tests for reference memory in mice. Genes Brain Behav 2002;1:55–69.
[25] Kim S, Lee S, Ryu S, Suk J, Park C. Comparative analysis of the anxiety-related behaviors in four inbred mice. Behav Processes 2002;60:81–190.
[26] Klapdor K, van der Staay FJ. The Morris water-escape task in mice: strain differences and effects of intra-maze contrast and brightness. Physiol Behav 1996;60:1247–54.
[27] Korelusova I, Cendelin J, Vozeh F. Motor and visuospatial abilities in a model of olivocerebellar and retinal degeneration–Lurcher mutant mice of C3H strain. Prague Med Rep 2007;108:37–48.
[28] Krizkova A, Vozeh F. Development of early motor learning and topical motor skills in a model of cerebellar degeneration. Behav Brain Res 2004;150:65–72.
[29] Lalonde R, Lamarre Y, Smith AM. Does the mutant mouse lurcher have deficits in spatially oriented behaviours? Brain Res 1988;455:24–30.
[30] Lalonde R, Botez MI, Joyal CC, Caumartin M. Motor abnormalities in Lurcher mutant mice. Physiol Behav 1992;51:523–5.
[31] Lalonde R, Joyal CC, Guastavino JM, Botez MI. Hole poking and motor coordination in lurcher mutant mice. Physiol Behav 1993;54:41–4.
[32] Lalonde R, Thifault S. Absence of an association between motor coordination and spatial orientation in lurcher mutant mice. Behav Genet 1994;24:497–501.
[33] Lalonde R, Filali M, Bensoula AN, Lestienne F. Sensorimotor learning in three cerebellar mutant mice. Neurobiol Learn Mem 1996;65:113–20.
[34] Lalonde R. Immobility responses in Lurcher mutant mice. Behav Genet 1998;28:309–14.
[35] Lorivel T, Hilber P. Effects of chlordiazepoxide on the emotional reactivity and motor capacities in the cerebellar Lurcher mutant mice. Behav Brain Res 2006;173:122–8.
[36] Manto M, Marmolino D. Animal models of human cerebellar ataxias: a cornerstone for the therapies of the twenty-first century. Cerebellum 2009;8:137–54.
[37] Markvartova V, Cendelin J, Vozeh F. Changes of motor abilities during ontogenetic development in Lurcher mutant mice. Neuroscience 2010;168:646–51.
[38] Markvartova V, Cendelin J, Vozeh F. Effect of dimethyl sulfoxide in cerebellar mutant Lurcher mice. Neurosci Lett 2013;543:142–5.
[39] Martin LA, Goldowitz D, Mittleman G. Sustained attention in the mouse: a study of the relationship with the cerebellum. Behav Neurosci 2006;120:477–81.
[40] Menalled L, El-Khodor BF, Hornberger M, Park L, Howland D, Brunner D. Effect of the rd1 mutation on motor performance in R6/2 and wild type mice. PLoS Curr 2012;4:RRN1303.
[41] Morris RGM. Development of a water–maze procedure for studying spatial learning in the rat. J Neurosci Meth 1984;11:47–64.
[42] Nadler JJ, Zou F, Huang H, Moy SS, Lauder J, Crawley JN, et al. Large-scale gene expression differences across brain regions and inbred strains correlate with a behavioral phenotype. Genetics 2006;174:1229–36.
[43] Ohkura N, Oishi K, Sekine Y, Atsumi G, Ishida N, Matsuda J, et al. Comparative study of circadian variation in numbers of peripheral blood cells among mouse strains: unique feature of C3H/HeN mice. Biol Pharm Bull 2007;30:1177–80.
[44] Owen EH, Logue SF, Rasmussen DL, Wehner JM. Assesment of learning by the Morris water task and fear conditioning in inbred mouse strains and F1 hybrids: Implications of genetic background for single gene mutations and quantitative trait loci analyses. Neuroscience 1997;80:1087–99.
[45] Pesarin F, Salmaso L. Permutation Tests for Complex Data: Theory, Application and Software. first ed. Wiltshire: John Wiley & Sons; 2010.
[46] Phillips RJS. 'Lurcher'. A new gene in linkage group XI of the house mouse. J Genet 1960;57:35–42.
[47] Porras-Garcia E, Cendelin J, Dominguez-del-Toro E, Vozeh F, Delgado-Garcia JM. Purkinje cell loss affects differentially the execution, acquisition and prepulse inhibition of skeletal and facial motor responses in Lurcher mice. Eur J Neurosci 2005;21:979–88.
[48] Porras-Garcia E, Sanchez-Campusano R, Martinez-Vargas D, Dominguez-del-Toro E, Cendelin J, Vozeh F, et al. Behavioral characteristics, associative learning capabilities, and dynamic association mapping in an animal model of cerebellar degeneration. J Neurophysiol 2010;104:346–65.
[49] Reader TA, Strazielle C, Botez MI, Lalonde R. Brain dopamine and amino acid concentrations in Lurcher mutant mice. Brain Res Bull 1998;45:489–93.
[50] Rossi F, Jankovski A, Sotelo C. Target neuron controls the integrity of afferent axon phenotype: a study on the Purkinje cell-climbing fiber system in cerebellar mutant mice. J Neurosci 1995;15:2040–56.
[51] Selimi F, Doughty M, Delhaye-Bouchaud N, Mariani J. Target-related and intrinsic neuronal death in Lurcher mutant mice are both mediated by caspase-3 activation. J Neurosci 2000;20:992–1000.
[52] Simon P, Dupuis R, Costentin J. Thigmotaxis as an index of anxiety in mice. Influence of dopaminergic transmissions. Behav Brain Res 1994;61:59–64.
[53] Tarantino LM, Gould TJ, Druhan JP, Bucan M. Behavior and mutagenesis screens: the importance of baseline analysis of inbred strains. Mamm Genome 2000;11:555–64.
[54] Trullas R, Skolnick P. Differences in fear motivated behaviours among inbred mouse strains. Psychopharmacology 1993;111:323–31.
[55] Tuma J, Cendelin J, Vozeh F. Maternal infanticide and low maternal ability in cerebellar mutants Lurcher. Neuro Endocrinol Lett 2013;34:101–6.
[56] van Gaalen MM, Steckler T. Behavioural analysis of four mouse strains in an anxiety test battery. Behav Brain Res 2000;115:95–106.
[57] Wahlsten D, Andison M. Patterns of cerebellar foliation in recombinant inbred mice. Brain Res 1991;557:184–9.
[58] Wahlsten D, Cooper SF, Crabbe JC. Different rankings of inbred mouse strains on the Morris maze and a refined 4-arm water escape task. Behav Brain Res 2005;165:36–51.
[59] Zanjani SH, Selimi F, Vogel MW, Haeberle AM, Boeuf J, Mariani J, et al. Survival of interneurons and parallel fiber synapses in a cerebellar cortex deprived of Purkinje cells: studies in the double mutant mouse Grid2$^{Lc/-}$;Bax$^{-/-}$. J Comp Neurol 2006;497:622–35.
[60] Zuo J, De Jager PL, Takahasi KJ, Jiang W, Linden DJ, Heintz H. Neurodegeneration in Lurcher mice caused by mutation of (2 glutamate receptor gene. Nature 1997;388:769–73.

Article 5

Vaclav Babuska, Zbynek Houdek, Jan Tuma, Zdenka Purkartova, Jana Tumova, Milena Kralickova, Frantisek Vozeh and Jan Cendelin

Transplantation of embryonic cerebellar grafts improves gait parameters in ataxic *Lurcher* mice

Cerebellum 2015; 14(6): 632-641

Cerebellum (2015) 14:632–641
DOI 10.1007/s12311-015-0656-x

ORIGINAL PAPER

Transplantation of Embryonic Cerebellar Grafts Improves Gait Parameters in Ataxic *Lurcher* Mice

Vaclav Babuska · Zbynek Houdek · Jan Tuma · Zdenka Purkartova · Jana Tumova · Milena Kralickova · Frantisek Vozeh · Jan Cendelin

Published online: 21 February 2015

Abstract Hereditary cerebellar ataxias are severe diseases for which therapy is currently not sufficiently effective. One of the possible therapeutic approaches could be neurotransplantation. *Lurcher* mutant mice are a natural model of olivocerebellar degeneration representing a tool to investigate its pathogenesis as well as experimental therapies for hereditary cerebellar ataxias. The effect of intracerebellar transplantation of embryonic cerebellar solid tissue or cell suspension on motor performance in adult *Lurcher* mutant and healthy wild-type mice was studied. Brain-derived neurotrophic factor level was measured in the graft and adult cerebellar tissue. Gait analysis and rotarod, horizontal wire, and wooden beam tests were carried out 2 or 6 months after the transplantation. Higher level of the brain-derived neurotrophic factor was found in the *Lurcher* cerebellum than in the embryonic and adult wild-type tissue. A mild improvement of gait parameters was found in graft-treated *Lurcher* mice. The effect was more marked in cell suspension grafts than in solid transplants and after the longer period than after the short one. *Lurcher* mice treated with cell suspension and examined 6 months later had a longer hind paw stride (4.11 *vs*. 3.73 mm, $P<0.05$) and higher swing speed for both forepaws (52.46 *vs*. 32.79 cm/s, $P<0.01$) and hind paws (63.46 *vs*. 43.67 cm/s, $P<0.001$) than controls. On the other hand, classical motor tests were not capable of detecting clearly the change in the motor performance. No strong long-lasting negative effect of the transplantation was seen in wild-type mice, suggesting that the treatment has no harmful impact on the healthy cerebellum.

Keywords Ataxia · Cerebellar transplantation · Gait analysis · *Lurcher* · Olivocerebellar degeneration

V. Babuska
Department of Medical Chemistry and Biochemistry, Faculty of Medicine in Pilsen, Charles University in Prague, Karlovarska 48, 301 66 Plzen, Czech Republic

Z. Houdek · J. Tuma · Z. Purkartova · F. Vozeh · J. Cendelin
Department of Pathophysiology, Faculty of Medicine in Pilsen, Charles University in Prague, alej Svobody 1655/76, 323 00 Plzen, Czech Republic

M. Kralickova
Department of Histology and Embryology, Faculty of Medicine in Pilsen, Charles University in Prague, Karlovarska 48, 301 66 Plzen, Czech Republic

J. Tuma · M. Kralickova · F. Vozeh · J. Cendelin (✉)
Laboratory of Neurodegenerative Disorders, Biomedical Center, Faculty of Medicine in Pilsen, Charles University in Prague, alej Svobody 1655/76, 323 00 Plzen, Czech Republic
e-mail: jan.cendelin@lfp.cuni.cz

J. Tumova
Department of Nutrition and Centre for Research on Diabetes, Metabolism and Nutrition, Third Faculty of Medicine, Charles University in Prague, Ruska 87, 100 00 Praha 10, Czech Republic

Introduction

Hereditary cerebellar degenerations represent a wide group of diseases [1] that may have a detrimental impact on patients since the cerebellum not only plays a key role in motor coordination control but is also involved in cognitive and affective functions. (For a review, see [2]). The effectiveness of therapy for cerebellar ataxias was mostly insufficient, but interesting approaches have started to appear in recent years in experimental studies [e.g., 3–5]. One of the hopeful therapies for cerebellar degenerations could be neurotransplantation, which, however, still needs in-depth investigation before it can become a routine method in humans. The variability of human hereditary cerebellar ataxias is also reflected in a wide spectrum of animal models [6]. Mutant ataxic mice are

used to investigate symptoms, pathogenesis, and cell death mechanisms, as well as to develop and test therapeutic approaches for these diseases [7].

One of the most frequently used natural models of genetically determined cerebellar degeneration is the *Lurcher* mutant mouse [8]. *Lurcher* mice are heterozygous for *Grid2*^{Lc} semi-dominant gain-of-function mutation in the δ2 glutamate receptor (GluRδ2) gene [9], which is predominantly expressed in cerebellar Purkinje cells and several hindbrain neurons [10]. The nature of the affection in *Lurcher* mice is similar to human olivopontocerebellar atrophy, and although the same mutation does not appear in humans, loss-of-function mutation of the same receptor causes cerebellar degeneration in humans [11]. *Lurcher* mice suffer from early onset postnatal Purkinje cell degeneration [12], which is cell autonomous and is a primary effect of the mutation [13, 14]. The extinction of Purkinje cells is accompanied by a secondary reduction of cerebellar interneurons and inferior olive neurons [12–15]. Three months after birth, *Lurcher* mice have lost almost every Purkinje cell, some 90 % of granule cells, and some 75 % of the inferior olive neurons [12]. The most evident manifestation of the cerebellar degeneration in *Lurchers* is cerebellar ataxia [16], and they fail in various motor tests [17–21].

Tomey and Heckroth [22] considered *Lurcher* mice to be advantageous for neurotransplantation research. They were used several times for investigating the transplantation of embryonic cerebellar tissue [22–27] or various types of stem cells [25, 28, 29]. Nevertheless, the functional effect of the transplantation has been examined only in a minority of the studies [26, 28], and for embryonic cerebellar cell suspension, it has not been assessed yet despite the fact that functional recovery is the crucial goal of neurotransplantation treatment.

The aim of this study was to assess the effect of intracerebellar transplantation of embryonic cerebellar solid tissue or cell suspension grafts on gait, motor skills, and motor learning ability in adult *Lurcher* mutant mice. The same procedure was accomplished with wild-type mice in order to assess the potential negative effect of transplantation into the healthy cerebellum.

Materials and Methods

Animals

Lurcher mutant and wild-type mice of the B6CBA strain were used. The mice were kept in standard conditions with a 12:12 h light/dark cycle (6 am to 6 pm), at a temperature of 22–24 °C. Food and water were available *ad libitum*. Donor embryos were obtained by cross-breeding enhanced green fluorescent protein (EGFP)-positive C57BL/6-Tg(ACTB-EGFP)1Osb/J males with B6CBA wild-type females. All experimental procedures were performed in compliance with EU guidelines for scientific experimentation on animals and with the permission of the Ethical Commission of the Faculty of Medicine in Pilsen. All efforts were made to minimize the number of animals used and their suffering.

Design of the Experiment

The mice were treated with transplantation of solid embryonic cerebellar grafts or embryonic cerebellar cell suspensions at the age of 90–120 days. Two or 6 months after the transplantation, spontaneous gait was analyzed and motor skills and motor learning were tested with a rotarod, horizontal wire, and wooden beam tests for 3 days. The mice were then euthanized for histological examination of the graft presence and structure. The scheme of the experiment is shown in Fig. 1. Only mice with surviving grafts were used for the behavioral data analysis. Untreated control mice were examined at a corresponding age. The numbers of mice involved in the individual experimental groups are indicated in Table 1. Next, six mice with a graft and two sham-operated controls were euthanized 3 days after the surgery to examine cell proliferation early after engraftment and/or injection of the vehicle. Levels of brain-derived neurotrophic factor (BDNF) were determined in the embryonic cerebellum and adult cerebellum, mesencephalon, and brainstem using an enzyme-linked immunosorbent assay (ELISA).

Transplantation

Donor females with conception-timed pregnancies were euthanized by overdose of thiopental on the 12th day of gestation, and the embryos were removed. Only EGFP-positive embryos were used. The embryonic cerebellum was dissected in the form of two pieces of tissue, and the pieces were then pooled in a cold aqueous solution of 0.9 % sodium chloride and 0.6 % glucose, which also served as a vehicle for graft administration. For the cell suspension preparation, the tissue was treated with trypsin for 10 min, washed with the vehicle, and mechanically dissociated. Cell concentration was adjusted to 50,000 cells/μl.

The host mice were anesthetized with an intraperitoneal administration of ketamine (100 mg/kg body weight (bw)) and xylazine (16 mg/kg bw). A solid cerebellar graft (one piece of tissue per host in 5 μl of the vehicle) was injected with a glass capillary, with the wide orifice toward the host cerebellum (bregma—6.2 mm, midline, depth bregma—2 mm). Cell suspension (1 μl per host) was injected into the cerebellum (bregma—6.2 mm, midline, depth bregma—3 mm) with a glass microcapillary (inner diameter 60 μm). The injection speed was 0.5 μl/min.

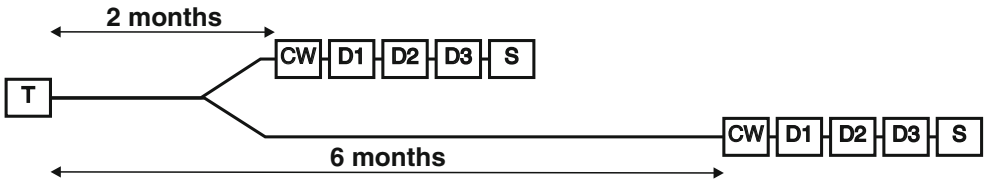

Fig. 1 Scheme of the experimental design. Transplantation day (*T*) was followed by 2 or 6 months of recovery. Then, the CatWalk gait test (*CW*) and three motor test day sessions (*D1*, *D2*, *D3*) were performed. Finally, the mice were sacrificed for histological examination (*S*)

Six mice with the graft and two sham-operated mice were injected with bromodeoxyuridine (BrdU) at the time of the surgery and then for the next 2 days in order to follow newly arising cells in the graft and at the site of the injection. BrdU (Sigma-Aldrich, Saint Louis, USA) was injected intraperitoneally in dose of 50 mg/kg. BrdU-treated mice were euthanized 3 days after the surgery, as described below.

Motor Function Examination

For automated gait analysis, CatWalk 7.1 (Noldus Information Technology BV, Wageningen, the Netherlands) was used. Animals were placed on a glass walkway (85 cm long and 8.5 cm wide) and allowed to move freely across the walkway. For each mouse, two tracks with a straight walking direction and without any interruption were analyzed, and data from these two tracks were averaged. The following parameters were assessed: walking speed (cm/s), stand (s), stride length (cm), and swing speed (cm/s). (For details, see [20]).

Motor skills were examined on the rotarod (RotaRod Advanced, TSE Systems Ltd., Germany), horizontal wire, and wooden beam for three consecutive day sessions (D1–D3). For the rotarod test, the cylinder diameter was 3.5 cm, rod width 6.5 cm, and rotation speed 5.5 rotations per minute. For the horizontal wire test, the mouse was hung by its forepaws on a wire (length 30 cm, diameter 1 mm) 55 cm above a table. For the wooden beam test, the mouse was placed on a horizontal cylindrical wooden rod (length 106 cm, diameter 7 cm). In all cases, fall latencies were measured. If the mouse reached a latency of 120 s, the trial was stopped. Four trials per day session were performed on individual tests, and for each

Table 1 Mean walking speed, stand, stride length, and swing speed ± SEM for forepaws and hind paws in *Lurcher* mutant and wild-type mice 2 or 6 months after transplantation of embryonic cerebellar cell suspension or solid graft and in age-matched controls

Experimental group	Speed (cm/s)	Stand ($s \times 10^{-2}$)		Stride length (cm)		Swing speed (cm/s)	
		Forepaws	Hind paws	Forepaws	Hind paws	Forepaws	Hind paws
Lurcher 2 months							
Cell suspension (n=17; 85 %)	28.63±1.94	12.3±0.6	14.3±1.0	4.14±0.10	4.17±0.09	53.18±3.90*	60.53±2.86
Solid graft (n=14; 64 %)	33.45±2.92	14.0±0.5	17.2±0.6	3.88±0.12	3.93±0.11	39.21±2.02	51.96±2.77
Control (n=20)	25.61±1.68	14.0±0.8$^{\#\#\#}$	16.9±1.0$^{\#\#\#}$	3.96±0.12$^{\#\#\#}$	3.99±0.12$^{\#\#\#}$	42.80±2.81$^{\#\#\#}$	53.40±2.91$^{\#\#\#}$
Lurcher 6 months							
Cell suspension (n=13; 68 %)	17.00±1.93	14.6±0.1	17.9±1.9	3.93±0.17	4.11±0.15*	52.46±7.01**	63.46±5.30***
Solid graft (n=8; 62 %)	18.39±1.22	14.8±1.3	17.5±1.6	3.82±0.13	3.89±0.10	41.00±3.80	53.69±4.90*
Control (n=24)	20.42±1.86	14.8±0.7$^{\#\#\#}$	18.1±0.9$^{\#\#\#}$	3.76±0.10$^{\#\#\#}$	3.73±0.10$^{\#\#\#}$	32.79±1.96$^{\#\#\#}$	43.67±1.88$^{\#\#\#}$
Wild-type 2 months							
Cell suspension (n=22; 100 %)	28.75±1.55	10.4±0.4	11.8±0.5	5.22±0.12	5.17±0.12	77.52±4.52	96.61±4.65
Solid graft (n=17; 77 %)	25.80±2.18	11.6±0.6	13.1±0.6	5.04±0.11*	5.01±0.10	65.82±3.90*	80.35±4.46*
Control (n=26)	26.08±1.38	9.8±0.3	11.0±0.4	5.37±0.11	5.32±0.11	80.10±4.16	96.31±4.52
Wild-type 6 months							
Cell suspension (n=20; 95 %)	16.31±1.33	11.2±0.5	12.1±0.7	5.37±0.19**	5.26±0.18**	86.40±6.08**	96.98±5.18
Solid graft (n=16; 76 %)	18.34±1.19	10.8±0.3	11.4±0.3	5.09±0.12*	5.08±0.12*	75.88±2.91*	85.88±4.04
Control (n=28)	23.22±1.26	11.1±0.3	12.6±0.4	4.71±0.10	4.67±0.10	64.07±3.84	78.41±3.97

Numbers of mice in individual experimental groups (n) are indicated. In the case of graft-treated mice, n shows number of mice with surviving grafts and this is followed by graft survival rate (in %)

$^{\#}$ vs. control in the wild-type experimental group; *vs. control in the same experimental group

*P<0.05; **P<0.01; ***P<0.001; $^{\#\#\#}$ P<0.001

test and mouse, the values were averaged. Motor learning was quantified using the ratio of latencies on D3 and D1 (D3/D1).

Histological Examination

Finally, the mice were sacrificed by overdose of thiopental, before then being transcardially perfused with Ringer's solution and 4 % phosphate-buffered paraformaldehyde (pH 7.4). The frontal 40 μm frozen sections of the cerebella and adjacent structures were prepared. The graft presence and morphology were assessed according to natural EGFP fluorescence of grafted and graft-derived cells.

An immunohistochemistry was used to verify the presence of Purkinje cells with anti-calbindin and to identify astrocytes with anti-glial fibrillary acidic protein (GFAP) staining in selected free-floating sections. For anti-calbindin staining, the sections were incubated with anti-calbindin primary antibody (ab11426, Abcam, Cambridge, UK; dilution 1:1000) overnight at room temperature and then with AlexaFluor® 594 secondary antibody (ab150076, Abcam, Cambridge, UK; dilution 1:400) for 2 h at room temperature. For anti-GFAP staining, sections were incubated with anti-GFAP primary antibody (clone G-A-5 Cy3 conjugate, Sigma-Aldrich, Saint Louis, USA, dilution 1:800) overnight at 4 °C.

The BrdU labeling was performed according to the modified protocol described by Kempermann et al. [30]. After the blocking in Tris-bufferred saline containing 2 % Triton X-100 and 10 % donkey serum (ab7475, Abcam, Cambridge, UK), the sections were treated with hydrochloric acid (2.0 M) for 30 min at 37 °C before being incubated in primary antibody anti-BrdU (ab1893, Abcam, Cambridge, UK; dilution 1:500) overnight at 4 °C. Finally, the sections were incubated with DyLight® 594 secondary antibody (ab96941, Abcam, Cambridge, UK; dilution 1:400) for 4 h at room temperature.

The specimens were visualized using a fluorescent Olympus BX41 microscope (Olympus Corporation, Japan) and an Olympus FV10I-DOC confocal laser scanning microscope (Olympus Corporation, Japan).

BDNF Assay

The level of BDNF was determined in the tissue cerebella of 12-day-old (e.g., the age of graft gaining) embryos and in the cerebella, mesencephalons, and brainstems of 3-month-old (e.g., the age of transplantation) *Lurcher* and wild-type mice. The adult tissue samples were taken from six *Lurcher* and six wild-type mice. The brainstem was processed only in five mice per group for technical reasons. Because the amount of tissue obtained from one embryo was too small for the processing, the cerebella of 32 embryos were collected and divided into three equal samples.

The level of BDNF was measured using the ELISA kit (Elmeca Bioscience, Breda, the Netherlands), according to the manufacturer's protocol. Data were normalized to the protein content using a bicinchoninic acid assay (Sigma-Aldrich, Saint Louis, USA). The specimens were processed in duplicates, and the values were then averaged.

Statistical Evaluation

Most of the data did not show normal distribution (verified with the Kolmogorov-Smirnov test). Therefore, nonparametric statistics was used. For walking speed, a permutational ANOVA (with mouse type, treatment, and time period as between-group factors) was used. Since other gait parameters showed correlation with walking speed, a permutational ANCOVA, with walking speed as a covariate, was used for the analysis of these data, rather than using an ANOVA. For the between-group planned comparison, a permutational *t* test was used. For motor test evaluation, a permutational ANOVA (with mouse type, treatment, and time period as between-group factors) with repeated measurements (with day session as a within-group factor) was used, and the between-group planned comparison was carried out using a permutational *t* test with Bonferroni correction for repeated measurements. For the evaluation of the BDNF level in adult mice, a two-way permutational ANOVA with mouse type and brain structure as between-group factors was used. For assessment of the BDNF level in the *Lurcher* mutant, a wild-type and embryonic cerebellum one-way permutational ANOVA was used. For the between-group planned comparison, a permutational *t* test was used. The reported *F* and *t* values were considered as *F*0 and *t*0 before the start of the permutational tests. The permutational ANOVA/ANCOVA and *t* tests were performed with a maximum of 5000 and 10,000 permutations, respectively [31]. $P<0.05$ was accepted as statistically significant. The data are presented as mean ± SEM.

Results

Graft Morphology

The number of mice with surviving grafts and the graft survival rate in individual experimental groups are shown in Table 1. Most of the cell suspension and the solid cerebellar grafts contained Purkinje cell-shaped cells (Fig. 2). Immunohistochemistry verified that such cells were calbindin-positive. Nevertheless, massive colonization of the host cerebellum with graft-derived cells was not seen, and EGFP-positive fibers connecting the graft with the host tissue were rare (Fig. 2). Furthermore, in *Lurcher* mice, the graft was mostly outside the cerebellum and did not show a tendency to invade it (Fig. 2a). Both types of grafts contained numerous GFAP-positive cells (astrocytes) of

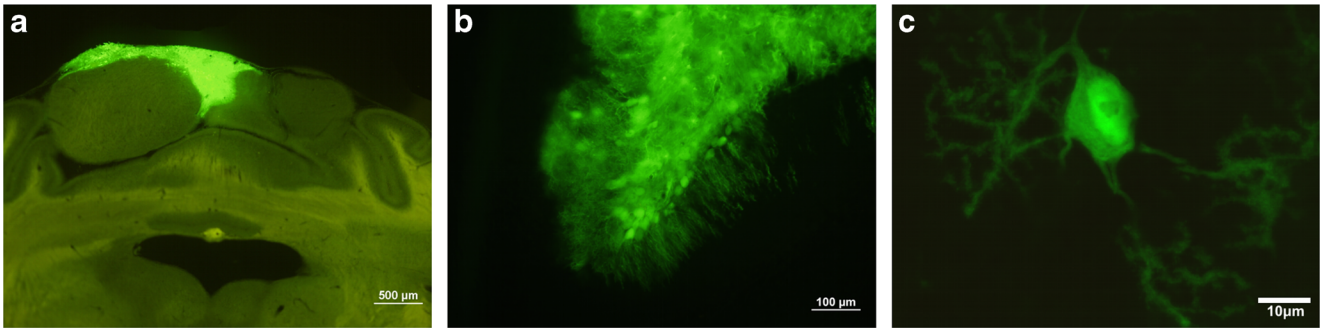

Fig. 2 A solid graft in a *Lurcher* mouse avoiding the host cerebellum (**a**). Detail of a solid graft containing Purkinje cell-shaped cells in a wild-type mouse (**b**). Detail of a Purkinje-shaped cell with deviated dendrite in a cell suspension graft (**c**). Natural EGFP fluorescence. Fluorescent Olympus BX41 microscope (**a**, **b**), Olympus FV10I-DOC confocal laser scanning microscope (**c**)

both host (EGFP-negative) and donor (EGFP-positive) origin (Fig. 3).

The grafts that were examined 3 days after engraftment appeared as small clusters of EGFP-positive tissue. They did not yet contain Purkinje cell-shaped cells. While in the surroundings of these grafts, a higher density of GFAP-positive cells was seen, and the graft mass was almost free of them (Fig. 4e). The BrdU immunohistochemistry showed accumulation of positive cells in the area of these graft injections but much less in the place of vehicle injection (compare Fig. 4a and Fig. 4c). Inside the graft, several cells were found that were positive for both BrdU and EGFP (Figs. 4b–d, f–h). On the other hand, there were many cells that were positive for BrdU but not for EGFP in the graft area (Figs. 4b–d, f–h).

BDNF Level

Significant effects of brain structure ($F_{(2,28)}$=8.96, P=0.0022) as well as the interaction of the brain structure and mouse type factors ($F_{(2,28)}$=7.79, P=0.0012) on BDNF level were found in adult mice. The sample origin had a significant effect on the BDNF level ($F_{(2,12)}$=31.72, P<0.0001) when comparing adult *Lurcher* mutants, wild-type and embryonic cerebella. The levels of BDNF were nearly identical in both wild-type and *Lurcher* mutant mesencephalon and brainstem, as well as in the wild-type cerebellum (Fig. 5). The *Lurcher* mutant cerebellum showed significantly higher BDNF levels than did the wild-type one. Embryonic cerebella, on the other hand, contained less BDNF than did the wild-type, as well as *Lurcher* mutant cerebellar tissue.

Gait Analysis

Walking speed, stand, stride length, and swing speed are shown in Table 1. Gait analysis did not show a significant effect of mouse type and treatment on walking speed. Stand (forepaws: $F_{(1,211)}$=75.63, P<0.0001; hind paws: $F_{(1,211)}$=100.28, P<0.0001), stride length (forepaws: $F_{(1,211)}$=234.39, P<0.0001; hind paws: $F_{(1,211)}$=226.13, P<0.0001), and

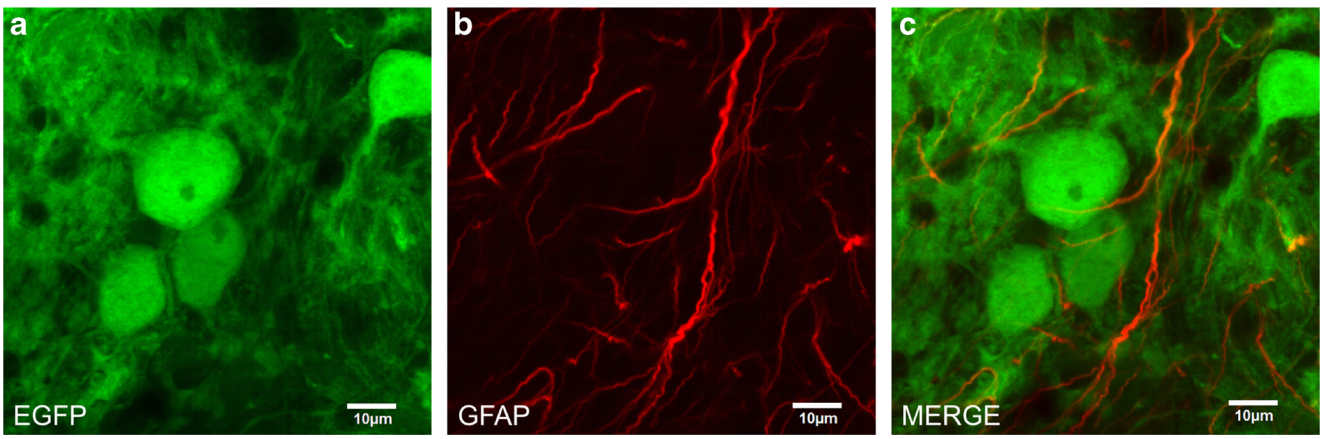

Fig. 3 Astrocytes in the embryonic cell suspension graft in a wild-type mouse—native fluorescence of EGFP (**a**), anti-GFAP immunohistochemistry (**b**), and merged figure (**c**). Only some of the astrocytes are EGFP-positive. Large EGFP-positive Purkinje cell-shaped cells are present. Olympus FV10I-DOC confocal laser scanning microscope

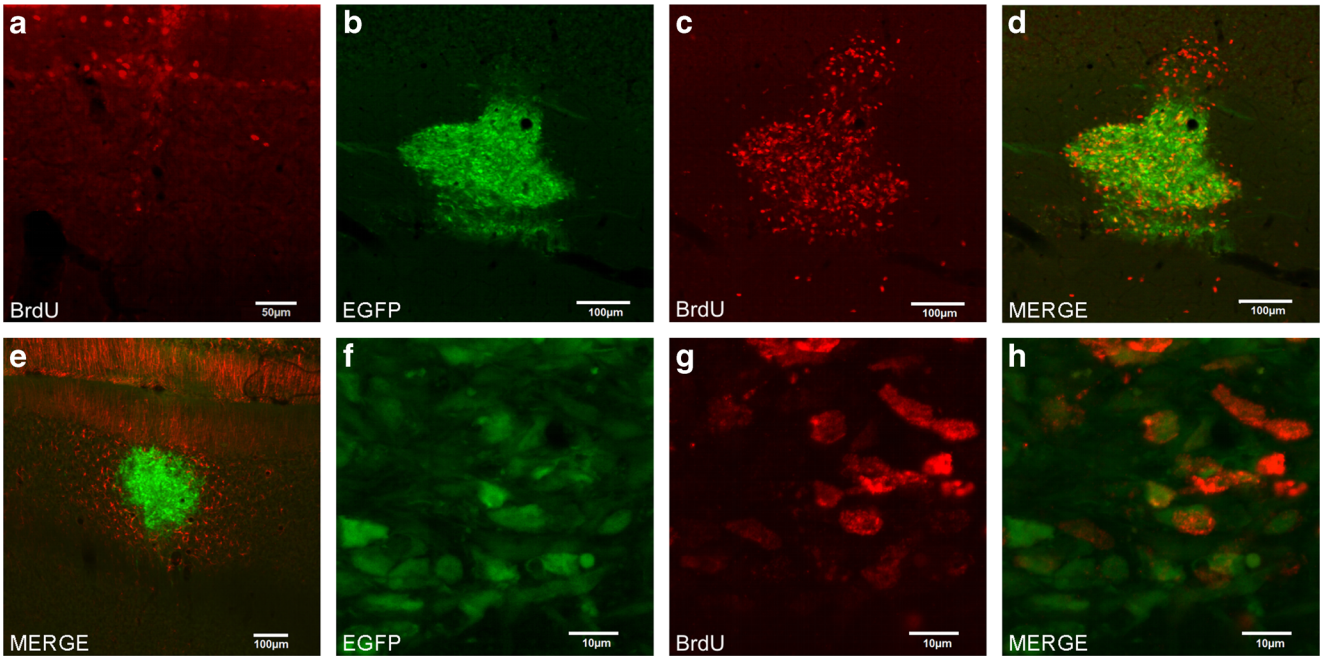

Fig. 4 Anti-BrdU immunohistochemistry (**a**, **c**, **g**), native fluorescence of EGFP (**b**, **f**), merge figure for anti-BrdU immunohistochemistry and native EGFP fluorescence (**d**, **h**), merge figure for anti-GFAP immunohistochemistry and native EGFP fluorescence (**e**), 3 days after surgery. BrdU-positive cells in the place of vehiculum injection (**a**). EGFP-positive cell suspension graft (**b**), BrdU-positive cells in the same localization (**c**), and merge figure (**d**). GFAP-positive cells in the area of EGFP-positive graft injection (**e**). A detail of EGFP-positive cells in the cell suspension graft (**f**), BrdU-positive cells in the same localization (**g**), and merge figure (**h**). Olympus FV10I-DOC confocal laser scanning microscope

swing speed (forepaws: $F_{(1,211)}$=141.93, P<0.0001; hind paws: $F_{(1,211)}$=176.27, P<0.0001) showed a significant effect of the mouse-type factor. Control *Lurcher* mice had a longer stand, shorter stride, and lower swing speed than control wild-type mice (Table 1).

Only stride length (forepaws: $F_{(2,211)}$=3.37, nonsignificant; hind paws: $F_{(2,211)}$=4.76, P=0.0276) and swing speed (forepaws: $F_{(2,211)}$=10.05, P<0.0001; hind paws: $F_{(2,211)}$=9.07, P<0.0001) showed a significant effect of the treatment factor. The results of between-group comparison are shown in

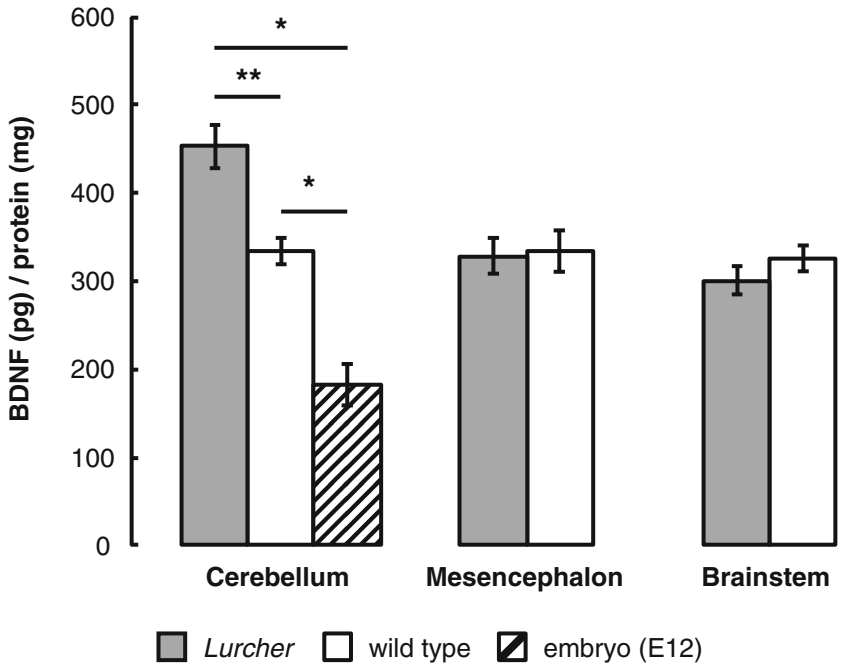

Fig. 5 The mean BDNF level (pg of BDNF per 1 mg of proteins) in adult *Lurcher* mutant and wild-type cerebellum, mesencephalon, and brainstem, as well as in embryonic cerebellum. *Error bars* represent SEM. P<0.05 is indicated by * and P<0.01 by **

Table 1. Cell suspension-treated *Lurcher* mice tested 2 months after the transplantation had only a higher forepaw swing speed than controls. *Lurcher* mice treated with cell suspension and examined 6 months later had a longer hind paw stride and higher swing speed for both forepaws and hind paws than controls. Solid graft-treated *Lurchers* achieved a higher hind paw swing speed than controls only when examined 6 months after the transplantation.

Wild-type mice treated with cell suspension and examined 2 months later did not differ from controls. However, when tested after 6 months, they had a longer stride and higher swing speed. Solid graft-treated wild-type mice tested 2 months after the surgery had a shorter forepaw stride and lower swing speed of both forepaws and hind paws than control mice. Those examined after 6 months had a longer forepaw and hind paw stride and higher forepaw swing speed.

Motor Skills

Fall latencies on the motor skill tests are shown in Fig. 6. For fall latencies on the rotarod ($F_{(1,212)}$=1634.15, P<0.0001), horizontal wire ($F_{(1,212)}$=77.34, P<0.0001), and wooden beam ($F_{(1,212)}$=683.71, P<0.0001) tests, a significant effect of the mouse type was found. *Lurcher* mice achieved shorter fall latencies than wild-type mice in all tests (compare Fig. 6). No significant effect of the treatment factor was detected in

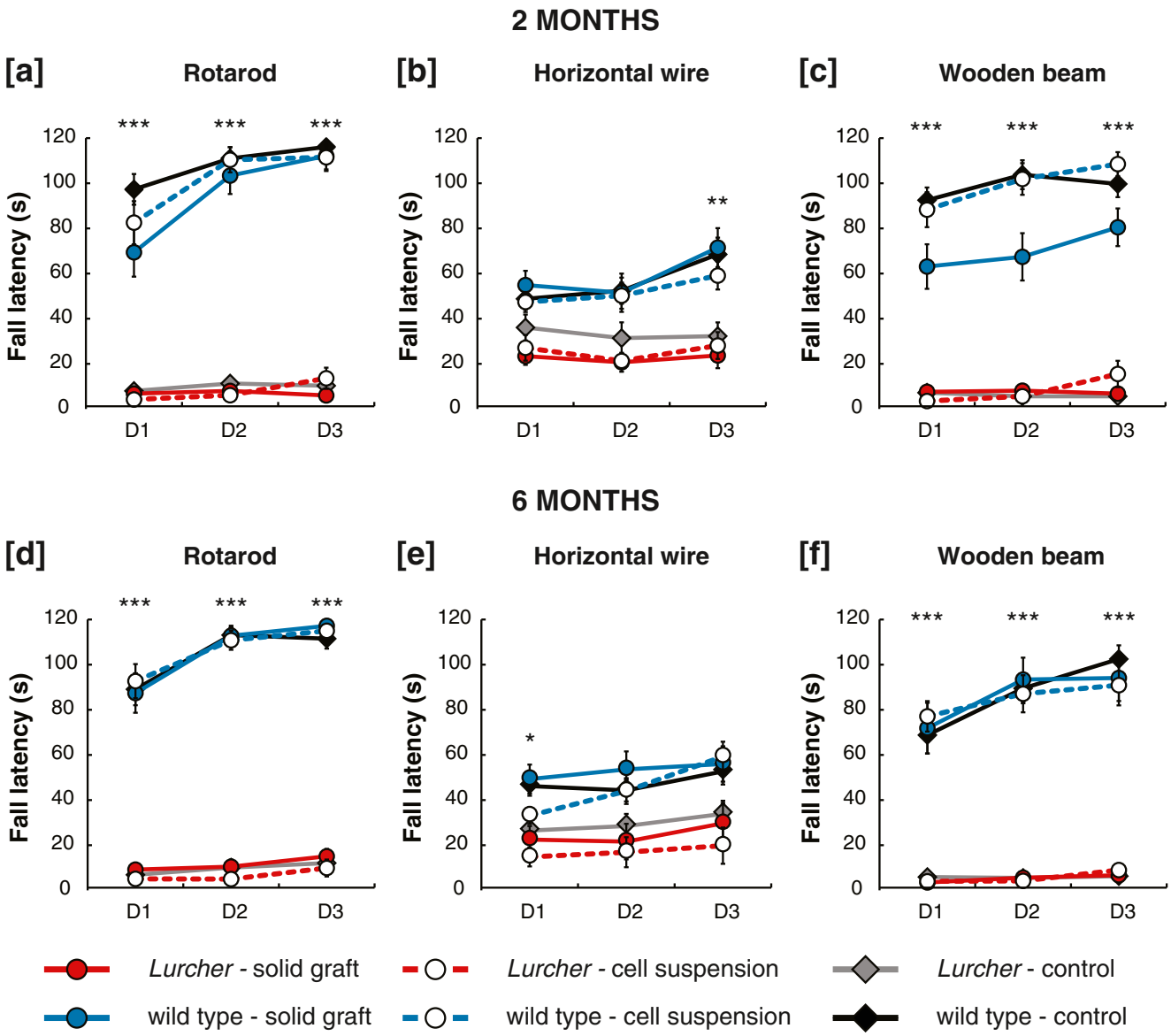

Fig. 6 Mean fall latencies (s) in 3 day sessions (D1–D3) of the rotarod (**a**, **d**), horizontal wire (**b**, **e**), and wooden beam (**c**, **f**) tests in *Lurcher* mutant and wild-type mice treated with suspension or solid grafts and tested 2 (**a**, **b**, **c**) or 6 months (**d**, **e**, **f**) later and in control groups. *Error bars* represent SEM. For comparison of control *Lurcher* and wild-type mice, P<0.05 is indicated by *, P<0.01 by **, and P<0.001 by ***

any motor test. For the D3/D1 ratio, no significant effect of the mouse type was found, but for the wooden beam test, significant effects of treatment ($F_{(2,212)}$=2.61, P=0.0338) and interaction of mouse type:treatment ($F_{(2,212)}$=7.49, P<0.0001) were found. *Lurcher* mice treated with cell suspension achieved a higher D3/D1 ratio of fall latencies than control mice (2 months after treatment: t=−2.44, P=0.0011;6 months after treatment: t=−2.38, P=0.0137). Solid graft-treated wild-type mice examined 2 months after the transplantation achieved a higher D3/D1 ratio than controls (t=−2.34, P=0.0192). On the other hand, cell suspension-treated wild-type mice tested after 6 months had a lower D3/D1 ratio than controls (t=2.13, P=0.0277) (Table 2).

Discussion

We found significant improvement in some gait parameters in adult ataxic *Lurcher* mutant mice after intracerebellar transplantation of embryonic cerebellar grafts. Up until now, embryonic solid cerebellar graft transplantation has been shown to have only a mild and inconsistent effect in *Lurcher* mice [26]. On the other hand, Jones et al. [28] observed a significant improvement in the performance on motor tests and increased Purkinje cell survival after transplantation of mesenchymal stem cells into the cerebellum of newborn *Lurchers*. It was suggested that grafted mesenchymal stem cells produced neurotrophic factors that supported the surviving Purkinje cells [28].

Among other cerebellar mutant mice, alleviation of ataxia was seen after transplantation of embryonic or fetal cerebellar cells in Purkinje cell degeneration (*pcd*) [32, 33] and spinocerebellar ataxia type 1 (*SCA1*) [34] mice. In *pcd* mice, the functional effect was explained by reconstruction of the neural circuitries [35]. However, proximity of the grafted Purkinje cells to the deep cerebellar nuclei is necessary [36] since the granular layer acts as a barrier that prevents nerve fibers from sprouting toward the deep cerebellar nuclei [37]. Transplantation of various types of stem cells also led to the improvement of motor function, e.g., in *nervous* [38], *SCA1* [39], and spinocerebellar ataxia type 2 (*SCA2*) [40] mice.

In the present study, graft structure examination confirmed our previous findings [24–27]. The grafts were able to survive for 6 months in both wild-type and *Lurcher* mice, and therefore, both their short- and long-term effects on the cerebellar ataxia could be examined. Most of the 2- or 6-month-old grafts seemed to be much larger than were the grafts that were examined 3 days after the transplantation. Growth of the graft was confirmed by the presence of newly generated EGFP-positive cells. In wild-type mice, the cell suspension graft showed some dispersion of the Purkinje-shaped cells and was similar to the graft seen recently in *SCA2* mice [41]. In *Lurcher* mice, the grafts showed a tendency to avoid the cerebellum, and fiber sprouting from the graft was rare. Therefore, numerous functional synaptic contacts between the graft and host cerebellum cannot be expected, and the graft structure in *Lurchers* did not promise any strong specific functional effects mediated by Purkinje cell replacement and neural circuitry reconnection. Since no abundant connections between the graft and the host structures were seen, the functional effect of the graft would probably be at least partially mediated by the supporting intrinsic brain plasticity through the presence of the grafted tissue. (For a review, see [42]). It has been reported several times that grafted cells do not substitute for the lost ones but instead prevented their degeneration, supported the function of surviving host Purkinje cells [28, 40, 43] in cerebellar mutant mice, or reduced glial activation and inflammatory responses in the cerebellum in the Niemann-Pick disease type C mouse model [44, 45]. These approaches, however, require timely engraftment before the extinction of the intrinsic Purkinje cells, and therefore, it would not be applicable in adult *Lurcher* mice with no Purkinje cells. The effect of the grafted tissue could be complex and may not be explained by one mechanism. There are large numbers of various trophic and morphogenetic factors that could be

Table 2 Mean D3/D1 ratios of fall latencies ± SEM in the rotarod, suspension wire, and wooden beam tests in *Lurcher* mutant and wild-type mice 2 or 6 months after transplantation of solid embryonic cerebellar graft or cell suspension and in age-matched controls

	Time period	Treatment	Rotarod	Horizontal wire	Wooden beam
Lurcher	2 months	Cell suspension	4.88±2.31	1.53±0.39	6.07±2.24
		Solid graft	1.17±0.18	1.01±0.15	1.36±0.37
		Control	2.04±0.70	1.46±0.51	1.01±0.18
	6 months	Cell suspension	1.88±0.62	2.18±1.02	3.19±1.06
		Solid graft	1.97±0.35	1.32±0.26	2.21±0.94
		Control	1.68±0.35	1.95±0.45	1.27±0.24
Wild type	2 months	Cell suspension	4.53±1.94	1.49±0.18	1.96±0.68
		Solid graft	4.87±1.83	1.51±0.22	2.00±0,41
		Control	3.47±1.58	1.50±0.17	1.17±0.10
	6 months	Cell suspension	1.70±0.35	2.36±0.44	1.17±0.10
		Solid graft	1.81±0.37	1.40±0.26	2.16±0.58
		Control	2.42±0.88	1.58±0.40	3.90±1.08

produced by the graft. Moreover, production of various factors could be induced in the host tissue due to the presence of the extraneous grafted tissue. Nevertheless, the induction of elevated levels of certain factors may not be required. We demonstrated that in the *Lurcher* cerebellum, BDNF is increased compared with the healthy cerebellar tissue and with both wild-type and *Lurcher* mutant mesencephalon and brainstems. Furthermore, the embryonic cerebellum contains less BDNF than does the postnatal one [46], and therefore, it does not seem to be a source of this factor delivery into the diseased host tissue.

Lurcher mice are well known for their severe motor deficits [16, 17, 19, 21], and in accordance with previous findings [20], we found a significant impact of the *Lurcher* phenotype on performance in the rotarod, horizontal wire, and wooden beam tests, as well as on several basic gait parameters. Although in the classical motor tests, no benefit of the transplantation was detected in *Lurcher* mice (except for slightly better learning on the wooden beam in cell suspension-treated ones), the gait analysis showed significant amelioration in graft-treated *Lurchers*, which was more marked in those treated with cell suspensions.

Since no significant difference was found in walking speed, improvements of swing speed and/or stride length parameters were not just artifacts due to faster walking. Examination of spontaneous gait as a natural movement appeared to be more sensitive for detecting the functional effect of the transplantation therapy. On the other hand, classical motor tests were not capable of clearly identifying those cases where only mild changes had already been seen [26]. After a longer interval between the transplantation and function examination, the improvement was more marked. This suggests that a long enough period is necessary to develop changes in the neural circuitries that determine functional manifestation.

Mild gait parameter changes were also seen in wild-type mice after cerebellar transplantation. In solid graft-treated ones, the changes were negative when examined 2 months after the surgery. This suggests a possible moderate negative effect of a solid piece of tissue growing in the cerebellum or of the trauma caused by its introduction. In our previous studies, we used double doses of solid cerebellar grafts, which in some cases, led to compression of the host cerebellum [26, 27]. Nevertheless, when the graft amount was reduced in the present experiment, such a negative phenomenon was not observed and the negative effect of the solid graft seemed to be transient only because after 6 months, the gait parameters were not worse than they were in untreated control mice.

Conclusion

A mild beneficial effect of embryonic cerebellar tissue transplantation into the cerebellum of *Lurcher* mice on spontaneous gait was found. Cell suspension seems to be more effective than solid grafts. Although in wild-type mice, no severe or long-lasting negative effects of the transplantation were observed, cell suspension application would probably also be a more gentle approach. Nevertheless, functional improvement is probably a slow and long-lasting process.

Acknowledgments The work was supported by COST grant nos. LD 12057 and LD12056 from the Ministry of Education, Youth, and Sport of the Czech Republic, student specific research project of Charles University, Charles University Grant Agency grant no. 408911, Charles University Research Fund P36, project CZ.1.05/2.1.00/03.0076 from the European Regional Development Fund and was co-financed by the European Social Fund and the state budget of the Czech Republic project no. CZ.1.07/2.3.00/30.0022.

Conflict of Interest The authors declare that they have no conflict of interest.

References

1. Manto MU. The wide spectrum of spinocerebellar ataxias (SCAs). Cerebellum. 2005;4:2–6.
2. Marien P, Beaton A. The enigmatic linguistic cerebellum: clinical relevance and unanswered questions on nonmotor speech and language deficits in cerebellar disorders. Cerebellum Ataxias. 2014;1:12.
3. Wang HL, Hu SH, Chou AH, Wang SS, Weng YH, Yeh TH. H1152 promotes the degradation of polyglutamine-expanded ataxin-3 or ataxin-7 independently of its ROCK-inhibiting effect and ameliorates mutant ataxin-3-induced neurodegeneration in the SCA3 transgenic mouse. Neuropharmacology. 2013;70:1–11.
4. Chort A, Alves S, Marinello M, Dufresnois B, Dornbierer JG, Tesson C, et al. Interferon β induces clearance of mutant ataxin 7 and improves locomotion in SCA7 knock-in mice. Brain. 2013;136:1732–45.
5. Power EM, Empson RM. Functional contributions of glutamate transporters at the parallel fibre to Purkinje neuron synapse-relevance for the progression of cerebellar ataxia. Cerebellum Ataxias. 2014;1:3.
6. Manto M, Marmolino D. Animal models of human cerebellar ataxias: a cornerstone for the therapies of the twenty-first century. Cerebellum. 2009;8:137–54.
7. Cendelin J. From mice to men: lessons from mutant ataxic mice. Cerebellum Ataxias. 2014;1:4.
8. Phillips RJS. 'Lurcher', a new gene in linkage group XI of the house mouse. J Genet. 1960;57:35–42.
9. Zuo J, DeJager PJ, Takahashi KA, Jiang W, Linden DJ, Heintz N. Neurodegeneration in Lurcher mice caused by mutation in δ2 glutamate receptor. Nature. 1997;388:769–73.
10. Araki K, Meguro H, Kushiya E, Takayama C, Inoue Y, Mishina M. Selective expression of the glutamate receptor channel delta 2 subunit in cerebellar Purkinje cells. Biochem Biophys Res Commun. 1993;197:1267–76.
11. Hills LB, Masri A, Konno K, Kakegawa W, Lam ATN, Lim-Melia E, et al. Deletions in GRID2 lead to a recessive syndrome of cerebellar ataxia and tonic upgaze in humans. Neurology. 2013;81:1378–86.
12. Caddy KWT, Biscoe TJ. Structural and quantitative studies on the normal C3H and Lurcher mutant mouse. Philos Trans R Soc B-Biol Sci. 1979;287:167–201.

13. Wetts R, Herrup K. Interaction of granule, Purkinje and inferior olivary neurons in lurcher chimeric mice I Qualitative studies. J Embryol Exp Morphol. 1982;68:87–98.
14. Wetts R, Herrup K. Interaction of granule, Purkinje and inferior olivary neurons in lurcher chimeric mice. II. Granule cell death. Brain Res. 1982;250:358–62.
15. Zanjani SH, Selimi F, Vogel MW, Haeberle AM, Boeuf J, Mariani J, et al. Survival of interneurons and parallel fiber synapses in a cerebellar cortex deprived of Purkinje cells: studies in the double mutant mouse Grid2$^{Lc/+}$;Bax$^{-/-}$. J Comp Neurol. 2006;497:622–35.
16. Fortier PA, Smith AM, Rossignol S. Locomotor deficits in the cerebellar mutant mouse, Lurcher. Exp Brain Res. 1987;66:271–86.
17. Lalonde R, Filali M, Bensoula AN, Lestienne F. Sensorimotor learning in three cerebellar mutant mice. Neurobiol Learn Mem. 1996;65:113–20.
18. Hilber P, Caston J. Motor skills and motor learning in Lurcher mutant mice during aging. Neuroscience. 2001;102:615–23.
19. Porras-Garcia E, Cendelin J, Dominguez-del-Toro E, Vozeh F, Delgado-Garcia JM. Purkinje cell loss affects differentially the execution, acquisition and prepulse inhibition of skeletal and facial motor responses in Lurcher mice. Eur J Neurosci. 2005;21:979–88.
20. Cendelin J, Voller J, Vozeh F. Ataxic gait analysis in a mouse model of the olivocerebellar degeneration. Behav Brain Res. 2010;210:8–15.
21. Cendelin J, Tuma J, Korelusova I, Vozeh F. The effect of genetic background on behavioral manifestation of Grid2^{Lc} mutation. Behav Brain Res. 2014;271:218–27.
22. Tomey DA, Heckroth JA. Transplantation of normal embryonic cerebellar cell suspensions into the cerebellum of Lurcher mutant mice. Exp Neurol. 1993;122:165–70.
23. Heckroth JA, Hobart NJH, Summers D. Transplanted neurons alter the course of neurodegenerative disease in Lurcher mutant mice. Exp Neurol. 1998;154:336–52.
24. Cendelin J, Babuska V, Korelusova I, Houdek Z, Vozeh F. Long-term survival of solid embryonic cerebellar grafts in Lurcher mice. Neurosci Lett. 2012;515:23–7.
25. Cedikova M, Houdek Z, Babuska V, Kulda V, Vozeh F, Zech N, et al. Fate of two types of cerebellar graft in wild type and cerebellar mutant mice. J Appl Biomed. 2014;12:17–23.
26. Cendelin J, Korelusova I, Vozeh F. The effect of cerebellar transplantation and enforced physical activity on motor skills and spatial learning in adult Lurcher mutant mice. Cerebellum. 2009;8:35–45.
27. Cendelin J, Korelusova I, Vozeh F. A preliminary study of solid embryonic cerebellar graft survival in adult B6CBA Lurcher mutant and wild type mice. Anat Rec. 2009;292:1986–92.
28. Jones J, Jaramillo-Merchan J, Bueno C, Pastor D, Viso-Leon M, Martinez S. Mesenchymal stem cells rescue Purkinje cells and improve motor functions in a mouse model of cerebellar ataxia. Neurobiol Dis. 2010;40:415–23.
29. Houdek Z, Cendelin J, Kulda V, Babuska V, Cedikova M, Kralickova M, et al. Intracerebellar application of P19-derived neuroprogenitor and naive stem cells to Lurcher mutant and wild type B6CBA mice. Med Sci Monitor. 2012;18:BR174–80.
30. Kempermann G, Gast D, Kronenberg G, Yamaguchi M, Gage FH. Early determination and long-term persistence of adult-generated new neurons in the hippocampus of mice. Development. 2003;130:391–9.
31. Pesarin F, Salmaso L. Permutation tests for complex data: theory, applications and software. 1st ed. Wiltshire: John Wiley & Sons; 2010.
32. Triarhou LC, Zhang W, Lee WH. Graft-induced restoration of function in hereditary cerebellar ataxia. Neuroreport. 1995;6:1827–32.
33. Triarhou LC, Zhang W, Lee WH. Amelioration of the behavioral phenotype in genetically ataxic mice through bilateral intracerebellar grafting of fetal Purkinje cells. Cell Transplant. 1996;5:269–77.
34. Kaemmerer WF, Low WC. Cerebellar allografts survive and transiently alleviate ataxia in a transgenic model of spinocerebellar ataxia type-1. Exp Neurol. 1999;158:301–11.
35. Sotelo C, Alvarado-Mallart RM. Reconstruction of the defective cerebellar circuitry in adult Purkinje cell degeneration mutant mice by Purkinje cell replacement through transplantation of solid embryonic implants. Neuroscience. 1987;20:1–22.
36. Keep M, Alvarado-Mallart RM, Sotelo C. New insight on the factors orienting the axonal outgrowth of grafted Purkinje cells in the pcd cerebellum. Dev Neurosci. 1992;14:153–65.
37. Carletti B, Williams IM, Leto K, Nakajima K, Magrassi L, Rossi F. Time constraints and positional cues in the developing cerebellum regulate Purkinje cell placement in the cortical architecture. Dev Biol. 2008;317:147–60.
38. Li JX, Imitola J, Snyder EY, Sidman RL. Neural stem cells rescue nervous Purkinje neurons by restoring molecular homeostasis of tissue plasminogen activator and downstream targets. J Neurosci. 2006;26:7839–48.
39. Matsuura S, Shuvaev AN, Iizuka A, Nakamura K, Hirai H. Mesenchymal stem cells ameliorate cerebellar pathology in a mouse model of spinocerebellar ataxia type 1. Cerebellum. 2014;13:323–30.
40. Chang YK, Chen MH, Chiang YH, Chen YF, Ma WH, Tseng CY, et al. Mesenchymal stem cell transplantation ameliorates motor function deterioration of spinocerebellar ataxia by rescuing cerebellar Purkinje cells. J Biomed Sci. 2011;18:54.
41. Purkartova Z, Tuma J, Pesta M, Kulda V, Hajkova L, Sebesta O, et al. Morphological analysis of embryonic cerebellar grafts in SCA2 mice. Neurosci Lett. 2014;558:154–8.
42. Rossi F, Cattaneo E. Opinion: Neural stem cell therapy for neurological diseases: dreams and reality. Nat Rev Neurosci. 2002;3:401–9.
43. Chintawar S, Hourez R, Ravella A, Gall D, Orduz D, Rai M, et al. Grafting neural precursor cells promotes functional recovery in an SCA1 mouse model. J Neurosci. 2009;29:13126–35.
44. Bae JS, Furuya S, Ahn SJ, Yi SJ, Hirabayashi Y, Jin HK. Neuroglial activation in Niemann-Pick type C mice is suppressed by intracerebral transplantation of bone marrow-derived mesenchymal stem cells. Neurosci Lett. 2005;381:234–6.
45. Bae JS, Carter JE, Jin HK. Adipose tissue-derived stem cells rescue Purkinje neurons and alleviate inflammatory responses in Niemann-Pick disease type C mice. Cell Tissue Res. 2010;340:357–69.
46. Sato M, Suzuki K, Nakanishi S. Expression profile of BDNF-responsive genes during cerebellar granule cell development. Biochem Biophys Res Commun. 2006;341:304–9.

4 DISCUSSION

4.1 Spatial behavior of cerebellar mutants

Because cerebellar disorders are associated with complex behavioral disturbances, deep behavioral analysis of cerebellar mutant mouse models is necessary to understand all of the factors involved in their phenotype. A detailed description of the specific features of their cognitive, emotional and motor functions is necessary to understand the involvement of the cerebellum in behavioral processes as well as for the assessment of their suitability as models of experimental therapy. It has already been shown that mouse models of olivocerebellar degeneration suffer from ataxia and cognitive and affective impairments (for details see above). Nevertheless, modern tracking and analysis systems, new statistical approaches, and the involvement of previously neglected factors, e.g. genetic background and sex, enable us to verify and extend our knowledge about the functional disturbances caused by olivocerebellar degeneration.

The main topic of this thesis was to assess a behavior deficit in two mouse models of olivocerebellar degeneration, *Lurcher* and *pcd* mice, with particular attention paid to their cognitive and emotional disturbances. *Lurcher* and *pcd* mice are two of the oldest and frequently used cerebellar mutants. Based on current knowledge, both mutants constitute a distinct type of mutation affecting the olivocerebellar system either exclusively (*Lurcher*) or inclusively (*pcd*) and determining a noticeable pathological phenotype. Their history and distinct histopatological similarities predestine these mutants to frequent mutual comparisons (for reviews see Vogel et al., 2007; Wang and Morgan, 2007). However, these comparisons were mostly indirect and none of the studies involved systematic behavioral analysis. Except for strong ataxia, spatial behavior impairment was one of the first behavioral deficits described in both *Lurcher* and *pcd* mice (Lalonde et al., 1988; Goodlett et al., 1992).

Orienting and navigating relative to the environment constitute fundamental tasks common to all organisms (Etienne and Jeffery, 2004; Wiltschko and Wiltschko, 2012; Collett et al., 2013). Gallistel (1990) defined spatial navigation as “a process of

determining and maintaining a course or trajectory from one place to another with respect to the known world". The capacity to plan and execute a goal-directed path consists of two elementary processes. First, dead reckoning (originally a nautical term), or path integration (biological term) (Mittelstaedt and Mittelstaedt, 1982), is the continuous process of determining a change in position by integrating directed speed with respect to time and second, an episodic process gives the position using fixed, visible cues (Gallistel, 1990). From this point of view, cerebellar degeneration could affect more particular components of spatial behavior. With regard to the type of mutation and extent of cerebellar degeneration in *Lurcher* and *pcd* mice, we primarily aimed to assess and compare spatial navigation and orientation as well as spatial learning and memory in these mutants.

Spatial behavior in *Lurcher* and *pcd* mice was tested using a Morris water maze (Morris et al., 1982; Morris, 1984; for reviews see D'Hooge and De Deyn, 2001; Wahlsten, 2011). The Morris water maze consists of a simple task with aversive stimulus (water) that motivates an animal to find an escape platform (hidden or visible). Despite the aversive nature of the task that could provoke unpredictable behavior in cerebellar mutants, we decided to use this test for the following reasons: 1) it is broadly accepted that swimming in these mice is less affected than gait by cerebellar ataxia (Fortier et al., 1987; Goodlett et al., 1992) and 2) for comparability with previously published studies. Nevertheless, we also tested exploration and anxiety in the open field (Hall and Ballachey, 1932; Hall, 1934; for reviews see Walsh and Cummins, 1976; Wahlsten, 2011), as well as depressive-like behavior in the Porsolt's forced swimming test (Porsolt et al., 1977; Porsolt et al., 1978; Porsolt et al., 1979; for reviews see Wahlsten, 2011; Slattery and Cryan, 2012) to describe a complex behavioral profile and to avoid a misleading interpretation of results obtained from the Morris water task.

We have confirmed severe impairments in cognitive and behavioral tests in both *Lurcher* and *pcd* mutant mice (**Article 2**: Tuma et al., 2015). Contrary to previous studies (Goodlett et al., 1992; Lalonde and Thifault, 1994), we have shown that overall performance in the Morris water maze test was better in *Lurcher* than in *pcd* mutants (**Article 2**: Tuma et al., 2015). We have found that navigation to the visible platform is only partially disabled in *Lurcher* mutants, but *pcd* mice failed in

both visual and hidden goal tests (**Article 2**: Tuma et al., 2015). On the basis of these behavioral findings and the extent of cerebellar and non-cerebellar affections, we proposed that the poor performance of cerebellar mutants in the water maze task could be caused by at least four types of factors, alone or in combination: 1) cognitive disturbances, 2) sensory disorders, 3) motor deficits, and 4) motivation and behavioral abnormalities (**Article 2**: Tuma et al., 2015). The intensity of employment of these basic mechanisms in the individual mouse is determined by various factors, such as mutations, genetic background (strain), and sex (**Article 2**: Tuma et al., 2015; **Article 4**: Cendelin et al., 2014).

4.1.1 Role of cognition

Spatial behavior requires two types of navigation: egocentric navigation (where the mouse determines the spatial relationships of features in the environment with respect to its own body) and allocentric navigation (where the mouse stores and uses information about the relationship of these features to each other) (for detail see Jeffery, 2003). For more sophisticated navigation and planning of the journey to find the optimal route, and also for recalibration of accumulated error resulting from egocentric navigation, the building of an internal representation of the environment, termed "cognitive map" is crucial (Tolman, 1948; O'Keefe and Nadel, 1978; for details see Jeffery, 2003).

The neural substrate of the cognitive map is in the hippocampus (O'Keefe and Dostrovsky, 1971; O'Keefe and Nadel, 1978), namely hippocampal place cells (O'Keefe and Dostrovsky, 1971). Nevertheless, later studies revealed that the cerebellum also plays a key role in the formation of a hippocampal spatial representation map (Burguiere et al., 2005; Rochefort et al., 2011; Passot et al., 2012; for review see Rochefort et al., 2013). Rochefort et al. (2011) demonstrated that mice that lack cerebellar protein kinase C (PKC)-dependent PF-PC LTD (L7-PKCI mice) showed exclusively impaired place cell properties when they had to rely on self-motion cues only. However, L7-PKCI mice were able to navigate using allocentric navigation (Rochefort et al., 2011). These findings suggested that cerebellar PF-PC LTD is not necessary for successful navigation in the Morris water maze when both allocentric and egocentric navigation are used. Nevertheless, the

dissociation of these types of navigation in PF-PC LTD deficient mice, such as L7-PKCI, as well as *Lurcher* and *pcd* could lead to effects on path integration and impaired place cell properties (Burguiere et al., 2005; Rochefort et al., 2011; Rochefort et al., 2013).

With regard to these findings, Rondi-Reig et al. (2014) suggested that the cerebellar cortex serves as an adaptive filter which transforms self-motion sensory signals, motor efference copy, and the previous sensory state into a prediction of the sensory signal expected from voluntary movements. Comparing the prediction with actual sensory signals, the cerebellum helps to detect novelty in the environment (Rondi-Reig et al., 2014). This computation could verify the expected sensory state during voluntary navigation or inform about the necessity to update the position in the environment (Rondi-Reig et al., 2014).

Since *Lurcher* and *pcd* mice have lost synapses on which the PF-PC LTD arises, a deficit in path integration could be expected (see above). Furthermore, both mutants failed in the Morris water maze enabling allocentric navigation (**Article 2**: Tuma et al., 2015; **Article 4**: Cendelin et al., 2014) impairment of this type of navigation could also be present. Contrary to L7-PKCI mice, *Lurcher* as well as *pcd* mice suffer not from selective lack of PF-PC LTD but from complete functional decortication of the cerebellum. Thus much wider functional impact is expectable.

Allocentric navigation using the internal representation of spatial context is complex process involving many neural structures, including the cerebellum (for details see Petrosini et al., 1998). The spatial context is a neural construct that enables to hippocampal place cells to respond not only to spatial aspects of an environment, but also to non-spatial "contextual" aspects, such as color or shape (Anderson et al., 2003). This construct enables the animal to navigate from one place to another using a non-spatial scheme and to plan a path to another place with the relation to landmarks array (Jeffery, 2003). To build a cognitive map, the processes for transforming egocentric sensory inputs into an allocentric form are required (Hartley et al., 2003). The collection of personally experienced events including contextual information, such as spatial layout and visual details concerning the location in which it occurred, indicate a possible link between spatial and episodic function (Hartley et al., 2003). Therefore, hippocampal spatial memory is also dependent on episodic

memory formed primarily in medial temporal cortex (O'Keefe and Nadel, 1978; Abrahams et al., 1997; Aggleton and Brown, 1999). The content of episodic memory can be defined as perceived information or feeling about an event that the subject is consciously aware of at the time (Moscovitch, 1995; Nadel and Moscovitch, 1997; Fujii et al., 2002a; Fujii et al., 2004). From this point of view, the content of the episodic memory is not the same as the event itself, but rather can be determined as the interaction between the subject and the event (Fujii et al., 2002b).

Activation of the cerebellar-hippocampal network during spatial context retrieval (Fujii et al., 2004; Paleja et al., 2014; Sami et al., 2014), and participation of the cerebellum in episodic memory (Andreasen et al., 1999; Fliessbach et al., 2007; Habas et al., 2009) were found. Thus, the alteration of these two memory functions could contribute to the deficit in allocentric navigation in both *Lurcher* and *pcd* mice.

A functional link between the cerebellum and hippocampus has been also demonstrated during eyeblink conditioning (Hoffmann and Berry, 2009; Wikgren et al., 2010). Eyeblink (or eyelid) conditioning is one of the most extensively studied forms of associative motor learning (Gruart et al., 1997; Medina et al., 2000; Kishimoto et al., 2001; Jimenez-Diaz et al., 2004; Heiney et al., 2014). It is supposed that simple associative learning is also related to animals' abilities to use internal representation of an absent object to guide adaptive behavior and acquire new information, and to represent multiple spatial, temporal, and object properties of complex events and event sequences (for review see Pickens and Holland, 2004). Both *Lurcher* and *pcd* mice show abnormalities in associative eyeblink conditioning (Chen et al., 1996; Porras-Garcia et al., 2005; Brown et al., 2010; Porras-Garcia et al., 2010; for review see Porras-Garcia et al., 2013).

Moreover, task solving in the Morris water maze requires not only declarative spatial memory, which involves the collection and recall of exact relations of environmental cues, but also procedural learning (Schenk and Morris, 1985; Petrosini et al., 1998; Leggio et al., 1999). Procedural aspects linked to how a spatial task is solved embrace different components (Whishaw, 1985; Whishaw and Gorny, 1991; Leggio et al., 1999). Consecutive improvement in the Morris water task can reflect improvement in the motor component of the task, which is *a priori* limited by ataxia in cerebellar mutants. Nevertheless, we have shown that *Lurcher* mice are able to

improve their motor skills (**Article 4**: Cendelin et al., 2014). With regard to the absence of PF-PC LTD (for details see chapter 1.4.1 Motor control and learning) in *Lurcher* mice, we have to take into account a different cellular (van Alphen and De Zeeuw, 2002; Schonewille et al., 2011) and/or non-cellular mechanism involved in the improvement of motor skills in these mutants.

4.1.2 Role of sensory deficits

Sensory inputs are essential for spatial navigation and orientation. The computational process during path integration depends on the integration of internal signals generated by vestibular cues, proprioception, and optic flow (Yoder et al., 2015). It has been reported that the cerebellum plays a key role in this integrative process (see chapter 1.3.2 Cognitive and affective functions; Angelaki and Hess, 2005; Yakusheva et al., 2007; Brooks and Cullen, 2009; Yakusheva et al., 2013). To avoid progressively degraded estimation of the current position given by the accumulation of errors during path integration, the navigator needs to recalibrate its position using an external reference frame, e.g. visual, olfactory, acoustic, and magnetic landmark cues (Etienne and Jeffery, 2004). In the Morris water task with visible external cues, the recalibration process places emphasis on continuous sighting fixation and on the visual following of an object by a moving individual. In *Lurcher* mice, abnormalities of the OKR and VOR were reported by van Alphen et al. (2002). Since the Purkinje cells control oculomotor coordination, including OKR and VOR (for reviews see Angelaki and Hess, 2005; Yakusheva et al., 2007), oculomotor problems could also be expected in *pcd* mice in which the VOR has, however, been found to be almost normal (Killian and Baker, 2002). Aside from its role in oculomotor control, the cerebellum is involved in perceptual processes at a higher level of sensory signal processing (for details see Baumann et al., 2015).

Moreover, *pcd* mice suffer from slow, progressive retinal degeneration (Blanks et al., 1982a; LaVail et al., 1982). Although we found only an insignificant reduction in photoreceptor density in the retinas of *pcd* mice at the age at which they were tested in the Morris water maze (**Article 2**: Tuma et al., 2015), the impact of vision problems on spatial behavior could not be excluded due to possible functional

imperfection of degenerating retina even before the reduction of photoreceptor number becomes evident (Marchena et al., 2011).

Taken together, the effects of oculomotor deficit, sensory integration, and possible poor vision (*pcd*, *Lurcher* C3H/Pde6b$^{rd/+}$) can play a significant role in navigation difficulties in these mice (**Article 2**: Tuma et al., 2015; **Article 4**: Cendelin et al., 2014). In the visible goal task, these problems may be less important than in the hidden goal task, since the goal represents a single and marked intramaze object of interest instead of the multiple extramaze landmarks necessary for hidden goal location.

4.1.3 Role of motor impairments

Motor deficit is the main distinct impairment in cerebellar mutants (for details see reviews Lalonde and Strazielle, 2007; Porras-Garcia et al., 2013; Cendelin, 2014). Despite the motor disorders in *Lurcher* (**Article 4**: Cendelin et al., 2014; **Article 5**: Babuska et al., 2015) and *pcd* mice (Mullen et al., 1976; Goodlett et al., 1992), some authors have reported that swimming capability in these mutants is competent and less affected by ataxia than their gait (Fortier et al., 1987; Goodlett et al., 1992; Martin et al., 2003). Fortier et al. (1987) showed that whereas on land *Lurchers* stumbled after only a few step cycles, in water they were capable of producing an extended series of consecutive swim cycles with a normal EMG pattern. Goodlett et al. (1992) demonstrated that, although terrestrial movement is also strongly affected in *pcd* mice, they could at times adopt a normal swimming posture comparable to that of littermate controls, with their head above the water, forepaws inhibited, propelling with alternating hind limb kicks, and using the tail in the water. However, they did not maintain this swimming pattern over long distances, and frequently broke into a "dog-paddle", in which they used both forelimbs and hind limbs for swimming (Goodlett et al., 1992).

We have shown that *Lurcher* mice achieved the same swimming speed as their healthy littermate controls (**Article 2**: Tuma et al., 2015; **Article 4**: Cendelin et al., 2014) but, despite the findings of Fortier et al. (1987), the mutants sometimes demonstrated an abnormal swimming posture (see Figure 2). Contrary to *Lurcher* mice, *pcd* mutants were not able to achieve the same swimming speed as their

controls (**Article 2**: Tuma et al., 2015). Low swimming speed in *pcd* mice could account for their low capability to maintain a normal swimming pattern over a long distance (Goodlett et al., 1992), but also for lower activity (see below) and/or worse fitness (**Article 2**: Tuma et al., 2015). Nevertheless, in both *Lurcher* and *pcd* mutants, we have observed a high incidence of rotating and almost no direct swim to the escape platform (**Article 2**: Tuma et al., 2015; **Article 4**: Cendelin et al., 2014). A low frequency of direct swim as well as an inability to reduce overall heading deviation from direct swim, even at the end of the visible platform task suggests that motor deficiency in cerebellar mutants could markedly influence trajectory shape and disable the maintenance of a straight course toward the goal (**Article 2**: Tuma et al., 2015).

With regard to these findings, it can be speculated that the disruption of trajectory shape and inability to maintain a swimming course primarily affects path integration in cerebellar mutants. Although path integration is a highly adaptive form of spatial navigation that enables rapid orientation in an unknown environment, continuously ongoing calculation of actual position is highly susceptible to rapid accumulation of errors (Etienne et al., 1988; Benhamou et al., 1990). The new position is always calculated from previous values and therefore, each small error is reflected in the next computation step (Kimchi et al., 2004; Tommasi et al., 2012). Frequent uncontrolled displacements from the intentional swimming path due to motor deficits accelerate error accumulation and thus decrease the precision and accuracy of this type of navigation in *Lurcher* and *pcd* mice.

Figure 2: Examples of abnormal swimming posture in *Lurcher* mutant mice.

4.1.4 Role of motivation and behavioral abnormalities

Although both *Lurcher* and *pcd* mutants failed in the Morris water task, behavioral manifestation in the maze was different (**Article 2**: Tuma et al., 2015; **Article 4**: Cendelin et al., 2014). While *Lurcher* mice spent the whole time in the water maze swimming intensively, *pcd* mutants showed low swimming activity and long periods of floating (**Article 2**: Tuma et al., 2015). A higher tendency toward inactivity in *pcd* mice and increased swimming activity in *Lurcher* mice were also seen in the forced swimming test (**Article 2**: Tuma et al., 2015). Floating is a behavioral phenomenon that may substantially influence the results of the water maze task (Llano Lopez et al., 2010) or may be a response to a difficult task as a manifestation of depressive-like behavior and learned helplessness (Porsolt et al., 1979). In *pcd* mice, a potential sight-related impairment due to retinal degeneration (see above) and poor fitness related to low body weight may make the spatial task too difficult and might induce learned helplessness (**Article 2**: Tuma et al., 2015). Although *Lurcher* mice showed significantly lower body weight than their healthy littermates, they did not demonstrate poor fitness as was seen in *pcd* mice (**Article 2**: Tuma et al., 2015). In contrast to *pcd* mice, *Lurcher* mutants showed inability to inhibit their swimming activity in the forced swimming test compared with healthy controls (**Article 2**: Tuma et al., 2015). This abnormal behavior could account for their behavioral disinhibition when they are exposed to anxiogenic situations (Frederic et al., 1997; Hilber et al., 2004).

Impaired capability to solve the Morris water task in both *Lurcher* and *pcd* mice could also result in decreased motivation to explore and/or effectively find the escape route from the maze. Although the mutants did not show distinct changes in exploratory behavior in the open field test compared with control groups (**Article 2**: Tuma et al., 2015), we can assume that behavior would differ in a more aversive environment, such as the water maze. Higher stress reactivity in *Lurcher* mice or depressive-like behavior in *pcd* mice could result in their inability to inhibit nonadaptive behavior (circling in the pool periphery, scrabbling at pool walls, inhibiting of exploratory behavior) and thus decrease their probability of solving the task.

4.1.5 Role of the mutation, strain background and sex

Grid2^{Lc} and *Agtpbp1*^{pcd} mutations not only differ in their mechanisms of cell death activation, but also in biochemical characteristics, which can modify behavior. Quantitative peptidomics of *pcd* mouse brains showed significantly altered levels of some peptide hormones and prohormones, e.g. melanin-concentrating hormone (MCH), proopiomelanocortin, and proenkephalin, (Berezniuk et al., 2013). MCH neuropeptide displays anxiolytic, antidepressant and/or anorectic properties (Hervieu, 2003). Nevertheless, in our experiment, *pcd* mice showed more depressive-like behavior (**Article 2**: Tuma et al., 2015).

Moreover, the spectrum of extracerebellar brain damage and the effect on other tissues is wider with the *Agtpbp1*^{pcd} mutation (see above). Particularly, retinal degeneration (Mullen et al., 1976; Blanks et al., 1982a), deficiency of CCP1 protein in skeletal muscles (Harris et al., 2000), and olfactory mitral cell degeneration (Diaz et al., 2012) are important factors that can influence mouse behavior. Thus it could be speculated that the overall worse performance of *pcd* mice in the Morris water maze compared with *Lurcher* mutants could be related to the broader spectrum of degenerative processes (**Article 2**: Tuma et al., 2015).

Since genetic background (strain) differences between B6CBA and B6.BR wild type mice were also found, it is difficult to unambiguously distinguish the specific mutation effect from the effect of strain-specific phenotypic traits, the importance of which was particularly shown for depressive-like behavior (**Article 2**: Tuma et al., 2015) or visual ability (Brown and Wong, 2007). Nevertheless, we have shown that genetic background can modify manifestations of the *Grid2*^{Lc} mutation in *Lurcher* mice (**Article 4**: Cendelin et al., 2014). However, the final phenotype seems to be a product of the superposition of the strain and *Grid2*^{Lc} mutation effect (**Article 4**: Cendelin et al., 2014).

Poor spatial performance is a strong phenotypic manifestation of particular mutations in *Lurcher* and *pcd* mice. Nevertheless, not only genetic background but also sex differences seem to slightly modulate the behavioral performance of these mice (**Article 2**: Tuma et al., 2015). Sex dimorphism as a function of brain structures related to both behavioral processes and motor control has been described (Arvidsson et al., 2014), and significant sex differences have even been reported in neurological

manifestations of mutations in mice (Walton et al., 2012; Truong et al., 2013). We have found that *pcd* females show a distinct behavioral response to stress in the forced swimming test compared with *pcd* males (**Article 2**: Tuma et al., 2015). Therefore, the sex factor should also be taken into account in the analysis of spatial behavior of cerebellar mutants.

4.2 Other behavioral abnormalities

Cerebellar mutant mice are known to have a wide spectrum of behavioral abnormalities (for reviews see: Lalonde and Strazielle, 2007; Porras-Garcia et al., 2013; Cendelin, 2014). We have shown that abnormal emotional processing and/or motor deficit could also lead to a higher incidence of maternal infanticide in *Lurcher* dams (**Article 1**: Tuma et al., 2013). Although some cerebellar mutants display poor maternal behavior or a complete inability to rear offspring, e.g. *pcd* (Mullen et al., 1976), *staggerer* (Guastavino, 1984), *reeler* (Guastavino et al., 1993), and *nervous* mice (Sidman and Green, 1970), maternal aggression towards own offspring in *Mus musculus* has been described as rare (McCarthy and vom Saal, 1985; for review see Weber and Olsson, 2008). Nevertheless, it has been reported that maternal cannibalism in mouse dams is related to emotionality and higher susceptibility to stress (Poley, 1974; Reeb-Whitaker et al., 2001). Therefore, we have suggested that in *Lurcher* females, maternal infanticide could be potentiated by the inability to inhibit impulsive actions (**Article 1**: Tuma et al., 2013) due to their behavioral disinhibition (Hilber et al., 2004). These findings are also supported by our results from open field and forced swimming tests (**Article 2**: Tuma et al., 2015). Moreover, regarding similar studies in other cerebellar mutants, we have confirmed that cerebellar degeneration could affect a distinct type of behavior, such as maternal behavior.

Although previously published studies using other cerebellar mutants did not assume a role of motor impairments in their low breeding capability (Bulloch et al., 1982; Boufares et al., 1993), low maternal ability and pup survival rate in *Lurcher* mice could be also related to motor deficit. Strazielle and Lalonde (1998) found that *Lurcher* mice showed a decreased number and duration of several grooming components, however, serial organization of grooming did not lack its cephalocaudal sequence. It is not clear whether or not reduced grooming in *Lurcher* mice is due to

motor impairments, but it was found that electrical stimulation of the midline cerebellum initiated grooming (Berntson et al., 1973; Berntson and Paulucci, 1979; Berntson et al., 1988). On the other hand, cerebellar affection in *weaver* mutants did not lead to a reduction in their grooming behavior (Coscia and Fentress, 1993). Nevertheless, it could be speculated that reduced grooming behavior and/or lower body weight in *Lurcher* dams could lead to poor maternal behavior and consequently, a low pup survival rate.

We can also hypothesize that *Lurcher* mice show impaired social communication. It was found that Purkinje cell loss in *Lurcher* mice modulates dopamine release in the prefrontal cortex and affects higher level cognitive processes, which are commonly deficient in autism spectrum disorders (Dickson et al., 2010; Rogers et al., 2013). Therefore, it could be speculated that impaired social cognition and communication could induce inappropriate maternal behavior in *Lurcher* females and in this way, reduce their breeding capability. Moreover, the cerebellum is related to speech motor planning, production as well as language perception (see above; for review see Marien et al., 2014). Abnormal vocalization has been found in *staggerer* (Heuze et al., 1997) and *reeler* (Romano et al., 2013) cerebellar mutant mice and thus we can assume that vocalization and its perception could be also disrupted in *Lurcher* mice.

4.3 Applicability for experimental therapy

Cerebellar mouse mutants constitute a wide spectrum of experimental models for understanding not only pathogenesis and its behavioral consequences but also functional recovery. One of the suggested hopeful therapies is neurotransplantation. However, it is currently still in the mostly experimental phase (Cendelin, 2015). It was found that embryonic cerebellar cells have the potential to survive (**Article 3**: Purkartova et al., 2014; **Article 5**: Babuska et al., 2015) and develop complex anatomical patterns (Sotelo and Alvarado-Mallart, 1987b; Triarhou, 1996) when grafted into the non-neurogenic cerebellum. They are even innervated by host axons in a target-specific manner (Strata and Rossi, 1998; Rossi et al., 2002), but there is no clear evidence that such transplants can establish appropriate efferent connections with distant host targets (Rossi and Cattaneo, 2002). The main problem in

reconstituting afferent projections of corticonuclear Purkinje cells seems to be attributed to the "physicochemical barrier" of a granular cell layer that prevents axonal sprouting of Purkinje cells (Sotelo et al., 1992; Triarhou, 1996).

We have found that transplantation of embryonic cell suspension into the *Lurcher's* cerebellum led to mild improvement in ataxic gait (**Article 5**: Babuska et al., 2015). However, the behavioral benefit that is observed in treated animals could be attributed to the trophic effect of grafted immature tissue, rather than rewiring of disrupted circuits (Mattsson et al., 1997; Rossi and Cattaneo, 2002). These findings support the opinion of Rossi and Cattaneo (Rossi and Cattaneo, 2002), that neurotransplantation therapy could have some importance, but is probably not sufficient on its own, in the treatment of neurodegenerative diseases, particularly for cerebellar degeneration. The possible positive effect of cerebellar neurotransplantation depends on many factors, e.g. pathogenesis of disease, progress and extent of neurodegeneration, biochemical composition of affected tissue or graft origin. In hereditary ataxias with slow progression, such as SCA2, pharmacological therapy seems to be more efficient and gentle (Scoles et al., 2012) than the intracerebellar intervention and ethically disputed transplantation of embryonic cells.

In spite of the fact that partial functional motor recovery brought about by cerebellar transplants has been reported in *pcd* (Triarhou et al., 1995; for review see Triarhou, 1996, 1996; Zhang et al., 1996) and *Lurcher* mice (**Article 5**: Babuska et al., 2015), the effect of intracerebellar transplantation on complex behavioral functions (e.g. cognitive and emotional processing) has not yet been studied. From this point of view, neurotransplantation holds no promise to become a sufficient and primary therapy for cerebellar neurodegenerative diseases, but only an alternative or complementary strategy, which might include neuroprotective therapy, neurosurgical approaches, and physical rehabilitation (Rossi and Cattaneo, 2002).

5 CONCLUSION

We have confirmed several behavioral impairments in both *Lurcher* and *pcd* mutant mice. Nevertheless, contrary to previous studies (Goodlett et al., 1992; Lalonde and Thifault, 1994), we have found that the manifestation of spatial behavior deficit is distinct in these two cerebellar mutants. The spatial task in the Morris water maze is solved by different behavioral components (Whishaw, 1985; Whishaw and Mittleman, 1986; Whishaw, 1991), including general procedures, such as inhibiting nonadaptive behavior, procedural learning, processing of self-movement idiothetic cues, and spatial procedures based on allothetic cues (Whishaw et al., 1997; for review see Leggio et al., 1999). With regard to the role of the cerebellum in each of these processes (see above), we have shown that the distinct pathogenesis of cerebellar degeneration in *Lurcher* and *pcd* mice could lead to differential solving of spatial tasks. Based on our findings, we proposed that the deficit of spatial performance in cerebellar mutants may potentially arise from a combination of 1) cognitive disturbances, 2) sensory deficits, 3) motor impairments, and finally, 4) affective disorder (**Article 2**: Tuma et al., 2015). Moreover, the resulting spatial behavior could be also modified by the specific effect of mutation, genetic background, and sex (**Article 2**: Tuma et al., 2015; **Article 4**: Cendelin et al., 2014). All of these four partial processes are integrated in the cerebellum and therefore, it is very hard to distinguish between them in the all-embracing Morris water maze task during the analysis of spatial behavior in cerebellar mutants.

Nevertheless, based on our findings, we suggest that an inability to solve the Morris water task arises in both *Lurcher* as well as *pcd* mice from a disturbed and aimless behavior, though different in nature (**Article 2**: Tuma et al., 2015). We have shown that *Lurcher* mutants are able to reach the visible platform and remember its position for several days (**Article 2**: Tuma et al., 2015). Therefore, we suppose that motor disability and cognitive deficit play only partial roles in spatial disturbance in these animals. On the other hand, *pcd* mice suffer from wide spectrum of extracerebellar brain damage (see above) and therefore, their spatial behavior could reflect more functional disturbances.

We have also shown that cerebellar degeneration in *Lurcher* mice could affect other distinct behavioral attributes, such as maternal behavior, and could lead to decreased breeding capability in *Lurcher* females. We have hypothesized that increased maternal infanticide and a low pup survival rate in *Lurcher* mice could arise not only from their motor disabilities or lower body weight of dams but also from their affective disturbances (**Article 1**: Tuma et al., 2013).

Although we have shown that an embryonic cerebellar graft survives well in both *Lurcher* (**Article 5**: Babuska et al., 2015) and SCA2 mice (**Article 3**: Purkartova et al., 2014), the morphology of the graft did not promise any strong specific behavioral effects. Furthermore, intracerebellar transplantation had only mild positive effects on gait parameters in *Lurcher* mice (**Article 5**: Babuska et al., 2015). From this point of view, intracerebellar transplantation does not seem to be a very effective therapy for degenerative diseases, but may serve only as an alternative or complementary strategy.

6 ANNEXES

List of articles not included in the thesis:

1. Glutamate receptor block in Lurcher mutant mice during ontogeny and its effect on hippocampal long-term potentiation

Jan Barcal, Jan Cendelin, Ivana Korelusova, Jan Tuma and Frantisek Vozeh

Prague Medical Report 2010; 111(2): 127-134

2. Evaluation of lipofuscin-like pigments as an index of lead-induced oxidative damage of the brain

Jana Patkova, Max Vojtisek, Jan Tuma, Frantisek Vozeh, Jana Knotkova, Pavlina Santorova and Jiri Wilhelm

Experimental and Toxicologic Pathology 2012; 64(1-2): 51-56

3. Near-complete adaptation of the PRiMA knockout to the lack of central acetylcholinesterase

Vladimir Farar, Franziska Mohr, Marie Legrand, Boris Lamotte d'Incamps, Jan Cendelin, Jacqueline Leroy, Marc Abitbol, Veronique Bernard, Frederic Baud, Vincent Fournet, Pascal Houze, Jochen Klein, Benoit Plaud, Jan Tuma, Martina Zimmermann, Philippe Ascher, Anna Hrabovska, Jaromir Myslivecek and Eric Krejci

Journal of Neurochemistry 2012; 122: 1065-1080

4. Intra-observer error of mouse long bone cross section digitalization

Alena Jindrova, Jan Tuma and Vladimir Sladek

Folia Zoologica 2012; 61(3-4): 340-349

7 REFERENCES

Abele M, Burk K, Schols L, Schwartz S, Besenthal I, Dichgans J, Zuhlke C, Riess O, Klockgether T (2002) The aetiology of sporadic adult-onset ataxia. *Brain* 125:961-968.

Abrahams S, Pickering A, Polkey CE, Morris RG (1997) Spatial memory deficits in patients with unilateral damage to the right hippocampal formation. *Neuropsychologia* 35:11-24.

Aggleton JP, Brown MW (1999) Episodic memory, amnesia, and the hippocampal-anterior thalamic axis. *Behav Brain Sci* 22:425-444; discussion 444-489.

Aguiar J, Fernandez J, Aguilar A, Mendoza Y, Vazquez M, Suarez J, Berlanga J, Cruz S, Guillen G, Herrera L, Velazquez L, Santos N, Merino N (2006) Ubiquitous expression of human SCA2 gene under the regulation of the SCA2 self promoter cause specific Purkinje cell degeneration in transgenic mice. *Neurosci Lett* 392:202-206.

Albus JS (1971) A theory of cerebellar function. *Math Biosci* 10:25-61.

Anand BK, Malhotra CL, Singh B, Dua S (1959) Cerebellar projections to limbic system. *J Neurophysiol* 22:451-457.

Anderson MI, Hayman R, Chakraborty S, Jeffery KJ (2003) The representation of spatial context. In: *The Neurobiology of Spatial Behaviour* (Jeffery, K. J., ed), p 316 Oxford: Oxford University Press, USA.

Andreasen NC, O'Leary DS, Paradiso S, Cizadlo T, Arndt S, Watkins GL, Ponto LL, Hichwa RD (1999) The cerebellum plays a role in conscious episodic memory retrieval. *Hum Brain Mapp* 8:226-234.

Andrezik JA, Dormer KJ, Foreman RD, Person RJ (1984) Fastigial nucleus projections to the brain stem in beagles: pathways for autonomic regulation. *Neuroscience* 11:497-507.

Angelaki DE, Hess BJ (2005) Self-motion-induced eye movements: effects on visual acuity and navigation. *Nat Rev Neurosci* 6:966-976.

Angelaki DE, McHenry MQ, Dickman JD, Newlands SD, Hess BJ (1999) Computation of inertial motion: neural strategies to resolve ambiguous otolith information. *J Neurosci* 19:316-327.

Anglade P, Vyas S, Javoy-Agid F, Herrero MT, Michel PP, Marquez J, Mouatt-Prigent A, Ruberg M, Hirsch EC, Agid Y (1997) Apoptosis and autophagy in nigral neurons of patients with Parkinson's disease. *Histol Histopathol* 12:25-31.

Annoni JM, Ptak R, Caldara-Schnetzer AS, Khateb A, Pollermann BZ (2003) Decoupling of autonomic and cognitive emotional reactions after cerebellar stroke. *Ann Neurol* 53:654-658.

Appollonio IM, Grafman J, Schwartz V, Massaquoi S, Hallett M (1993) Memory in patients with cerebellar degeneration. *Neurology* 43:1536-1544.

Araki K, Meguro H, Kushiya E, Takayama C, Inoue Y, Mishina M (1993) Selective expression of the glutamate receptor channel delta 2 subunit in cerebellar Purkinje cells. *Biochem Biophys Res Commun* 197:1267-1276.

Armstrong CL, Duffin CA, McFarland R, Vogel MW (2011) Mechanisms of compartmental purkinje cell death and survival in the lurcher mutant mouse. *Cerebellum* 10:504-514.

Arvidsson E, Viereckel T, Mikulovic S, Wallen-Mackenzie A (2014) Age- and sex-dependence of dopamine release and capacity for recovery identified in the dorsal striatum of C57/Bl6J mice. *PLoS One* 9:e99592.

Babuska V, Houdek Z, Tuma J, Purkartova Z, Tumova J, Kralickova M, Vozeh F, Cendelin J (2015) Transplantation of Embryonic Cerebellar Grafts Improves Gait Parameters in Ataxic Lurcher Mice. *Cerebellum* 14:632-641.

Bagnall M, du Lac S, Mauk M (2012) Cerebellum. In: *Fundamental Neuroscience* (Squire, L. et al., eds), p 1152 New York: Academic Press.

Baillieux H, De Smet HJ, Paquier PF, De Deyn PP, Marien P (2008) Cerebellar neurocognition: insights into the bottom of the brain. *Clin Neurol Neurosurg* 110:763-773.

Baltanas FC, Berciano MT, Valero J, Gomez C, Diaz D, Alonso JR, Lafarga M, Weruaga E (2013) Differential glial activation during the degeneration of Purkinje cells and mitral cells in the PCD mutant mice. *Glia* 61:254-272.

Baltanas FC, Casafont I, Lafarga V, Weruaga E, Alonso JR, Berciano MT, Lafarga M (2011) Purkinje cell degeneration in pcd mice reveals large scale chromatin reorganization and gene silencing linked to defective DNA repair. *J Biol Chem* 286:28287-28302.

Bares M, Lungu O, Liu T, Waechter T, Gomez CM, Ashe J (2007) Impaired predictive motor timing in patients with cerebellar disorders. *Exp Brain Res* 180:355-365.

Barmack NH (2003) Central vestibular system: vestibular nuclei and posterior cerebellum. *Brain Res Bull* 60:511-541.

Barmack NH, Yakhnitsa V (2008) Functions of interneurons in mouse cerebellum. *J Neurosci* 28:1140-1152.

Barski JJ, Hartmann J, Rose CR, Hoebeek F, Morl K, Noll-Hussong M, De Zeeuw CI, Konnerth A, Meyer M (2003) Calbindin in cerebellar Purkinje cells is a critical determinant of the precision of motor coordination. *J Neurosci* 23:3469-3477.

Bastian AJ, Martin TA, Keating JG, Thach WT (1996) Cerebellar ataxia: abnormal control of interaction torques across multiple joints. *J Neurophysiol* 76:492-509.

Bastian AJ, Zackowski KM, Thach WT (2000) Cerebellar ataxia: torque deficiency or torque mismatch between joints? *J Neurophysiol* 83:3019-3030.

Baumann O, Borra RJ, Bower JM, Cullen KE, Habas C, Ivry RB, Leggio M, Mattingley JB, Molinari M, Moulton EA, Paulin MG, Pavlova MA, Schmahmann JD, Sokolov AA (2015) Consensus paper: the role of the cerebellum in perceptual processes. *Cerebellum* 14:197-220.

Baurle J, Grusser-Cornehls U (1994) Axonal torpedoes in cerebellar Purkinje cells of two normal mouse strains during aging. *Acta Neuropathol* 88:237-245.

Bell CC (2002) Evolution of cerebellum-like structures. *Brain Behav Evol* 59:312-326.

Belzung C, Chapillon P, Lalonde R (2001) The effects of the lurcher mutation on object localization, T-maze discrimination, and radial arm maze tasks. *Behav Genet* 31:151-155.

Ben-Arie N, Bellen HJ, Armstrong DL, McCall AE, Gordadze PR, Guo Q, Matzuk MM, Zoghbi HY (1997) Math1 is essential for genesis of cerebellar granule neurons. *Nature* 390:169-172.

Benhamou S, Sauve J-P, Bovet P (1990) Spatial memory in large scale movements: Efficiency and limitation of the egocentric coding process. *J Theor Biol* 145:1-12.

Berezniuk I, Sironi J, Callaway MB, Castro LM, Hirata IY, Ferro ES, Fricker LD (2010) CCP1/Nna1 functions in protein turnover in mouse brain: Implications for cell death in Purkinje cell degeneration mice. *FASEB J* 24:1813-1823.

Berezniuk I, Sironi JJ, Wardman J, Pasek RC, Berbari NF, Yoder BK, Fricker LD (2013) Quantitative peptidomics of Purkinje cell degeneration mice. *PLoS One* 8:e60981.

Berezniuk I, Vu HT, Lyons PJ, Sironi JJ, Xiao H, Burd B, Setou M, Angeletti RH, Ikegami K, Fricker LD (2012) Cytosolic carboxypeptidase 1 is involved in processing alpha- and beta-tubulin. *J Biol Chem* 287:6503-6517.

Berntson GG, Jang JF, Ronca AE (1988) Brainstem systems and grooming behaviors. *Ann N Y Acad Sci* 525:350-362.

Berntson GG, Paulucci TS (1979) Fastigial modulation of brainstem behavioral mechanisms. *Brain Res Bull* 4:549-552.

Berntson GG, Potolicchio SJ, Jr., Miller NE (1973) Evidence for higher functions of the cerebellum: eating and grooming elicited by cerebellar stimulation in cats. *Proc Natl Acad Sci U S A* 70:2497-2499.

Bidaud I, Mezghrani A, Swayne LA, Monteil A, Lory P (2006) Voltage-gated calcium channels in genetic diseases. *Biochim Biophys Acta* 1763:1169-1174.

Blanks JC, Mullen RJ, LaVail MM (1982a) Retinal degeneration in the pcd cerebellar mutant mouse. II. Electron microscopic analysis. *J Comp Neurol* 212:231-246.

Blanks JC, Mullen RJ, LaVail MM (1982b) Retinal degeneration in the pcd cerebellar mutant mouse. II. Electron microscopic analysis. *J Comp Neurol* 212:231-246.

Blanks JC, Spee C (1992) Retinal degeneration in the pcd/pcd mutant mouse: accumulation of spherules in the interphotoreceptor space. *Exp Eye Res* 54:637-644.

Bliss TV, Collingridge GL (1993) A synaptic model of memory: long-term potentiation in the hippocampus. *Nature* 361:31-39.

Bodranghien F, Bastian A, Casali C, Hallett M, Louis ED, Manto M, Marien P, Nowak DA, Schmahmann JD, Serrao M, Steiner KM, Strupp M, Tilikete C, Timmann D, van Dun K (2015) Consensus Paper: Revisiting the Symptoms and Signs of Cerebellar Syndrome. *Cerebellum*.

Boufares S, Guastavino JM, Larsson K (1993) Restoration of staggerer mouse maternal behavior following long-term breeding selection. *Physiol Behav* 53:1151-1155.

Bourgeois JA, Cogswell JB, Hessl D, Zhang L, Ono MY, Tassone F, Farzin F, Brunberg JA, Grigsby J, Hagerman RJ (2007) Cognitive, anxiety and mood disorders in the fragile X-associated tremor/ataxia syndrome. *Gen Hosp Psychiatry* 29:349-356.

Bourgeois JA, Seritan AL, Casillas EM, Hessl D, Schneider A, Yang Y, Kaur I, Cogswell JB, Nguyen DV, Hagerman RJ (2011) Lifetime prevalence of mood and anxiety disorders in fragile X premutation carriers. *J Clin Psychiatry* 72:175-182.

Bower JM (1997) Control of sensory data acqusition. In: *The Cerebellum and Cognition*, vol. 41 (Schmahmann, J. D., ed), pp 489-513 San Diego: Academic.

Brochu G, Maler L, Hawkes R (1990) Zebrin II: a polypeptide antigen expressed selectively by Purkinje cells reveals compartments in rat and fish cerebellum. *J Comp Neurol* 291:538-552.

Brooks JX, Cullen KE (2009) Multimodal integration in rostral fastigial nucleus provides an estimate of body movement. *J Neurosci* 29:10499-10511.

Brown KL, Agelan A, Woodruff-Pak DS (2010) Unimpaired trace classical eyeblink conditioning in Purkinje cell degeneration (pcd) mutant mice. *Neurobiol Learn Mem* 93:303-311.

Brown RE, Wong AA (2007) The influence of visual ability on learning and memory performance in 13 strains of mice. *Learn Mem* 14:134-144.

Brusse E, Maat-Kievit JA, van Swieten JC (2007) Diagnosis and management of early- and late-onset cerebellar ataxia. *Clin Genet* 71:12-24.

Buckner RL (2013) The cerebellum and cognitive function: 25 years of insight from anatomy and neuroimaging. *Neuron* 80:807-815.

Bulloch K, Hamburger RN, Loy R (1982) Nest-building behavior in two cerebellar mutant mice: staggerer and weaver. *Behav Neural Biol* 36:94-97.

Burguiere E, Arleo A, Hojjati M, Elgersma Y, De Zeeuw CI, Berthoz A, Rondi-Reig L (2005) Spatial navigation impairment in mice lacking cerebellar LTD: a motor adaptation deficit? *Nat Neurosci* 8:1292-1294.

Butts T, Wilson L, Wingate RJ (2007) Specification of granule cells and Purkinje cells. In: *Handbook of the Cerebellum and Cerebellar Disorders* (Manto, M. et al., eds), pp 1499-1520 New York: Springer Verlag.

Caddy KW, Biscoe TJ (1975) Preliminary observations on the cerebllum in the mutant mouse Lurcher. *Brain Res* 91:276-280.

Caddy KW, Biscoe TJ (1979) Structural and quantitative studies on the normal C3H and Lurcher mutant mouse. *Phil Trans R Soc B* 287:167-201.

Caddy KW, Biscow TJ (1976) The number of Purkinje cells and olive neurones in the normal and Lurcher mutant mouse. *Brain Res* 111:396-398.

Carrascosa C, Torres-Aleman I, Lopez-Lopez C, Carro E, Espejo L, Torrado S, Torrado JJ (2004) Microspheres containing insulin-like growth factor I for treatment of chronic neurodegeneration. *Biomaterials* 25:707-714.

Cartelli D, Ronchi C, Maggioni MG, Rodighiero S, Giavini E, Cappelletti G (2010) Microtubule dysfunction precedes transport impairment and mitochondria damage in MPP+ -induced neurodegeneration. *J Neurochem* 115:247-258.

Caston J, Chianale C, Delhaye-Bouchaud N, Mariani J (1998) Role of the cerebellum in exploration behavior. *Brain Res* 808:232-237.

Cataldo AM, Hamilton DJ, Barnett JL, Paskevich PA, Nixon RA (1996) Properties of the endosomal-lysosomal system in the human central nervous system:

disturbances mark most neurons in populations at risk to degenerate in Alzheimer's disease. *J Neurosci* 16:186-199.

Cendelin J (2014) From mice to men: lessons from mutant ataxic mice. *Cerebellum & Ataxias* 1:4.

Cendelin J (2015) Transplantation and Stem Cell Therapy for Cerebellar Degenerations. *Cerebellum*.

Cendelin J, Babuska V, Korelusova I, Houdek Z, Vozeh F (2012) Long-term survival of solid embryonic cerebellar grafts in Lurcher mice. *Neurosci Lett* 515:23-27.

Cendelin J, Korelusova I, Vozeh F (2008) The effect of repeated rotarod training on motor skills and spatial learning ability in Lurcher mutant mice. *Behav Brain Res* 189:65-74.

Cendelin J, Korelusova I, Vozeh F (2009a) The effect of cerebellar transplantation and enforced physical activity on motor skills and spatial learning in adult Lurcher mutant mice. *Cerebellum* 8:35-45.

Cendelin J, Korelusova I, Vozeh F (2009b) A preliminary study of solid embryonic cerebellar graft survival in adult B6CBA Lurcher mutant and wild type mice. *Anat Rec* 292:1986-1992.

Cendelin J, Tuma J, Korelusova I, Vozeh F (2014) The effect of genetic background on behavioral manifestation of Grid2(Lc) mutation. *Behav Brain Res* 271:218-227.

Cendelin J, Voller J, Vozeh F (2010) Ataxic gait analysis in a mouse model of the olivocerebellar degeneration. *Behav Brain Res* 210:8-15.

Cendelin J, Vozeh F (2007) Lurcher mouse. In: *Handbook of the Cerebellum and Cerebellar Disorders* (Manto, M. et al., eds), pp 1499-1520 New York: Springer Verlag.

Cerminara NL, Aoki H, Loft M, Sugihara I, Apps R (2013) Structural basis of cerebellar microcircuits in the rat. *J Neurosci* 33:16427-16442.

Ciosk R, DePalma M, Priess JR (2004) ATX-2, the C. elegans ortholog of ataxin 2, functions in translational regulation in the germline. *Development* 131:4831-4841.

Collett M, Chittka L, Collett TS (2013) Spatial memory in insect navigation. *Curr Biol* 23:R789-800.

Consalez GG, Florio M, Massimino L, Croci L (2007) Proneural genes and cerebellar neurogenesis in ventricular zone abd upper rhombic lip. In: *Handbook of the Cerebellum and Cerebellar Disorders* (Manto, M. et al., eds), pp 1499-1520 New York: Springer Verlag.

Corrales JD, Blaess S, Mahoney EM, Joyner AL (2006) The level of sonic hedgehog signaling regulates the complexity of cerebellar foliation. *Development* 133:1811-1821.

Corrales JD, Rocco GL, Blaess S, Guo Q, Joyner AL (2004) Spatial pattern of sonic hedgehog signaling through Gli genes during cerebellum development. *Development* 131:5581-5590.

Coscia EM, Fentress JC (1993) Neurological dysfunction expressed in the grooming behavior of developing weaver mutant mice. *Behav Genet* 23:533-541.

Coutelier M, Burglen L, Mundwiller E, Abada-Bendib M, Rodriguez D, Chantot-Bastaraud S, Rougeot C, Cournelle MA, Milh M, Toutain A, Bacq D, Meyer V, Afenjar A, Deleuze JF, Brice A, Heron D, Stevanin G, Durr A (2015) GRID2 mutations span from congenital to mild adult-onset cerebellar ataxia. *Neurology* 84:1751-1759.

Crook J, Hendrickson A, Robinson FR (2006) Co-localization of glycine and gaba immunoreactivity in interneurons in Macaca monkey cerebellar cortex. *Neuroscience* 141:1951-1959.

D'Hooge R, De Deyn PP (2001) Applications of the Morris water maze in the study of learning and memory. *Brain Res Rev* 36:60-90.

Dahmane N, Ruiz i Altaba A (1999) Sonic hedgehog regulates the growth and patterning of the cerebellum. *Development* 126:3089-3100.

Damrath E, Heck MV, Gispert S, Azizov M, Nowock J, Seifried C, Rub U, Walter M, Auburger G (2012) ATXN2-CAG42 sequesters PABPC1 into insolubility and induces FBXW8 in cerebellum of old ataxic knock-in mice. *PLoS Genet* 8:e1002920.

Dansithong W, Paul S, Figueroa KP, Rinehart MD, Wiest S, Pflieger LT, Scoles DR, Pulst SM (2015) Ataxin-2 regulates RGS8 translation in a new BAC-SCA2 transgenic mouse model. *PLoS Genet* 11:e1005182.

De Jager PL, Zuo J, Cook SA, Heintz N (1997) A new allele of the lurcher gene, lurcherJ. *Mamm Genome* 8:647-650.

De Smet HJ, Baillieux H, Catsman-Berrevoets C, De Deyn PP, Marien P, Paquier PF (2007) Postoperative motor speech production in children with the syndrome of 'cerebellar' mutism and subsequent dysarthria: a critical review of the literature. *Eur J Paediatr Neurol* 11:193-207.

De Smet HJ, Marien P (2012) Posterior fossa syndrome in an adult patient following surgical evacuation of an intracerebellar haematoma. *Cerebellum* 11:587-592.

De Zeeuw CI, Hansel C, Bian F, Koekkoek SK, van Alphen AM, Linden DJ, Oberdick J (1998) Expression of a protein kinase C inhibitor in Purkinje cells blocks cerebellar LTD and adaptation of the vestibulo-ocular reflex. *Neuron* 20:495-508.

De Zeeuw CI, Yeo CH (2005) Time and tide in cerebellar memory formation. *Curr Opin Neurobiol* 15:667-674.

Delgado-Garcia JM, Gruart A (2002) The role of interpositus nucleus in eyelid conditioned responses. *Cerebellum* 1:289-308.

Dempesy CW, Tootle DM, Fontana CJ, Fitzjarrell AT, Garey RE, Heath RG (1983) Stimulation of the paleocerebellar cortex of the cat: increased rate of synthesis and release of catecholamines at limbic sites. *Biol Psychiatry* 18:127-132.

Di Donato S (1998) The complex clinical and genetic classification of inherited ataxias. I. Dominant ataxias. *Ital J Neurol Sci* 19:335-343.

Di Donato S, Gellera C, Mariotti C (2001) The complex clinical and genetic classification of inherited ataxias. II. Autosomal recessive ataxias. *Neurol Sci* 22:219-228.

Diaz D, Lepousez G, Gheusi G, Alonso JR, Lledo PM, Weruaga E (2012) Bone marrow cell transplantation restores olfaction in the degenerated olfactory bulb. *J Neurosci* 32:9053-9058.

Dickson PE, Rogers TD, Del Mar N, Martin LA, Heck D, Blaha CD, Goldowitz D, Mittleman G (2010) Behavioral flexibility in a mouse model of developmental cerebellar Purkinje cell loss. *Neurobiol Learn Mem* 94:220-228.

Dieudonne S, Dumoulin A (2000) Serotonin-driven long-range inhibitory connections in the cerebellar cortex. *J Neurosci* 20:1837-1848.

Doulazmi M, Hadj-Sahraoui N, Frederic F, Mariani J (2002) Diminishing Purkinje cell populations in the cerebella of aging heterozygous Purkinje cell degeneration but not heterozygous nervous mice. *J Neurogenet* 16:111-123.

Drepper J, Timmann D, Kolb FP, Diener HC (1999) Non-motor associative learning in patients with isolated degenerative cerebellar disease. *Brain* 122 (Pt 1):87-97.

Duffin CA, McFarland R, Sarna JR, Vogel MW, Armstrong CL (2010) Heat shock protein 25 expression and preferential Purkinje cell survival in the lurcher mutant mouse cerebellum. *J Comp Neurol* 518:1892-1907.

Dugue GP, Dumoulin A, Triller A, Dieudonne S (2005) Target-dependent use of co-released inhibitory transmitters at central synapses. *J Neurosci* 25:6490-6498.

Dum RP, Strick PL (2003) An unfolded map of the cerebellar dentate nucleus and its projections to the cerebral cortex. *J Neurophysiol* 89:634-639.

Dumesnil-Bousez N, Sotelo C (1992) Early development of the Lurcher cerebellum: Purkinje cell alterations and impairment of synaptogenesis. *J Neurocytol* 21:506-529.

Dumesnil-Bousez N, Sotelo C (1993) Partial reconstruction of the adult Lurcher cerebellar circuitry by neural grafting. *Neuroscience* 55:1-21.

Dusart I, Guenet JL, Sotelo C (2006) Purkinje cell death: differences between developmental cell death and neurodegenerative death in mutant mice. *Cerebellum* 5:163-173.

Ebner TJ (2007) Cerebellum and internal models. In: *Handbook of the Cerebellum and Cerebellar Disorders* (Manto, M. et al., eds), pp 1499-1520 New York: Springer Verlag.

Ebner TJ, Hewitt AL, Popa LS (2011) What features of limb movements are encoded in the discharge of cerebellar neurons? *Cerebellum* 10:683-693.

Ekerot CF, Garwicz M, Schouenborg J (1991) Topography and nociceptive receptive fields of climbing fibres projecting to the cerebellar anterior lobe in the cat. *J Physiol* 441:257-274.

Elden AC, Kim HJ, Hart MP, Chen-Plotkin AS, Johnson BS, Fang X, Armakola M, Geser F, Greene R, Lu MM, Padmanabhan A, Clay-Falcone D, McCluskey L, Elman L, Juhr D, Gruber PJ, Rub U, Auburger G, Trojanowski JQ, Lee VM, Van Deerlin VM, Bonini NM, Gitler AD (2010) Ataxin-2 intermediate-length polyglutamine expansions are associated with increased risk for ALS. *Nature* 466:1069-1075.

Etienne AS, Jeffery KJ (2004) Path integration in mammals. *Hippocampus* 14:180-192.

Etienne AS, Maurer R, Saucy F (1988) Limitations in the assessment of path dependent information. *Behaviour* 106:81-111.

Felix R (2000) Channelopathies: ion channel defects linked to heritable clinical disorders. *J Med Genet* 37:729-740.

Fernandez-Gonzalez A, La Spada AR, Treadaway J, Higdon JC, Harris BS, Sidman RL, Morgan JI, Zuo J (2002) Purkinje cell degeneration (pcd) phenotypes caused by mutations in the axotomy-induced gene, Nna1. *Science* 295:1904-1906.

Filla A, De Michele G (2012) Overview of autosomal recessive ataxias. In: *Ataxic Disorders* (Subramony, S. H. and Dürr, A., eds), pp 265-274 London: Elsevier B.V.

Fliessbach K, Trautner P, Quesada CM, Elger CE, Weber B (2007) Cerebellar contributions to episodic memory encoding as revealed by fMRI. *Neuroimage* 35:1330-1337.

Fortier PA, Smith AM, Rossignol S (1987) Locomotor deficits in the mutant mouse, Lurcher. *Exp Brain Res* 66:271-286.

Frederic F, Chautard T, Brochard R, Chianale C, Wollman E, Oliver C, Delhaye-Bouchaud N, Mariani J (1997) Enhanced endocrine response to novel environment stress and endotoxin in Lurcher mutant mice. *Neuroendocrinology* 66:341-347.

Frysinger RC, Bourbonnais D, Kalaska JF, Smith AM (1984) Cerebellar cortical activity during antagonist cocontraction and reciprocal inhibition of forearm muscles. *J Neurophysiol* 51:32-49.

Fujii T, Okuda J, Tsukiura T, Ohtake H, Suzuki M, Kawashima R, Itoh M, Fukuda H, Yamadori A (2002a) Encoding-related brain activity during deep processing of verbal materials: a PET study. *Neurosci Res* 44:429-438.

Fujii T, Okuda J, Tsukiura T, Ohtake H, Suzuki M, Yamadori A (2002b) Episodic memory encoding and the medial temporal lobe. In: *Frontiers in Human Memory* (Yamadori, A. et al., eds), pp 253-262 Sendai: Tohoku University Press.

Fujii T, Suzuki M, Okuda J, Ohtake H, Tanji K, Yamaguchi K, Itoh M, Yamadori A (2004) Neural correlates of context memory with real-world events. *Neuroimage* 21:1596-1603.

Gallistel CR (1990) The organization of learning. Cambridge, MA: Bradford Books/MIT Press.

Garwicz M, Ekerot CF, Jorntell H (1998) Organizational Principles of Cerebellar Neuronal Circuitry. *News Physiol Sci* 13:26-32.

Ghetti B, Norton J, Triarhou LC (1987) Nerve cell atrophy and loss in the inferior olivary complex of "Purkinje cell degeneration" mutant mice. *J Comp Neurol* 260:409-422.

Glickstein M, Doron K (2008) Cerebellum: connections and functions. *Cerebellum* 7:589-594.

Glickstein M, Strata P, Voogd J (2009) Cerebellum: history. *Neuroscience* 162:549-559.

Goodlett CR, Hamre KM, West JR (1992) Dissociation of spatial navigation and visual guidance performance in Purkinje cell degeneration (pcd) mutant mice. *Behav Brain Res* 47:129-141.

Gottwald B, Wilde B, Mihajlovic Z, Mehdorn HM (2004) Evidence for distinct cognitive deficits after focal cerebellar lesions. *J Neurol Neurosurg Psychiatry* 75:1524-1531.

Green AM, Angelaki DE (2004) An integrative neural network for detecting inertial motion and head orientation. *J Neurophysiol* 92:905-925.

Greer CA, Shepherd GM (1982) Mitral cell degeneration and sensory function in the neurological mutant mouse Purkinje cell degeneration (PCD). *Brain Res* 235:156-161.

Gruart A, Pastor AM, Armengol JA, Delgado-Garcia JM (1997) Involvement of cerebellar cortex and nuclei in the genesis and control of unconditioned and conditioned eyelid motor responses. *Prog Brain Res* 114:511-528.

Guastavino JM (1984) Environmental features determining successful rearing in the mutant mouse staggerer. *Physiol Behav* 32:225-228.

Guastavino JM, Larsson K, Allain C, Jaisson P (1993) Neonatal vestibular stimulation and mating in cerebellar mutants. *Behav Genet* 23:265-269.

Habas C, Kamdar N, Nguyen D, Prater K, Beckmann CF, Menon V, Greicius MD (2009) Distinct cerebellar contributions to intrinsic connectivity networks. *J Neurosci* 29:8586-8594.

Haines DE, Dietrichs E (1984) An HRP study of hypothalamo-cerebellar and cerebello-hypothalamic connections in squirrel monkey (Saimiri sciureus). *J Comp Neurol* 229:559-575.

Hall CS (1934) Emotional behavior in the rat: Defecation and urination as measures of individual differences in emotionality. *J Comp Psychol* 18:385-403.

Hall CS, Ballachey EL (1932) A study of the rat's behavior in a field: a contribution to method in comparative psychology. *University of California Publications in Psychology* 6:1-12.

Hall DA, Birch RC, Anheim M, Jonch AE, Pintado E, O'Keefe J, Trollor JN, Stebbins GT, Hagerman RJ, Fahn S, Berry-Kravis E, Leehey MA (2014) Emerging topics in FXTAS. *J Neurodev Disord* 6:31.

Handel MA, Lane PW, Schroeder AC, Davisson MT (1988) New mutation causing sterility in the mouse. *Gamete Res* 21:409-423.

Hansen ST, Meera P, Otis TS, Pulst SM (2013) Changes in Purkinje cell firing and gene expression precede behavioral pathology in a mouse model of SCA2. *Hum Mol Genet* 22:271-283.

Harding AE (1993) Clinical features and classification of inherited ataxias. In: *Inherited ataxias*, vol. 61 (Harding, A. E. and Deufel, T., eds), pp 1-14 New York: Raven.

Harper JW, Heath RG (1973) Anatomic connections of the fastigial nucleus to the rostral forebrain in the cat. *Exp Neurol* 39:285-292.

Harris A, Morgan JI, Pecot M, Soumare A, Osborne A, Soares HD (2000) Regenerating motor neurons express Nna1, a novel ATP/GTP-binding protein related to zinc carboxypeptidases. *Mol Cell Neurosci* 16:578-596.

Hartley T, King JA, Burgess N (2003) Studies of the neural basis of human navigation and memory. In: *The Neurobiology of Spatial Behaviour* (Jeffery, K. J., ed), p 316 Oxford: Oxford University Press, USA.

Hartmann N, Martrette JM, Westphal A (2001) Influence of the Lurcher mutation on myosin heavy chain expression in skeletal and cardiac muscles. *J Cell Biochem Suppl* Suppl 36:222-231.

Hashimoto K, Kano M (2013) Synapse elimination in the developing cerebellum. *Cell Mol Life Sci* 70:4667-4680.

Heath RG (1973) Fastigial nucleus connections to the septal region in monkey and cat: a demonstration with evoked potentials of a bilateral pathway. *Biol Psychiatry* 6:193-196.

Heckroth JA (1994a) Quantitative morphological analysis of the cerebellar nuclei in normal and lurcher mutant mice. I. Morphology and cell number. *J Comp Neurol* 343:173-182.

Heckroth JA (1994b) A quantitative morphological analysis of the cerebellar nuclei in normal and lurcher mutant mice. II. Volumetric changes in cytological components. *J Comp Neurol* 343:183-192.

Heckroth JA, Goldowitz D, Eisenman LM (1990) Olivocerebellar fiber maturation in normal and lurcher mutant mice: defective development in lurcher. *J Comp Neurol* 291:415-430.

Heckroth JA, Hobart NJ, Summers D (1998) Transplanted neurons alter the course of neurodegenerative disease in Lurcher mutant mice. *Exp Neurol* 154:336-352.

Heiney SA, Wohl MP, Chettih SN, Ruffolo LI, Medina JF (2014) Cerebellar-dependent expression of motor learning during eyeblink conditioning in head-fixed mice. *J Neurosci* 34:14845-14853.

Hervieu G (2003) Melanin-concentrating hormone functions in the nervous system: food intake and stress. *Expert Opin Ther Targets* 7:495-511.

Heuze P, Feron C, Baudoin C (1997) Early behavioral development of mice is affected by staggerer mutation as soon as postnatal day three. *Dev Brain Res* 101:81-84.

Hilber P, Caston J (2001) Motor skills and motor learning in Lurcher mutant mice during aging. *Neuroscience* 102:615-623.

Hilber P, Jouen F, Delhaye-Bouchaud N, Mariani J, Caston J (1998) Differential roles of cerebellar cortex and deep cerebellar nuclei in learning and retention of a spatial task: studies in intact and cerebellectomized lurcher mutant mice. *Behav Genet* 28:299-308.

Hilber P, Lalonde R, Caston J (1999) An unsteady platform test for measuring static equilibrium in mice. *J Neurosci Methods* 88:201-205.

Hilber P, Lorivel T, Delarue C, Caston J (2004) Stress and anxious-related behaviors in Lurcher mutant mice. *Brain Res* 1003:108-112.

Hills LB, Masri A, Konno K, Kakegawa W, Lam AT, Lim-Melia E, Chandy N, Hill RS, Partlow JN, Al-Saffar M, Nasir R, Stoler JM, Barkovich AJ, Watanabe M, Yuzaki M, Mochida GH (2013) Deletions in GRID2 lead to a recessive syndrome of cerebellar ataxia and tonic upgaze in humans. *Neurology* 81:1378-1386.

Hirano T (2014) Around LTD hypothesis in motor learning. *Cerebellum* 13:645-650.

Hoffmann LC, Berry SD (2009) Cerebellar theta oscillations are synchronized during hippocampal theta-contingent trace conditioning. *Proc Natl Acad Sci U S A* 106:21371-21376.

Holmes G (1917) The symptoms of acute cerebellar injuries due to gunshot injuries. *Brain* 40:461-535.

Holmes G (1922) Clinical symptoms of cerebellar disease and their interpretation. *Lancet* 2:59-65.

Hoshino M, Nakamura S, Mori K, Kawauchi T, Terao M, Nishimura YV, Fukuda A, Fuse T, Matsuo N, Sone M, Watanabe M, Bito H, Terashima T, Wright CV, Kawaguchi Y, Nakao K, Nabeshima Y (2005) Ptf1a, a bHLH transcriptional gene, defines GABAergic neuronal fates in cerebellum. *Neuron* 47:201-213.

Houdek Z, Cendelin J, Kulda V, Babuska V, Cedikova M, Kralickova M, Pachernik J, Stefano GB, Vozeh F (2012) Intracerebellar application of P19-derived neuroprogenitor and naive stem cells to Lurcher mutant and wild type B6CBA mice. *Med Sci Monit* 18:BR174-180.

Huang C, Ricklefs RE (2007) Cerebellum and human evolution: A comparative and information theory perspective. In: *Handbook of the Cerebellum and Cerebellar Disorders* (Manto, M. et al., eds), pp 1337-1357 New York: Springer Verlag.

Huynh DP, Figueroa K, Hoang N, Pulst SM (2000) Nuclear localization or inclusion body formation of ataxin-2 are not necessary for SCA2 pathogenesis in mouse or human. *Nat Genet* 26:44-50.

Huynh DP, Scoles DR, Nguyen D, Pulst SM (2003) The autosomal recessive juvenile Parkinson disease gene product, parkin, interacts with and ubiquitinates synaptotagmin XI. *Hum Mol Genet* 12:2587-2597.

Chakrabarti L, Eng J, Ivanov N, Garden GA, La Spada AR (2009) Autophagy activation and enhanced mitophagy characterize the Purkinje cells of pcd mice prior to neuronal death. *Mol Brain* 2:24.

Chakrabarti L, Zahra R, Jackson SM, Kazemi-Esfarjani P, Sopher BL, Mason AG, Toneff T, Ryu S, Shaffer S, Kansy JW, Eng J, Merrihew G, MacCoss MJ, Murphy A, Goodlett DR, Hook V, Bennett CL, Pallanck LJ, La Spada AR (2010) Mitochondrial dysfunction in NnaD mutant flies and Purkinje cell degeneration mice reveals a role for Nna proteins in neuronal bioenergetics. *Neuron* 66:835-847.

Chang AC, Ghetti B (1993) Embryonic cerebellar graft development during acute phase of gliosis in the cerebellum of pcd mutant mice. *Chin J Physiol* 36:141-149.

Chang B, Hawes NL, Hurd RE, Davisson MT, Nusinowitz S, Heckenlively JR (2002) Retinal degeneration mutants in the mouse. *Vision Res* 42:517-525.

Chang YK, Chen MH, Chiang YH, Chen YF, Ma WH, Tseng CY, Soong BW, Ho JH, Lee OK (2011) Mesenchymal stem cell transplantation ameliorates motor function deterioration of spinocerebellar ataxia by rescuing cerebellar Purkinje cells. *J Biomed Sci* 18:54.

Chen L, Bao S, Lockard JM, Kim JK, Thompson RF (1996) Impaired classical eyeblink conditioning in cerebellar-lesioned and Purkinje cell degeneration (pcd) mutant mice. *J Neurosci* 16:2829-2838.

Chen L, Bao S, Thompson RF (1999) Bilateral lesions of the interpositus nucleus completely prevent eyeblink conditioning in Purkinje cell-degeneration mutant mice. *Behav Neurosci* 113:204-210.

Cheng SS, Heintz N (1997) Massive loss of mid- and hindbrain neurons during embryonic development of homozygous lurcher mice. *J Neurosci* 17:2400-2407.

Chizhikov VV, Lindgren AG, Currle DS, Rose MF, Monuki ES, Millen KJ (2006) The roof plate regulates cerebellar cell-type specification and proliferation. *Development* 133:2793-2804.

Ito M (1970) Neurophysiological aspects of the cerebellar motor control system. *Int J Neurol* 7:162-176.

Ito M (1982) Cerebellar control of the vestibulo-ocular reflex--around the flocculus hypothesis. *Annu Rev Neurosci* 5:275-296.

Ito M (1989) Long-term depression. *Annu Rev Neurosci* 12:85-102.

Ito M (2002) The molecular organization of cerebellar long-term depression. *Nat Rev Neurosci* 3:896-902.

Ito M (2012) The cerebellum: Brain for an implicit self. New Jersey: FT Press.

Jaarsma D, Dino MR, Ohishi H, Shigemoto R, Mugnaini E (1998) Metabotropic glutamate receptors are associated with non-synaptic appendages of unipolar brush cells in rat cerebellar cortex and cochlear nuclear complex. *J Neurocytol* 27:303-327.

Jeffery KJ (2003) Introduction. In: *The Neurobiology of Spatial Behaviour* (Jeffery, K. J., ed), p 316 Oxford: Oxford University Press, USA.

Jen JC (2008) Hereditary episodic ataxias. *Ann N Y Acad Sci* 1142:250-253.

Jen JC, Graves TD, Hess EJ, Hanna MG, Griggs RC, Baloh RW, investigators C (2007) Primary episodic ataxias: diagnosis, pathogenesis and treatment. *Brain* 130:2484-2493.

Jimenez-Diaz L, Navarro-Lopez Jde D, Gruart A, Delgado-Garcia JM (2004) Role of cerebellar interpositus nucleus in the genesis and control of reflex and conditioned eyelid responses. *J Neurosci* 24:9138-9145.

Jones J, Jaramillo-Merchan J, Bueno C, Pastor D, Viso-Leon M, Martinez S (2010) Mesenchymal stem cells rescue Purkinje cells and improve motor functions in a mouse model of cerebellar ataxia. *Neurobiol Dis* 40:415-423.

Juncos JL, Lazarus JT, Graves-Allen E, Shubeck L, Rusin M, Novak G, Hamilton D, Rohr J, Sherman SL (2011) New clinical findings in the fragile X-associated tremor ataxia syndrome (FXTAS). *Neurogenetics* 12:123-135.

Kalashnikova LA, Zueva YV, Pugacheva OV, Korsakova NK (2005) Cognitive impairments in cerebellar infarcts. *Neurosci Behav Physiol* 35:773-779.

Kanazawa I (1999) Molecular pathology of dentatorubral-pallidoluysian atrophy. *Phil Trans R Soc B* 354:1069-1074.

Kashiwabuchi N, Ikeda K, Araki K, Hirano T, Shibuki K, Takayama C, Inoue Y, Kutsuwada T, Yagi T, Kang Y, et al. (1995) Impairment of motor coordination, Purkinje cell synapse formation, and cerebellar long-term depression in GluR delta 2 mutant mice. *Cell* 81:245-252.

Kawato M (1999) Internal models for motor control and trajectory planning. *Curr Opin Neurobiol* 9:718-727.

Kawato M, Furukawa K, Suzuki R (1987) A hierarchical neural-network model for control and learning of voluntary movement. *Biol Cybern* 57:169-185.

Keele SW, Ivry R (1990) Does the cerebellum provide a common computation for diverse tasks? A timing hypothesis. *Ann N Y Acad Sci* 608:179-207; discussion 207-111.

Kegel KB, Kim M, Sapp E, McIntyre C, Castano JG, Aronin N, DiFiglia M (2000) Huntingtin expression stimulates endosomal-lysosomal activity, endosome tubulation, and autophagy. *J Neurosci* 20:7268-7278.

Kelly RM, Strick PL (2003) Cerebellar loops with motor cortex and prefrontal cortex of a nonhuman primate. *J Neurosci* 23:8432-8444.

Kiehl TR, Nechiporuk A, Figueroa KP, Keating MT, Huynh DP, Pulst SM (2006) Generation and characterization of Sca2 (ataxin-2) knockout mice. *Biochem Biophys Res Commun* 339:17-24.

Kiehl TR, Shibata H, Pulst SM (2000) The ortholog of human ataxin-2 is essential for early embryonic patterning in C. elegans. *J Mol Neurosci* 15:231-241.

Killian JE, Baker JF (2002) Horizontal vestibuloocular reflex (VOR) head velocity estimation in Purkinje cell degeneration (pcd/pcd) mutant mice. *J Neurophysiol* 87:1159-1164.

Kimchi T, Etienne AS, Terkel J (2004) A subterranean mammal uses the magnetic compass for path integration. *Proc Natl Acad Sci U S A* 101:1105-1109.

Kishimoto Y, Kawahara S, Fujimichi R, Mori H, Mishina M, Kirino Y (2001) Impairment of eyeblink conditioning in GluRdelta2-mutant mice depends on the temporal overlap between conditioned and unconditioned stimuli. *Eur J Neurosci* 14:1515-1521.

Klionsky DJ, Emr SD (2000) Autophagy as a regulated pathway of cellular degradation. *Science* 290:1717-1721.

Klockgether T (2007) Ataxias. *Parkinsonism Relat Disord* 13 Suppl 3:S391-394.

Klockgether T (2010) Sporadic ataxia with adult onset: classification and diagnostic criteria. *Lancet Neurol* 9:94-104.

Klockgether T (2012) Sporadic adult-onset ataxia of unknown etiology. In: *Ataxic Disorders* (Subramony, S. H. and Dürr, A., eds), pp 253-262 London: Elsevier B.V.

Koekkoek SK, Hulscher HC, Dortland BR, Hensbroek RA, Elgersma Y, Ruigrok TJ, De Zeeuw CI (2003) Cerebellar LTD and learning-dependent timing of conditioned eyelid responses. *Science* 301:1736-1739.

Kohda K, Kakegawa W, Matsuda S, Yamamoto T, Hirano H, Yuzaki M (2013) The delta2 glutamate receptor gates long-term depression by coordinating interactions between two AMPA receptor phosphorylation sites. *Proc Natl Acad Sci U S A* 110:E948-957.

Kohda K, Kamiya Y, Matsuda S, Kato K, Umemori H, Yuzaki M (2003) Heteromer formation of delta2 glutamate receptors with AMPA or kainate receptors. *Mol Brain Res* 110:27-37.

Komuro H, Rakic P (1998) Distinct modes of neuronal migration in different domains of developing cerebellar cortex. *J Neurosci* 18:1478-1490.

Komuro H, Yacubova E (2003) Recent advances in cerebellar granule cell migration. *Cell Mol Life Sci* 60:1084-1098.

Komuro Y, Fahrion JK, Foote KD, Fenner KB, Kumada T, Ohno N, Komuro H (2007) Granule cell migration and differentiation. In: *Handbook of the Cerebellum and Cerebellar Disorders* (Manto, M. et al., eds), pp 1499-1520 New York: Springer Verlag.

Krizkova A, Vozeh F (2004) Development of early motor learning and topical motor skills in a model of cerebellar degeneration. *Behav Brain Res* 150:65-72.

Kurihara H, Hashimoto K, Kano M, Takayama C, Sakimura K, Mishina M, Inoue Y, Watanabe M (1997) Impaired parallel fiber-->Purkinje cell synapse stabilization during cerebellar development of mutant mice lacking the glutamate receptor delta2 subunit. *J Neurosci* 17:9613-9623.

Kyuhou S, Kato N, Gemba H (2006) Emergence of endoplasmic reticulum stress and activated microglia in Purkinje cell degeneration mice. *Neurosci Lett* 396:91-96.

Laine J, Axelrad H (1994) The candelabrum cell: a new interneuron in the cerebellar cortex. *J Comp Neurol* 339:159-173.

Laine J, Axelrad H (1998) Lugaro cells target basket and stellate cells in the cerebellar cortex. *Neuroreport* 9:2399-2403.

Lalonde R (1994) Motor learning in lurcher mutant mice. *Brain Res* 639:351-353.

Lalonde R (1998) Immobility responses in Lurcher mutant mice. *Behav Genet* 28:309-314.

Lalonde R, Botez MI, Joyal CC, Caumartin M (1992) Motor abnormalities in lurcher mutant mice. *Physiol Behav* 51:523-525.

Lalonde R, Filali M, Bensoula AN, Lestienne F (1996) Sensorimotor learning in three cerebellar mutant mice. *Neurobiol Learn Mem* 65:113-120.

Lalonde R, Joyal CC, Cote C, Botez MI (1993a) Simultaneous visual discrimination learning in lurcher mutant mice. *Brain Res* 618:19-22.

Lalonde R, Joyal CC, Guastavino JM, Botez MI (1993b) Hole poking and motor coordination in lurcher mutant mice. *Physiol Behav* 54:41-44.

Lalonde R, Lamarre Y, Smith AM (1988) Does the mutant mouse lurcher have deficits in spatially oriented behaviours? *Brain Res* 455:24-30.

Lalonde R, Strazielle C (2007) Spontaneous and induced mouse mutations with cerebellar dysfunctions: behavior and neurochemistry. *Brain Res* 1140:51-74.

Lalonde R, Thifault S (1994) Absence of an association between motor coordination and spatial orientation in lurcher mutant mice. *Behav Genet* 24:497-501.

Lalouette A, Guenet JL, Vriz S (1998) Hotfoot mouse mutations affect the delta 2 glutamate receptor gene and are allelic to lurcher. *Genomics* 50:9-13.

Landis SC, Mullen RJ (1978) The development and degeneration of Purkinje cells in pcd mutant mice. *J Comp Neurol* 177:125-143.

Landsend AS, Amiry-Moghaddam M, Matsubara A, Bergersen L, Usami S, Wenthold RJ, Ottersen OP (1997) Differential localization of delta glutamate receptors in the rat cerebellum: coexpression with AMPA receptors in parallel fiber-spine synapses and absence from climbing fiber-spine synapses. *J Neurosci* 17:834-842.

Larsell O (1967) The Comparative Anatomy and Histology of the Cerebellum from Myxinoids Through Birds. Minneapolis: University of Minnesota Press.

Lastres-Becker I, Brodesser S, Lutjohann D, Azizov M, Buchmann J, Hintermann E, Sandhoff K, Schurmann A, Nowock J, Auburger G (2008) Insulin receptor and lipid metabolism pathology in ataxin-2 knock-out mice. *Hum Mol Genet* 17:1465-1481.

LaVail MM, Blanks JC, Mullen RJ (1982) Retinal degeneration in the pcd cerebellar mutant mouse. I. Light microscopic and autoradiographic analysis. *J Comp Neurol* 212:217-230.

Le Marec N, Caston J, Lalonde R (1997) Impaired motor skills on static and mobile beams in lurcher mutant mice. *Exp Brain Res* 116:131-138.

Le Marec N, Hebert C, Botez MI, Botez-Marquard T, Marchand L, Reader TA (1999) Serotonin innervation of Lurcher mutant mice: basic data and manipulation with a combination of amantadine, thiamine and L-tryptophan. *Brain Res Bull* 48:195-201.

Le Marec N, Lalonde R (1997) Sensorimotor learning and retention during equilibrium tests in Purkinje cell degeneration mutant mice. *Brain Res* 768:310-316.

Le Marec N, Lalonde R (1998) Treadmill performance of mice with cerebellar lesions: 1. Purkinje cell degeneration mutant mice. *Behav Neurosci* 112:225-232.

Le Marec N, Lalonde R (2000) Treadmill performance of mice with cerebellar lesions: 2. Lurcher mutant mice. *Neurobiol Learn Mem* 73:195-206.

Lee PH, Kim JW, Bang OY, Ahn YH, Joo IS, Huh K (2008) Autologous mesenchymal stem cell therapy delays the progression of neurological deficits in patients with multiple system atrophy. *Clin Pharmacol Ther* 83:723-730.

Leggio MG, Neri P, Graziano A, Mandolesi L, Molinari M, Petrosini L (1999) Cerebellar contribution to spatial event processing: characterization of procedural learning. *Exp Brain Res* 127:1-11.

Leiner HC (2010) Solving the mystery of the human cerebellum. *Neuropsychol Rev* 20:229-235.

Leiner HC, Leiner AL, Dow RS (1986) Does the cerebellum contribute to mental skills? *Behav Neurosci* 100:443-454.

Lewis PM, Gritli-Linde A, Smeyne R, Kottmann A, McMahon AP (2004) Sonic hedgehog signaling is required for expansion of granule neuron precursors and patterning of the mouse cerebellum. *Dev Biol* 270:393-410.

Li J, Gu X, Ma Y, Calicchio ML, Kong D, Teng YD, Yu L, Crain AM, Vartanian TK, Pasqualini R, Arap W, Libermann TA, Snyder EY, Sidman RL (2010) Nna1 mediates Purkinje cell dendritic development via lysyl oxidase propeptide and NF-kappaB signaling. *Neuron* 68:45-60.

Lie CH, Specht K, Marshall JC, Fink GR (2006) Using fMRI to decompose the neural processes underlying the Wisconsin Card Sorting Test. *Neuroimage* 30:1038-1049.

Liu J, Tang TS, Tu H, Nelson O, Herndon E, Huynh DP, Pulst SM, Bezprozvanny I (2009) Deranged calcium signaling and neurodegeneration in spinocerebellar ataxia type 2. *J Neurosci* 29:9148-9162.

Llano Lopez L, Hauser J, Feldon J, Gargiulo PA, Yee BK (2010) Evaluating spatial memory function in mice: a within-subjects comparison between the water maze test and its adaptation to dry land. *Behav Brain Res* 209:85-92.

Llinas R, Sugimori M (1980) Electrophysiological properties of in vitro Purkinje cell dendrites in mammalian cerebellar slices. *J Physiol* 305:197-213.

Lorivel T, Gras M, Hilber P (2010) Effects of corticosterone synthesis inhibitor metyrapone on anxiety-related behaviors in Lurcher mutant mice. *Physiol Behav* 101:309-314.

Louvi A, Alexandre P, Metin C, Wurst W, Wassef M (2003) The isthmic neuroepithelium is essential for cerebellar midline fusion. *Development* 130:5319-5330.

Lu W, Tsirka SE (2002) Partial rescue of neural apoptosis in the Lurcher mutant mouse through elimination of tissue plasminogen activator. *Development* 129:2043-2050.

Machold R, Fishell G (2005) Math1 is expressed in temporally discrete pools of cerebellar rhombic-lip neural progenitors. *Neuron* 48:17-24.

Manto M, Marmolino D (2009) Animal models of human cerebellar ataxias: a cornerstone for the therapies of the twenty-first century. *Cerebellum* 8:137-154.

Manto MU (2005) The wide spectrum of spinocerebellar ataxias (SCAs). *Cerebellum* 4:2-6.

Marcinkiewicz M, Morcos R, Chretien M (1989) CNS connections with the median raphe nucleus: retrograde tracing with WGA-apoHRP-Gold complex in the rat. *J Comp Neurol* 289:11-35.

Marchena M, Lara J, Aijon J, Germain F, de la Villa P, Velasco A (2011) The retina of the PCD/PCD mouse as a model of photoreceptor degeneration. A structural and functional study. *Exp Eye Res* 93:607-617.

Marien P, Ackermann H, Adamaszek M, Barwood CH, Beaton A, Desmond J, De Witte E, Fawcett AJ, Hertrich I, Kuper M, Leggio M, Marvel C, Molinari M, Murdoch BE, Nicolson RI, Schmahmann JD, Stoodley CJ, Thurling M,

Timmann D, Wouters E, Ziegler W (2014) Consensus paper: Language and the cerebellum: an ongoing enigma. *Cerebellum* 13:386-410.

Marien P, De Smet HJ, Wijgerde E, Verhoeven J, Crols R, De Deyn PP (2013) Posterior fossa syndrome in adults: a new case and comprehensive survey of the literature. *Cortex* 49:284-300.

Marin F, Puelles L (1995) Morphological fate of rhombomeres in quail/chick chimeras: a segmental analysis of hindbrain nuclei. *Eur J Neurosci* 7:1714-1738.

Marr D (1969) A theory of cerebellar cortex. *J Physiol* 202:437-470.

Martin LA, Goldowitz D, Mittleman G (2003) The cerebellum and spatial ability: dissection of motor and cognitive components with a mouse model system. *Eur J Neurosci* 18:2002-2010.

Martinez S, Alvarado-Mallart RM (1989) Rostral Cerebellum Originates from the Caudal Portion of the So-Called 'Mesencephalic' Vesicle: A Study Using Chick/Quail Chimeras. *Eur J Neurosci* 1:549-560.

Massaquoi SG (2012) Physiology of clinical dysfunction of the cerebellum. In: *Ataxic Disorders* (Subramony, S. H. and Dürr, A., eds), pp 37-62 London: Elsevier B.V.

Matilla-Duenas A (2008) The highly heterogeneous spinocerebellar ataxias: from genes to targets for therapeutic intervention. *Cerebellum* 7:97-100.

Matilla-Duenas A, Ashizawa T, Brice A, Magri S, McFarland KN, Pandolfo M, Pulst SM, Riess O, Rubinsztein DC, Schmidt J, Schmidt T, Scoles DR, Stevanin G, Taroni F, Underwood BR, Sanchez I (2014) Consensus paper: pathological mechanisms underlying neurodegeneration in spinocerebellar ataxias. *Cerebellum* 13:269-302.

Matilla-Duenas A, Goold R, Giunti P (2006) Molecular pathogenesis of spinocerebellar ataxias. *Brain* 129:1357-1370.

Mattsson B, Sorensen JC, Zimmer J, Johansson BB (1997) Neural grafting to experimental neocortical infarcts improves behavioral outcome and reduces thalamic atrophy in rats housed in enriched but not in standard environments. *Stroke* 28:1225-1231; discussion 1231-1222.

Mayat E, Petralia RS, Wang YX, Wenthold RJ (1995) Immunoprecipitation, immunoblotting, and immunocytochemistry studies suggest that glutamate receptor delta subunits form novel postsynaptic receptor complexes. *J Neurosci* 15:2533-2546.

McCarthy MM, vom Saal FS (1985) The influence of reproductive state on infanticide by wild female house mice (Mus musculus). *Physiol Behav* 35:843-849.

Medina JF, Nores WL, Ohyama T, Mauk MD (2000) Mechanisms of cerebellar learning suggested by eyelid conditioning. *Curr Opin Neurobiol* 10:717-724.

Miale IL, Sidman RL (1961) An autoradiographic analysis of histogenesis in the mouse cerebellum. *Exp Neurol* 4:277-296.

Miall RC, Christensen LO, Cain O, Stanley J (2007) Disruption of state estimation in the human lateral cerebellum. *PLoS Biol* 5:e316.

Middleton FA, Strick PL (2001) Cerebellar projections to the prefrontal cortex of the primate. *J Neurosci* 21:700-712.

Millen KJ, Gleeson JG (2008) Cerebellar development and disease. *Curr Opin Neurobiol* 18:12-19.

Mittelstaedt H, Mittelstaedt M-L (1982) Homing by path integration. In: *Avian Navigation* (Papi, F. and Wallraff, H. G., eds), pp 290-297 New York: Springer.

Monnier C, Lalonde R (1995) Elevated (+)-maze and hole-board exploration in lurcher mutant mice. *Brain Res* 702:169-172.

Morris R (1984) Developments of a water-maze procedure for studying spatial learning in the rat. *J Neurosci Methods* 11:47-60.

Morris RG, Garrud P, Rawlins JN, O'Keefe J (1982) Place navigation impaired in rats with hippocampal lesions. *Nature* 297:681-683.

Moscovitch M (1995) Recovered consciousness: a hypothesis concerning modularity and episodic memory. *J Clin Exp Neuropsychol* 17:276-290.

Moseley ML, Zu T, Ikeda Y, Gao W, Mosemiller AK, Daughters RS, Chen G, Weatherspoon MR, Clark HB, Ebner TJ, Day JW, Ranum LP (2006) Bidirectional expression of CUG and CAG expansion transcripts and intranuclear polyglutamine inclusions in spinocerebellar ataxia type 8. *Nat Genet* 38:758-769.

Moulton EA, Schmahmann JD, Becerra L, Borsook D (2010) The cerebellum and pain: passive integrator or active participator? *Brain Res Rev* 65:14-27.

Mullen RJ, Eicher EM, Sidman RL (1976) Purkinje cell degeneration, a new neurological mutation in the mouse. *Proc Natl Acad Sci U S A* 73:208-212.

Nadel L, Moscovitch M (1997) Memory consolidation, retrograde amnesia and the hippocampal complex. *Curr Opin Neurobiol* 7:217-227.

Naito Y, Newman A, Lee WS, Beykirch K, Honrubia V (1995) Projections of the individual vestibular end-organs in the brain stem of the squirrel monkey. *Hear Res* 87:141-155.

Neau JP, Arroyo-Anllo E, Bonnaud V, Ingrand P, Gil R (2000) Neuropsychological disturbances in cerebellar infarcts. *Acta Neurol Scand* 102:363-370.

Nieuwenhuys R (1967) Comparative anatomy of the cerebellum. *Prog Brain Res* 25:1-93.

Nishiyama J, Matsuda K, Kakegawa W, Yamada N, Motohashi J, Mizushima N, Yuzaki M (2010) Reevaluation of neurodegeneration in lurcher mice:

constitutive ion fluxes cause cell death with, not by, autophagy. *J Neurosci* 30:2177-2187.

Nishiyama J, Yuzaki M (2010) Excitotoxicity and autophagy: lurcher may not be a model of "autophagic cell death". *Autophagy* 6:568-570.

Nixon RA, Cataldo AM, Mathews PM (2000) The endosomal-lysosomal system of neurons in Alzheimer's disease pathogenesis: a review. *Neurochem Res* 25:1161-1172.

Nonhoff U, Ralser M, Welzel F, Piccini I, Balzereit D, Yaspo ML, Lehrach H, Krobitsch S (2007) Ataxin-2 interacts with the DEAD/H-box RNA helicase DDX6 and interferes with P-bodies and stress granules. *Mol Biol Cell* 18:1385-1396.

Nonis D, Schmidt MH, van de Loo S, Eich F, Dikic I, Nowock J, Auburger G (2008) Ataxin-2 associates with the endocytosis complex and affects EGF receptor trafficking. *Cell Signal* 20:1725-1739.

Norman DJ, Feng L, Cheng SS, Gubbay J, Chan E, Heintz N (1995) The lurcher gene induces apoptotic death in cerebellar Purkinje cells. *Development* 121:1183-1193.

O'Gorman S (1985) Degeneration of thalamic neurons in "Purkinje cell degeneration" mutant mice. II. Cytology of neuron loss. *J Comp Neurol* 234:298-316.

O'Gorman S, Sidman RL (1985) Degeneration of thalamic neurons in "Purkinje cell degeneration" mutant mice. I. Distribution of neuron loss. *J Comp Neurol* 234:277-297.

O'Keefe J, Dostrovsky J (1971) The hippocampus as a spatial map. Preliminary evidence from unit activity in the freely-moving rat. *Brain Res* 34:171-175.

O'Keefe J, Nadel L (1978) The hippocampus as a cognitive map: Oxford University press.

Onuki Y, Van Someren EJ, De Zeeuw CI, Van der Werf YD (2015) Hippocampal-cerebellar interaction during spatio-temporal prediction. *Cereb Cortex* 25:313-321.

Palau F, Espinos C (2006) Autosomal recessive cerebellar ataxias. *Orphanet J Rare Dis* 1:47.

Paleja M, Girard TA, Herdman KA, Christensen BK (2014) Two distinct neural networks functionally connected to the human hippocampus during pattern separation tasks. *Brain Cogn* 92C:101-111.

Parsons LM, Petacchi A, Schmahmann JD, Bower JM (2009) Pitch discrimination in cerebellar patients: evidence for a sensory deficit. *Brain Res* 1303:84-96.

Passot JB, Sheynikhovich D, Duvelle E, Arleo A (2012) Contribution of cerebellar sensorimotor adaptation to hippocampal spatial memory. *PLoS One* 7:e32560.

Paulesu E, Frith CD, Frackowiak RS (1993) The neural correlates of the verbal component of working memory. *Nature* 362:342-345.

Perrett SP, Ruiz BP, Mauk MD (1993) Cerebellar cortex lesions disrupt learning-dependent timing of conditioned eyelid responses. *J Neurosci* 13:1708-1718.

Petersen A, Larsen KE, Behr GG, Romero N, Przedborski S, Brundin P, Sulzer D (2001) Expanded CAG repeats in exon 1 of the Huntington's disease gene stimulate dopamine-mediated striatal neuron autophagy and degeneration. *Hum Mol Genet* 10:1243-1254.

Petersen SE, Fox PT, Posner MI, Mintun M, Raichle ME (1989) Positron emission tomographic studies of the processing of singe words. *J Cogn Neurosci* 1:153-170.

Petrosini L, Leggio MG, Molinari M (1998) The cerebellum in the spatial problem solving: a co-star or a guest star? *Prog Neurobiol* 56:191-210.

Phillips RJS (1960) ‘Lurcher’, a new gene in linkage group XI of the house mouse. *J Genet* 57:35-42.

Pickens CL, Holland PC (2004) Conditioning and cognition. *Neurosci Biobehav Rev* 28:651-661.

Poley W (1974) Emotionality related to maternal cannibalism in BALB and C57BL mice. *Anim Learn Behav* 2:241-244.

Pollack IF (1997) Posterior fossa syndrome. *Int Rev Neurobiol* 41:411-432.

Porras-Garcia E, Cendelin J, Dominguez-del-Toro E, Vozeh F, Delgado-Garcia JM (2005) Purkinje cell loss affects differentially the execution, acquisition and prepulse inhibition of skeletal and facial motor responses in Lurcher mice. *Eur J Neurosci* 21:979-988.

Porras-Garcia E, Sanchez-Campusano R, Martinez-Vargas D, Dominguez-del-Toro E, Cendelin J, Vozeh F, Delgado-Garcia JM (2010) Behavioral characteristics, associative learning capabilities, and dynamic association mapping in an animal model of cerebellar degeneration. *J Neurophysiol* 104:346-365.

Porras-Garcia ME, Ruiz R, Perez-Villegas EM, Armengol JA (2013) Motor learning of mice lacking cerebellar Purkinje cells. *Front Neuroanat* 7:4.

Porsolt RD, Bertin A, Blavet N, Deniel M, Jalfre M (1979) Immobility induced by forced swimming in rats: effects of agents which modify central catecholamine and serotonin activity. *Eur J Pharmacol* 57:201-210.

Porsolt RD, Bertin A, Jalfre M (1978) "Behavioural despair" in rats and mice: strain differences and the effects of imipramine. *Eur J Pharmacol* 51:291-294.

Porsolt RD, Le Pichon M, Jalfre M (1977) Depression: a new animal model sensitive to antidepressant treatments. *Nature* 266:730-732.

Pulst SM, Nechiporuk A, Nechiporuk T, Gispert S, Chen XN, Lopes-Cendes I, Pearlman S, Starkman S, Orozco-Diaz G, Lunkes A, DeJong P, Rouleau GA,

Auburger G, Korenberg JR, Figueroa C, Sahba S (1996) Moderate expansion of a normally biallelic trinucleotide repeat in spinocerebellar ataxia type 2. *Nat Genet* 14:269-276.

Pulst SM, Santos N, Wang D, Yang H, Huynh D, Velazquez L, Figueroa KP (2005) Spinocerebellar ataxia type 2: polyQ repeat variation in the CACNA1A calcium channel modifies age of onset. *Brain* 128:2297-2303.

Purkartova Z, Tuma J, Pesta M, Kulda V, Hajkova L, Sebesta O, Vozeh F, Cendelin J (2014) Morphological analysis of embryonic cerebellar grafts in SCA2 mice. *Neurosci Lett* 558:154-158.

Purkartova Z, Vozeh F (2013) Cerebellar degeneration in Lurcher mice under confocal laser scanning microscope. *Microsc Res Tech* 76:545-551.

Rahmati N, Owens CB, Bosman LW, Spanke JK, Lindeman S, Gong W, Potters JW, Romano V, Voges K, Moscato L, Koekkoek SK, Negrello M, De Zeeuw CI (2014) Cerebellar potentiation and learning a whisker-based object localization task with a time response window. *J Neurosci* 34:1949-1962.

Reader TA, Ase AR, Le Marec N, Lalonde R (2000) Differential effects of L-trytophan and buspirone on biogenic amine contents and metabolism in Lurcher mice cerebellum. *Neurosci Lett* 280:171-174.

Reader TA, Strazielle C, Botez MI, Lalonde R (1998) Brain dopamine and amino acid concentrations in Lurcher mutant mice. *Brain Res Bull* 45:489-493.

Reeb-Whitaker CK, Paigen B, Beamer WG, Bronson RT, Churchill GA, Schweitzer IB, Myers DD (2001) The impact of reduced frequency of cage changes on the health of mice housed in ventilated cages. *Lab Anim* 35:58-73.

Resibois A, Cuvelier L, Goffinet AM (1997) Abnormalities in the cerebellum and brainstem in homozygous lurcher mice. *Neuroscience* 80:175-190.

Rogers TD, Dickson PE, McKimm E, Heck DH, Goldowitz D, Blaha CD, Mittleman G (2013) Reorganization of circuits underlying cerebellar modulation of

prefrontal cortical dopamine in mouse models of autism spectrum disorder. *Cerebellum* 12:547-556.

Rogowski K, van Dijk J, Magiera MM, Bosc C, Deloulme JC, Bosson A, Peris L, Gold ND, Lacroix B, Bosch Grau M, Bec N, Larroque C, Desagher S, Holzer M, Andrieux A, Moutin MJ, Janke C (2010) A family of protein-deglutamylating enzymes associated with neurodegeneration. *Cell* 143:564-578.

Rochefort C, Arabo A, Andre M, Poucet B, Save E, Rondi-Reig L (2011) Cerebellum shapes hippocampal spatial code. *Science* 334:385-389.

Rochefort C, Lefort JM, Rondi-Reig L (2013) The cerebellum: a new key structure in the navigation system. *Front Neural Circuits* 7:35.

Romano E, Michetti C, Caruso A, Laviola G, Scattoni ML (2013) Characterization of neonatal vocal and motor repertoire of reelin mutant mice. *PLoS One* 8:e64407.

Rondi-Reig L, Paradis AL, Lefort JM, Babayan BM, Tobin C (2014) How the cerebellum may monitor sensory information for spatial representation. *Front Syst Neurosci* 8:205.

Rossi F, Cattaneo E (2002) Opinion: neural stem cell therapy for neurological diseases: dreams and reality. *Nat Rev Neurosci* 3:401-409.

Rossi F, Saggiorato C, Strata P (2002) Target-specific innervation of embryonic cerebellar transplants by regenerating olivocerebellar axons in the adult rat. *Exp Neurol* 173:205-212.

Ruigrok TJ (2011) Ins and outs of cerebellar modules. *Cerebellum* 10:464-474.

Saab CY, Willis WD (2003) The cerebellum: organization, functions and its role in nociception. *Brain Res Rev* 42:85-95.

Sami S, Robertson EM, Miall RC (2014) The time course of task-specific memory consolidation effects in resting state networks. *J Neurosci* 34:3982-3992.

Sapp E, Schwarz C, Chase K, Bhide PG, Young AB, Penney J, Vonsattel JP, Aronin N, DiFiglia M (1997) Huntingtin localization in brains of normal and Huntington's disease patients. *Ann Neurol* 42:604-612.

Scoles DR, Pflieger LT, Thai KK, Hansen ST, Dansithong W, Pulst SM (2012) ETS1 regulates the expression of ATXN2. *Hum Mol Genet* 21:5048-5065.

Selimi F, Doughty M, Delhaye-Bouchaud N, Mariani J (2000a) Target-related and intrinsic neuronal death in Lurcher mutant mice are both mediated by caspase-3 activation. *J Neurosci* 20:992-1000.

Selimi F, Vogel MW, Mariani J (2000b) Bax inactivation in lurcher mutants rescues cerebellar granule cells but not purkinje cells or inferior olivary neurons. *J Neurosci* 20:5339-5345.

Sgaier SK, Millet S, Villanueva MP, Berenshteyn F, Song C, Joyner AL (2005) Morphogenetic and cellular movements that shape the mouse cerebellum; insights from genetic fate mapping. *Neuron* 45:27-40.

Shibata H, Huynh DP, Pulst SM (2000) A novel protein with RNA-binding motifs interacts with ataxin-2. *Hum Mol Genet* 9:1303-1313.

Schenk F, Morris RG (1985) Dissociation between components of spatial memory in rats after recovery from the effects of retrohippocampal lesions. *Exp Brain Res* 58:11-28.

Schilling K, Oberdick J, Rossi F, Baader SL (2008) Besides Purkinje cells and granule neurons: an appraisal of the cell biology of the interneurons of the cerebellar cortex. *Histochem Cell Biol* 130:601-615.

Schmahmann JD (1991) An emerging concept. The cerebellar contribution to higher function. *Arch Neurol* 48:1178-1187.

Schmahmann JD (2004) Disorders of the cerebellum: ataxia, dysmetria of thought, and the cerebellar cognitive affective syndrome. *J Neuropsychiatry Clin Neurosci* 16:367-378.

Schmahmann JD, Pandya DN (1997a) Anatomic organization of the basilar pontine projections from prefrontal cortices in rhesus monkey. *J Neurosci* 17:438-458.

Schmahmann JD, Pandya DN (1997b) The cerebrocerebellar system. *Int Rev Neurobiol* 41:31-60.

Schmahmann JD, Sherman JC (1997) Cerebellar cognitive affective syndrome. *Int Rev Neurobiol* 41:433-440.

Schonewille M, Belmeguenai A, Koekkoek SK, Houtman SH, Boele HJ, van Beugen BJ, Gao Z, Badura A, Ohtsuki G, Amerika WE, Hosy E, Hoebeek FE, Elgersma Y, Hansel C, De Zeeuw CI (2010) Purkinje cell-specific knockout of the protein phosphatase PP2B impairs potentiation and cerebellar motor learning. *Neuron* 67:618-628.

Schonewille M, Gao Z, Boele HJ, Veloz MF, Amerika WE, Simek AA, De Jeu MT, Steinberg JP, Takamiya K, Hoebeek FE, Linden DJ, Huganir RL, De Zeeuw CI (2011) Reevaluating the role of LTD in cerebellar motor learning. *Neuron* 70:43-50.

Schwaller B, Meyer M, Schiffmann S (2002) 'New' functions for 'old' proteins: the role of the calcium-binding proteins calbindin D-28k, calretinin and parvalbumin, in cerebellar physiology. Studies with knockout mice. *Cerebellum* 1:241-258.

Schwartz LM, Smith SW, Jones ME, Osborne BA (1993) Do all programmed cell deaths occur via apoptosis? *Proc Natl Acad Sci U S A* 90:980-984.

Sidman RL, Green MC (1970) “Nervous,” a new mutant mouse with cerebellar disease. In: *Les mutants pathologiques ches l'animal*, pp 69-79 Saboury M. Paris: Centre National De la Recherche.

Simat M, Parpan F, Fritschy JM (2007) Heterogeneity of glycinergic and gabaergic interneurons in the granule cell layer of mouse cerebellum. *J Comp Neurol* 500:71-83.

Slattery DA, Cryan JF (2012) Using the rat forced swim test to assess antidepressant-like activity in rodents. *Nat Protoc* 7:1009-1014.

Smith AM (1981) The coactivation of antagonist muscles. *Can J Physiol Pharmacol* 59:733-747.

Snider RS, Stowell A (1944) Receiving areas of the tactile, auditory, and visual systems in the cerebellum. *J Neurophysiol* 7:331-357.

Sotelo C, Alvarado-Mallart RM (1986) Growth and differentiation of cerebellar suspensions transplanted into the adult cerebellum of mice with heredodegenerative ataxia. *Proc Natl Acad Sci U S A* 83:1135-1139.

Sotelo C, Alvarado-Mallart RM (1987a) Embryonic and adult neurons interact to allow Purkinje cell replacement in mutant cerebellum. *Nature* 327:421-423.

Sotelo C, Alvarado-Mallart RM (1987b) Reconstruction of the defective cerebellar circuitry in adult Purkinje cell degeneration mutant mice by Purkinje cell replacement through transplantation of solid embryonic implants. *Neuroscience* 20:1-22.

Sotelo C, Alvarado-Mallart RM, Keep M (1992) Fate of axons of embryonic Purkinje cells grafted in the adult cerebellum of the pcd mutant mouse. In: *The nerve growth cone* (Letourneau, P. C. et al., eds), pp 505-517 New York: Raven Press.

Sotelo C, Rossi F (2007) Purkinje cell migration and differentiation. In: *Handbook of the Cerebellum and Cerebellar Disorders* (Manto, M. et al., eds), pp 1499-1520 New York: Springer Verlag.

Stoodley CJ, Schmahmann JD (2010) Evidence for topographic organization in the cerebellum of motor control versus cognitive and affective processing. *Cortex* 46:831-844.

Strata P, Rossi F (1998) Plasticity of the olivocerebellar pathway. *Trends Neurosci* 21:407-413.

Strazielle C, Lalonde R (1998) Grooming in Lurcher mutant mice. *Physiol Behav* 64:57-61.

Strazielle C, Lalonde R, Reader TA (2000) Autoradiography of glutamate receptor binding in adult Lurcher mutant mice. *J Neuropathol Exp Neurol* 59:707-722.

Strazielle C, Lalonde R, Riopel L, Botez MI, Reader TA (1996) Regional distribution of the 5-HT innervation in the brain of normal and lurcher mice as revealed by [3H]citalopram quantitative autoradiography. *J Chem Neuroanat* 10:157-171.

Sugihara I (2011) Compartmentalization of the deep cerebellar nuclei based on afferent projections and aldolase C expression. *Cerebellum* 10:449-463.

Sultan F, Konig T, Mock M, Thier P (2002) Quantitative organization of neurotransmitters in the deep cerebellar nuclei of the Lurcher mutant. *J Comp Neurol* 452:311-323.

Swisher DA, Wilson DB (1977) Cerebellar histogenesis in the lurcher (Lc) mutant mouse. *J Comp Neurol* 173:205-218.

Takeuchi T, Ohtsuki G, Yoshida T, Fukaya M, Wainai T, Yamashita M, Yamazaki Y, Mori H, Sakimura K, Kawamoto S, Watanabe M, Hirano T, Mishina M (2008) Enhancement of both long-term depression induction and optokinetic response adaptation in mice lacking delphilin. *PLoS One* 3:e2297.

Thach WT (1968) Discharge of Purkinje and cerebellar nuclear neurons during rapidly alternating arm movements in the monkey. *J Neurophysiol* 31:785-797.

Thangima Zannat M, Bhattacharjee RB, Bag J (2011) Depletion of cellular poly (A) binding protein prevents protein synthesis and leads to apoptosis in HeLa cells. *Biochem Biophys Res Commun* 408:375-381.

Thier P, Haarmeier T, Treue S, Barash S (1999) Absence of a common functional denominator of visual disturbances in cerebellar disease. *Brain* 122 (Pt 11):2133-2146.

Thompson RF (2005) In search of memory traces. *Annu Rev Psychol* 56:1-23.

Thullier F, Lalonde R, Cousin X, Lestienne F (1997) Neurobehavioral evaluation of lurcher mutant mice during ontogeny. *Dev Brain Res* 100:22-28.

Tian ZM, Chen T, Zhong N, Li ZC, Yin F, Liu S (2009) Clinical study of transplantation of neural stem cells in therapy of inherited cerebellar atrophy. *Beijing Da Xue Xue Bao* 41:456-458.

Timmann D, Drepper J, Frings M, Maschke M, Richter S, Gerwig M, Kolb FP (2010) The human cerebellum contributes to motor, emotional and cognitive associative learning. A review. *Cortex* 46:845-857.

Tolman EC (1948) Cognitive maps in rats and men. *Psychol Rev* 55:189-208.

Tomey DA, Heckroth JA (1993) Transplantation of normal embryonic cerebellar cell suspensions into the cerebellum of lurcher mutant mice. *Exp Neurol* 122:165-170.

Tommasi L, Chiandetti C, Pecchia T, Sovrano VA, Vallortigara G (2012) From natural geometry to spatial cognition. *Neurosci Biobehav Rev* 36:799-824.

Triarhou LC (1996) The cerebellar model of neural grafting: structural integration and functional recovery. *Brain Res Bull* 39:127-138.

Triarhou LC (1998) Rate of neuronal fallout in a transsynaptic cerebellar model. *Brain Res Bull* 47:219-222.

Triarhou LC, Zhang W, Lee WH (1995) Graft-induced restoration of function in hereditary cerebellar ataxia. *Neuroreport* 6:1827-1832.

Triarhou LC, Zhang W, Lee WH (1996) Amelioration of the behavioral phenotype in genetically ataxic mice through bilateral intracerebellar grafting of fetal Purkinje cells. *Cell Transplant* 5:269-277.

Truong DT, Bonet A, Rendall AR, Rosen GD, Fitch RH (2013) A behavioral evaluation of sex differences in a mouse model of severe neuronal migration disorder. *PLoS One* 8:e73144.

Tukaj C (2013) The significance of macroautophagy in health and disease. *Folia Morphol* 72:87-93.

Tuma J, Cendelin J, Vozeh F (2013) Maternal infanticide and low maternal ability in cerebellar mutants Lurcher. *Neuroendocrinol Lett* 34:618-623.

Tuma J, Kolinko Y, Vozeh F, Cendelin J (2015) Mutation-related differences in exploratory, spatial, and depressive-like behavior in pcd and Lurcher cerebellar mutant mice. *Front Behav Neurosci* 9:116.

Turner BM, Paradiso S, Marvel CL, Pierson R, Boles Ponto LL, Hichwa RD, Robinson RG (2007) The cerebellum and emotional experience. *Neuropsychologia* 45:1331-1341.

Uemura T, Lee SJ, Yasumura M, Takeuchi T, Yoshida T, Ra M, Taguchi R, Sakimura K, Mishina M (2010) Trans-synaptic interaction of GluRdelta2 and Neurexin through Cbln1 mediates synapse formation in the cerebellum. *Cell* 141:1068-1079.

Valero J, Berciano MT, Weruaga E, Lafarga M, Alonso JR (2006) Pre-neurodegeneration of mitral cells in the pcd mutant mouse is associated with DNA damage, transcriptional repression, and reorganization of nuclear speckles and Cajal bodies. *Mol Cell Neurosci* 33:283-295.

van Alphen AM, De Zeeuw CI (2002) Cerebellar LTD facilitates but is not essential for long-term adaptation of the vestibulo-ocular reflex. *Eur J Neurosci* 16:486-490.

van Alphen AM, Schepers T, Luo C, De Zeeuw CI (2002) Motor performance and motor learning in Lurcher mice. *Ann N Y Acad Sci* 978:413-424.

van de Loo S, Eich F, Nonis D, Auburger G, Nowock J (2009) Ataxin-2 associates with rough endoplasmic reticulum. *Exp Neurol* 215:110-118.

van de Warrenburg BP, Hendriks H, Durr A, van Zuijlen MC, Stevanin G, Camuzat A, Sinke RJ, Brice A, Kremer BP (2005) Age at onset variance analysis in spinocerebellar ataxias: a study in a Dutch-French cohort. *Ann Neurol* 57:505-512.

Vig PJ, Subramony SH, Burright EN, Fratkin JD, McDaniel DO, Desaiah D, Qin Z (1998) Reduced immunoreactivity to calcium-binding proteins in Purkinje cells precedes onset of ataxia in spinocerebellar ataxia-1 transgenic mice. *Neurology* 50:106-113.

Vogel MW, Caston J, Yuzaki M, Mariani J (2007) The Lurcher mouse: fresh insights from an old mutant. *Brain Res* 1140:4-18.

Voogd J, Bigare F (1980) Topographical distribution of oli- vary and cortico nuclear fibers in the cerebellum: a review. In: *The Inferior Olivary Nucleus: Anatomy and Physiology* (Courville, J. et al., eds), pp 207-234 New York: Raven.

Voogd J, Glickstein M (1998) The anatomy of the cerebellum. *Trends Neurosci* 21:370-375.

Wahlsten D (2011) Mouse behavioral testing. London, Burlington, San Diego: Elsevier.

Walsh RN, Cummins RA (1976) The Open-Field Test: a critical review. *Psychol Bull* 83:482-504.

Walton JC, Schilling K, Nelson RJ, Oberdick J (2012) Sex-dependent behavioral functions of the Purkinje cell-specific Galphai/o binding protein, Pcp2(L7). *Cerebellum* 11:982-1001.

Wang QJ, Ding Y, Kohtz DS, Mizushima N, Cristea IM, Rout MP, Chait BT, Zhong Y, Heintz N, Yue Z (2006) Induction of autophagy in axonal dystrophy and degeneration. *J Neurosci* 26:8057-8068.

Wang T, Morgan JI (2007) The Purkinje cell degeneration (pcd) mouse: an unexpected molecular link between neuronal degeneration and regeneration. *Brain Res* 1140:26-40.

Weber EM, Olsson AS (2008) Maternal behaviour in *Mus musculus* sp.: An ethological review. *Appl Anim Behav Sci* 114:1-22.

Welsh JP, Yamaguchi H, Zeng XH, Kojo M, Nakada Y, Takagi A, Sugimori M, Llinas RR (2005) Normal motor learning during pharmacological prevention of Purkinje cell long-term depression. *Proc Natl Acad Sci U S A* 102:17166-17171.

Wenning GK, Ben Shlomo Y, Magalhaes M, Daniel SE, Quinn NP (1994) Clinical features and natural history of multiple system atrophy. An analysis of 100 cases. *Brain* 117 (Pt 4):835-845.

Wenning GK, Colosimo C, Geser F, Poewe W (2004) Multiple system atrophy. *Lancet Neurol* 3:93-103.

Whishaw IQ (1985) Cholinergic receptor blockade in the rat impairs locale but not taxon strategies for place navigation in a swimming pool. *Behav Neurosci* 99:979-1005.

Whishaw IQ (1991) Latent learning in a swimming pool place task by rats: evidence for the use of associative and not cognitive mapping processes. *Q J Exp Psychol B* 43:83-103.

Whishaw IQ, Gorny BP (1991) Postprandial scanning by the rat (Rattus norvegicus): the importance of eating time and an application of "warm-up" movements. *J Comp Psychol* 105:39-44.

Whishaw IQ, McKenna JE, Maaswinkel H (1997) Hippocampal lesions and path integration. *Curr Opin Neurobiol* 7:228-234.

Whishaw IQ, Mittleman G (1986) Visits to starts, routes, and places by rats (Rattus norvegicus) in swimming pool navigation tasks. *J Comp Psychol* 100:422-431.

Wikgren J, Nokia MS, Penttonen M (2010) Hippocampo-cerebellar theta band phase synchrony in rabbits. *Neuroscience* 165:1538-1545.

Wilson DB (1976) Histological defects in the cerebellum of adult lurcher (Lc) mice. *J Neuropathol Exp Neurol* 35:40-45.

Wilson LJ, Myat A, Sharma A, Maden M, Wingate RJ (2007) Retinoic acid is a potential dorsalising signal in the late embryonic chick hindbrain. *BMC Dev Biol* 7:138.

Wiltschko W, Wiltschko R (2012) Global navigation in migratory birds: tracks, strategies, and interactions between mechanisms. *Curr Opin Neurobiol* 22:328-335.

Wolpert DM, Miall RC, Kawato M (1998) Internal models in the cerebellum. *Trends Cogn Sci* 2:338-347.

Wu CY, Bao XF, Zhang C, Zhang QL (1991) Fetal tissue grafts for cerebellar atrophy. *Chin Med J (Engl)* 104:198-203.

Wullner U, Loschmann PA, Weller M, Klockgether T (1995) Apoptotic cell death in the cerebellum of mutant weaver and lurcher mice. *Neurosci Lett* 200:109-112.

Wullner U, Weller M, Schulz JB, Krajewski S, Reed JC, Klockgether T (1998) Bcl-2, Bax and Bcl-x expression in neuronal apoptosis: a study of mutant weaver and lurcher mice. *Acta Neuropathol* 96:233-238.

Xue L, Fletcher GC, Tolkovsky AM (1999) Autophagy is activated by apoptotic signalling in sympathetic neurons: an alternative mechanism of death execution. *Mol Cell Neurosci* 14:180-198.

Yakusheva TA, Blazquez PM, Chen A, Angelaki DE (2013) Spatiotemporal properties of optic flow and vestibular tuning in the cerebellar nodulus and uvula. *J Neurosci* 33:15145-15160.

Yakusheva TA, Shaikh AG, Green AM, Blazquez PM, Dickman JD, Angelaki DE (2007) Purkinje cells in posterior cerebellar vermis encode motion in an inertial reference frame. *Neuron* 54:973-985.

Yoder RM, Goebel EA, Koppen JR, Blankenship PA, Blackwell AA, Wallace DG (2015) Otolithic information is required for homing in the mouse. *Hippocampus*.

Yue Z (2010) Autophagy in lurcher mice: indicted but yet to be acquitted for the death of Purkinje cells. *Autophagy* 6:571-572; discussion 573.

Yue Z, Horton A, Bravin M, DeJager PL, Selimi F, Heintz N (2002) A novel protein complex linking the delta 2 glutamate receptor and autophagy: implications for neurodegeneration in lurcher mice. *Neuron* 35:921-933.

Yuzaki M (2004) The delta2 glutamate receptor: a key molecule controlling synaptic plasticity and structure in Purkinje cells. *Cerebellum* 3:89-93.

Zanjani H, Rondi-Reig L, Vogel M, Martinou JC, Delhaye-Bouchaud N, Mariani J (1998a) Overexpression of a Hu-bcl-2 transgene in Lurcher mutant mice delays Purkinje cell death. *C R Acad Sci III* 321:633-640.

Zanjani HS, McFarland R, Cavelier P, Blokhin A, Gautheron V, Levenes C, Bambrick LL, Mariani J, Vogel MW (2009) Death and survival of heterozygous Lurcher Purkinje cells in vitro. *Dev Neurobiol* 69:505-517.

Zanjani HS, Vogel MW, Martinou JC, Delhaye-Bouchaud N, Mariani J (1998b) Postnatal expression of Hu-bcl-2 gene in Lurcher mutant mice fails to rescue Purkinje cells but protects inferior olivary neurons from target-related cell death. *J Neurosci* 18:319-327.

Zhang W, Lee WH, Triarhou LC (1996) Grafted cerebellar cells in a mouse model of hereditary ataxia express IGF-I system genes and partially restore behavioral function. *Nat Med* 2:65-71.

Ziemus B, Baumann O, Luerding R, Schlosser R, Schuierer G, Bogdahn U, Greenlee MW (2007) Impaired working-memory after cerebellar infarcts paralleled by changes in BOLD signal of a cortico-cerebellar circuit. *Neuropsychologia* 45:2016-2024.

Zoghbi HY, Orr HT (2000) Glutamine repeats and neurodegeneration. *Annu Rev Neurosci* 23:217-247.

Zuo J, De Jager PL, Norman DJ, Heintz N (1995) Generation of a high-resolution genetic map and a YAC contig of the Lurcher locus on mouse chromosome 6. *Genome Res* 5:381-392.

Zuo J, De Jager PL, Takahashi KA, Jiang W, Linden DJ, Heintz N (1997) Neurodegeneration in Lurcher mice caused by mutation in delta2 glutamate receptor gene. *Nature* 388:769-773.